EAS 572 The Atmospheric Boundary Layer

J.D. Wilson

6 Nov. 2012

Contents

Contents **i**

I Orientation, Tools 1

1 Review of Fluid Mechanics **2**
1.1 What is "turbulence"? . . . 2
1.2 Dimensional Analysis . . . 4
1.2.1 Example: pendulum . . . 4
1.2.2 Example: canopy wind profile . . . 5
1.2.3 Example: highway collision rate . . . 6
1.2.4 Method of Indices . . . 6
1.2.5 Example: plane Poiseuille flow . . . 7
1.3 Similarity Theory . . . 9
1.3.1 Example: flow past a cylinder . . . 9
1.4 Developing the Conservation Equations of Fluid Mechanics . . . 11
1.4.1 Use of tensor notation . . . 11
1.4.2 Continuum Hypothesis . . . 12
1.4.3 Diffusive and Convective Flux Densities . . . 13
Fourier's law of conduction . . . 13
Fick's law of binary diffusion . . . 14
Newton's law of viscosity and the shear stress tensor . . . 14
Convective Flux Densities . . . 17
1.4.4 The Lagrangian (Material) Derivative . . . 18
1.4.5 Deriving a conservation equation . . . 19
1.4.6 Special cases . . . 21
The continuity equation . . . 21
Water vapour conservation . . . 21
Momentum equations . . . 22
1.4.7 Cauchy's Equation of Motion . . . 22
1.4.8 Stress-Strain Relationship for a Newtonian Fluid . . . 23
1.5 The Navier-Stokes Equations . . . 24
1.5.1 Exact Solutions to the Navier-Stokes Equations . . . 24
1.5.2 Definition of Incompressibility . . . 25
1.5.3 Special Classes of Flows . . . 25
Inviscid flow . . . 26
Two-dimensional flow . . . 26

Non-divergent flow . . . 26
Irrotational flow . . . 26
Potential flow . . . 26
1.5.4 Helmholtz Theorem . . . 26
1.5.5 The Energy Cascade . . . 27
1.5.6 Kolmogorov's theory of Locally Isotropic Turbulence . . . 28
1.6 The Boussinesq Approximation . . . 29
1.6.1 Summary . . . 29

2 Key turbulence statistics **31**
2.1 Velocity Statistics . . . 31
2.2 Some vital terminology . . . 35
2.3 Time scales and length scales of turbulence . . . 35

3 Governing Equations for Atmospheric Statistics **37**
3.1 Resolved and Unresolved Scales of Motion . . . 37
3.2 Reynolds-Averaging the Governing Equations . . . 39
3.2.1 Example: water vapour . . . 40
3.3 Average form of the continuity equation . . . 42
3.4 Mean momentum equations . . . 43
3.5 Mean pressure . . . 44
3.6 Reynolds stress budget . . . 44
3.7 Turbulent Kinetic Energy equation . . . 45
3.8 Temperature statistics . . . 46
3.9 Statistics of a passive scalar . . . 47

4 Preliminary view of uniform PBL **49**
4.1 Mean Velocity . . . 49
4.1.1 Mean vertical velocity . . . 50
4.1.2 Mean horizontal velocity . . . 50
4.1.3 First-order closures . . . 52
Analytical Wind Profiles for the hh-ABL . . . 52
4.2 The hh-ASL identified as a constant flux layer . . . 53
4.3 Surface drag . . . 54
4.4 Friction velocity and other wind statistics . . . 54
4.5 Neutral wind profile in log layer . . . 54
4.6 Mean humidity . . . 56
4.7 Turbulent kinetic energy . . . 57
4.7.1 Variance of streamwise velocity, $\overline{u'^2}$ . . . 57
4.7.2 Variance of vertical velocity, $\overline{w'^2}$ . . . 57
4.7.3 Turbulent kinetic energy budget . . . 58
Pressure redistribution . . . 58
Local Equilibrium . . . 60
TKE budget . . . 60
Flux Richardson Number . . . 60
4.8 Shear stress budget . . . 61
4.8.1 Weakness of K-theory . . . 61

4.9 Heat flux budget 61

II The Ideal Atmospheric Surface Layer 63

5 Horizontally-Uniform Surface-Layer 64
5.1 Logical basis of Monin-Obukhov Similarity Theory 64
5.1.1 Non-dimensionalized governing equations 65
5.2 The friction velocity and the Obukhov Length 69
5.3 Exchange coefficients 70
5.4 Flux and Gradient Richardson Numbers 71
5.5 Key experiments on MO functions 71
5.5.1 New South Wales Experiments 71
5.5.2 Kansas Experiments 72
5.5.3 ITCE76 73
5.6 Mean Profiles 74
5.6.1 Stable stratification 74
5.6.2 Unstable stratification 74
5.7 Velocity Standard Deviations 75
5.7.1 Velocity standard deviations in unstable stratification 76
5.7.2 Velocity standard deviations in stable stratification 76
5.8 Velocity Spectra 76
5.9 Turbulent Prandtl- and Schmidt Numbers 77
5.10 Local free convection scaling 78
5.11 Origin and effectiveness 79

6 Surface-air exchange 80
6.1 The surface energy balance 80
6.2 Eddy-Covariance 82
6.3 Flux-gradient methods 83
6.4 Flux loss and energy-balance non-closure 86
6.5 Bulk Transfer Coefficients 89
6.6 Refinement over MOST profiles near $z = z_0$ 90
6.6.1 Profiles very near $z = 0$ 92
6.7 Convective boundary-layer budgeting (CBLB) 94
6.8 The flux footprint 95
6.8.1 An oversimplified analytical flux footprint 96
6.9 Evapotranspiration 97
6.10 Inverse dispersion method 100

III Above and Below the Surface Layer 103

7 The "Horizontally-Uniform" ABL 104
7.1 Partial list of ABL experiments 106
7.2 Multi-layer description of very convective CBL over land 107
Quasi-equilibrium of the CBL 107
Velocity statistics in the CBL 108

7.3 Velocity spectra . . . 108
7.3.1 Velocity spectra for the unstable ABL . . . 108
7.4 The stable boundary layer (SBL) . . . 112
7.4.1 Intermittency in the SBL . . . 115
7.4.2 Velocity spectra for the stable ASL . . . 117
7.5 Theories for time-evolution of ABL depth . . . 117

8 The micrometeorology of "Uniform" Plant Canopies 119
8.1 Need for horizontal averaging . . . 120
8.1.1 A Spatial Average . . . 121
8.2 Intermittency in plant canopies . . . 124
8.2.1 Ramps and Microfronts . . . 124
8.2.2 Quadrant analysis . . . 126
8.2.3 Governing equations for a uniform canopy . . . 127
8.3 Canopy profiles . . . 128
8.3.1 Canopy shear-stress profile . . . 128
8.3.2 Canopy wind profile . . . 128
8.3.3 Turbulence profiles . . . 131
8.3.4 Layer-resolved energy budget in the plant canopy . . . 131
8.3.5 TKE transformations (wake production) . . . 133
8.3.6 Modelling TKE transformations . . . 133
8.4 Velocity and TKE profiles computed from a simple closure . . . 134
8.4.1 Application to "uniform canopies" . . . 135
"Furry Hill" . . . 135
"Tombstone Canopy" . . . 135
8.5 Countergradient transport in plant canopies . . . 136
8.6 The renewal model . . . 138
8.7 Canopy wind spiral . . . 139
8.8 Coherent structures in canopy flows . . . 139

9 Thermals and Roll Vortices 140
9.1 The Dust Devil (columnar vortices) . . . 141
9.2 ASL-CBL flow continuity . . . 141
9.3 Thermals . . . 142
9.3.1 Thermals in a uniform CBL . . . 144
9.4 Roll vortices . . . 145
9.5 Hairpin (horseshoe) vortices . . . 146
9.6 Bird flight in the ABL . . . 147

IV Disturbed Flows 148

10 Introduction 149
10.1 Paradigm of the Internal Boundary Layer (IBL) . . . 150

11 Local Advection 152

12 Windbreak Flows **155**
12.0.1 Windbreak experiments . . . 156
12.0.2 Overview of Windbreak Aerodynamics . . . 157
Characterizing the approach flow and the barrier . . . 157
Mean velocity field . . . 159
Turbulent velocity field . . . 159
12.0.3 Mean Pressure . . . 160
12.0.4 Governing Equations for mean flow and turbulence . . . 160
12.0.5 TKE sources . . . 162
12.0.6 Evolution of theories of porous barrier flow . . . 162
12.0.7 Modern (numerical) simulations of windbreak flow . . . 163

13 Hierarchy of turbulence closures **167**
13.1 First-order (K-theory) closures . . . 168
13.1.1 Eddy Viscosity of the Approach Flow ("K_0") . . . 168
13.1.2 Prandtl closure ("K_{P_r}") . . . 168
13.1.3 One-Equation Closure ("K_k") . . . 168
13.1.4 Two-Equation Closures: k-ϵ model . . . 170
13.2 Higher-order closures . . . 171

V Turbulent Dispersion **173**

14 Dispersion in the Uniform ABL **174**
14.1 "Relative" versus "Absolute" Dispersion . . . 175
14.1.1 Plume . . . 175
14.1.2 Puff . . . 176
14.2 Project Prairie Grass . . . 176
14.3 Eulerian Approach . . . 177
14.3.1 Simplifications due to Symmetry . . . 177
14.3.2 First-order Closures . . . 177
"Gaussian Puff" and "Gaussian Plume" Models . . . 179
Instantaneous Point Source . . . 179
Empirical Prescriptions for Plume Widths . . . 182
More-general First-Order Models for the hh-ASL . . . 183
Near field correction . . . 183
Lateral dispersion . . . 183
14.4 Turbulent Schmidt Number and C_0 . . . 186

15 Lagrangian approach to scalar dispersion **187**
15.1 General Expression for Ensemble Mean Concentration . . . 188
15.2 Taylor's Lagrangian Theory . . . 189
15.2.1 Comparison with Classical Eddy-Diffusion Solution . . . 191
15.2.2 Asymptotic results . . . 192
15.3 Lagrangian stochastic (LS) models . . . 193
15.3.1 Deterministic vs. stochastic form of LS model . . . 194
15.3.2 Reminder on relevant time scales . . . 194

15.3.3 Hierarchy of LS models . . . 195
15.3.4 Well-mixed condition . . . 196
15.3.5 Unique 1-D LS model . . . 197
Project Prairie Grass (The O'Neill Experiment) . . . 198
LS simulations of PPG . . . 198
15.3.6 Lateral dispersion in the atmosphere . . . 199
15.3.7 Multi-dimensional LS models . . . 202
Gaussian inhomogeneous turbulence . . . 202
15.3.8 Link between C_0 and S_c . . . 203
15.3.9 Reflection at Boundaries . . . 204
15.3.10 Partially-absorbing boundaries . . . 205
15.3.11 LS models for non-Gaussian turbulence . . . 205
Convective BL . . . 205
Profiles of vertical velocity statistics for the CBL . . . 206
Validity of reflection algorithm . . . 206
Model coefficient . . . 207
Example: CBL simulation of Du et al. . . . 207
LS models for a plant/forest canopy . . . 210
15.4 Fundamental Superiority of Lagrangian models . . . 212
15.5 Heavy particle dispersion . . . 214
15.5.1 Inertial particle models . . . 214
15.5.2 Heuristic driving fluid velocity for IP model . . . 215
15.5.3 Langevin class of particle trajectory models . . . 216
Turbophoresis . . . 217
15.5.4 Suffield heavy particle dispersion trials . . . 218
15.6 LS models applicable in disturbed flows . . . 222

16 Lagrangian similarity theory **223**

Bibliography **227**

Index **252**

Part I

Tools & Orientation to Turbulence Statistics and their Governing Equations

Chapter 1

REVIEW OF FLUID MECHANICS PERTINENT TO THE TURBULENT ABL

1.1 What is "turbulence"?

If the wind near ground were not turbulent, these notes would be but a few pages long, and there would not be much mystery; we should have an elegant equation for all properties of the wind, at any height. The variability of the wind, on all time and space scales, is what makes its study both difficult and interesting. And the fastest scale of variation is what we call "turbulence." This is not necessarily the same thing as we mean by our everyday term, "gustiness," because under the heading of "turbulence" we include not only the observable gusts, but also fluctuations of a scale so small and a lifetime so short as to escape notice, as well as changes so slow (compared to our attention span) that they also might pass unremarked. In short, "turbulence" usually involves a huge range of scales of motion. (P. Bradshaw, in "An Introduction to Turbulence and its Measurement", Pergamon Press, 1971: "Turbulence is a three-dimensional time-dependent motion in which vortex stretching causes velocity fluctuations to spread to all wavelengths between a minimum determined by viscous forces and a maximum determined by the boundary conditions of the flow. It is the usual state of fluid motion except at low Reynolds numbers")

What are the limits to that scale range? Turbulence[1] is a property of a *flow* (not a

[1]There is a useful complementary viewpoint as to what we mean by "turbulence" and "turbulent transport" and their study, relating to one's recognition that in scientific description of a flow one will never be able to "know" the flow properties at all points and times — unless the flow of interest is "laminar", i.e. highly ordered (loosely, the Reynolds number of the flow is very small). In modern fluid mechanics, and especially in computation of flow (e.g. weather modelling) one unavoidably is forced to declare that one will describe the flow in terms of averages. The averages are most intuitively thought of as being volume averages, in a weather model over an area of about 10 km $\times$ 10 km and depth of about 0.1 km. Then, all "scales of motion" that are smeared out by the volume averaging are called "unresolved scales of motion." The study of turbulence (largely) equates to the study of these unresolved scales of motion, and their impact on the resolved properties.

property of a fluid, per se), and it is a *continuum* phenomenon, in the sense that the smallest eddies (charactieristic size λ_K) are very large compared to the mean free path l of the molecules of air, $\lambda_K \gg l$. At the other end of the scale range, the largest eddies (of the "energy-containing range") tend to be of a size reflecting the size of the "conduit" in which they arise; that size, in the atmosphere, being about equal to the depth (δ) of the "planetary boundary layer" (PBL; or Atmospheric Boundary Layer, ABL) across which wind speed decreases from a large, relatively steady (non-turbulent) value (U_G) far aloft, to zero, and across which excess heat dumped at the sunlit ground is transported by thermals and other inscrutable "transport agents." A "cascade" of (kinetic) energy occurs, from larger to smaller scales of motion, as the turbulent vortices mutually stretch and tilt each other; the result is a irregular, rotational and certainly three-dimensional field of motion, although the largest eddies (such as thermals and boundary-layer roll vortices) may have a marked coherency and a high degree of spatial symmetry.

Owing to this cascade of turbulent kinetic energy, and the action of viscosity which, working at the smallest scales of motion, damps the motion and converts kinetic energy to heat, we say that turbulence is *dissipative*, meaning that in the absence of an energy supply, it rapidly decays. It is also *diffusive*, in the sense of causing the rapid mixing of mass, momentum, and energy; but we must be clear that *convection* is the main actor: by stretching any given blob of fluid into elongated, entangled filaments, turbulent convection rapidly increases the interfacial surface area between (initially) distinguishable masses of fluid, and thereby abets an ultimate homogenization due to molecular diffusion across this ever enlarging boundary.

Finally, though we associate the notions of irregularity and randomness with a fluid in turbulent motion, and are forced to adopt (and greatly benefit by) a statistical description, all is not random: there is always a measurable temporal and spatial correlation in a "turbulent" property-field (such as velocity), and where we can identify "coherent structures" such as thermals, the coherent circulation may seem more essential and "real" than do the (mere) "fine-scale eddies" that nibble at their forms. It is considered by some that turbulence can most usefully be regarded as the random occurrence of "coherent structures." But exactly what types of structure occur, in what combinations, where and under what conditions, and in what manner interacting with each other, remains to be worked out fully.

If we had but observations alone from which to build an understanding of (patterns in) the wind, we should be greatly hampered in our ability to generalize, despite any amount of skill in the organization of data along the lines offered by dimensional analysis and similarity theory. Fortunately the conservation principles (mass, momentum and energy) provide us "governing equations," which upon manipulation yield equations for the statistics of the turbulent wind. Unfortunately however, those equations are unclosed — any set containing N of these equations involves more than N unknowns (the turbulence closure problem). This

means that working theories of turbulence are necessarily, to some extent, empirical.

With those few words of introduction, we begin the study of the wind near ground with a quick review of fluid mechanics and related concepts.

1.2 Dimensional Analysis

Dimensional analysis (Bridgman, 1922; Langhaar, 1951; Panton, 1984; Schmidt & Housen, 1995) is a tool of great power in the examination of any physical system, guiding not only the theoretician but also the design and analysis of experiments. According to Drazin and Reid (2004), the use of dimensional analysis in fluid mechanics was encouraged by Reynolds' discovery that the stability (sustained plane-parallel, or laminar, motion) of Poiseuille flow in a pipe depends only on the numerical value of a dimensionless "Reynolds number" $R_e = Ud/\nu$ (U=velocity, d=diameter, ν = kinematic viscosity of air).

It is obvious, though we may never have remarked the fact, that physical laws must be dimensionally homogeneous. If $A = B + C$ is a meaningful law of a sensible physical system, then the dimensions $[A], [B], [C]$ of the terms must be equal: a valid equation cannot (additively) mix terms having units of kilograms with terms having units of seconds. As a consequence of this commonplace, the Buckingham Pi Theorem (Buckingham, 1914; Schmidt & Housen, 1995) states that:

> "If an equation in n variables is dimensionally homogeneous with respect to m fundamental dimensions it can be expressed as a relation between $n - m$ independent dimensionless groups."
> Buckingham (1914)

1.2.1 Example: pendulum

Suppose an observer suspects or hypothesizes that the period T of a simple pendulum is controlled by its mass M, length L, and gravity g (see Fig. 1.1). The number of variables involved is $n = 4$ and we have $m = 3$ fundamental dimensions[2]. Thus the governing equation must involve only $n - m = 1$ non-dimensional variables.

Therefore s/he should seek an equation of form $N = \text{const.}$, where N is dimensionless. Only a single non-dimensional number can be formed from T, M, L, g, namely $\frac{T}{\sqrt{L/g}}$, thus

$$\boxed{\frac{T}{\sqrt{L/g}} = \text{const.}}$$

[2]Time t has not been counted by this astute thinker, for he stipulates the process under investigation is a non-decaying, purely oscillatory motion, and does not ask to know any characteristic of the motion that *might* evolve in time.

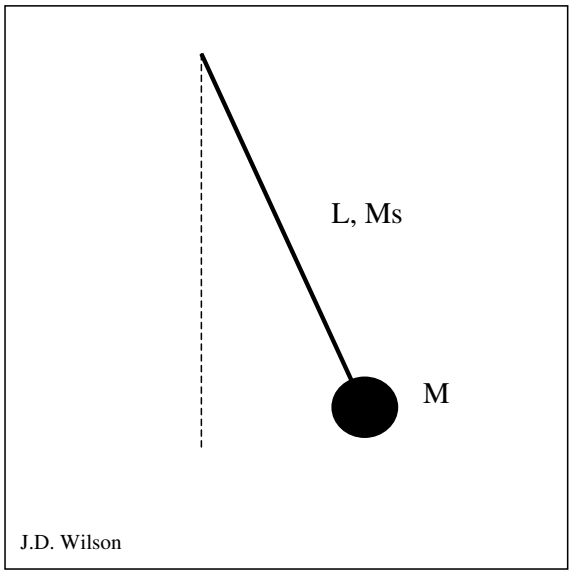


Figure 1.1: The period (T) of a pendulum in a gravity field of strength (g, $\mathrm{m\,s^{-2}}$) is suspected to depend on the masses (M, M_s) and the length of the connection (L).

We say that the "controlling timescale" is $\sqrt{L/g}$. The validity of this prediction is confirmed by a force balance, which for small amplitude motion yields the unambiguous result that $T/\sqrt{L/g} = 2\pi$.

The mass M has been found to be irrelevant. The inclusion of irrelevant variables adds work but does not invalidate the procedure. The omission of a truly relevant variable will yield a relationship that does not agree with reality.

If we add the possibility that the mass of the string M_s may be important, we now have $n = 5, m = 3$. The prediction is then:

$$\frac{T}{\sqrt{L/g}} = F\left(\frac{M}{M_s}\right)$$

and we know that $F \to 2\pi$ as $M/M_s \to \infty$.

1.2.2 Example: canopy wind profile

You would like to determine the factors that control the mean wind speed U_h at the top of a forest whose depth is h, whose planting density is $n\,[\mathrm{m^{-2}}]$ and whose foliage area density is $\alpha\,[\mathrm{m^{-1}}]$ (a constant). The foliage drag constant is c_d, dimensionless and also a constant, and you suspect U_h might be proportional to the friction velocity $u_* \equiv \sqrt[4]{\overline{u'w'}^2 + \overline{v'w'}^2}$.

We have $n = 6$ and $m = 2$ (thus $n - m = 4$). The relation sought is:

$$\frac{U_h}{u_*} = f\left(c_d, \alpha h, nh^2\right) \ . \tag{1.1}$$

How does your result change if you include as relevant variables the air density ρ_0 and temperature T_0?

1.2.3 Example: highway collision rate

Suppose you want to find a law for the collision rate $C\,[\mathrm{m}^{-1}\,\mathrm{s}^{-1}]$ in the (two) eastbound lanes of a motorway. The traffic density in these lanes is $\rho_i\,[\mathrm{m}^{-1}]$, $(i = 1, 2)$ and the means and standard deviations of the vehicle speeds are u_i, σ_i. The lane exchange rate is $\alpha\,[\mathrm{m}^{-1}\,\mathrm{s}^{-1}]$, assumed the same for both lanes (i.e. for each car moving from 1 to 2 there is another moving from 2 to 1). In this case $n = 8$, $m = 2$ and one obtains

$$\frac{C}{\alpha} = f\left(\frac{\rho_1}{\rho_2}, \frac{u_1}{u_2}, \frac{\sigma_1}{\sigma_2}, \frac{\sigma_1}{u_1}, \frac{u_1\rho_1^2}{\alpha}\right) \ . \tag{1.2}$$

Of course this result ignores many factors, e.g. state of the road surface, visibility, time of day, and much else.

Now suppose $\alpha = 0$. This would seem a bit awkward. There could still be collisions. One might instead choose as the scale for C the combination $\rho_1\rho_2\sqrt{u_1u_2}$. But again, what if one lane were empty?

1.2.4 Method of Indices

Often, finding the non-dimensional variables is easy. In case not, there are methodical ways to find the non-dimensional ratios *given* the variables involved. One such is the Method of Indices, covered by Schlichting (1968) and by Arya (1988, Section 9.3.2).

As an example, suppose that an investigator suspects the drag force F_D per unit of cross-stream length on a cylinder in a steady, uniform fluid stream depends only on the speed U of the fluid, the diameter d of the cylinder, and the density ρ and (dynamic) viscosity μ of the fluid. The first step in the Method of Indices is to assume the dependent variable F_D may be written in the form of a series, each term of which is a dimensionally correct product of independent variables:

$$F_D = \sum\nolimits_i c_i\, U^{\alpha_i}\, d^{\beta_i}\, \rho^{\gamma_i}\, \mu^{\delta_i}$$

where the c_i are dimensionless constants. Dimensional homogeneity requires that:

$$[F_D] = [U]^{\alpha_i}\ [d]^{\beta_i}\ [\rho]^{\gamma_i}\ [\mu]^{\delta_i}\ ,$$

where the bracket $[q]$ implies "units of q." This in turn implies that:

$$\begin{aligned} \text{kg}: \quad 1 &= \gamma_i + \delta_i \ , \\ \text{m}: \quad 0 &= \alpha_i + \beta_i - 3\gamma_i - \delta_i \ , \\ \text{s}: \quad -2 &= -\alpha_i - \delta_i \ . \end{aligned} \tag{1.3}$$

Here we have 3 equations in 4 unknowns, so 3 unknowns may be expressed in terms of the other one. If we choose δ_i as the single surviving unknown, then the i^{th} term may be written:

$$c_i \, U^{2-\delta_i} \, d^{1-\delta_i} \, \rho^{1-\delta_i} \, \mu^{\delta_i} = c_i \, U^2 \, \rho \, d \left(\frac{\mu}{\rho U d} \right)^{\delta_i} \ . \tag{1.4}$$

Thus:

$$\frac{F_D}{\rho \, U^2 \, d} = \sum\nolimits_i c_i \left(\frac{Ud}{\nu} \right)^{-\delta_i} = F \left(\frac{Ud}{\nu} \right) . \tag{1.5}$$

The drag, made dimensionless on the scale $\rho \, U^2 \, d$ (whose units are pressure $\times$ length, or equivalently force per metre), is a function only of the Reynolds number Ud/ν (the dynamic viscosity μ and the kinematic viscosity ν, $[\text{m}^2\text{s}^{-1}]$ are related by $\nu = \mu/\rho$). This result suggests the investigator should plot his observations in the form $F_D/(\rho U^2 d)$ versus Ud/ν in the hope of finding a universal relationship – a valuable clue. (Check for yourselves that the correct number of dimensionless ratios have arisen, ie. our result is consistent with the Pi theorem.)

Selection of the relevant parameters is the critical step. The process may rely on intuition, on limited experimental data, or, most mechanically but most reliably, on a knowledge of the governing equations and their boundary and initial conditions (even if the latter cannot be solved).

1.2.5 Example: plane Poiseuille flow

Consider a non-turbulent (i.e. steady) flow in the region $-D \le z \le D$ between two infinite smooth walls (at $z = \pm D$) separated by a distance $2D$. Assume the motion is unidirectional and oriented along the x-axis (see Fig. 1.2), such that the velocity vector $\mathbf{u}$ expressed in Cartesian coordinates is

$$\mathbf{u} = \vec{u} = u_i = (u, v, w) = (u, 0, 0) \tag{1.6}$$

where, in view of the symmetries *assumed*, $u = u(z)$. We would like to deduce this "velocity profile."

To keep things simple, let the fluid have constant density ρ and kinematic viscosity ν. Of course, by the "no slip condition," the motion u must vanish at the flow boundaries, $z = \pm D$. The "incompressible continuity equation" (proven later) reads

$$\nabla \cdot \mathbf{u} = \frac{\partial u}{\partial x} + \frac{\partial v}{\partial x} + \frac{\partial w}{\partial x} = 0 \ , \tag{1.7}$$

but tells us nothing we had not already *assumed*. However incompressibility allows us to express the u-momentum equation (one component of the Navier-Stokes equations) in "transport" (or "flux") form

$$\frac{\partial u}{\partial t} + \frac{\partial u^2}{\partial x} + \frac{\partial uv}{\partial y} + \frac{\partial uw}{\partial z} = \frac{-1}{\rho}\frac{\partial p}{\partial x} + \nu\nabla^2 u \,, \tag{1.8}$$

where t is time, p is the pressure, and ∇^2 is the Laplacian operator whose expression in Cartesian coordinates is $\nabla^2 \equiv \partial^2/\partial x^2 + \partial^2/\partial y^2 + \partial^2/\partial z^2$ (we shall soon discuss the origin of this equation, but for now, please take it as given).

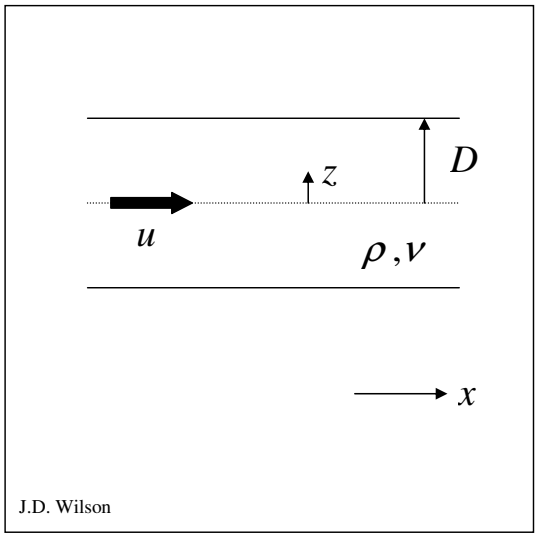


Figure 1.2: Laminar flow along the x-axis between two plates. How does velocity $u(z)$ vary with cross-stream position z?

Several terms, including the local time derivative, vanish. We can extract from the equation and boundary conditions the following variables, which it is helpful to classify in terms of their origin:

- Variables characterizing the fluid: ρ, ν
- Variables characterizing the flow: $\frac{\partial p}{\partial x}$ (the "forcing")
- Geometric variables: D (arising from the boundary conditions)
- Location variables: z
- Dependent variable of interest u

Now we have $n = 6, m = 3$ (fundamental dimensions are length, time mass). Thus we seek a relationship between $n - m = 3$ non-dimensional ratios. These ratios can be found by inspection (or if needbe, by the method of indices) to be:

$$\frac{z}{D} \ , \ \frac{uz}{\nu} \ , \ \frac{D^3}{\nu^2 \rho} \frac{\partial p}{\partial x} \tag{1.9}$$

Hence the outcome of our dimensional analysis is the prediction that

$$\frac{uz}{\nu} = F\left(\frac{D^3}{\nu^2 \rho} \frac{\partial p}{\partial x}, \frac{z}{D}\right) \ . \tag{1.10}$$

Note also that we can find other non-dimensional ratios, such as $uz/\nu \times D/z$: but these are not independent of the chosen three. The chosen three are not unique, but there can be only three and they must be independent. Finally, it would be more helpful to replace the left hand side with the ratio $(z/D)^{-1} \times uz/\nu = uD/\nu$, a step we are perfectly entitled to take for we continue to have three independent variables. Then,

$$\frac{u}{\nu/D} = f\left(\frac{D^3}{\nu^2 \rho} \frac{\partial p}{\partial x}, \frac{z}{D}\right) \ , \tag{1.11}$$

and our "scale" for the velocity is now a constant; the function $f()$ of course must differ from the earlier $F()$.

1.3 Similarity Theory

Atmospheric surface-layer flow past a fence and wind-tunnel flow over a barrier mounted on a roughened floor are two distinct flows which fall into the same class. One wonders to what extent they are "similar." The concept of "similarity" in fact has a precise meaning, for this and any other class of physical problems.

> "Complete similarity between systems A and B is said to obtain
> if the governing equations (and boundary and initial conditions),
> expressed in non-dimensional form with the use of scale factors
> (dimensionless groupings of scales for the physical variables),
> can be made identical."

1.3.1 Example: Incompressible flow of an unbounded viscous fluid past a cylinder

We consider flows A, B, C... involving fluids of different densities and viscosities, around cylinders of different radii (R). Let the cylinder(s) lie along the y-axis (see Fig. 1.3). The

governing equations, in "transport form" and expressed relative to rectangular Cartesian coordinates are:

$$\begin{aligned}
\frac{\partial u}{\partial x}+\frac{\partial v}{\partial y}+\frac{\partial w}{\partial z} &= 0 \\
\frac{\partial u}{\partial t}+\frac{\partial u^2}{\partial x}+\frac{\partial uv}{\partial y}+\frac{\partial uw}{\partial z} &= \frac{-1}{\rho}\frac{\partial p}{\partial x}+\nu\nabla^2 u \\
\frac{\partial v}{\partial t}+\frac{\partial uv}{\partial x}+\frac{\partial v^2}{\partial y}+\frac{\partial vw}{\partial z} &= \frac{-1}{\rho}\frac{\partial p}{\partial y}+\nu\nabla^2 v \\
\frac{\partial w}{\partial t}+\frac{\partial uw}{\partial x}+\frac{\partial vw}{\partial y}+\frac{\partial w^2}{\partial z} &= \frac{-1}{\rho}\frac{\partial p}{\partial z}+\nu\nabla^2 w-g\ , \qquad (1.12)
\end{aligned}$$

(again, for the time being please take these equations as given). The boundary conditions are:

$$\begin{aligned}
u=v=0 \quad &, \quad \text{on } x^2+z^2=R^2 \\
u=U_0, v=w=0, p=p_0 \quad &, \quad \text{at } z=\pm\infty \text{ and at } x=-\infty \qquad (1.13)
\end{aligned}$$

(p_0 is the "background" pressure, far from any disturbance to the flow). Note that no matter how far downstream we go, we cannot say both u and p recover because the drag on the cylinder implies momentum is removed from the flow: Force $=\frac{\partial}{\partial t}$ (momentum), so there has to be a velocity or pressure difference (or both) between $x=-\infty$ and $x=+\infty$.

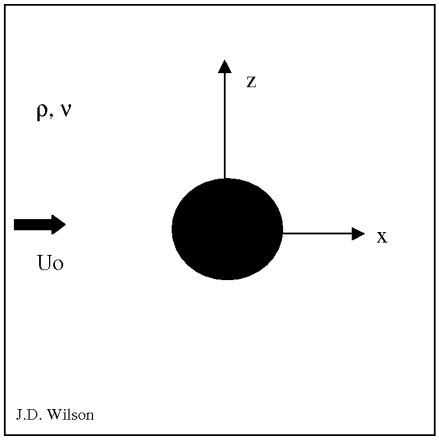


Figure 1.3: Velocity field in flow about a cylinder of radius R aligned along the y-axis.

Let us non-dimensionalize the streamwise momentum equation. The dimensions involved are length, time, mass (or alternatively length, velocity, pressure). Let us use scaling parameters U_0 for velocity, R for length, and $\rho {U_0}^2$ for pressure, so that:

- $u_* = \frac{u}{U_0}$, dimensionless velocity
- $x_* = \frac{x}{R}$ (etc.), dimensionless positions

- $p_* = \frac{p}{\rho {U_0}^2}$, dimensionless pressure
- $t_* = \frac{t}{R/U_0}$, dimensionless time

where the subscript (*) implies a dimensionless variable. Multiply through the streamwise momentum equation (which has dimensions velocity^2/length) by $R/{U_0}^2$ to obtain:

$$\frac{\partial u_*}{\partial t_*} + \frac{\partial {u_*}^2}{\partial x_*} + \frac{\partial u_* v_*}{\partial y_*} + \frac{\partial u_* w_*}{\partial z_*} = -\frac{\partial p_*}{\partial x_*} + \frac{\nu}{RU_0}\left(\frac{\partial^2 u_*}{\partial {x_*}^2} + \frac{\partial^2 u_*}{\partial {y_*}^2} + \frac{\partial^2 u_*}{\partial {z_*}^2}\right) .$$

A similar operation on the w-equation gives us a similar result, but with an additional dimensionless term $-gR/{U_0}^2$ arising from the gravitational acceleration. No new dimensionless ratios will arise from the v-equation, nor from the "no-slip and no leak" boundary conditions on the cylinder (i.e. $u_* = v_* = w_* = 0$ at ${x_*}^2 + {z_*}^2 = 1$). However the upstream and side boundary conditions yield a condition that $p_0/\rho {U_0}^2$ be constant:

$$u_* = 1,\ v_* = w_* = 0,\ p_* = \frac{p_0}{\rho U_0^2} \text{ at } \ z_* = \pm\infty \text{ and at } x_* = -\infty .$$

This can be satisfied by setting $p_0 = 0$ (we are free to do this because only pressure *gradients* appear in the governing equations – pressure is said to be a "relative variable" in flows with this character).

Now getting back to our exploration of concepts of *similarity* of flows, we may ask: *under what condition do these non-dimensional equations govern* all *of the flows*, A, B, C ....? The answer is, on the condition that the dimensionless numbers

$$\begin{aligned} R_e &= \frac{R\,U_0}{\nu} , \\ F_r &= \frac{U_0}{\sqrt{g\,R}} , \end{aligned}$$

respectively a Reynolds number and a Froude number, *are the same for each member of the set* A,B,C... *of flows*. Note that (if unrestricted) the set of flows might contain examples with very low R_e (laminar flow), very high R_e (turbulent flow), and intermediate R_e (cylinder wake near or at transition from laminar to turbulent).

1.4 Developing the Conservation Equations of Fluid Mechanics

1.4.1 Use of tensor notation

It will be convenient to make use of the notation of Cartesian tensors, e.g. the "stress tensor" τ_{ij} which you can think of as a $2-d$ matrix having nine components,

$$\tau_{ij} = \begin{pmatrix} \tau_{xx} & \tau_{xy} & \tau_{xz} \\ \tau_{yx} & \tau_{yy} & \tau_{yz} \\ \tau_{zx} & \tau_{zy} & \tau_{zz} \end{pmatrix} . \tag{1.14}$$

The stress tensor is a "rank-2 tensor" and gives the rate of transfer (per unit area) of "x-wise momentum" along the x-direction, and so on (details later).

Now what would a *first* rank tensor be? Merely a vector. For example, u_i is simply the tensor notation for the vector $\mathbf{u}$ (or $\vec{u}$) whose Cartesian components (i.e. whose projections onto three mutually perpendicular axes) are (u, v, w). There is nothing special about the symbol i. One could as easily have used j. So, $u_j = (u, v, w)$. We see that the subscripts range over $1, 2, 3$ (for x, y, z).

Each term in an equation MUST have the same tensor character: each term must have the same rank; in each term the same subscripts (assuming they are not repeated within that term) must appear – though not necessarily in the same order.

Summation Convention

If a symbolic subscript (i or j or k or whatever) appears more than once in a tensor expression, summation over (x, y, z) is implied, e.g.

$$u_i u_i \equiv u^2 + v^2 + w^2 \ ,$$

which is a "scalar." Another example is

$$u_j \frac{\partial u_i}{\partial x_j} \equiv u \frac{\partial u_i}{\partial x} + v \frac{\partial u_i}{\partial y} + w \frac{\partial u_i}{\partial z} \ ,$$

(a vector). The latter could also be expressed in vector notation as $(\mathbf{u} \cdot \nabla)\ \mathbf{u}$, but the meaning is less clear.

1.4.2 Continuum Hypothesis

The conservation equations are non-linear partial differential equations valid at a "point." To derive them one must invoke the "continuum hypothesis," which is valid provided the smallest scales of motion are much larger than the molecular mean free path; then it is meaningful to speak of values at a point, where the property values (density ρ, pressure p, etc.) are considered an average over a volume whose scale is simultaneously much larger than the mean free path, and much smaller than the smallest inhomogeneities of the motion; such properties are continuous in space.

According to the classical Kolmogorov theory (e.g. Frisch, 1995), a length scale typical of the smallest scales of motion is the "Kolmogorov length"

$$\eta_K = \left(\frac{\nu^3}{\epsilon} \right)^{\frac{1}{4}} \ , \tag{1.15}$$

where ϵ $[\mathrm{m}^2\,\mathrm{s}^{-3}]$ is the "turbulent kinetic energy dissipation rate", and ν $[\mathrm{m}^2\,\mathrm{s}^{-1}]$ is the kinematic viscosity.

The *Handbook of Physics and Chemistry* gives for the mean free paths of N_2 and O_2 (at 20° C and 1 Atmosphere) 9.29×10^{-8} m and 9.93×10^{-8} m, respectively. At this temperature, for air, $\nu = 1.5 \times 10^{-5}\ \mathrm{m^2\,s^{-1}}$. To evaluate ϵ we could simply note it is of the order of $U^2\,T^{-1}$, where U is a typical turbulent velocity, and T is a timescale for the longevity of turbulent fluctuations. If we specify $U = 1\,\mathrm{m\,s^{-1}}$ and $T = 10$ s (for example), we have $\epsilon \approx 0.1$ m (within an order of magnitude). Alternatively we could use the value predicted by theory (which we will see later) for the undisturbed atmospheric surface layer under neutral thermal stratification, namely:

$$\epsilon = \frac{{u_*}^3}{k_v z} \tag{1.16}$$

where $k_v = 0.4$ is the (dimensionless) von Karman constant, z is height above ground, and u_* is the "friction" velocity, an easily determined velocity scale (that is height-independent). Taking $u_* = 0.2\,\mathrm{m\,s^{-1}}$ and $z = 0.5$ m, this gives $\epsilon = 0.04$ m and we have for our ratio of the smallest scale of motion to the MFP

$$\frac{\eta_K}{\mathrm{MFP}} > 10^3\ .$$

This indicates we can satisfactorily define a fluid element that contains many molecules, but remains very much smaller than the smallest eddies. It is common to see the term "particle" (or "fluid particle") used to refer to a fluid element. The continuum hypothesis is not valid very high in the atmosphere (MFP very long) nor in a shock wave.

1.4.3 Diffusive and Convective Flux Densities

The term "species flux density" is attributed to the vector $\mathbf{F}$ whose instantaneous direction and magnitude at any point tell us the rate of transport of the species (mass, momentum, energy, number) per unit area along the specified direction. The following are the empirical laws describing the macroscopic (observable) consequences of microscopic (hidden, molecular or atomic) motion.

Fourier's law of conduction

The proto-typical form for many transport laws, Fourier's law relates the heat flux density $\mathbf{Q}_H$ (or $\vec{Q}_H$) at a given space-time point to the local temperature gradient:

$$\mathbf{Q}_H = -k\,\nabla T\ [\mathrm{J\,m^{-2}s^{-1}}]\ . \tag{1.17}$$

Here k is the molecular conductivity, and is related to the thermal diffusivity κ by $\kappa = (\rho\,c)^{-1}\,k$ where ρ is the density and c the specific heat capacity of the material: thus we may also write

$$\mathbf{Q}_H = -\rho\,c\,\kappa\,\nabla T \tag{1.18}$$

(it is always nice to express such equations using diffusivities, for *irrespective of the transported entity* diffusivies *always* have the unit $\mathrm{m}^2\,\mathrm{s}^{-1}$). It is especially interesting to note that according to Fourier's law, the heat flux at point **P** is fully determined by the temperature gradient at **P** (and nowhere else); that is, the heat flux is *locally determined*. When we pass on to describe *turbulent* heat (and mass and momentum) fluxes, we shall find that, despite being assigned similar names and symbols and having the same meaning (rate of transport of the entity), they *do not* have this property of being locally determined.

Fick's law of binary diffusion

The mass flux density $\mathbf{n}_A$ $[\mathrm{kg}\,\mathrm{m}^{-2}\,\mathrm{s}^{-1}]$ of species A in a binary mixture of species A and B is given by (Bird et al. 1960):

$$\mathbf{n}_A = \rho_A\,\mathbf{u} - \rho\,D_{AB}\,\nabla\left(\frac{\rho_A}{\rho}\right) \tag{1.19}$$

where $\rho = \rho_A + \rho_B$ is the total density; ρ_A/ρ is the "mass fraction" of species A; $D_{AB} = D_{BA}$ is the "mass diffusivity" $[\mathrm{m}^2\,\mathrm{s}^{-1}]$ of A in A+B and of B in A+B; and $\mathbf{u}$ is the "mass average" or bulk velocity. The first term, being due to the bulk flow, is a *convective* flux density — discussed further below. Note that diffusive mass transport cannot occur in a single species gas because $\nabla(\rho_A/\rho_A) \equiv \nabla(1) = 0$.

In a turbulent flow, except near boundaries, convective fluxes are normally overwhelmingly dominant. This can be phrased in terms of the Peclet number

$$P_e = \frac{U\,L}{D} \tag{1.20}$$

where U, L are turbuelnt velocity and length scales, and D is the (generic) molecular diffusivity. If P_e is large, then molecular fluxes can be neglected. This is not the same as saying they "do nothing." Consider a drop of ink placed in a beaker of water. If the beaker is stirred, the ink stretches out into a filament that grows increasingly long. This increases the surface area of conact between (mostly) ink and (mostly) water, such that the efficacy of molecular diffusion is increased. Ultimately the ink molecules becomes homogeneously mixed, courtesy of molecular diffusion. But (in the presence of stirring, i.e. convection) the delay between introduction of the ink and the first non-zero signal from an "ink detector" placed some way from the drop is controlled by the rate of convection.

Newton's law of viscosity and the shear stress tensor

For a "Newtonian fluid" (such as air or water[3]) it is an observed fact that the fluid above the imaginary surface z_1 exerts a tangential force (a shear stress) upon the fluid below that

[3] A "Newtonian fluid" is one for which Stokes's stress-strain relationship (given later) applies.

surface (see Fig. 1.4). This force may equally well be regarded as a tangential pull of the fluid below z_1 on the fluid above. Labelling this shearing stress τ_{xz}, because it is the force on a surface whose normal points in the z direction whereas the force is directed along the x direction, Newton's law of viscosity reads:

$$\tau_{xz} = \mu \frac{\partial u}{\partial z} \, , \tag{1.21}$$

where μ is the dynamic viscosity (depending on one's sign convention, one might insert a minus sign on the rhs). Note that τ_{xz} is the shearing force per unit area of the interface, and has the units of pressure (if we had used the kinematic viscosity ν in Eq. 1.21, then our τ_{xz} would have been the "kinematic" shear stress, with unit $\mathrm{m}^2\,\mathrm{s}^{-2}$). The velocity gradient may be termed the "strain rate," and Newton's law is thus a stress-strain relation for a fluid continuum. The component τ_{xz} is but one of nine components of τ_{ij}, the "stress tensor," which is symmetric, ie. unchanged upon exchange of the order of i, j. The shear stress can be regarded as – indeed *is* – a flux density of momentum. Its pressure units can be regarded as (dimensionally) the product [velocity $\times$ (density $\times$ velocity) = velocity $\times$ (momentum per unit volume)].

A more general expression of Newton's law of viscosity, using tensor notation and preferring the kinematic stress, is

$$\tau_{ij} = \nu \left(\frac{\partial u_i}{\partial x_j} + \frac{\partial u_j}{\partial x_i} \right) \tag{1.22}$$

where $\partial u_i / \partial x_j$ is the velocity gradient tensor

$$\frac{\partial u_i}{\partial x_j} = \begin{pmatrix} \partial u/\partial x & \partial u/\partial y & \partial u/\partial z \\ \partial v/\partial x & \partial v/\partial y & \partial v/\partial z \\ \partial w/\partial x & \partial w/\partial y & \partial w/\partial z \end{pmatrix} \, . \tag{1.23}$$

Clearly the velocity gradient tensor does not possess subscript exchange symmetry, whereas the stress tensor *does*. Thus the velocity gradient has to be "symmetrized", producing the "strain rate tensor"

$$S_{ij} = \tfrac{1}{2} \left(\frac{\partial u_i}{\partial x_j} + \frac{\partial u_j}{\partial x_i} \right) \tag{1.24}$$

in terms of which the kinematic (molecular) shear stress tensor $\tau_{ij} = 2\nu S_{ij}$. If we add $p\,\delta_{ij}$ (i.e. insert the pressure in each term on the diagonal) we have the full molecular stress tensor – these diagonal terms are said to be the "normal" (as opposed to tangential) stresses.

Fig. (1.5) shows an element of (imaginary) surface with area dS, a "face", in three different inclinations. In case (i), the face is vertical. By definition of the stress tensor, the rate of transfer of z-momentum across the face is $\tau_{xz} dS$ (units are Newtons). Similarly, the rate of transfer of x-momentum across the face of case (i) is $\tau_{xx} dS$.

In case (ii), the face is horizontal. The rate of transfer of z-momentum (or x-momentum) across the face is $\tau_{zz} dS$ (or $\tau_{zx} dS$).

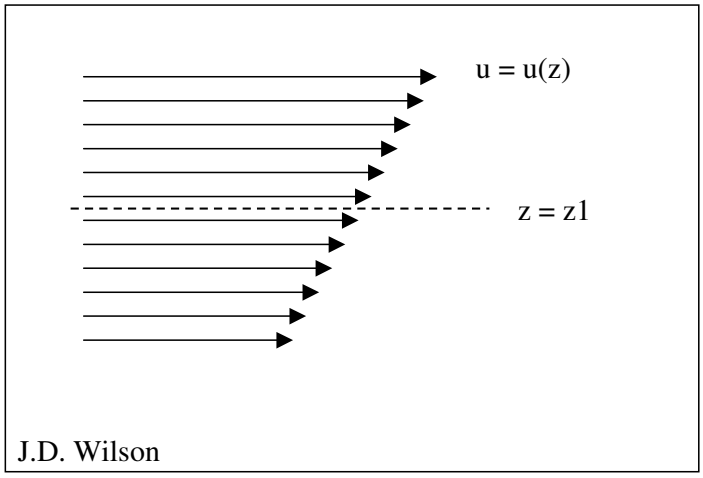


Figure 1.4: Velocity shear along the z-axis results in the layer above the plane $z = z_1$ dragging on the layer below z_1.

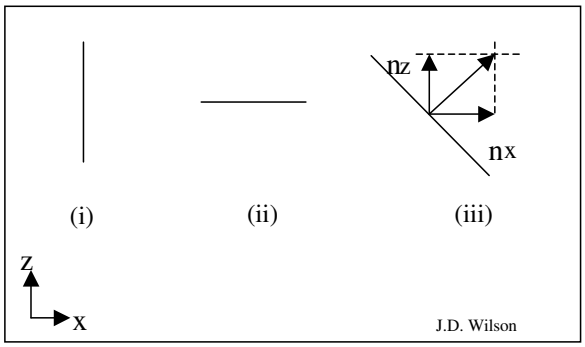


Figure 1.5: Three surface elements at differing inclinations, showing the surface normal $\mathbf{n}$ and its x- and z- components for case (iii).

In case (iii) the rate of transfer of z-momentum across the face is $(\tau_{zz} n_z + \tau_{xz} n_x)\ dS$. If we adjust the inclination in case (iii) such that $n_z \to 1, n_x \to 0$ we recover case (ii).

For a general inclination of surface element dS, the rate of transfer of z-momentum across the face is

$$(\tau_{xz} n_x + \tau_{yz} n_y + \tau_{zz} n_z)\, dS = \tau_{iz}\, n_i\, dS \equiv \tau_{zi}\, n_i\, dS\ . \tag{1.25}$$

Now we can infer that the rate of transfer of i-momentum across the (imaginary) surface (S)

of an imaginary volume (V) is therefore

$$\int_S \tau_{ij}\, n_j\, dS\ , \tag{1.26}$$

where $\mathbf{n}$ is the local normal to the surface element dS. Of course if no other forces were acting, this transfer of momentum across the walls of the volume V (a "surface force ") must result in an acceleration of the volume V.

Convective Flux Densities

A convective flux relative to a given frame of reference is simply a flux caused by a systematic bulk motion of the fluid (as distinct from and superposed over to its microscopic and randomly-oriented thermal molecular motion) which carries along an admixture of the species of interest. Consider dust, blowing in the wind: if there is no bulk movement of the air (no wind), then there is no transport (no flux of dust); and if there is no dust in the air, then (equally) there is no dust transport (no flux). So quite intuitively, the general form for a convective flux density is

$$\mathbf{F} = \mathbf{u}\,\phi\ , \tag{1.27}$$

where ϕ is the concentration [amount per unit volume] of the species of interest. (The sign convention for the fluxes will follow the sign convention for velocities). Looking back to Fick's law, we see that the convective part of the mass flux density has exactly this form.

Examples:

1. The convective flux (density) $\rho\, u_i$ of "air," whose concentration is simply the density ρ
2. The convective flux (density) $u_i\, \rho_v$ of water vapour (ρ_v being the conventional symbol for the "absolute humidity")
3. The convective flux (density) of $u_i\, n$ of neutrally-buoyant suspended particles whose number concentration is n [m^{-3}]
4. Note that if u is the "streamwise" (or "alongstream") velocity component then $\rho\, u$ is the streamwise momentum per unit volume — a concentration of momentum. So $u_i\, (\rho\, u)$ is a convective momentum flux of u-momentum: ρu^2 = flux of u-mtm along x, ρuv = flux of u-mtm along y, ρuw = flux of u-mtm along z
5. Similarly, $\rho(u^2 + v^2 + w^2)/2$ is the concentration of fluid kinetic energy, and $\rho u_i(u^2 + v^2 + w^2)/2$ is the vector convective flux density of fluid kinetic energy.

It becomes a little tedious to carry all the adjectives needed to unambiguously specify the meaning of a particular "flux density", and so they are often dropped. It is healthy to make the habit of mentally re-inserting them, from a pool of available specifiers: diffusive, convective, radiative, average, eddy, vertical, streamwise, cross-stream, turbulent...

1.4.4 The Lagrangian (Material) Derivative

Consider the trajectory (see Fig. 1.6) of a particular "fluid particle" (a "fluid particle" or "fluid element" is a volume so small as to be considered a point, yet contains vast numbers of molecules). If $X_i(t)$ labels the position of this particle[4] then its velocity is $U_i = \frac{dX_i}{dt} = (U, V, W)$. Unlike the coordinate x_i, the variable X_i is not a "field variable," ie. it makes

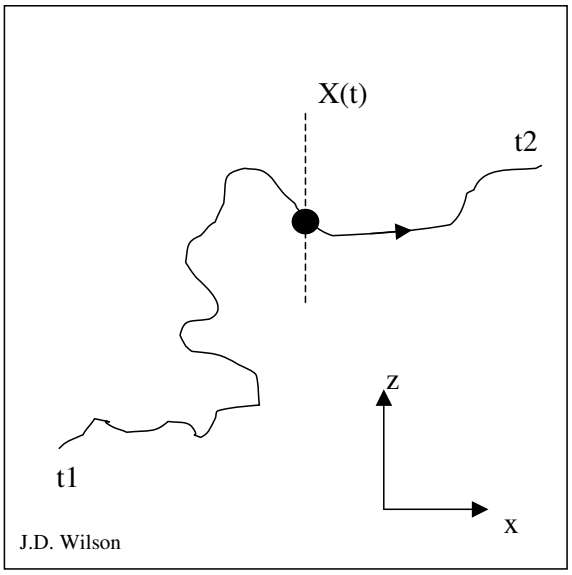


Figure 1.6: A fluid element (particle) trajectory, showing the particle at time t when its position on the x-axis is X.

no sense to write $X_i = X_i(x_i)$, for a given particle cannot be at more than one position at a given time.

Let $q = q(x_i, t)$ be any continuum property of the fluid. Then the fluid element that is at $X_i(t)$ at time t "carries" $q(X_i(t), t)$ and by the chain rule of differentiation, the change in $q = q(X_i(t), t)$ over interval dt is

$$dq = \left(\frac{\partial q}{\partial t}\right)_{x_i = X_i(t)} dt + \left(\frac{\partial q}{\partial X_i}\right)_t dX_i \tag{1.28}$$

where I have added subscripts to emphasize which variables are held constant during the partial differentiation, and (of course) the repeated subscript i implies summation. We may make the substitution $dX_i = U_i\, dt$.

[4]Note: We shall generally use capitals to distinguish a "Lagrangian" (ie. particle-following or flow-following) property.

How do we interpret $\left(\frac{\partial q}{\partial X_i}\right)_t$? If t is to be held fixed, then how can we have a dX_i, ie. a change in particle position? Well, what we want is the spatial gradient of q at time t at the location then occupied by our particle, that is, at $x_i = X_i(t)$. So we may write[5]

$$\left(\frac{\partial q}{\partial X_i}\right)_t \equiv \left(\frac{\partial q}{\partial x_i}\right)_t . \tag{1.29}$$

Upon introducing this simplification and dividing by dt we have:

$$\frac{dq}{dt} = \frac{\partial q}{\partial t} + U_i \frac{\partial q}{\partial x_i} = \frac{\partial q}{\partial t} + \mathbf{u} \cdot \nabla q \tag{1.30}$$

which expresses the "total" (or "Lagrangian" or "material") time derivative d/dt as the sum of the "local tendency" $\partial/\partial t$ and "advection". I have dropped the subscripts on the partial derivatives, for compactness.

Having introduced the Lagrangian derivative we now have the choice to express our flow equations in alternative forms (examples below).

1.4.5 Eulerian Derivation of a Generalized Conservation Equation

The following derivation applies to two-dimensional flow, but the generalisation is obvious. Let c quantify the amount of a certain property per unit volume of the fluid, having units like, for example, [kg m^{-3}]; thus defined, c is called an "intensive" variable. Consider a "control volume", an imaginary surface (see Fig. 1.7) through which the fluid freely moves, and having dimensions $(\Delta x, \Delta z)$. Both diffusion and convection are able to transfer "c" across the control volume (cv) walls[6]. And the property *may* be created or destroyed at any point, so that there is a "volumetric production rate" written symbolically as (say) Q, [kg m^{-3} s^{-1}].

At any time the total amount of c in the cv is $c(t)\Delta x \Delta z$ (where c and Q are for now considered to be average values throughout the small control volume). This – and as an aside, note that it is an "extensive" quantity – changes over time Δt by an amount $\Delta c\ \Delta x\ \Delta z$, due to internal production and net gain/loss across the walls.

Let F_x, F_z be respectively the total (convective + diffusive) flux components of c along x and along z, with units (like) [kg m^{-2} s^{-1}]. Then:

$$\begin{aligned} \Delta c \Delta x \Delta z &= \Delta z \Delta t \left[F_x(x) - F_x(x + \Delta x)\right] \\ &+ \Delta x \Delta t \left[F_z(z) - F_z(z + \Delta z)\right] + Q \Delta x \Delta z \Delta t , \end{aligned} \tag{1.31}$$

where (evidently, for this to be true) the fluxes must be considered to be average values along the (small) faces. Now divide by $\Delta x\, \Delta z\, \Delta t$ and let $(\Delta x, \Delta z, \Delta t)$ all become infinitesimal.

[5] This may not be very evident.

[6] More generally, if c quantified an energy density, we'd need to include radiative fluxes as well. Again, the generalization is easy.

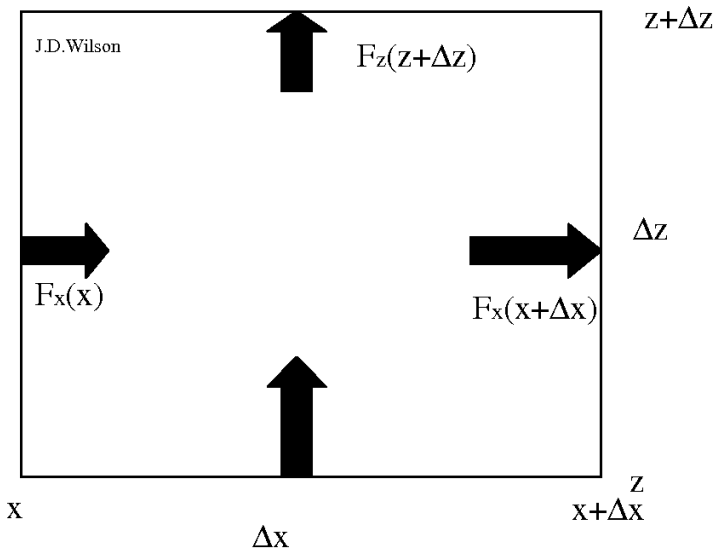


Figure 1.7: An imaginary control volume through which the fluid flows freely, and the interfacial fluxes $\mathbf{F} = (F_x, F_y, F_z)$ of "c" carried by the flow. Arrows define a convention for the direction of positive flux.

We obtain the differential equation:

$$\frac{\partial c}{\partial t} = -\frac{\partial F_x}{\partial x} - \frac{\partial F_z}{\partial z} + Q \tag{1.32}$$

or generalising to 3d,

$$\frac{\partial c}{\partial t} = -\frac{\partial F_x}{\partial x} - \frac{\partial F_y}{\partial y} - \frac{\partial F_z}{\partial z} + Q \; . \tag{1.33}$$

This conservation equation may also be written in the following elegant and *coordinate-independent* forms:

$$\frac{\partial c}{\partial t} = -\frac{\partial F_i}{\partial x_i} + Q \; , \tag{1.34}$$

and

$$\frac{\partial c}{\partial t} = -\nabla \cdot \mathbf{F} + Q \; . \tag{1.35}$$

In words, the local time rate of change ("local tendency") of the concentration of a fluid attribute is driven by the divergence of the flux of that attribute, and/or internal production/destruction.

The left hand side (LHS) is a "storage term." The first term on the right is a "transport term," so-identified because it is of the form of a spatial derivative. And the second term on the right is (obviously) a "source term." There are only these three types of terms in *all* of the transport equations[7] of fluid mechanics: or rather, this useful 3-fold classification of terms is infallible and useful.

[7] An equation like the ideal gas law $p = \rho RT$ is not a transport equation: it is a constitutive law of the system.

1.4.6 Special Cases derived from the Generalized Conservation Equation

The continuity equation

Set $c = \rho$, the air density. The flux of air is $F_i = \rho\, u_i$, and is entirely convective (refer back to the section on Fick's law to see why there is no diffusive flux). The continuity equation is:

$$\frac{\partial \rho}{\partial t} = -\nabla \cdot (\rho \mathbf{u}) \ . \tag{1.36}$$

This may be expanded to:

$$\frac{\partial \rho}{\partial t} = -\rho \nabla \cdot \mathbf{u} - \mathbf{u} \cdot \nabla \rho \ , \tag{1.37}$$

or (using the Lagrangian derivative):

$$\frac{d\rho}{dt} = -\rho \nabla \cdot \mathbf{u} \ . \tag{1.38}$$

Thus

$$\frac{1}{\rho}\frac{d\rho}{dt} = -\nabla \cdot \mathbf{u} \ . \tag{1.39}$$

$\nabla \cdot \mathbf{u} = \partial u_i / \partial x_i$, the velocity divergence, is also called the "rate of volumetric dilatation[8] of a material element," the "rate of dilatation," and the "rate of expansion." Following a fluid element, density changes only due to the divergence of the local velocity field at the present location of that element.

Water vapour conservation

Let $c = \rho_v$, the absolute humidity or vapour density [kg m^{-3}]. The equation expressing conservation of water vapour is

$$\frac{\partial \rho_v}{\partial t} = -\nabla \cdot (\mathbf{u}\, \rho_v \ - \ D_v\, \nabla \rho_v) + \ Q_v \ , \tag{1.41}$$

where the flux of water vapour has been expressed as the sum of its convective and diffusive components, and D_v is the molecular diffusivity of water vapour in dry air. We shall learn that for most practical purposes in the study of the ABL, terms involving molecular transport may be neglected because molecular fluxes (except very close to boundaries) are far smaller than convective fluxes.

[8] Substituting $\alpha = 1/\rho$ into Eq. (1.39) and carrying through the derivatives on the l.h.s., one obtains

$$\frac{1}{\alpha}\frac{d\alpha}{dt} = \nabla \cdot \mathbf{u} \ , \tag{1.40}$$

i.e. positive divergence $\nabla \cdot \mathbf{u}$ implies that the fractional rate of change of specific volume following a fluid element is positive (expansion).

Momentum equations

We can derive a heuristic equation for momentum conservation, but to do so we need to identify the appropriate fluxes and sources. Consider the conservation of vertical momentum, whose concentration is ρw. Presumably we have something like:

$$\frac{\partial \rho w}{\partial t} = -\nabla \cdot [\mathbf{u}\, \rho\, w - \nu \nabla(\rho w)\,] \ . \tag{1.42}$$

Assuming constant density, this is just:

$$\frac{\partial w}{\partial t} + \mathbf{u}\ \cdot \nabla w = \nu \nabla^2 w \tag{1.43}$$

which is not so good — we missed a body force, gravity, and a surface force, the vertical pressure gradient (the two major forces for most atmospheric flows, certainly for synoptic scale flow). We need to be more systematic.

1.4.7 Cauchy's Equation of Motion

Two types of force may act on an element of a continuous medium: "external" (or "body") forces are "volume" forces, and act throughout the volume (eg. gravity); and "internal," (or "contact" or "surface") forces act on a fluid element through its bounding surface, i.e. momentum is passed across the surface[9].

Cauchy's equation of motion, which we shall not prove, reads:

$$\rho\, \frac{du_i}{dt} = \ \rho\, F_i + \ \frac{\partial \tau_{ij}}{\partial x_j}\ . \tag{1.44}$$

Note the appearance of the two types of force: F_i is the body force per unit mass in the i-direction (normally $F_i = -g\,\delta_{3i}$ in meteorological flows), and τ_{ij} is the stress tensor, whose *divergence* appears in the equation. This equation is valid for *any* continuum, no matter how the stress tensor relates to the rate of strain (ie. to the state of motion of the continuum, specifically, the velocity derivatives).

Euler's equation of motion is obtained from Cauchy's equation by dropping all but the normal surface forces (ie. retaining only the diagonal components of the stress tensor $\tau_{11} = \tau_{22} = \tau 33 = -p$).

Problem: If $\tau_{ij} = 0, F_i = -g\delta_{3i}, u_i = (0,0,0)$ at $t = 0$, then solve Cauchy's equation of motion for $u_i(t)$. Interpret your result.

[9] As earlier shown, surface forces depend on the rate at which the fluid is strained by the velocity field present in it. We describe surface forces by means of the "stress tensor" τ_{ij}, which is symmetric: eg, τ_{xz} is the rate of transfer per unit area along the x-direction of z-momentum, and equals the rate of transfer along the z-direction of x-momentum. And for a general inclination of the surface element dS having unit normal vector $\hat{n}$, the rate of transfer of z-mtm across the face is $\tau_{iz} n_i dS$ (summation convention implied).

1.4.8 Stress-Strain Relationship for a Newtonian Fluid

The relationship between the stress tensor and the strain rate is an empirical "constitutive equation" for any continuum.

If point A with coordinates (x, y, z) moves at velocity (u, v, w) then neighbouring point B with coordinates $(x + dx, y + dy, z + dz)$ moves at a velocity whose components are

$$u + du = u + \frac{\partial u}{\partial x}dx + \frac{\partial u}{\partial y}dy + \frac{\partial u}{\partial z}dz = u + \frac{\partial u}{\partial x_j}dx_j \tag{1.45}$$

etc. Therefore the relative motion of nearby points is described by the "velocity gradient tensor," $\partial u_i/\partial x_j$.

Now the velocity gradient tensor is not symmetric, whereas the shear stress tensor τ_{ij} *is* symmetric. This is a hint that we should *not* seek a simple relationship between the two. However we can express the velocity gradient tensor as a sum of symmetric and anti-symmetric parts,

$$\frac{\partial u_i}{\partial x_j} = \frac{1}{2}\left(\frac{\partial u_i}{\partial x_j} + \frac{\partial u_j}{\partial x_i}\right) + \frac{1}{2}\left(\frac{\partial u_i}{\partial x_j} - \frac{\partial u_j}{\partial x_i}\right) . \tag{1.46}$$

The anti-symmetric part is a matrix whose diagonal elements vanish and whose off diagonal components are simply (one half) the components of the vorticity vector $\omega = \nabla \times \mathbf{u}$. The symmetric part is of more interest in the present context, and is called the "strain rate tensor,"

$$S_{ij} = \frac{1}{2}\left(\frac{\partial u_i}{\partial x_j} + \frac{\partial u_j}{\partial x_i}\right) . \tag{1.47}$$

Note that upon "contracting" the strain rate tensor (i.e. setting its two subscripts equal) we obtain its "trace"

$$S_{ii} = S_{xx} + S_{yy} + S_{zz} = \nabla \cdot \mathbf{u} , \tag{1.48}$$

a scalar, and which is simply the velocity divergence.

Schlichting (1968) shows that the most general possible motion may be decomposed as the superposition of

1. A pure translation
2. A rigid body rotation, described by components of $\Omega = \nabla \times \mathbf{u}$
3. A volumetric dilatation, described by $S_{ii} = \nabla \cdot \mathbf{u}$
4. A volume-preserving distortion in shape, described by S_{ij} with $i \neq j$

Only the last two types of motion produce deformation of a fluid element, so the strain rate tensor is also called the "deformation tensor."

For an "isotropic Newtonian fluid," one seeks a linear relationship between the stress tensor (actually, the "deviatoric stress tensor," obtained by adding the pressure p to each

term along the diagonal of the stress tensor) and the deformation tensor (ie. that part of the velocity gradient tensor which causes deformation). With the aid of Stoke's hypothesis one obtains:

$$\tau_{ij} = -p\,\delta_{ij} + \mu\left(\frac{\partial u_i}{\partial x_j} + \frac{\partial u_j}{\partial x_i} - \frac{2}{3}\,\delta_{ij}\,\frac{\partial u_k}{\partial x_k}\right) \tag{1.49}$$

where μ is the dynamic viscosity (related to the kinematic viscosity by $\mu = \rho\nu$). Substituting this expression for τ_{ij} into Cauchy's equation of motion, we obtain the Navier-Stokes equations (Batchelor, 1985, p147; Schlichting, 1968, p61; Hinze, 1975, p19; Monin & Yaglom, 1977, p29; Aris, 1989, p113).

1.5 The Navier-Stokes Equations

Neglecting gradients in the dynamic viscosity μ, the Navier-Stokes equations expressing conservation of momentum in an isotropic Newtonian fluid read

$$\rho\frac{du_i}{dt} = \rho F_i - \frac{\partial p}{\partial x_i} + \mu\nabla^2 u_i + \frac{\mu}{3}\frac{\partial}{\partial x_i}\frac{\partial u_k}{\partial x_k}\,, \tag{1.50}$$

where for incompressible flows, for which $\nabla\cdot\mathbf{u} \equiv \partial u_k/\partial x_k = 0$, the final term on the rhs vanishes. Eq.(1.50) may easily be transformed into either of the equivalent statements:

$$\frac{\partial u_i}{\partial t} + u_j\frac{\partial u_i}{\partial x_j} = F_i - \frac{1}{\rho}\frac{\partial p}{\partial x_i} + \nu\nabla^2 u_i + \frac{\nu}{3}\frac{\partial}{\partial x_i}\frac{\partial u_k}{\partial x_k} \tag{1.51}$$

(the advection form), or:

$$\frac{\partial u_i}{\partial t} + \frac{\partial}{\partial x_j}\left(u_i\,u_j\right) = F_i - \frac{1}{\rho}\frac{\partial p}{\partial x_i} + \nu\nabla^2 u_i + \frac{\nu}{3}\frac{\partial}{\partial x_i}\frac{\partial u_k}{\partial x_k} - u_i\frac{\partial u_k}{\partial x_k} \tag{1.52}$$

(the "flux" or "transport" form). To repeat, terms in the velocity divergence $\partial u_k/\partial x_k$ vanish for an incompressible flow — the relevance of this being that the wind field in the atmospheric boundary layer may be treated as being (effectively) incompressible. The body force F_i includes, for our purposes, gravity, and the Coriolis force: $F_i = -g\delta_{i3} - (\nabla\times\mathbf{u})_i$.

Exercise: classify the terms of the N/S equations as to whether they are storage, transport, or source/sink terms.

1.5.1 Exact Solutions to the Navier-Stokes Equations

Exercise 1. Obtain the velocity field $u = u(z)$ for "Plane Couette Flow" in a channel spanning $|z| \le D/2$, ie. for the flow between two infinite, parallel, rigid plates. Assume the upper plate is moving at velocity U along the x-direction relative to the lower plate. Restrict your derivation to steady, plane-parallel ($v = w = 0$), incompressible ($\rho = $ const.), "shear-driven" (ie. no pressure gradients) flow.

Exercise 2. Obtain the velocity field, the shear stress, and the volume flow rate $Q, [\mathrm{m}^3\ \mathrm{s}^{-1}]$ for laminar pipe flow: pressure-driven, steady, incompressible flow down an infinite pipe with only the axial (x) velocity component (u) non-zero. Assume the flow is in streamwise equilibrium (all x-derivatives except pressure gradient vanish).

Note: Expressed in cylindrical coordinates (radial r, alongstream x, azimuthal ϕ), the ∇^2 operator is:

$$\nabla^2 = \frac{1}{r}\frac{\partial}{\partial r}\left(r\frac{\partial}{\partial r}\right) + \frac{1}{r^2}\frac{\partial^2}{\partial \phi^2} + \frac{\partial^2}{\partial x^2} \tag{1.53}$$

(Bird *et al.*, 1960, p46; Schlichting, 1968, p11).

1.5.2 Definition of Incompressibility

"A fluid is said to be "incompressible" when the density of an element of fluid is not affected by changes in the pressure" (Batchelor, 1985, p75). But we know the density of a fluid element *can* (and does) change, with associated volumetric dilatation, as a result of heat transfer across its boundaries – otherwise there could be no temperature fluctuations. Quote: "a statement that the fluid is effectively incompressible is usually taken to imply... that the density of each mass element of the fluid remains constant" (Batchelor, 1985, p75), ie. $\rho = \text{const.}$ along trajectories, $d\rho/dt = 0$.

A gas/fluid could not transport heat if it were truly incompressible. Consider trajectories in the atmosphere near ground on a hot afternoon. A cool fluid element approaches the ground, where it is surrounded by hotter air. If it were truly incompressible, its density would remain constant as it swept down to the surface and later blew away. No heat transfer would be accomplished. In fact, even though the approximation of incompressibility is used for boundary-layer flow, what happens is that heat transfer to/from the element causes dilatation and density changes. The element gets hot (and its density decreases) at the ground and it takes this heat off with it up to cooler parts of the flow.

1.5.3 Special Classes of Flows

Before going on to the complexity of turbulent atmospheric flow, we'll note a few simple "types" of flow: these are not applicable to turbulent atmospheric winds, but are nevertheless of direct use to the micrometeorologist for related problems. For example, potential flow about a half-sphere is an unacceptable description of flow over a hill, but useful to understand the function of the "pressure-sphere" anemometer sometimes used to measure turbulent boundary-layer winds[10].

[10]The pressure sphere is a small sphere (diameter $d \sim 5 - 10$ cm) with (typically, 5) ports drilled in its surface (central port C, surrounded by ports to north N etc). Fine tubes conduct differential pressure signals $\Delta p_{E-W}, \Delta p_{N-S}, \Delta p_{NSEW-C}$ from pairs of ports to a sensitive differential pressure transducer, and all three components of the velocity vector may be inferred, making use of the theoretical surface distribution of pressure over the sphere.

Inviscid ("frictionless") flow

Here the fluid viscosity is neglected, $\nu = 0$, and one speaks of "inviscid flow."

Two-dimensional flow

The Navier-Stokes equations in two space dimensions do not "permit" the type of motion we call turbulence. However a turbulent flow field may have the property that its velocity *statistics* are invariant along one coordinate direction, in which case, owing to this symmetry, it is sometimes named a 2-dimensional flow. If velocity statistics are invariant along two coordinate directions, this may be called a 1-dimensional flow.

Non-divergent flow

As noted earlier, this means $\operatorname{div} \mathbf{u} \equiv \nabla \cdot \mathbf{u} = 0$.

Irrotational flow

Here the *vorticity* vanishes,

$$\Omega_i = (\nabla \times \mathbf{u})_i = \epsilon_{ijk} \frac{\partial u_k}{\partial x_j} = 0$$

where ϵ_{ijk} is the alternating tensor, taking values $(0, \pm 1)$

Potential flow

Irrotational and non-divergent.

1.5.4 Helmholtz Theorem

Any vector field (so any velocity field) may be expressed as (decomposed or split into) the sum of a non-divergent part plus an irrotational part:

$$\mathbf{u} = \mathbf{u}_{irr} + \mathbf{u}_{nd} \ . \tag{1.54}$$

The irrotational part $\mathbf{u}_{irr}$ may be derived from a scalar potential,

$$\mathbf{u}_{irr} = \nabla \Phi \ , \tag{1.55}$$

while $\mathbf{u}_{nd}$ may be derived from a vector potential,

$$\mathbf{u}_{nd} = \nabla \times \mathbf{\Psi} \ . \tag{1.56}$$

1.5.5 The Energy Cascade

It is an observed fact that the length of a filament of tracer in a turbulent flow (eg. ink in stirred water) increases, corresponding to loss of order. We do not expect any event to shrink the increasingly complex pattern back to the initial ordered state (blob) – though the stretching of a tracer filament in viscous flow may be reversed by reversing the motion. Bradshaw (1978) notes that any two particles in an unbounded turbulent flow experience continuing increase in their expected separation. Tennekes and Lumley (1972, p75) state: "The scale of a vortex which is stretched decreases – this is the mechanism for passing energy from larger to smaller scales."

- In turbulent flows energy is generally fed from large vortices (generated by flow interaction with the surfaces, or by buoyancy) to smaller and smaller. "The interaction of vortices (mutual stretching and tilting) leads to a chaotic process (turbulence) in which energy is fed from large vortices to smaller and smaller vortices (the energy cascade) and finally dissipated by molecular viscosity."

- "A limit to the decrease of vortex tube diameter is set when viscosity diffuses vorticity away from the axis as fast as stretching reduces the diameter" (Bradshaw 1978).

- "Kinetic energy passes from the mean flow (if a mean strain rate is present) down through vortex motions of smaller and smaller scale until it is converted into thermal internal energy by viscosity. This process is independent of viscosity except in the final stage. So the rate of energy transfer to the smallest motions is independent of viscosity. Viscosity causes dissipation but does not control its rate; the intensity and scale of the small scale motion adjust themselves so as to dissipate all the energy transfered from larger scales, and the smaller the viscosity the smaller the motions that can survive." (Bradshaw 1978).

- "One might expect that at large $R_e = Ud/\nu$ the relative magnitude of viscosity is so small that viscous effects in a flow tend to become vanishingly small. The non-linear terms in the Navier-Stokes equations counteract this threat by generating motion at scales small enough to be affected by viscosity" (Tennekes & Lumley, 1972).

- The rate of spectral energy transfer ϵ is determined by properties of the large eddies. If L is the scale of the flow domain and ΔU is the mean velocity variation across the domain, the order of magnitude of ϵ is $(\Delta U)^3/L$ (Landau & Lifshitz, p118).

Big whorls have little whorls,
Which feed on their velocity;
And little whorls have lesser whorls,

And so on to viscosity.
- L.F. Richardson, 1922.

1.5.6 Kolmogorov's theory of Locally Isotropic Turbulence

Since the large eddies obtain their energy from the mean flow (shear production) or from buoyancy effects, they will not be isotropic. (Definition of *Isotropic Turbulence*: statistical properties have no directional bias). On the other hand, at scales that are very much smaller than the scales at which energy is input to the cascade, one would expect any directional bias in the original energy feeding to have been lost. The Kolmogorov hypotheses:

1. In all turbulent flows with sufficiently high Reynolds number there will exist small scale motions whose statistics are isotropic and homogeneous and depend only on the mean TKE dissipation rate ϵ and the coefficient of viscosity ν (the universal equilibrium range)

2. In turbulent flows with large Re there is a large separation in time and space scales between the production and dissipation mechanisms. At scales that are very small compared to production end scales and very large compared to dissipation range scales, the statistical character of the fluctuations will be isotropic and homogeneous and will NOT depend on ν (the inertial subrange)

According to Hypothesis I, the characteristic scales of the largest fluctuations on which viscosity exerts an influence must be derived as a dimensional combination of ϵ [m^2 s^{-3}] and ν [m^2 s^{-1}]. Thus the Kolmogorov "inner scales" for length, velocity and time are:

$$\eta_K = \left(\nu^3/\epsilon\right)^{1/4}, \tag{1.57}$$

$$v_K = \left(\nu\epsilon\right)^{1/4}, \tag{1.58}$$

$$t_K = \eta/v_K = \sqrt{\nu/\epsilon}\,. \tag{1.59}$$

Dimensional analysis also yields a relationship for the turbulent energy spectrum $E(k)$, where k is the wavenumber [m^{-1}]. The spectrum is defined such that:

$$\int_0^\infty E(k)\,dk = \frac{1}{2}\left(\overline{u'^2} + \overline{v'^2} + \overline{w'^2}\right) \tag{1.60}$$

where $\overline{u'^2} \equiv {\sigma_u}^2$ is the variance of the streamwise velocity u (etc). In the inertial subrange, Kolmogorov's theory implies:

$$E(k) = c\,\epsilon^{2/3}\,k^{-5/3} \tag{1.61}$$

where c is a dimensionless constant, considered universal.

If we wish to express the spectrum in terms of frequency, we transform, using the relationship $E(k)dk = S(f)df$ where k is related to the "wavelength" of an eddy by $k = 2\pi/\lambda$.

Assuming that the eddy is "frozen" and drifts past our sensor at the windspeed U, the frequency of the eddy and its size λ are inter-related through U by the wave equation $U = f\lambda$. Then one finds

$$S(f) = \hat{c}\, U^{2/3}\, \epsilon^{2/3}\, f^{-5/3} \tag{1.62}$$

where $\hat{c}$ is another universal dimensionless constant.

1.6 The Boussinesq Approximation

In the Planetary Boundary-Layer there are mean gradients (strongest in the vertical) in pressure and temperature (and therefore density), as well as turbulent fluctuations p', ρ', T'. This could make it messy when we come to average the N/S eqns to get the Reynolds equations (which govern the statistics of the flow): the term $-(1/\rho)\,\nabla p$ will be troublesome — how does one average a ratio whose numerator and denominator both fluctuate? Furthermore, life would be easier if we could say that the velocity field is non-divergent (solenoidal) — for then the N/S eqns simplify.

The Boussinesq approximation is applicable to many interesting flows, including the winds in the atmospheric boundary layer. Time does not permit to cover it in the lectures; for more detail than provided here, see Batchelor (1985, p167), Businger (1984) in Nieustadt and van Dop (1984) and Calder (1968, p88).

1.6.1 Summary of the Boussinesq Approx

Density is treated as constant in time except where multiplied by gravity (ie. except as it affects buoyancy). This is valid provided:

- $U^2 \ll c^2$, where U is the turbulent velocity scale and c is the speed of sound ,
- $L \ll c^2/g$, where L is the length scale for vertical motion .

Detailed consequences are:

(i) we may make the approximation that $\nabla \cdot \mathbf{u} = 0$

(ii) we may transform the sum of the pressure-gradient and gravity terms in the Navier-Stokes equations such that

$$\frac{-1}{\rho}\frac{\partial p}{\partial x_i} - g\,\delta_{3i} \rightarrow \frac{-1}{\rho_R}\frac{\partial \tilde{p}}{\partial x_i} + g\,\frac{\tilde{T}}{T_R}\,\delta_{3i} \tag{1.63}$$

where p_R (etc.) are values for a hypothetical hydrostatic and adiabatic rest state and $\tilde{p}$ (etc.) are the departures from that state, ie. $p = p_R + \tilde{p}$, $\rho = \rho_R + \tilde{\rho}$, $T = T_R + \tilde{T}$. With these assumptions,

$$\frac{du_i}{dt} = \frac{\partial u_i}{\partial t} + \frac{\partial}{\partial x_j}\,(u_i\, u_j) = -\frac{1}{\rho_R}\,\frac{\partial \tilde{p}}{\partial x_i} + g\frac{\tilde{T}}{T_R}\delta_{3i} + \nu\,\nabla^2 u_i \tag{1.64}$$

In the following sections I drop this tilde on the instantaneous pressure and temperature departures from reference state.

Chapter 2

A brief tour of some key statistics of turbulence

Since the atmospheric properties (wind, temperature, humidity, CO_2 concentration, concentration of pollutant gases,...) near the ground undergo turbulent fluctuations, it is the universal habit to report observations in terms of statistics of the variables. In fact, we will declare that the resolved variables are to be statistics. There are three common notations for the average value of a variable, viz.

$$\overline{u}_i = \langle u_i \rangle = U_i = \frac{1}{N} \sum_1^N u_i \ , \tag{2.1}$$

and these may be used interchangeably (in these notes $\overline{u}_i$ is most common).

In micrometeorology, averaging is usually in the form of time averaging (space-averaging requires duplication of expensive and flow-disturbing instruments, gross conditions are never sufficiently invariant to permit ensemble averaging). What is shown here generalises to either of the alternatives anyway.

I'll illustrate using the alongwind (streamwise) component of velocity, $u(t)$. Presumably we will choose to average u over a period long compared to the slowest turbulent fluctuations, say 15 min, at least. This is not an instrumentation course: suffice it to say one can derive quantitative criteria for the interrelationship between instrument response time, sampling interval, and averaging duration.

2.1 Velocity Statistics

Reiterating, the variable is decomposed (Fig. 2.1) into a mean part plus a departure from the mean (or fluctuation),

$$u(t) = \overline{u} + u'(t) \ .$$

The statistics of the fluctuation u' are of interest. Its mean value $\overline{u'} = 0$. It has mean square value

$$\overline{u'^2} = \overline{(u - \overline{u})^2} = \frac{1}{N}\sum_{1}^{N} u'^2 \,, \tag{2.2}$$

which is by definition the variance of u (over the averaging interval), and is sometimes termed the "power" in u'. Note that unless the instrument used is fast enough to see (give full response to) even the fastest fluctuations in u', this statistic will not be measured properly: what we will get is the mean square value of the measured value.

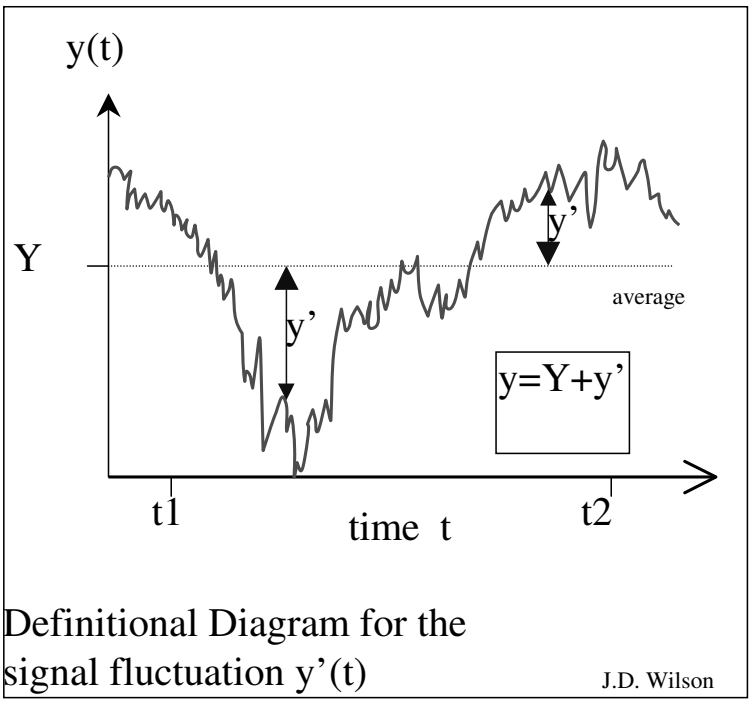


Figure 2.1: Signal: definition of the fluctuation.

In any case, from the measured mean square, the standard deviation of u is:

$$\sigma_u = \sqrt{\overline{u'^2}} \tag{2.3}$$

The third moment of u about its mean is:

$$\overline{u'^3} = \frac{1}{N}\sum_{i} u'^3 \tag{2.4}$$

and the dimensionless "skewness" based on this is:

$$Sk_u = \frac{\overline{u'^3}}{{\sigma_u}^3} \tag{2.5}$$

We could go on to define kurtosis. Or the power spectrum (Fig. 2.2) $S_{uu}(f)$ [$\mathrm{m}^2\ \mathrm{s}^{-2}/\mathrm{s}^{-1} = \mathrm{m}^2\ \mathrm{s}^{-1}$], which gives the range of frequencies (f) within which the variance in u occurs:

$$\sigma_u{}^2 = \int_0^\infty S_{uu}(f)\ df\ . \tag{2.6}$$

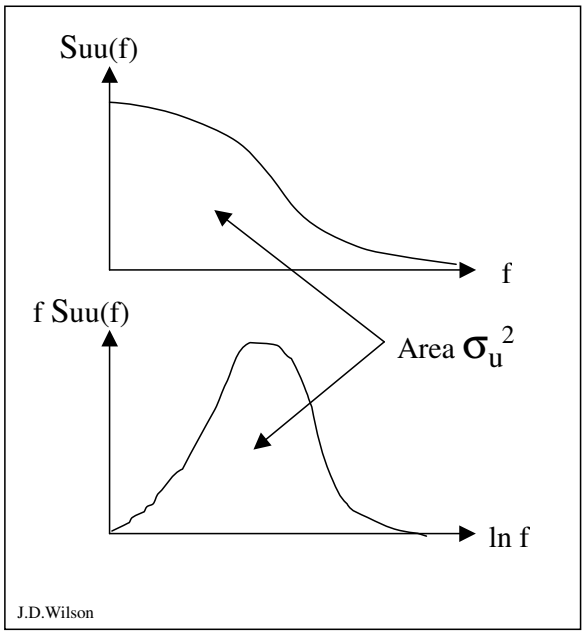


Figure 2.2: Schematic of two common plot styles for the power spectrum of the fluctuation u'. In each case, the area under the curve gives the variance.

But pausing, clearly $\overline{u}, \overline{v}, \overline{w}, \sigma_u, \sigma_v, \sigma_w$ tell us a very great deal about the flow and turbulence. If u happened to have the Gaussian (Normal) probability density function ("Gaussian turbulence")

$$f(u) = \frac{1}{\sqrt{2\pi}\ \sigma_u}\ \exp\left(-\frac{(u-\overline{u})^2}{2{\sigma_u}^2}\right) \tag{2.7}$$

then its distribution see (Fig. 2.3) would be entirely determined by the mean and standard deviation ($\overline{u}$ and σ_u).

We have as yet encountered no statistic relating to the *duration* of the velocity fluctuations, nor to whether the fluctuations in u, v, w tend to correlate with each other. Well, consider the *covariance* of two velocity fluctuation, e.g.

$$\overline{u'\ w'} = \frac{1}{N}\sum_i u'_i\ w'_i\ . \tag{2.8}$$

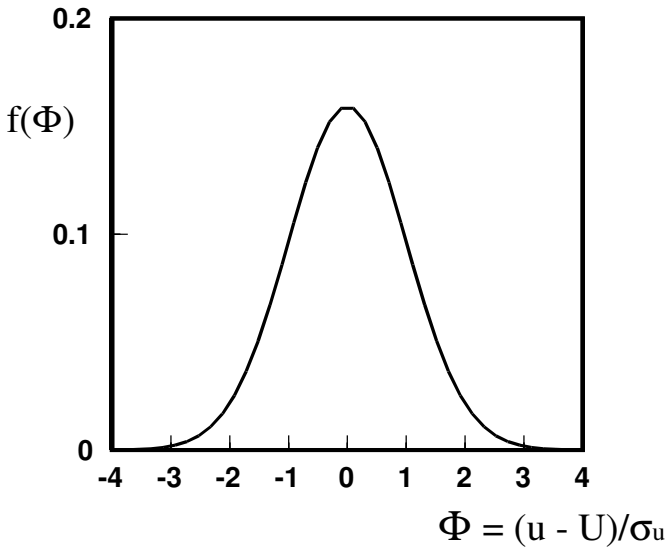


Figure 2.3: A Gaussian probability density function (pdf), $f(\Phi)$. The random variable (in this context, a velocity) has been "standardized", by subtracting the mean U and scaling upon the standard deviation σ_u: thus the normalised velocity is $\Phi = (u-U)/\sigma_u$. Area under the curve is 1.

What does it mean? If we treat the air density ρ as being constant, we may regard $\rho\overline{u'\ w'}$ as being the average value of a convective momentum flux, specifically, the average vertical flux of u-momentum. This is a vitally important statistic, for in fact the fluctuations in horizontal and vertical velocity *do* co-vary. The fluctuations in u and w are correlated, with correlation coefficient:

$$R_{uw} = \frac{\overline{u'\ w'}}{\sigma_u\ \sigma_w}\ . \tag{2.9}$$

But why? In the atmospheric boundary layer, when the wind blows down ($w' < 0$) the horizontal velocity tends to be larger than normal ($u' > 0$). This is because the downdraft brings a parcel from further aloft, where the mean horizontal velocity is greater. The resulting covariance is of great dynamical significance. It is the momentum supply to the sluggish air lying against the ground (which, remember, is a no-slip surface). The downward travelling parcels, arriving with an excess of horizontal momentum ($u' > 0$), give up this momentum to their (sluggish) environment. Conversely, rising parcels carry aloft a deficit of horizontal momentum. This is the process of turbulent momentum transport, vastly more effective than molecular (viscous) momentum transport. We'll see later that in the budget equation

for the average alongwind momentum (obtained by averaging the Navier-Stokes equation for u) the term $-\partial\overline{u'w'}/\partial z$, the vertical divergence of the rate of propagation down the vertical of x-momentum, appears on the RHS. A given layer of air in the boundary-layer has a force balance involving large-scale pressure gradient, Coriolis, and friction terms. The friction term is precisely the above "momentum flux divergence."

2.2 Some vital terminology

Stationary turbulence means that the statistics of the turbulence are not changing with time.

Homogeneous turbulence is turbulence within which statistics are independent of position. Turbulence may be (commonly is) homogeneous along one or more coordinate directions. For example, the turbulence of the undisturbed atmospheric surface layer is inhomogeneous only along the vertical coordinate.

Eulerian statistics are statistics formed from measurements made at a fixed point.

Lagrangian statistics are formed from measurements made following a trajectory.

2.3 Time scales and length scales of turbulence

What about statistics to do with the duration of fluctuations? Let us define an Eulerian two-time velocity covariance

$$C^E{}_{ww}(\mathbf{x},\tau) = \overline{w'(\mathbf{x},t)\; w'(\mathbf{x},t+\tau)} \tag{2.10}$$

where both velocities are measured at the same fixed point, but at two different times (time separation τ is often called the "lag"). Assuming stationarity of the turbulence (statistics not changing in time; which in a sense was already assumed, since t was not indicated as being one of the independent variables upon which $C^E{}_{ww}$ depends), $C^E{}_{ww}$ can be normalised by the local variance ${\sigma_w}^2$ to obtain a dimensionless autocorrelation coefficient:

$$R^E{}_{ww}(\mathbf{x},\tau) = \frac{\overline{w'(\mathbf{x},t)\; w'(\mathbf{x},t+\tau)}}{{\sigma_w}^2}\ . \tag{2.11}$$

For very short time separations ($\mathrm{Lim}_{\tau\to 0}$) $R^E{}_{ww}(\tau)$ tends to 1 (perfect correlation). For very long separations, $R^E{}_{ww}(\tau)$ tends to zero (see Fig. 2.4).

We define the "Eulerian integral timescale" as simply the area under the above graph:

$$\Gamma^E{}_{ww}(\mathbf{x}) = \int_0^\infty R^E{}_{ww}(\tau)\; d\tau \tag{2.12}$$

This is a time scale with a precise definition. It is a measurable. Qualitatively, we may interpret it as giving the typical persistence time for vertical velocity fluctuations. Measurements

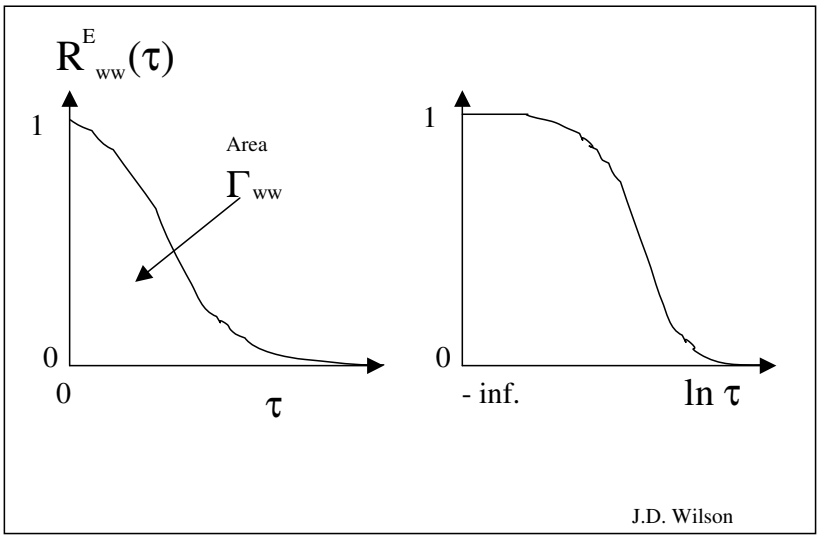


Figure 2.4: Schematic of an autocorrelation function, indicating definition of the integral timescale. Slope at infinitely small lag (τ) must vanish, since due to viscous damping there are no "infinitely fast" eddies.

show that in the undisturbed atmospheric surface layer (generally, adjacent to any flat wall) this timescale increases linearly with distance from the wall, essentially[1] vanishing "at the ground."

Now we are ready to derive governing equations for any/many of the statistics that describe turbulent flow.

[1]Why "essentially"? Because "at ground" is an oversimplification. There will always be scales at which the ground is not flat. How far are we from the ground, relative to these scales? We cannot usually define "at" the ground. If we are truly "at" a solid wall the velocity has to vanish: the "no-slip, no-leak" condition.

Chapter 3

The Reynolds Equations for Statistical Properties

3.1 Resolved and Unresolved Scales of Motion

The atmosphere is a continuum. The smallest eddies are very much larger than the molecular mean free path, so one can define each fluid "point" as being actually a small volume containing many molecules and having well-defined pressure, temperature, etc. Regarding the atmospheric continuum, meteorologists clearly never have complete (every-point, every-instant) knowledge of its state. Therefore in any description of the atmosphere (whether it be concerned with global meteorology, the meso-scale, or micro-meteorology) it is helpful to introduce the notion of "resolved" and "unresolved" scales of motion. We split any variable, say w, the vertical velocity, into resolved and unresolved parts[1], thus:

$$w = \overline{w} + w' \tag{3.1}$$

where $w(x, y, z, t)$ is the total instantaneous vertical velocity, $\overline{w}(x, y, z, t)$ is the resolved motion[2], and w' is the deviation from the resolved motion, the "unresolved motion" or "fluctuation." We then declare that we are concerned to predict/describe the "resolved fields" — of velocity $(\overline{u}, \overline{v}, \overline{w})$, of temperature $\overline{T}$, of absolute humidity $\overline{\rho}_v$, and so forth. But it is an inescapable fact that the unresolved field seldom has a negligible influence on the evolution of the resolved field.

Now what might this "resolved" field $\overline{w}$ be? In what sense is $\overline{w}$ a "filtered" field? As a first example, let us suppose we are concerned with the "synoptic scale." I consider "synoptic scale" to mean that we are working with dependent variables which have been averaged in the horizontal plane (or on a pressure surface) over distances (X, Y) large enough to average

[1] Wyngaard's (2010) textbook notation differs, viz. (p30) he prefers and uses: $\tilde{w} = W + w$.

[2] Common alternative notations for the resolved field are the upper case, W and the angle-bracket $\langle w \rangle$.

out microscale and mesoscale variations, e.g.

$$\overline{w} = \frac{1}{XY} \int_{-X/2}^{X/2} \int_{-Y/2}^{Y/2} w(x,y,z)\, dx\, dy\ . \tag{3.2}$$

Note that we could and probably should have also averaged in the vertical, since we cannot resolve all detail along *any* space dimension.

This averaging operation smooths out the sharp updrafts and downdrafts about a range of hills, or the updrafts about a sharp lake-land or ocean-land boundary, or the intense updrafts within individual cumulus clouds: and we are left with a spatially-averaged vertical velocity $\overline{w}$, which is presumably smaller in magnitude than the instantaneous, local values of w. The mean $\overline{w}$ remains a function of x, y, but it is a *smoother* function of x, y than is the raw velocity w. Detail (unresolved structure) has been "filtered" out.

Now, does the existence of an *unresolved* field w' have any effect on the evolution of $\overline{w}$? Yes. For example, a population of cumulus, though each too small to be a resolved feature (cloud width $L \ll X, Y$) as the synoptic scale level of analysis/prediction, collectively causes very efficient vertical heat and vapour transport, that results in a vertical heat flux carried by the "unresolved flow" that may even exceed the resolved heat flux $\overline{Q}_H = \rho\, c_p\, \overline{w}\, \overline{T}$.

In micrometeorology the resolved field is often obtained (in practise) as a time average over a sufficiently long interval T (in practise T ranges from about 15 minutes to an hour) to average through even the "slowest" turbulent scales" (there is a problem here because the horizontal velocity field fluctuates even on very "slow" timescales due to changes in the larger-scale weather situation). Thus we might define

$$\overline{w}(x,y,z,t,T) = \frac{1}{T} \int_{t-T}^{t} w(x,y,z,t')\, dt' \tag{3.3}$$

etc. The unresolved field is then the fluctuation from the long-time (T; say 30 minute) average. In a wind tunnel simulation of the turbulent atmospheric boundary layer, the necessary averaging time T is much shorter because the eddies in the tunnel are smaller and "faster."

Suppose for the purposes of simulating the ABL we volume average in such a way that we smooth out the smaller scales of the turbulence, but leave "resolved" the time-space dependence of eddies whose size is larger than the averaging volume (ie. we average w and other variables throughout a volume XYZ whose size might be $50 \times 50 \times 50$ [m^3]). That approach is named "Large Eddy Simulation" of turbulence (LES).

We have established that in any scale of meteorology, one should commence by settling the issue of scales to be resolved. That done, we need to find "evolution equations" (prognostic or governing equations) for the resolved field $\overline{u}$ etc., ie. we want differential equations for

$\partial\overline{u}/\partial t$, etc. And we must show, formally and quantitatively, the way in which the unresolved field affects the evolution of the resolved field. This is straightforward. We simply average the governing equations, a procedure pioneered by Reynolds (Reynolds, 1895).

3.2 Reynolds-Averaging the Governing Equations

Let f and g be arbitrary flow variables. Then the so-called "Reynolds decomposition" reads

$$\begin{aligned} f &= \overline{f} + f' \,, \\ g &= \overline{g} + g' \,. \end{aligned} \tag{3.4}$$

The Reynolds average, which is an idealization, is purported to satisfy the following four conditions:

$$\begin{aligned} \overline{f+g} &= \overline{f} + \overline{g} \,, \\ \overline{\alpha\, f} &= \alpha\, \overline{f} \,, \\ \overline{\frac{\partial f}{\partial s}} &= \frac{\partial \overline{f}}{\partial s} \,, \\ \overline{\overline{f}\, g} &= \overline{f}\, \overline{g} \,, \end{aligned} \tag{3.5}$$

where α is (any) constant and $s = x_1, x_2, x_3$ or t. To the extent that these four requirements are met, then in addition the following further properties hold true (prove for yourselves):

$$\begin{aligned} \overline{\overline{f}} &= \overline{f} \,, \\ \overline{f'} &= 0 \,, \\ \overline{\overline{f}\,\overline{g}} &= \overline{f}\,\overline{g} \,, \\ \overline{\overline{f}\, g'} &= 0 \,. \end{aligned} \tag{3.6}$$

What about practicable (real) averaging schemes, such as we might apply to real measurements (data)? The time-averaging operator defined by[3]

$$\overline{f} = \frac{1}{T} \int_{t-T}^{t} f(t')dt' \tag{3.7}$$

certainly satisfies rules $(1, 2)$. However it can be shown that rule 3 is not generally satisfied, because

$$\frac{\partial \overline{f}}{\partial t} = \overline{\frac{\partial f}{\partial t}} + \frac{f(t) - f(t-T)}{T} \,. \tag{3.8}$$

[3] If the data were discrete, i.e. a time series, the integral would be replaced by a summation.

Nevertheless provided the averaging interval T is long, this is (practically) acceptable. Rule 4 also is generally not satisfied. It can be shown that

$$\overline{\overline{f}\,\overline{g}} \approx \overline{f}\,\overline{g}\,\left[1 + \mathrm{O}\left(\frac{T}{\Gamma}\right)\right]\,, \tag{3.9}$$

where Γ is a timescale for changes in the average values $\overline{f}, \overline{g}$. Now no matter what we pick for an averaging duration T, most atmospheric statistics are not stationary. There are variations on all timescales in the temperature, for example (seconds through to millenia). If in micrometeorology we pick a half hour averaging time to ensure ${\sigma_u}^2 \equiv \overline{u'^2}$ (the variance in the fluctuation u' from the resolved velocity $\overline{u}$) includes "most" of the power in fluctuations of horizontal velocity, we inevitably miss longer scales due to mesoscale or frontal systems. An exception is the vertical velocity w. Close to ground, the spectrum of w contains no low frequency power: one cannot drive air through the ground. Thus close to ground a relatively short averaging time will cover all the power in w.

Similar comments apply to spatial averaging, which, likewise, does not exactly satisfy our rules. However, *we shall proceed to average the equations as if our averaging operation were ideal.* Anthes (1977) is more careful about this; and Wyngaard (2010) looks systematically at different types of averaging and the convergence of averages.

3.2.1 Example: Averaging the Vapour Conservation Equation

Conservation of water vapour is expressed by:

$$\frac{\partial \rho_v}{\partial t} = -\nabla \cdot \mathbf{F}_v \; + Q_v \tag{3.10}$$

where $\mathbf{F}_v$ [kg m^{-2} s^{-1}] is the (total) vector flux density of water vapour. Now because both are linear operations, the averaging operation commutes with differentiation, so that

$$\overline{\frac{\partial \rho_v}{\partial t}} = \frac{\partial \overline{\rho}_v}{\partial t}$$

and

$$\overline{\nabla \cdot \mathbf{F}_v} = \nabla \cdot \overline{\mathbf{F}}_v\,. \tag{3.11}$$

It follows that the average form of the vapour conservation equation is:

$$\frac{\partial \overline{\rho}_v}{\partial t} = -\nabla \cdot \overline{\mathbf{F}}_v + \overline{Q}_v\,. \tag{3.12}$$

We can safely neglect molecular diffusion of water vapour, so the mean flux density $\overline{\mathbf{F}}_v$ reduces to (using Cartesian coordinates):

$$\overline{\mathbf{F}}_v = (\overline{u\,\rho_v}, \overline{v\,\rho_v}, \overline{w\,\rho_v})\,. \tag{3.13}$$

Now substitute $u = \overline{u} + u'$ (etc.) and multiply to get

$$\begin{aligned} \overline{F}_{vx} &= \overline{u\ \rho_v} \\ &= \overline{(\overline{u} + u')\ (\overline{\rho_v} + \rho_v')} \\ &= \overline{u}\ \overline{\rho_v}\ +\ \overline{u'\ \rho_v'} \end{aligned} \tag{3.14}$$

and so on. Notice the emergence of two terms — a vapour flux carried by the mean flow, and the eddy flux of vapour carried by the unresolved (turbulent) flow.

We will temporarily neglect the source term Q_v (though it can easily be put back in — and needs to be, to account for evaporation/condensation with respect to any liquid water present). Then the averaged form of the equation, ie. the evolution equation for $\overline{\rho}_v$ is:

$$\begin{aligned} \frac{\partial \overline{\rho}_v}{\partial t} = &- \frac{\partial}{\partial x}\ \overline{u}\ \overline{\rho}_v - \frac{\partial}{\partial y}\ \overline{v}\ \overline{\rho}_v - \frac{\partial}{\partial z}\ \overline{w}\ \overline{\rho}_v \\ &- \frac{\partial}{\partial x}\ \overline{u'\rho_v'} - \frac{\partial}{\partial y}\ \overline{v'\rho_v'} - \frac{\partial}{\partial z}\ \overline{w'\rho_v'}\ . \end{aligned} \tag{3.15}$$

The first three terms on the rhs involve the resolved variables (and their gradients) and are simply "resolved advection," or, advection by the resolved flow, expressed in transport form. It is the second three terms that are novel. They are new unknowns, and represent the divergence of fluxes of water vapour carried by the unresolved flow. That is to say, $\overline{w'\ \rho_v'}$ is a convective vertical flux density of water vapour, carried by the unresolved flow (turbulent eddies), and so on. And if $\overline{w'\ \rho_v'}$ changes with height, there results an influence on the resolved humidity field $\overline{\rho}_v$. Whereas the governing equation for ρ_v is "closed" if we regard the velocity field and Q_v as known (1 equation in 1 unknown, ρ_v), the equation we have derived for the evolution of the resolved humidity is unclosed, for even if we know $\overline{u}, \overline{v}, \overline{w}, \overline{Q}_v$, there appear in our equation in addition to $\overline{\rho}_v$ the unknown unresolved fluxes. This proliferation of unknowns is called "the closure problem."

- In order to "close" the budget equations to get a diagnostic or predictive model for turbulence statistics, it is necessary to invoke empirical rules or equations or relationships, and we will shortly cover some of these: there are many variants of "first-order" (or "eddy viscosity/diffusivity") closure; of "higher-order" closure; and of Large Eddy Simulation

- However the unclosed set of equations may be used *interpretatively* without simplification – e.g. in the analysis of experimental data.

Returning to the main point, the form of the influence of unresolved flow upon the resolved flow is that there arise fluxes carried by the unresolved flow, and the divergences of those fluxes appear as a "forcing" in the evolution equation for the resolved flow. We have now

covered the decomposition into resolved and unresolved scales, which should be the starting point of virtually any scientific enterprise in meteorology. We have seen that the fluxes carried by the unresolved motion feed back on the resolved fields of motion and temperature and humidity, and that the evolution equation for the resolved field is unclosed, until we specify (by some means) the magnitudes of the unresolved fluxes (the closure problem).

Now we have seen that we can derive governing equations not only for the resolved fields $\overline{u}_i, \overline{T}, \overline{\rho}_v$ of velocity, temperature, humidity, etc. We can also derive governing equations for statistics like $\overline{u_i' u_j'}$ (the "kinematic" shear stress tensor or kinematic Reynolds stress) which upon simplification give us the budget equation for each element of the stress tensor, (e.g. setting $i = j = 1$)

$$\sigma_u{}^2 = \overline{u'\, u'} = \overline{u'^2}\ , \tag{3.16}$$

which is the variance of the fluctuation u' about the mean $\overline{u}$ (σ_u is just the standard deviation of the u-velocity). The equations we shall derive for some of the wind statistics are very complex, and we shall delay *interpretation* of terms to a later chapter, where we simplify the equations to the case of a stationary, horizontally-uniform ABL.

3.3 Average form of the continuity equation

Under the Boussinesq approximation our continuity equation is:

$$\nabla \cdot \mathbf{u} = \frac{\partial u_i}{\partial x_i} = \frac{\partial u}{\partial x} + \frac{\partial v}{\partial y} + \frac{\partial w}{\partial z} = 0 \tag{3.17}$$

where the vector- and tensor- expressions are coordinate-independent, while the right-most form applies to the case of Cartesian coordinates. Now if we substitute the Reynolds decomposition we have

$$\frac{\partial u_i}{\partial x_i} = \frac{\partial \overline{u}_i}{\partial x_i} + \frac{\partial u_i'}{\partial x_i} = 0\ . \tag{3.18}$$

Now average this equation to obtain

$$\overline{\frac{\partial \overline{u}_i}{\partial x_i} + \frac{\partial u_i'}{\partial x_i}} = 0\ . \tag{3.19}$$

Because the average of a sum is the sum of the averages, and because differentiation commutes with averaging, this becomes

$$\frac{\partial \overline{\overline{u}}_i}{\partial x_i} + \frac{\partial \overline{u_i'}}{\partial x_i} = 0\ , \tag{3.20}$$

which simplifies to

$$\frac{\partial \overline{u}_i}{\partial x_i} = 0\ . \tag{3.21}$$

The mean flow is non-divergent. Now subtract this result from the un-averaged form above:

$$\frac{\partial u_i'}{\partial x_i} = 0\ . \tag{3.22}$$

The instantaneous velocity field $u_i(t)$, the average velocity field $\overline{u}_i(t)$ and the velocity fluctuation field $u'_i(t)$ are *all* non-divergent.

3.4 Mean momentum equations

Begin by substituting the Reynolds decomposition into the Navier-Stokes equations (under the Boussinesq approximation, and preferably in transport form). Recall that under the Boussinesq approximation we had introduced a decomposition

$$\begin{aligned} p &= p_R + \tilde{p} \\ \rho &= \rho_R + \tilde{\rho} \\ T &= T_R + \tilde{T} \end{aligned}$$

where p_R, ρ_R, T_R define a hydrostatic and adiabatic reference state (the subscript is switched to '0' in this chapter). With the understanding that the tilde is implied, we write the momentum equations as

$$\begin{aligned} \frac{\partial(\overline{u}_i + u'_i)}{\partial t} &+ \frac{\partial}{\partial x_j}\left[\, (\overline{u}_i + u'_i)\,(\overline{u}_j + u'_j)\,\right] = \\ &- \frac{1}{\rho_0}\frac{\partial(\overline{p} + p')}{\partial x_i} + g\frac{(\overline{T} + T')}{T_0}\,\delta_{3i} + \nu\,\nabla^2(\overline{u}_i + u'_i)\,, \end{aligned} \tag{3.23}$$

in which (for example) $\overline{T}$ is the *mean* departure from the reference state, and T' the instantaneous deviation (fluctuation) from this mean departure — such that the total temperature $T = T_0 + \overline{T} + T'$.

Now we expand the non-linear term

$$(\overline{u}_i + u'_i)\,(\overline{u}_j + u'_j) = \overline{u}_i\,\overline{u}_j + u'_i\,u'_j + \overline{u}_i\,u'_j + \overline{u}_j\,u'_i \tag{3.24}$$

and substitute into eqn(3.23). Upon averaging according to the earlier rules, we obtain the mean momentum equations:

$$\frac{\partial \overline{u}_i}{\partial t} + \frac{\partial}{\partial x_j}\left(\overline{u}_i\,\overline{u}_j + \overline{u'_i\,u'_j}\right) = -\frac{1}{\rho_0}\frac{\partial \overline{p}}{\partial x_i} + g\frac{\overline{T}}{T_0}\,\delta_{3i} + \nu\,\nabla^2\overline{u}_i \tag{3.25}$$

(c.f. Wyngaard, 2010, p57, Eq. 3.7; but note the difference in notation: his full velocity is $\tilde{u}_i$ and its expansion is $\tilde{u}_i = U_i + u_i$). This is similar to the original momentum equation (1.64), but with a new term, the divergence of the Reynolds stress tensor [4].

[4] In the next chapter we shall simplify this equation for the horizontally-uniform case, in an attempt to find a law for the wind profile $\overline{u}(z)$.

3.5 Mean pressure

By the operation $\partial/\partial x_i$ on the Navier-Stokes equations we may obtain an elliptic equation for the pressure. Under the Boussinesq approximation, the result is

$$\frac{1}{\rho_0}\nabla^2 p = -\frac{\partial u_i}{\partial x_j}\frac{\partial u_j}{\partial x_i} - \frac{g}{T_0}\frac{\partial T}{\partial z} - \frac{\partial}{\partial t}\frac{\partial u_i}{\partial x_i} \tag{3.26}$$

where p, T are departures from the reference state. Upon Reynolds averaging we obtain

$$\frac{1}{\rho_0}\nabla^2 \overline{p} = -\frac{\partial \overline{u}_i}{\partial x_j}\frac{\partial \overline{u}_j}{\partial x_i} - \overline{\frac{\partial u_i'}{\partial x_j}\frac{\partial u_j'}{\partial x_i}} - \frac{g}{T_0}\frac{\partial \overline{T}}{\partial z} - \frac{\partial}{\partial t}\frac{\partial \overline{u}_i}{\partial x_i}\,. \tag{3.27}$$

The final term, according to the Boussinesq equation, must vanish; however in numerical models it may be retained, to provide a stabilizing numerical feedback between the computed velocity field and pressure field.

3.6 Reynolds stress budget

The procedure for finding higher moments of velocity (etc.) is quite tedious, but not difficult (according to Chou (1945), the Reynolds stress budget equation was first given by Keller and Friedmann in 1924). The starting point is to derive a governing equation for the *instantaneous* velocity u_i' (and in the context of other statistics, for the temperature fluctuation, and so forth). Subtracting 3.25 from 3.23 we obtain:

$$\begin{aligned}\frac{\partial u_i'}{\partial t} &+ \frac{\partial}{\partial x_j}\left(u_i'\,u_j' + \overline{u_i}\,u_j' + \overline{u_j}\,u_i' - \overline{u_i'\,u_j'}\right)\\ &= -\frac{1}{\rho_0}\frac{\partial p'}{\partial x_i} + g\frac{T'}{T_0}\,\delta_{3i} + \nu\,\nabla^2 u_i'\,.\end{aligned} \tag{3.28}$$

Now we multiply this equation by u_j' to obtain an equation for $u_j'\,\partial u_i'/\partial t$, and we create also the partner equation obtained by swopping the indices i, j. Then we add, to obtain the equation for $u_j'\,\partial u_i'/\partial t + u_i'\,\partial u_j'/\partial t = \partial(u_i'u_j')/\partial t$. Upon averaging this, we obtain the conservation equation for $\overline{u_i'u_j'}$ (c.f. Wyngaard, 2010, Eq. 8.70; Lumley & Khajeh-Nouri, 1974),

$$\begin{aligned}\frac{d\overline{u_i'u_j'}}{dt} &= \frac{\partial \overline{u_i'u_j'}}{\partial t} + \overline{u}_j\frac{\partial \overline{u_i'u_j'}}{\partial x_j}\\ &= -\overline{u_i'u_k'}\frac{\partial \overline{u}_j}{\partial x_k} - \overline{u_j'u_k'}\frac{\partial \overline{u}_i}{\partial x_k} - \overline{\left(\frac{\partial p'}{\partial x_i}u_j' + \frac{\partial p'}{\partial x_j}u_i'\right)}\\ &- \frac{\partial}{\partial x_k}\overline{u_i'u_j'u_k'} - 2\nu\,\overline{\frac{\partial u_i'}{\partial x_l}\frac{u_j'}{x_l}} + \nu\nabla^2\overline{u_i'u_j'}\,.\end{aligned} \tag{3.29}$$

For all high Reynolds number (R_e) flows, viscous transport (in general; here, the last term on the rhs) may be neglected[5].

It is common to expand the pressure term as the sum of a transport term (T_{ij}, 'pressure transport') and a 'deviatoric term'

$$\begin{aligned}\Pi_{ij} &\equiv \overline{\left(\frac{\partial p'}{\partial x_i}\, u'_j + \frac{\partial p'}{\partial x_j}\, u'_i\right)} \\ &= \frac{\partial}{\partial x_k}\left(\overline{p'\, u'_i\, \delta_{jk} + p'\, u'_j\, \delta_{ik}}\right) - \overline{p'\, \left(\frac{\partial u'_i}{\partial x_j} + \frac{\partial u'_j}{\partial x_i}\right)} \\ &= T_{ij} - P_{ij} \end{aligned} \tag{3.31}$$

where the deviatoric term (P_{ij})is called the 'pressure-strain' or 'pressure rate-of-strain' term because it involves the fluctuating velocity strain tensor. With this rearrangement, an alternative expression for the stress budget is (Hanjalic and Launder, 1972)

$$\begin{aligned}\frac{d\,\overline{u'_i u'_j}}{dt} &= -\left[\overline{u'_i u'_k}\,\frac{\partial \overline{u}_j}{\partial x_k} - \overline{u'_j u'_k}\,\frac{\partial \overline{u}_i}{\partial x_k}\right] - \left[2\nu\overline{\frac{\partial u'_i}{\partial x_k}\frac{\partial u'_j}{\partial x_k}} + \overline{p'\,\left(\frac{\partial u'_i}{\partial x_j} + \frac{\partial u'_j}{\partial x_i}\right)}\right] \\ &- \frac{\partial}{\partial x_k}\left[\overline{u'_i u'_j u'_k} - \nu\,\overline{\frac{u'_i u'_j}{\partial x_k}} + \overline{p'\,\left(u'_i\,\delta_{jk} + u'_j\,\delta_{ik}\right)}\right] \end{aligned} \tag{3.32}$$

The pressure-strain term is called the 'redistribution term' because it vanishes upon contraction ($i = j$) and so does not affect the total TKE, whereas in general it acts to equalize the partitioning of TKE into its components. Pressure transport is difficult to measure, but there have been some observations (e.g. McBean & Elliot, 1975).

3.7 Turbulent Kinetic Energy equation

If we set $i = j$ in Eq.3.29 (and divide throughout by 2) we obtain the conservation equation for the turbulent kinetic energy ("TKE"), defined

$$k = \frac{1}{2}\,\overline{u'_i u'_i} \equiv \frac{1}{2}\,\left(\overline{u'^2} + \overline{v'^2} + \overline{w'^2}\right) \tag{3.33}$$

(strictly, the turbulent kinetic energy per unit mass). The TKE equation is

$$\begin{aligned}\frac{\partial k}{\partial t} + \overline{u}_j\,\frac{\partial k}{\partial x_j} &= -\overline{u'_i u'_j}\,\frac{\partial \overline{u}_i}{\partial x_j} + \frac{g}{T_0}\,\overline{T' u'_i}\,\delta_{i3} \\ &- \frac{\partial}{\partial x_j}\left[\overline{u'_j\,\left(\tfrac{1}{2}\,u'_i u'_i\right)} + \overline{u'_j\,p'/\rho_0}\right] \\ &- \nu\,\overline{\frac{\partial u'_i}{\partial x_j}\,\frac{\partial u'_i}{\partial x_j}} + \nu\,\nabla^2 k\,. \end{aligned} \tag{3.34}$$

[5]Also, high R_e is usually considered to mean that:

$$2\nu\overline{\frac{\partial u'_i}{\partial x_k}\frac{\partial u'_j}{\partial x_k}} = \frac{2}{3}\,\delta_{ij}\,\epsilon \tag{3.30}$$

where ϵ is called the dissipation rate of turbulent kinetic energy.

The first terms on the rhs is traditionally known as "shear production." The second is the "buoyant production." The second line on the rhs gives the transport term (turbulent and pressure transport). The first term in the third line is viscous dissipation (conversion of TKE to heat by the action of viscous forces, usually called "ϵ") and the final term is molecular transport of TKE. For high Reynolds number (R_e) flows such as occur in the ABL, viscous transport may be neglected.

3.8 Temperature statistics

Under the Boussinesq approximation, the instantaneous thermodynamic energy equation is:

$$\rho_0 \, c_p \frac{\partial T}{\partial t} + \; \rho_0 \, c_p \; \frac{\partial}{\partial x_j} \; (u_j \, T) = \epsilon + \; k \, \nabla^2 T + Q_T \tag{3.35}$$

where c_p is the specific heat of air at constant pressure, k is the molecular conductivity of air, ϵ is the rate of conversion of turbulent kinetic energy (TKE) to internal energy (heat) by viscous forces (discussed later in the context of the TKE equation) and the source term Q_T absorbs condensation-evaporation (latent heat exchange) and radiative divergence (both of which we will neglect). We may regard $\rho_0 c_p T$ as the concentration of sensible heat in the airstream [J m^{-3}]. A good reference here is Calder (1968). It is easy to show that the rate of heating due to ϵ is negligibly small, so we shall drop that term too.

Then the conservation equation for the mean temperature (conservation of sensible heat) is

$$\frac{\partial \overline{T}}{\partial t} + \; \frac{\partial}{\partial x_j} \; \left(\overline{u}_j \, \overline{T} + \; \overline{u'_j \, T'} \right) = \kappa \, \nabla^2 \overline{T} \tag{3.36}$$

where $\kappa = k/(\rho_0 c_p)$ is the molecular diffusivity of air.

It is straightforward to construct an equation for the fluctuation, $\partial T'/\partial t$, which we may multiply by a velocity fluctuation u'_i. Adding this to the equation for $T' \, \partial u'_i/\partial t$, we obtain (after Reynolds decomposition and averaging) the heat-flux budget equation

$$\begin{aligned} \frac{\partial \overline{u'_i T'}}{\partial t} + \; \overline{u}_j \; \frac{\partial \overline{u'_i T'}}{\partial x_j} \;\; &= \;\; - \; \overline{u'_j T'} \; \frac{\partial \overline{u}_i}{\partial x_j} - \; \overline{u'_i u'_j} \; \frac{\partial \overline{T}}{\partial x_j} - \; \frac{\partial}{\partial x_j} \; \overline{u'_i u'_j T'} \\ &- \;\; \frac{1}{\rho_0} \; \overline{T' \; \frac{\partial p'}{\partial x_i}} + \frac{g}{T_0} \; \overline{T'^2} \; \delta_{3i} \\ &- \;\; (\nu + \; \kappa) \; \overline{\frac{\partial u'_i}{\partial x_j} \; \frac{\partial T'}{\partial x_j}} \end{aligned} \tag{3.37}$$

(c.f. Wyngaard, 2010, p99, Eq. 5.39). As with many equations in this Chapter, we shall find that upon application of symmetry assumptions they become much simpler and give us very direct insight into processes in the ABL – without any need to actually solve them (fortunately).

The budget equation for temperature variance is

$$\begin{aligned}\frac{\partial\overline{T'^2}}{\partial t} + \overline{u}_j \frac{\partial\overline{T'^2}}{\partial x_j} &= -2\,\overline{u'_j T'}\,\frac{\partial\overline{T}}{\partial x_j} - \frac{\partial}{\partial x_j}\,\overline{u'_j T'^2} \\ &\quad - 2\,k\,\overline{\frac{\partial T'}{\partial x_j}\,\frac{\partial T'}{\partial x_j}} + k\,\frac{\partial^2\overline{T'^2}}{\partial x_j\,\partial x_j}\end{aligned} \tag{3.38}$$

3.9 Statistics of a passive scalar

The Eulerian approach to the transport of a passive scalar (non-inertial, non-reacting scalar additive) hinges on the transport equations for the various moments of concentration c.

We decompose the scalar concentration $c = \overline{c} + c'$. By the same procedure as applied above for temperature, the equation for mean scalar concentration is

$$\frac{\partial\overline{c}}{\partial t} + \overline{u}_j \frac{\partial\overline{c}}{\partial x_j} = -\frac{\partial}{\partial x_j}\left(\overline{u'_j\,c'} - k_c\,\frac{\partial\overline{c}}{\partial x_j}\right) . \tag{3.39}$$

This is in advection form, but readily converted to flux form; and it has been assumed that there is no internal (volumetric) source; k_c is the molecular diffusivity of the species in air.

The scalar flux budget equation is

$$\begin{aligned}\frac{\partial\overline{u'_i c'}}{\partial t} + \overline{u}_j \frac{\partial\overline{u'_i c'}}{\partial x_j} &= -\overline{u'_j c'}\,\frac{\partial\overline{u}_i}{\partial x_j} - \overline{u'_i u'_j}\,\frac{\partial\overline{c}}{\partial x_j} - \frac{\partial}{\partial x_j}\,\overline{u'_i u'_j c'} \\ &\quad - \frac{1}{\rho_0}\overline{c'\,\frac{\partial p'}{\partial x_i}} + \nu\,\overline{c'\,\frac{\partial^2 u'_i}{\partial x_j\,\partial x_j}} \\ &\quad + k_c\,\overline{u'_i\,\frac{\partial^2 c'}{\partial x_j\,\partial x_j}} + \frac{g}{T_0}\,\overline{c'T'}\,\delta_{3i}\end{aligned} \tag{3.40}$$

(c.f. Wyngaard, 2010, p99, Eq. 5.39) and the scalar variance equation

$$\begin{aligned}\frac{\partial\overline{c'^2}}{\partial t} + \overline{u}_j \frac{\partial\overline{c'^2}}{\partial x_j} &= -2\,\overline{u'_j c'}\,\frac{\partial\overline{c}}{\partial x_j} - \frac{\partial}{\partial x_j}\,\overline{u'_j c'^2} \\ &\quad - 2\,k_c\,\overline{\frac{\partial c'}{\partial x_j}\,\frac{\partial c'}{\partial x_j}} + k_c\,\frac{\partial^2\overline{c'^2}}{\partial x_j\,\partial x_j} .\end{aligned} \tag{3.41}$$

The first term on the rhs is called "free air production"; a mass flux along a concentration gradient results in the production of concentration variance. The second term is "turbulent transport". The molecular transport term $k_c\,\nabla^2\overline{c'^2}$ is seldom important (except very near a boundary). The term which involves k_c and the covariance of gradients in instantaneous concentration is the main destruction term for scalar variance. We must not lose sight of what scalar variance is – a measure of the *variability* in concentration, so a crucial (important) descriptor in some contexts. The mean level of a contaminant may not be dangerous, but if the peaks exceed a threshold, combustion may occur, or a human may be poisoned.

We could go on to create budget equations for higher moments. Note though, that if the pdf for concentration were Gaussian, equations for the evolution of $\overline{c}$ and $\overline{c'^2} \equiv {\sigma_c}^2$ would suffice to fully determine it. Of course, these equations are unclosed. And note that they involve *joint* statistics of velocity and concentration.

Chapter 4

Preliminary insights for case of a horizontally-homogeneous ABL

Before thinking about the full complexity of ABL flow over inhomogeneous terrain and cover, it is imperative to understand ABL flow in the "undisturbed case," when the flow has travelled for a long distance over an unvarying lower boundary. This is a good point to introduce the concept (idealization) of a horizontally-homogeneous flow:

Horizontally-homogeneous flow: Velocity statistics are independent of location on horizontal planes, but may vary along the vertical coordinate. We shall often use the shorthand hh_ABL to indicate a horizontally-homogeneous ABL.

In boundary-layers in general, an "inner layer" (known variously as the "wall region" or the "surface layer") and an "outer layer" are recognised (Tennekes & Lumley, 1972, p147; Hinze, 1975, p618; Monin & Yaglom, 1977, p298). This is because it is expected that in a thin region near the wall the flow will be controlled by small length scales (ν/U for a smooth wall, U being a scale for velocity fluctuations; or the height of the roughness elements, for a rough wall). But far from the wall, the depth δ of the entire layer will be the controlling length scale. This expectation is founded on the principle of "Reynolds number similarity" — that for sufficiently large $R_e = U\delta/\nu$, the direct effect of viscosity is probably restricted to a shallow layer of strong velocity gradients adjacent to the wall, while outside that layer, the mean velocity does not depend on ν or R_e.

4.1 Mean Velocity

We can make $\overline{v} = 0$ at ground by choice of the coordinate orientation, but due to turning of the mean wind with height (due to the Coriolis terms), $\overline{v}$ will not vanish aloft (this turning is often neglected in the "surface-layer"). For now we will define the surface layer ("ASL") to be a shallow layer adjacent to ground, with depth of order $\delta/10$ where δ is the depth of the entire PBL; in this ASL the vertical gradients in windspeed, temperature, and humidity are

very strong, but across the ASL the changes in the corresponding vertical fluxes are small relative to their surface values.

4.1.1 Mean vertical velocity

The mean velocity field being non-divergent, clearly

$$\frac{\partial \overline{w}}{\partial z} = -\frac{\partial \overline{u}}{\partial x} - \frac{\partial \overline{y}}{\partial y} \, .$$

Then because (by the no leak condition) vertical velocity vanishes at the surface, it follows at once that in horizontally-homogeneous flow over a flat surface the mean vertical velocity $\overline{w} = 0$.

However we can learn something useful from the vertical momentum equation, despite the fact we already know $\overline{w} = 0$. Under the assumption of horizontal uniformity (which allows us to set horizontal derivatives to zero where they operate on an averaged quantity), and neglecting viscous momentum fluxes, this is:

$$\frac{\partial \overline{w'^2}}{\partial z} = -\frac{1}{\rho_0}\frac{\partial \overline{p}}{\partial z} + g\frac{\overline{T}}{T_0} \tag{4.1}$$

where $\overline{p}$ is the mean hydrostatic departure and $\overline{T}$ the mean departure from adiabatic reference state. Now differentiating w.r.t. x (and reversing the order of differentiation on p) we obtain:

$$\frac{\partial}{\partial z}\frac{\partial \overline{p}}{\partial x} = \frac{\partial}{\partial x}\left(\rho_0 \, g \, \frac{\overline{T}}{T_0} - \, \rho_0 \, \frac{\partial \overline{w'^2}}{\partial z}\right) \tag{4.2}$$

By definition of horizontal uniformity, the rhs vanishes. Similarly, differentiating by y we would conclude $\partial\overline{p}/\partial y$ does not change with height. So there is no vertical variation of the mean horizontal pressure gradient. The synoptic-scale pressure gradient is impressed upon the PBL. Note however that any flow disturbance (building, hill, fence...) will result in *local* mean pressure gradients which *are* height-dependent. Note also that we have made a critical assumption — horizontal uniformity. Horizontal non-uniformity is probably the rule rather than the exception, even in uniform terrain. Stubbley and Rooney (1986) argue that PBL structure is very sensitive to "baroclinicity" (height-dependence of horizontal pressure gradient).

4.1.2 Mean horizontal velocity

Now we turn to the mean alongwind velocity. Neglecting viscous momentum fluxes the governing equation for mean alongwind momentum is

$$\frac{\partial \overline{u}}{\partial t} + \overline{u}\,\frac{\partial \overline{u}}{\partial x} + \overline{v}\,\frac{\partial \overline{u}}{\partial y} + \overline{w}\,\frac{\partial \overline{u}}{\partial z} \;\; = \;\; -\frac{1}{\rho}\frac{\partial \overline{p}}{\partial x} - \frac{\partial \overline{u'^2}}{\partial x} - \frac{\partial \overline{u'\,w'}}{\partial z} + f\overline{v} \, . \tag{4.3}$$

The assumption of stationarity lets us set the local time derivative to zero. The assumption of horizontal uniformity again entitles us to set horizontal derivatives to zero (remember though, only where they operate on an averaged quantity) except in the case of the alongwind pressure-gradient: for the latter is non-zero, and is equal to the synoptic-scale pressure gradient (or its component along our chosen x-axis) which is imposed on the boundary-layer. So, the equation reduces to

$$\frac{\partial \overline{u'w'}}{\partial z} = -\frac{1}{\rho}\frac{\partial \overline{p}}{\partial x} + f\overline{v} \; . \tag{4.4}$$

The divergence of the shear stress $\Delta\overline{u'w'}/\Delta z$ across a layer Δz is balanced by the pressure-gradient and Coriolis forces. We will see below that $\overline{u'w'}$ has its largest vertical gradient at ground — but nevertheless it is usual to call that layer adjacent to ground over which it changes by less than about 10% the "constant stress layer" (we return to this below).

At the top of the PBL, by definition there is no turbulence and we may assume the flow to be steady and (on the micro-meteorological scale) horizontally-uniform. Then if we neglect viscous friction, the vector force balance is:

$$0 = -\frac{1}{\rho}\nabla p - 2\mathbf{\Omega} \times \mathbf{u} \tag{4.5}$$

($\mathbf{\Omega}$ is the angular velocity of the earth, with a magnitude of about $2\pi/(24{\times}3600)$ [radians s^{-1}]). Since $\mathbf{\Omega} \times \mathbf{u}$ is parallel to ∇p, $\mathbf{u}$ must be perpendicular to ∇p.

Back to why I wanted to introduce the "free atmosphere" momentum equations: we may conveniently use the components of the Geostrophic wind

$$\begin{aligned} U_g &= -\frac{1}{\rho f}\frac{\partial \overline{p}}{\partial y} \\ V_g &= \frac{1}{\rho f}\frac{\partial \overline{p}}{\partial x} \end{aligned} \tag{4.6}$$

to replace the (height-independent) horizontal pressure gradients within the governing equations for the PBL

$$\begin{aligned} 0 &= -\frac{\partial \overline{u'w'}}{\partial z} + f(\overline{v} - V_g) \; , \\ 0 &= -\frac{\partial \overline{v'w'}}{\partial z} - f(\overline{u} - U_g) \; . \end{aligned} \tag{4.7}$$

These equations show that the shear stress gradient in the PBL is controlled by the Geostrophic deficit. Since $\overline{v} = 0$ at ground (by choice of coordinates), the geostrophic deficit $\overline{v} - V_g$ is a maximum at ground: so $\overline{u'w'}$ varies with height most rapidly at ground.

But surely $w = \overline{w} = w' = 0$ at ground? Yes, though exactly where ground "is" on the z-axis is loosely defined. There is always a layer adjacent to ground, an "unresolved basal

layer" (Wilson & Flesch, 1993), across which velocity statistics drop rapidly as the ground is approached. This layer might constitute a forest canopy, or the layer of grass. Optionally, we could attempt to resolve the flow in this layer — usually a difficult task.

The accompanying figure shows the variation of shear stress with height through the PBL, into the surface layer, and through a forest.

4.1.3 First-order closures

The above equations are unclosed. But if we could specify the shear stresses in terms of the velocities $\overline{u}, \overline{v}$ we would then have a pair of 2^{nd}-order differential equations in two unknowns, $\overline{u}, \overline{v}$.

The Boussinesq eddy-viscosity (K) closure

$$\overline{u_i' u_j'} = -K \left(\frac{\partial \overline{u_i}}{\partial x_j} + \frac{\partial \overline{u_j}}{\partial x_i} \right) + \frac{2}{3} k \, \delta_{ij} \tag{4.8}$$

is often a useful approximation for the shearing stresses, e.g.

$$\overline{u'w'} = -K \left(\frac{\partial \overline{u}}{\partial z} + \frac{\partial \overline{w}}{\partial x} \right), \tag{4.9}$$

but is less satisfactory with respect to normal stresses, and so adjustments (that violate the ij-symmetry) are often introduced. K [$\mathrm{m^2\ s^{-1}}$] is called the "eddy viscosity" (or eddy diffusivity for momentum, or exchange coefficient).

Assuming horizontal homogeneity, the shear stress is expressed

$$\overline{u'w'} = -K \frac{\partial \overline{u}}{\partial z} \, . \tag{4.10}$$

It is to be emphasized that this is only a *model* (it can be taken to define K), by analogy with Newton's law of viscosity for momentum exchange via molecular collisions; but K vastly exceeds the molecular viscosity ν.

Analytical Wind Profiles for the hh-ABL

Suppose the Geostrophic deficit equations are closed by the adoption of K-theory (with a constant K) to model the shear stresses. And suppose we adopt as the boundary conditions

$$\begin{aligned} \overline{u} = U_g, \overline{v} = V_g \quad \text{at} \quad z = \infty \, , \\ \overline{u} = 0, \overline{v} = 0 \quad \text{at} \quad z = 0 \, . \end{aligned} \tag{4.11}$$

An analytical solution is easily found, the classical "Ekman spiral." Because in reality $K = K(z)$ is a strong function of height (especially in the surface layer), the Ekman solution is unrealistic. However a very useful "2-layer" solution can be obtained (Bergstrom, 1986), by

matching at height $z = h$ an outer Ekman layer with an inner surface layer. In the surface layer, variation of wind direction with height is neglected ($\overline{v} = 0$ throughout the surface layer), and the mean wind $\overline{u}$ is given by the Monin-Obukhov similarity theory (to be covered later). Wilson and Flesch (2004) have revised this idea so that the upper boundary condition is applied at a finite depth δ, the depth of the boundary-layer. Needless to say, one could also add a forest (or crop) canopy layer, matched at canopy height h_c to the MO surface layer wind, to obtain a 3-layer model resolving the wind in the canopy. To date, this has not been done.

4.2 The hh-ASL identified as a constant flux layer

Let's put in some numbers for the rate of variation of the shear stress near ground. Assume the Coriolis parameter $f = 10^{-4}\mathrm{s}^{-1}$ (a mid latitude value) and $V_g = 5\ \mathrm{m\,s}^{-1}$. Then

$$\frac{\partial \overline{u'w'}}{\partial z} = -fV_g = 5\ \times\ 10^{-4}\ . \tag{4.12}$$

A typical surface value of $-\overline{u'w'} = {u_*}^2$ is of order 0.1. Over a height of 20 m the change in the stress is about 10% of such a surface value. Thus, loosely, we may talk of a "constant stress layer" at the base of the PBL. Similarly, consider the mean temperature equation for a horizontally-homogeneous PBL ("hh-PBL"),

$$\rho\ c_p \frac{\partial \overline{T}}{\partial t} = -\rho\ c_p \frac{\partial \overline{w'T'}}{\partial z} = -\frac{\partial Q_H}{\partial z}\ . \tag{4.13}$$

Assume $\overline{T}$ is changing by about $+4^{\mathrm{o}}$K/hour ($10^{-3}\,\mathrm{K\,s}^{-1}$), that $\rho \approx 1[\mathrm{kg\ m}^{-3}]$, and note that $c_p \approx 1000\,[\mathrm{J\ kg}^{-1}\ \mathrm{K}^{-1}]$. Then, $LHS = RHS \approx 1$. Thus the sensible heat flux Q_H decreases with increasing height at a rate of about $1\mathrm{W\,m}^{-2}$ per metre. Given that Q_H is likely of order $100\,\mathrm{W\,m}^{-2}$, and can be measured directly (by eddy correlation, or other means) only to within a likely error of order 5%, even this (atypically large) variation with height is immeasurable.

We can thus speak of the horizontally-uniform ASL as a "constant heat flux layer," and, since the shear stress is also a flux (of momentum), we generalize and call the horizontally-uniform ASL a "constant flux layer." Here "constant" (flux layer) simply means that the *fractional* variation of the fluxes across a uniform ASL is small. The idea of the surface layer as being a "constant flux layer" is a fiction – but a convenient one.

4.3 Surface drag

The drag of the ground on the atmosphere is commonly and conveniently quantified by the 'surface' values (height $z \to 0$) of the turbulent shear stresses

$$\begin{aligned} \tau_{0x} &= -\rho \lim_{z\to 0} \overline{u'\, w'} \\ \tau_{0y} &= -\rho \lim_{z\to 0} \overline{v'\, w'} \end{aligned} \tag{4.14}$$

where as always ρ is air density, (u', v', w') are the turbulent velocity fluctuations, and the overline denotes a time average; the friction velocity u_{*0} is defined by

$$\rho^2\, u_{*0}^4 = \tau_{0x}^2 + \tau_{0y}^2 \tag{4.15}$$

(see Weber, 1999, for a discussion of nuances in the definition of the friction velocity).

Note that the surface shear stress need not necessarily be parallel to the mean wind direction. However it is common to assume that the only non-zero stress component on ground is parallel to the mean wind direction (ie. parallel to our x axis, assuming our chosen orientation for the axes is that $\overline{v} = 0$ at some reference height near ground). Then the friction velocity is simply

$$u_* = \sqrt{-\overline{u'w'}}\ . \tag{4.16}$$

4.4 Friction velocity and other wind statistics

We will see that in the surface layer the turbulent kinetic energy per unit mass (to be denoted TKE or simply k) is proportional to ${u_*}^2$, and that likewise $\sigma_w \propto u_*$. Indeed, all velocity statistics in the undisturbed surface layer scale with u_*.

4.5 Neutral wind profile for the surface layer via K-theory and dimensional reasoning

From the $\overline{u}$-momentum balance we deduced $\overline{u'w'}$ can be regarded as height-independent within a surface-layer adjacent to ground. Now, what does constancy of $\overline{u'w'}$ tell us about the mean wind, $\overline{u}$? Nothing. So far, we only know know $\overline{u} = 0$ at ground; and we know it increases aloft.

To obtain a formula for $\overline{u}(z)$ for the neutrally-stratified and horizontally-uniform surface layer, we will turn to the closure assumption (tentatively assumed useful), which relates the velocity *gradient* to the shear stress:

$$\overline{u'w'} = -K_m\, \frac{\partial \overline{u}}{\partial z}\ . \tag{4.17}$$

This model has already been introduced (but notice that the subscript 'm' has been added to the eddy viscosity, identifying this as the eddy diffusivity for momentum, whereas we will also have eddy diffusivites for heat K_h, for water vapour K_v, and so forth). To recapitulate, K-theory was introduced by the pioneers as a model for the turbulent convective fluxes, which they recognised as needing to be known but were unable to measure. K-theory *represents* turbulent convection *as if* it were a diffusive process, i.e. it models turbulent convection by analogy to molecular diffusion. It is therefore fundamentally wrong – but it works, in simple situations.

Now the eddy viscosity $K_m[\mathrm{m}^2\ \mathrm{s}^{-1}]$ is (dimensionally) the product of a velocity scale times a length scale. It has (qualitatively) to do with the efficiency of the turbulence (ie. the unresolved scales of motion) in causing down-gradient transfer of momentum. So why not choose σ_w as the velocity scale? No vertical motion – no mixing. Also, $\sigma_w \propto u_*$ and u_* relates to TKE; so we can pick either u_* or σ_w as our velocity scale. It is conventional to pick u_*.

For a length scale, remember that observations show the integral timescale Γ_{ww} increases linearly with distance from ground (this is only true quite close to ground: it does not increase indefinitely). This suggests using as our length scale a multiple of z, say $k_v z$ (where k_v is called the von Karman constant). Doing so, we have:

$$-{u_*}^2 = -k_v\ z\ u_* \frac{\partial \overline{u}}{\partial z} \tag{4.18}$$

or rearranging:

$$\frac{\partial \overline{u}}{\partial z} = \frac{u_*}{k_v\ z}\ . \tag{4.19}$$

If we define a constant of integration z_0 (the "surface roughness length") as the height where $\overline{u} = 0$, we can integrate to get the "log wind profile"

$$\overline{u}(z) = \frac{u_*}{k_v}\ \ln\left(\frac{z}{z_0}\right)\ . \tag{4.20}$$

Experiments show that with $k_v = 0.4$ this is a good description of the mean wind in the undisturbed surface-layer under neutral stratification, provided we are not too close to ground ($z \gg z_0$). This of course prohibits use of the log profile within and close above crops. We will later see how the Monin-Obukhov similarity theory generalises our finding for the stratified (but still horizontally-uniform) surface layer.

The surface roughness length correlates crudely with surface roughness. For tall canopies (height h_c), for example, $z_0 \sim h_c/10$. For typical pasture, z_0 is on the order of 0.01 m. Note that the wind speed aloft is rather insensitive to z_0 (due to its effect being through $-\ln(z_0)$) except for very small z, where the log law is anyway invalid (though usually used anyway, because we can't do better without a lot of trouble). And by measuring the mean wind $\overline{u}$ at

two (but preferably several) heights we can deduce the friction velocity from the slope:

$$\frac{\Delta \overline{u}}{\Delta \ln(z)} = \frac{u_*}{k_v} \tag{4.21}$$

(and we can obtain z_0 from the $\overline{u} = 0$ intercept). Thus, bearing in mind that once we know u_* we can infer many other properties of the surface layer (surface drag τ, turbulence TKE, σ_w, etc.), a very great deal of information can be obtained simply by measuring the mean wind profile.
Remember: the log law is severely limited in its validity.

4.6 Mean humidity

Again assuming horizontal uniformity, neglecting molecular fluxes, and assuming no sources or sinks (no condensation/evapn) the water vapour budget equation reduces to:

$$\frac{\partial \overline{\rho}_v}{\partial t} = -\frac{\partial \overline{w'\rho'_v}}{\partial z} \ . \tag{4.22}$$

This tells us that under horizontally uniform conditions (ie. in the absence of advection), the humidity of a layer changes in time only if there is a difference in the turbulent humidity flux $\overline{w'\rho'_v}$ across the layer. Since the rate of change of humidity is observed to be small, it is common to adopt the approximation of stationarity (though it is not strictly valid) and conclude that the surface-layer is a layer across which the flux of water-vapour is constant (generalising, to speak of a constant flux layer). Then adopting K-theory allows us to find the vertical gradient in humidity in terms of the vapour flux,

$$E = \overline{w'\rho'_v} = -K_v \frac{\partial \overline{\rho}_v}{\partial z} \ . \tag{4.23}$$

Now assume $K_v = K_m = k_v u_* z$ (identity of K_m and K_v has been suggested experimentally by some experiments, in neutral stratification, but there is no intuitive or obvious reason for it necessarily to be the case. Note that the value of K_m/K_v in the neutral limit is by definition the "turbulent Schmidt number" for water vapour, S_{cv}). We easily deduce a log law:

$$\overline{\rho}_v = \overline{\rho}_{v0} - \frac{E}{k_v \ u_*} \ln\left(\frac{z}{z_{ov}}\right) \tag{4.24}$$

General conclusion? We neglect the small height dependence of the evaporative flux in the hh-ASL, ie. consider E constant. Near ground, the eddy diffusivity K_v is small, and small K_v implies the necessity for a large height-gradient to "drive" the eddy flux. The gradient weakens as we progress away from ground. But again, this result needs to be generalised for arbitrary thermal stratification, and due to the weakness of the underlying model, it can breakdown completely: for example, mean vapour fluxes travelling against the mean gradient in humidity can occur, within a crop canopy.

4.7 Turbulent kinetic energy

4.7.1 Variance of streamwise velocity, $\overline{u'^2}$

The budget equation for $\overline{u'^2}$ in the horizontally-uniform case is:

$$\frac{\partial \overline{u'^2}}{\partial t} = 0 \;=\; -2\,\overline{u'w'}\,\frac{\partial \overline{u}}{\partial z} \;-\; \frac{\partial \overline{w'u'^2}}{\partial z} \;+\; \frac{2}{\rho_0}\,\overline{p'\,\frac{\partial u'}{\partial x}} + \nu\,\nabla^2\,\overline{u'^2} - 2\nu\,\overline{\frac{\partial u'}{\partial x_j}\,\frac{\partial u'}{\partial x_j}}\,. \tag{4.25}$$

Note that the summation convention applies in the last term. This is a balance between:

- Shear production: $-2\,\overline{u'w'}\,\frac{\partial \overline{u}}{\partial z}$
- Turbulent transport: $\frac{\partial \overline{w'u'^2}}{\partial z}$
- Redistribution (part of the pressure-rate of strain tensor): this term arises from the velocity-pressure gradient term $-\frac{2}{\rho_0}\,\overline{u'\,\partial p'/\partial x}$, which can be re-expressed as

$$-\frac{2}{\rho_0}\,\overline{u'\,\frac{\partial p'}{\partial x}} \rightarrow -\frac{2}{\rho_0}\,\left(\frac{\partial \overline{u'p'}}{\partial x} - \overline{p'\,\frac{\partial u'}{\partial x}}\right)\,. \tag{4.26}$$

  In view of the (assumed) horizontal-homogeneity, the transport term $\partial/\partial x\,\overline{u'p'} = 0$.

- Mean viscous transport: $\nu\,\nabla^2\,\overline{u'^2}$ (negligible)
- Dissipation: $\epsilon_u = -2\nu\,\overline{\frac{\partial u'}{\partial x_j}\,\frac{\partial u'}{\partial x_j}}$

There is no bouyancy term. Note that the presence of wind shear causes a direct feeding of energy into power in u'. An analogous balance-equation holds for $\overline{v'^2}$, but there is no shear production term.

4.7.2 Variance of vertical velocity, $\overline{w'^2}$

The budget equation for $\overline{w'^2}$ in the horizontally-uniform case is

$$\frac{\partial \overline{w'^2}}{\partial t} = 0 \;=\; -\,\frac{\partial \overline{w'^3}}{\partial z} \;+\; \frac{2}{\rho_0}\,\overline{p'\,\frac{\partial w'}{\partial z}} + 2\,\frac{g}{T_0}\,\overline{w'T'} + \nu\,\nabla^2\,\overline{w'^2} - 2\nu\,\overline{\frac{\partial w'}{\partial x_j}\,\frac{\partial w'}{\partial x_j}} \tag{4.27}$$

There is no shear production term. In the presence of an upward heat flux $\overline{w'T'} > 0$, buoyancy acts as a source for variance in w, while if $\overline{w'T'} < 0$, bouyancy is a sink for energy in w. The transport term $\partial \overline{w'^3}/\partial z$ corresponds to convective transport of energy in w', and is often small. The molecular transport term is negligible, but not so the dissipation term

$$\epsilon_w \equiv 2\nu\,\overline{\frac{\partial w'}{\partial x_j}\,\frac{\partial w'}{\partial x_j}}\,. \tag{4.28}$$

4.7.3 Turbulent kinetic energy budget

The TKE (strictly, per unit mass) is defined by:

$$k = \frac{1}{2}\left({\sigma_u}^2 + {\sigma_v}^2 + {\sigma_w}^2\right) \tag{4.29}$$

so that its budget equation is the sum of the equations for the individual velocity variances.

Pressure redistribution

What do we mean by "pressure redistribution" terms? You can see what will happen if we add together the two equations:

$$\frac{\partial \overline{u'}^2}{\partial t} + \frac{\partial \overline{w'}^2}{\partial t} = \tag{4.30}$$

On the rhs will appear:

$$\frac{2}{\rho_0}\left(\overline{p'\frac{\partial u'}{\partial x}} + \overline{p'\frac{\partial w'}{\partial z}}\right) = \frac{2}{\rho_0}\,\overline{p'\left(\frac{\partial u'}{\partial x} + \frac{\partial w'}{\partial z}\right)} \tag{4.31}$$

And when we add to this the equation for v'-variance, this term will be $(2/\rho_0)\,\overline{p'\,\nabla\cdot\mathbf{u}'}$ which is zero, due to the non-divergence of the velocity field. Thus these terms merely redistribute energy among components (see Fig. 4.1). Under neutral stratification there is no direct input of energy into the (v', w') fluctuations: these components receive their "power" indirectly, courtesy of pressure redistribution from u'.

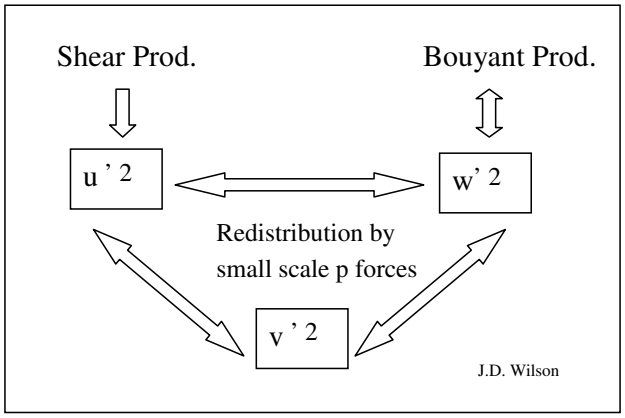


Figure 4.1: TKE sources and sinks, and redistribution of TKE amongst the variance pools.

Now returning to the sum of the individual variance-budgets, if we neglect molecular transport the TKE budget for steady state, horizontally-homogeneous flow is (c.f. Wyngaard,

2010, Eq. 10.43)

$$\begin{aligned} \frac{\partial k}{\partial t} = 0 \quad &= \quad -\overline{u'w'}\,\frac{\partial \overline{u}}{\partial z} + \frac{g}{T_0}\overline{w'T'} \\ &- \quad \frac{\partial}{\partial z}\,\overline{w'\left(\frac{p'}{\rho_0} + \tfrac{1}{2}\,\left(u'^2 + v'^2 + w'^2\right)\right)} \\ &+ \quad \nu\,\overline{\frac{\partial u_i'}{\partial x_j}\,\frac{\partial u_i'}{\partial x_j}} \end{aligned} \tag{4.32}$$

The first term on the rhs is called "shear production." The stresses due to unresolved scales work on the mean flow, converting MKE (mean KE) to TKE[1]. The second term on the rhs is buoyant production, the mean rate of working (force x velocity) by the bouyancy force $\overline{(g\ T'/T_0)\ w'}$.

The third term on the rhs is a TKE transport term.

The final term (involving ν) is the rate of conversion of TKE to heat, by viscous damping. It is usually given the notation $-\epsilon$. Fig. (4.2) shows the energy conversion pathways in a horizontally-uniform PBL.

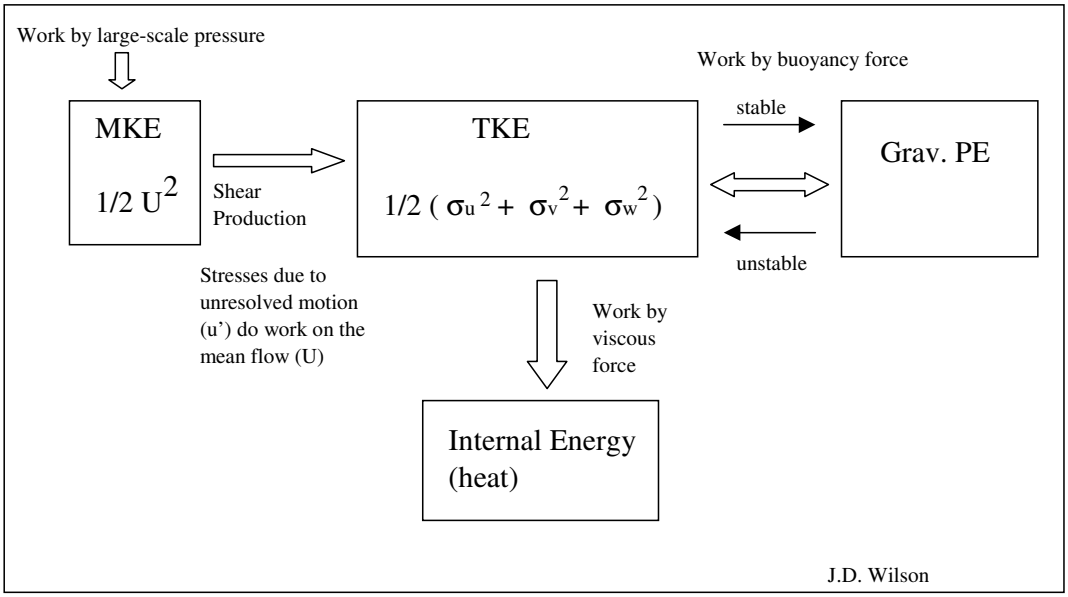


Figure 4.2: Pools of Energy and transformation pathways between them.

[1]Lettau (1954 and (independently) McNaughton (2006) have given a novel interpretation of the term usually named "shear production," according to which it is better viewed as the divergence of a downward convective flux of kinetic energy.

Local Equilibrium

The term "local equilibrium" describes the situation when the transport term is negligible, so that local production balances local dissipation

$$\frac{\partial k}{\partial t} = 0 = -\overline{u'w'}\,\frac{\partial \overline{u}}{\partial z} + \frac{g}{T_0}\overline{w'T'} - \epsilon\ . \tag{4.33}$$

TKE budget for the neutral, horizontally-uniform PBL in local equilibrium

With the added restriction of neutrality, the TKE budget reduces

$$\frac{\partial k}{\partial t} = 0 = -\overline{u'w'}\,\frac{\partial \overline{u}}{\partial z} - \epsilon \tag{4.34}$$

which is often written as:

$$P = -\overline{u'w'}\,\frac{\partial \overline{u}}{\partial z} = \epsilon \tag{4.35}$$

where P is the TKE production rate.

Now we have already seen that the wind shear is $u_*/k_v z$, so we have:

$$P = \epsilon = \frac{{u_*}^3}{k_v\ z}\ . \tag{4.36}$$

It is often assumed that, not too close to the surface ($z \gg z_0$) the horizontally-uniform atmospheric surface layer is in local equilibrium (and this is supported by the observations of Charuchittipan & Wilson, 2009). This is the situation one normally assumes in describing the undisturbed flow approaching (say) a hill or a fence.

Flux Richardson Number

The Flux Richardson number measures the ratio of the two energy source terms in the TKE budget

$${R_i}^f = \frac{\frac{g}{T_0}\,\overline{w'T'}}{\overline{u'w'}\,\frac{\partial \overline{u}}{\partial z}} \tag{4.37}$$

${R_i}^f$ is negative in an unstably stratified layer, zero in a neutrally stratified layer, and positive in a stably stratified layer (wherein buoyancy forces suppress vertical motion, and thus act as a sink for TKE).

4.8 Shear stress budget

Again, assuming steady state and horizontal homogeneity, the stress budget reduces to (c.f. Wyngaard, 2010, Eq. 10.45; here the pressure term is given in an alternative form)

$$\begin{aligned} \frac{\partial \overline{u'w'}}{\partial t} = 0 \;\; &= \;\; - \overline{w'^2} \;\; \frac{\partial \overline{u}}{\partial z} \\ &- \;\; \frac{\partial}{\partial z} \left(\overline{w'u'w' \;+\; u'p'/\rho_0} \right) \\ &+ \;\; \frac{1}{\rho_0} \overline{p' \left(\frac{\partial u'}{\partial z} + \frac{\partial w'}{\partial x} \right)} \\ &+ \;\; \frac{g}{T_0} \; \overline{u'T'} - 2\nu \overline{\frac{\partial u'}{\partial x_j} \; \frac{\partial w'}{\partial x_j}} \; . \end{aligned} \tag{4.38}$$

The pressure strain term is believed to act to try to return the turbulence towards isotropy, in which state there can be no shear stress. Thus it is commonly *modelled* as a "stress-destruction" term:

$$\frac{1}{\rho_0} \overline{p' \left(\frac{\partial u'}{\partial z} + \frac{\partial w'}{\partial x} \right)} = - \frac{\sqrt{k}}{\lambda} \; \overline{u'w'} \; \equiv - \frac{\overline{u'w'}}{\Gamma} \; , \tag{4.39}$$

where $\sqrt{k}$ is a velocity scale, λ is a length scale, Γ is a time scale ($\Gamma = \lambda/\sqrt{k}$).

4.8.1 Weakness of K-theory

If we drop turbulent transport, viscous transport, and pressure transport from the stress budget equation (4.38), and adopt the flux-destruction model (eqn. 4.39) for the pressure-strain term, the stress budget reduces to

$$\frac{\partial \overline{u'w'}}{\partial t} = 0 = - \; \overline{w'^2} \; \frac{\partial \overline{u}}{\partial z} \; - \; \frac{\sqrt{k}}{\lambda} \; \overline{u'w'} \; . \tag{4.40}$$

Upon rearrangement, this reads like K-theory

$$\overline{u'w'} = - \; \frac{{\sigma_w}^2}{\sqrt{k}} \; \lambda \; \frac{\partial \overline{u}}{\partial z} \tag{4.41}$$

with an effective viscosity $\lambda \; {\sigma_w}^2/\sqrt{k} \equiv \sigma_w^2 \Gamma$. Bearing in mind the train of assumptions that have been made to reduce the stress budget to Eq.(4.41), we can understand how far K-theory is from being generally true.

4.9 Heat flux budget

Assuming horizontal homogeneity and stationarity, neglecting molecular transport, and switching to the potential temperature, the general heat flux budget Eqn. 3.37 reduces to

$$\frac{\partial \overline{w'\theta'}}{\partial t} = 0 = - \; \overline{w'^2} \; \frac{\partial \overline{\theta}}{\partial z} - \; \frac{\partial}{\partial z} \; \overline{w'w'\theta'} - \; \frac{1}{\rho_0} \; \overline{\theta' \; \frac{\partial p'}{\partial z}} + \; \frac{g}{\theta_0} \; \overline{\theta'^2} \tag{4.42}$$

(c.f. Wyngaard, 2010, Eq. 10.48). A mean heat flux carried by turbulent eddies is produced whenever and wherever a non-zero vertical velocity variance and a mean vertical potential temperature gradient co-exist — which is always, unless the atmosphere is adiabatic. Potential temperature flucuations always make a positive contribution (i.e. mitigate towards an upward heat flux). The term in p' is believed to be the main flux destruction term.

Part II

The Ideal Atmospheric Surface Layer

Chapter 5

The Horizontally-Uniform Atmospheric Surface-Layer

Monin and Obukhov (1954) gave a similarity theory ("MOST", in effect a scaling scheme) for the surface layer profiles of mean wind, temperature, humidity, CO_2 concentration (etc) and other key statistics such as σ_w. Why do we need a similarity theory? Because the governing equations for the mean flow are unclosed, and even when closure assumptions are supplied, they cannot be solved except numerically.

The MO theory is very simple, and has proven very successful — although it is certainly imperfect and is regularly criticized. Its use is now standard in a vast array of environmental models. Note though, that MOST is valid only in *horizontally-uniform* conditions, and only at heights $z \gg z_0$. Wilson (2008) gives a critical review of MOST; Yaglom's (1990) obituary for Obukhov is an interesting read; and Foken (2006) reviews the impact of the theory.

It is important to establish from the outset that MOST is applicable only *above the "roughness sublayer"*, whose structure reflects the particularities of the underying surface and any plant cover. The roughness sublayer extends to some two-three times the height h_c of the plant or forest canopy. The layer within which MOST applies is often named the "inertial sublayer."

5.1 Logical basis of Monin-Obukhov Similarity Theory

Monin and Obukhov assumed there is a layer far enough above ground that scales of surface roughness do not affect the flow, yet close enough to ground that the depth δ of the PBL does not affect the flow. Within this layer $z_0 \ll z \ll \delta$ it is assumed that the turbulence is "controlled" by:

- the kinematic heat flux through the surface layer $\overline{w'T'} = Q_H/(\rho c_p)$
- the kinematic momentum flux through the surface layer[1], $\overline{u'w'} = -\,{u_*}^2$.

[1] To allow for a general orientation of the coordinate system one more generally defines the friction velocity

- a buoyancy parameter g/T_0, where T_0 is the mean (Kelvin) temperature

From the dimensional vantage point, this suggests using the following scales for non-dimensionalization:

$$u_* = \sqrt[4]{\overline{u'w'}^2 + \overline{v'w'}^2}\,, \tag{5.1}$$

$$T_* = -\frac{Q_H}{\rho c_p\, u_*}\,, \tag{5.2}$$

$$L = \frac{-{u_*}^3}{k_v\, \frac{g}{T_0}\, \frac{Q_H}{\rho\, c_p}}\,. \tag{5.3}$$

The von Karman constant k_v is inserted into the definition of L by convention. Note that T_0 would have been an unhelpful choice for a temperature scale, whose purpose is to quantify the influence of stratification, ie. of a heat flux through the surface layer. T_0 contains no information on that flux: a surface layer having $T_0 = 300$ K could be stable, neutral, or unstable. Often the above definitions are revised in terms of the *potential* rather than actual temperature, and in case it is necessary to account for the buoyancy effects of moisture, one may use the (potential or actual) *virtual* temperature, defined

$$T_v = T\ (1 + 0.61\ q) \tag{5.4}$$

where $q = \overline{\rho}_v/\rho$ is the specific humidity.

With this choice of scales, for the wind shear we would write:

$$\frac{k_v z}{u_*}\ \frac{\partial \overline{u}}{\partial z} = \phi_m\left(\frac{z}{L}\right) \tag{5.5}$$

where $\phi_m(.)$ is some unknown dimensionless "universal function" of its argument. Of course $k_v z$ might equally as well be replaced by L, in which case we should have a different function on the rhs, $\phi^*_m(.)$.

5.1.1 Non-dimensionalized governing equations hint at MO scaling

The premises of MOST may seem arbitrary. An interesting angle on Monin-Obukhov scaling arises by considering the criteria for "complete similarity" of the ASL from one state to another. We should have a universal description of the surface layer if the non-dimensionalised governing equations (and b/conds) could be made universal. We cannot "prove" MO similarity in this manner, because to do so we should have to cover an infinite set of coupled partial differential equations for all the moments — and their boundary conditions (Wilson,

---

as

$$u_*^4 = \overline{u'w'}^2 + \overline{v'w'}^2\,,$$

i.e. from (the fourth root of the magnitude of) the *resultant* of the two (perpendicular) components of the surface stresses.

2008). However it is interesting to see how easily the momentum equations can be cast in a universal form.

Neglecting Coriolis and viscous terms, the N/S equations under the Boussinesq approximation may be written:

$$\frac{\partial u_i}{\partial t} + u_j \frac{\partial u_i}{\partial x_j} = -\frac{1}{\rho_0} \frac{\partial p}{\partial x_i} + g \frac{T}{T_0} \delta_{3i} \tag{5.6}$$

where p is hydrostatic departure and T departure from an adiabatic reference state.

Introduce arbitrary scales V, L, T_*, P. Non-dimensionalising on these scales, and writing $\tilde{u}_i = u_i/V$ (etc.) the N/S equation becomes:

$$\frac{\partial \tilde{u}_i}{\partial \tilde{t}} + \tilde{u}_j \frac{\partial \tilde{u}_i}{\partial \tilde{x}_j} = -\left(\frac{P}{\rho_0 V^2}\right) \frac{\partial \tilde{p}}{\partial \tilde{x}_i} + \left(\frac{g T_* L}{T_0 V^2}\right) \tilde{T} \delta_{3i} \; . \tag{5.7}$$

Two dimensionless ratios appear. If these could be kept constant, regardless of the state of the atmospheric surface layer, we would have a universal equation for the non-dimensional velocity $\tilde{u}_i$ (etc).We have already argued that the sensible heat flux Q_H and the momentum flux $\tau = -\rho {u_*}^2$ are approximately constant across the surface layer. This suggests that natural velocity, temperature and pressure scales would be

$$u_* \; , \; T_* = -\frac{Q_H}{\rho c_p u_*} \; , \; P = \rho_0 {u_*}^2 \; .$$

With this choice, we are reduced to a single dimensionless ratio

$$\frac{g T_* L}{T_0 V^2} = \frac{g L Q_H}{\rho_0 c_p {u_*}^3 T_0} \; . \tag{5.8}$$

But we are free to choose the length scale L however we wish. So why not choose:

$$L = \frac{-{u_*}^3}{k_v \, \frac{g}{T_0} \, \frac{Q_H}{\rho_0 \, c_p}} \; ? \tag{5.9}$$

This choice (where the k_v and the negative sign are included simply by convention) fixes the second dimensionless ratio. Thus scaled, our equation governs scaled velocities which are independent of the "external" properties Q_H, u_* that control the state of the ASL. We could repeat this for the thermodynamic equation, humidity conservation equation (etc). A scaling parameter for the absolute humidity profile is defined from the vapour flux (by exact analogy with T_*) as:

$$\rho_{v*} = \frac{-\overline{w' \rho_v'}}{u_*} \tag{5.10}$$

and a scale for specific humidity would be $q* = \rho_{v*}/\rho$. Similarly for any passive tracer emitted at ground with spatially- and temporally-constant source-strength Q, we define a concentration scale $c_* = -Q/u_*$. We can in fact make the governing equations for all the interesting ASL statistics dimensionless in this way, without needing to introduce any dimensionless scale factors that go beyond those of MOST. However this does not constitute

a "proof" of MOST valid, because we have not considered the boundary conditions — the possible diversity of source distributions for heat, moisture, momentum[2] and so forth results in the inability of pure MOST to embrace *all* states of the ASL. Thus MOST is justified by its utility and parsimony, not by its rigour.

Now the purpose of the similarity theory is to find compact and useful formulae for the properties of the surface-layer: and properties of dominant interest are the profiles of the mean wind $\overline{u}$, temperature $\overline{T}$, and humidity $\overline{\rho}_v$. Since scales pertaining to the ground have not been included, we will work with the gradients in these properties. We write:

$$\begin{aligned} \frac{k_v z}{u_*}\frac{\partial \overline{u}}{\partial z} &= \phi_m\left(\frac{z}{L}\right) , \\ \frac{k_{vh} z}{T_*}\frac{\partial \overline{T}}{\partial z} &= \phi_h\left(\frac{z}{L}\right) , \\ \frac{k_{vw} z}{\rho_{v*}}\frac{\partial \overline{\rho_v}}{\partial z} &= \phi_w\left(\frac{z}{L}\right) , \\ \frac{k_{vc} z}{c_*}\frac{\partial \overline{c}}{\partial z} &= \phi_c\left(\frac{z}{L}\right) . \end{aligned} \tag{5.11}$$

Here $k_v z$ (etc.) could with equal validity be replaced by z or by L. This merely changes the numerical values of the dimensionless Monin-Obukhov universal similarity functions which appear on the rhs. The argument of these functions is the dimensionless height z/L. We begin by intentionally distinguishing the various von Karman constants, ie. $k_v, k_{vh}, k_{vw}, k_{vc}$, in order to require that the universal functions $\phi_m, \phi_h, \phi_w, \phi_c$ take unit value in the neutral limit, $z/L \to 0$.

But there is one aspect of the above expressions that needs to be modified. The mean temperature profile that corresponds to the state of zero heat flux (ie. neutrality, $T_* = 0$) is not $\partial\overline{T}/\partial z = 0$ but

$$\frac{\partial \overline{T}}{\partial z} = \Gamma \tag{5.12}$$

where $\Gamma = \frac{g}{c_p} \approx 0.01$ [K m^{-1}] is the "adiabatic lapse rate". Alternatively, of the neutrally-stratified layer we may say that the mean *potential* temperature $\overline{\theta}$ is uniform,

$$\frac{\partial \overline{\theta}}{\partial z} = 0 . \tag{5.13}$$

The ASL is sufficiently deep that we need to re-write our equation for the temperature profile as:

$$\frac{k_{vh} z}{T_*}\left(\frac{\partial \overline{T}}{\partial z} - \Gamma\right) = \phi_h\left(\frac{z}{L}\right) \tag{5.14}$$

[2]We may speak of "bottom up" sources, e.g. evaporation into the base of the ABL, or "top down" sources, such as result from entrainment at the top of the ABL (Wyngaard & Brost, 1984).

or better as

$$\frac{k_{vh} z}{\theta_{v*}} \frac{\partial \overline{\theta}}{\partial z} = \phi_h \left(\frac{z}{L} \right) \tag{5.15}$$

where θ_{v*} is the scale derived from the flux of the virtual potential temperature θ_v such that $-u_* \, \theta_{v*}$ is the buoyancy flux[3].

Now we have expressions for the gradients in wind, temperature, humidity. This doesn't get us far till we know the universal dimensionless (ϕ) functions. These have been the subject of a handful of major micrometeorological "flux-gradient" experiments (so called because they established the relationships between fluxes and gradients) in the past three decades, and are now well-established. Before looking at the functions, a word about the Obukhov length L, and about the concept of eddy diffusivity (which has not arisen so far in this similarity analysis).

[3]The virtual temperature is $T_v = T \, (1 + \, 0.61q)$, where q is the specific humidity. The virtual potential temperature is $\theta_v = \theta \, (1 + \, 0.61q)$.

5.2 The friction velocity and the Obukhov Length

Recall that in neutral stratification, and assuming the von Karman constant is a given constant (e.g. $k_v = 0.4$), the friction velocity can be deduced from the slope of a plot of mean wind speed verus height,

$$u_* = k_v \frac{\Delta \overline{u}}{\Delta \ln z} \,. \tag{5.16}$$

Bearing in mind that the stress on (or momentum flux to) the surface is $\tau = \rho u_*^2$ one can anticipate that u_* will depend both on the nature of the surface, i.e. how "rough" it is, and the strength of the wind. A typical range of values is about $0.1 - 0.5\,\mathrm{m\,s^{-1}}$ for light to moderate winds. Figure 5.1 gives the values observed in an experiment over an extensive uniform desert surface (this being rather a "smooth" surface, whose roughness length was only about $z_0 = 0.2 - 0.5$ mm).

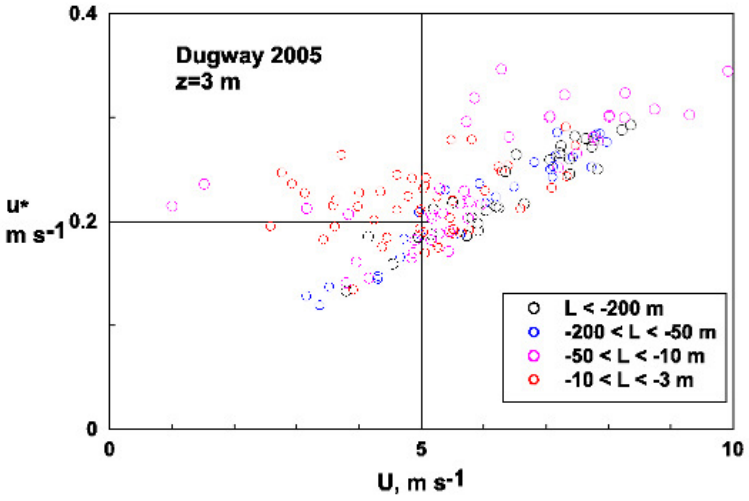


Figure 5.1: Observations from a sonic anemometer at $z = 3$ m over a desert surface (Dugway Proving Grounds, Utah, 2005).

Loosely speaking, the Obukhov length L (sometimes called the Monin-Obukhov length) is a "stability parameter," positive in stable stratification, negative in unstable stratification, and infinite (+ or -) under neutral stratification. It appears in the universal functions of MOST as the ratio z/L, and to avoid the discontinuities that occur as stratification changes from stable to unstable (through neutral, where $|L| = \infty$) it is often more useful to plot variables versus $1/L$. Note that the state of the MO layer is *effectively* neutral in the limit $z/|L| \to 0$, so that there are two ways to attain neutrality: either as z becomes small (irrespective of the value of L), or, as $|L|$ becomes large.

The Obukhov length L is sometimes named the "height of the substrate of dynamic turbulence," because its magnitude indicates (speaking qualitatively) the depth of the layer

within which shear production

$$P_s = -\overline{u'w'}\,\frac{\partial \overline{u}}{\partial z} - \overline{v'w'}\,\frac{\partial \overline{v}}{\partial z} \tag{5.17}$$

of TKE is overwhelmingly more important in the TKE balance than buoyant production/destruction

$$P_b = \frac{g}{T_0}\,\overline{w'T'}\,. \tag{5.18}$$

The ratio of these terms in the TKE budget is by definition the flux Richardson number, and the flux-gradient experiments have shown that

$$R_i^f = \frac{\frac{g}{T_0}\,\overline{w'T'}}{\overline{u'w'}\,\frac{\partial \overline{u}}{\partial z}} \;\approx\; \frac{z}{L}\,. \tag{5.19}$$

Thus by definition, if $|R_i^f| = 1$ then the two production mechanisms have equal magnitude; and this occurs at height $z \approx |L|$. Clearly even if the heat flux is quite large so that $|L|$ is *not* large, at small heights z the strong wind shear

$$\frac{\partial \overline{u}}{\partial z} = \frac{u_*}{k_v z}\,\phi_m\left(\frac{z}{L}\right)$$

means that shear production dominates over buoyant.

5.3 Exchange coefficients

The MO similarity theory does not depend on the introduction of K-theory. However if we wish to introduce the eddy viscosity (eg.), we have by definition:

$$\overline{u'w'} = -K_m\,\frac{\partial \overline{u}}{\partial z} \tag{5.20}$$

and comparison with the above relation for the wind shear shows that we must have

$$K_m = \frac{k_v u_* z}{\phi_m(z/L)}\,. \tag{5.21}$$

Similarly,

$$K_h = \frac{k_v u_* z}{\phi_h(z/L)}\,, \tag{5.22}$$

$$K_w = \frac{k_v u_* z}{\phi_w(z/L)}\,. \tag{5.23}$$

Thus we are supplied with closure relations, but these are valid only under those conditions under which MO similarity applies: not too close to the "ground" or canopy, in a horizontally-uniform ASL.

5.4 Relationship between Flux and Gradient Richardson Numbers

We've already encountered the flux Richardson number, defined by eqn (5.19). Substituting the Monin-Obukhov expressions for the the wind shear it follows that:

$$R_i^f = \frac{z}{L}\,\frac{1}{\phi_m}\ . \tag{5.24}$$

The gradient Richardson number is another dimensionless stability parameter, which can be evaluated from gradients alone:

$$R_i^g = \frac{g}{T_0}\,\frac{\partial\overline{T}/\partial z}{\left(\partial\overline{u}/\partial z\right)^2}\ . \tag{5.25}$$

Using the MO expressions for the temperature and velocity gradients, this may be written

$$R_i{}^g = \frac{z}{L}\frac{\phi_h}{\phi_m^2} = \frac{\phi_h}{\phi_m}\,R_i^f\ . \tag{5.26}$$

Many analyses of experimental data support the relationship $\phi_h \cong \phi_m^2$.

5.5 Key experiments on evaluation of the MO universal ϕ -functions.

Yaglom (1977) gives an excellent discussion of the difficulty of the experiments to determine the MO functions. The desire to determine these ϕ's spurred development of fast-response sensors for direct measurement of the fluxes (eddy correlation). In the days before computers, the need for fast sampling and cross multiplication of signals lead to some very ingenious electronic work (analog processing rather than digital); papers by Halstead et al. (1957), Fritschen and van Bavel (1963) and Dyer et al. (1967) give a fascinating insight into the concepts and evolving equipment of micro-meteorology in the 1950s and 1960s.

5.5.1 New South Wales Experiments

Carried out by a CSIRO (Australia) group and analysed by (among others) Dyer and Hicks (1967). Direct measurement of sensible heat flux by eddy correlation, some direct measurement of shear stress and vapour flux too. Results for the MO functions are fairly consistent with presently-accepted values. For the range $|z/L| \le 1$, Dyer and Hicks recommended

$$\begin{aligned}\phi_m &= \left(1-16\,\frac{z}{L}\right)^{-\frac{1}{4}}\ ,\\ \phi_h &= \phi_w = \left(1-16\frac{z}{L}\right)^{-\frac{1}{2}}\ .\end{aligned} \tag{5.27}$$

This formulation was well-liked for its convenient property that ${\phi_m}^2/\phi_h = 1$, which implies that $R_i^g = z/L$.

5.5.2 Kansas Experiments

Carried out by Air Force Cambridge Research Labs (AFCRL) and analysed by (among others) Businger et al. (1971). Sonic anemometers allowed eddy correlation for shear stress, heat and vapour flux. Shear stress also measured by "drag plates." The Kansas results were very influential, but are to some extent now superceded, because there is a widespread belief (e.g. Wieringa, 1980) that the electronics for their sonic anemometers (large boxes on the tower) distorted the flow, and thus contaminated their results.

The Kansas results were very useful and remain influential. One should be aware of the hypothesis (Wieringa, 1980; Wyngaard et al., 1981; Wyngaard, 1981; Gill, 1982) that the electronics for their sonics (large boxes on the tower) distorted the flow and thus affected the Kansas results. Original corrections for cup overspeeding were quite arbitrary and perhaps naive.

Businger et al. (1971) gave for the Kansas ϕ's in the unstable case[4]

$$\begin{aligned} \phi_m &= \left(1 - 15\,\frac{z}{L}\right)^{-\frac{1}{4}}, \\ \phi_h &= 0.74\left(1 - 9\frac{z}{L}\right)^{-\frac{1}{2}}, \end{aligned} \tag{5.28}$$

and for the stable case

$$\begin{aligned} \phi_m &= 1 + 4.7\,\frac{z}{L}, \\ \phi_h &= 0.74 + 4.7\,\frac{z}{L}. \end{aligned} \tag{5.29}$$

The Kansas experimenters found a 33% discrepancy between the shear stress measured by the drag plate and by eddy correlation. They obtained what is now considered an anomalously small estimate for the von Karman constant, $k_v = 0.35$, and concluded that (in the neutral limit) the ratio of the diffusivities for heat and momentum[5] was:

$$\left(\frac{K_h}{K_m}\right)_{|L|=\infty} = 1.34 \tag{5.30}$$

This result is generally held in doubt now. Many people now believe that (above the roughness sublayer) the eddy diffusivities are all equal in the neutral limit, and given by $k_v u_* z$ with $k_v = 0.4$.

A word on von Karman's constant k_v. The definition of k_v is

$$\left(\frac{\partial \overline{u}}{\partial z}\right)_{|L|=\infty} = \frac{u_*}{k_v\, z}, \tag{5.31}$$

[4]Note that these forms for the ϕ functions do not have the correct free convection limit, see Section**??**.

[5]This ratio is by definition the reciprocal of the "turbulent Prandtl number" P_r.

and so its evaluation necessitates measurement of u_* (i.e. the turbulent momentum fluxes, or shear stresses) and the velocity gradient. The shear stress(es), as we know, vary with height. Thus right off the bat there is some "slop" in the definition of k_v. Furthermore the shear stress is a notoriously difficult measurement, susceptible to errors due to incorrect alignment w.r.t. the ground (which error rotates a component of u into w), flow distortion by the anemometer itself, false electronic correlation, and a number of other errors particular to the earliest instruments (e.g. friction, inertia and inexact cosine response of 3D propellor anemometers).

Even measuring the wind shear is not trivial. In practise, the experiments have used cup anemometers, which measure the horizontal speed $s = \sqrt{u^2 + v^2}$ rather than $\overline{u}$. A binomial expansion shows that the inter-relationship is show that:

$$\overline{s} \approx \overline{u} \left(1 + \frac{\overline{u'^2} + \overline{v'^2}}{2\,\overline{u}^2} \right) . \tag{5.32}$$

Even if perfectly calibrated in a steady wind tunnel flow, cup anemometers "overspeed" in turbulence (they accelerate in gusts more rapidly than they decelerate in lulls). Their effective error may depend on z through $\sigma_u/\overline{u}$.

With careful attention to the above problems, Hogstrom (1985) determined that: $k_v = 0.40 \pm 0.01$.

5.5.3 ITCE (International Turbulence Comparison Experiment, 1976)

This experiment was led by CSIRO, with participation by Argonne National Labs. (USA) and a group from the Soviet Union. The site was flat, open grazing land in New South Wales, with a slopeof less than 2 parts in 10000. Instruments included fast response sensors to determine all covariances (fluxes) and turbulence statistics. Also used were drag plates for surface stress (τ_0), and a Lysimeter for evapotransiration rate (E_0). Cup anemometers were used to measure the wind profiles. Important papers stemming from this work include Francey and Garratt (1981) and Dyer and Bradley (1982).

The "alternative" analysis of ITCE76 by Dyer and Bradley (1982) does not presuppose the value of k_v. Their starting point is:

$$\begin{aligned} \frac{k_{vm} z}{u_*} \frac{\partial \overline{u}}{\partial z} &= \phi_m \left(\frac{z}{L} \right) \\ \frac{k_{vh} z}{T_*} \frac{\partial \overline{T}}{\partial z} &= \phi_h \left(\frac{z}{L} \right) \\ \frac{k_{vw} z}{\rho_{v*}} \frac{\partial \overline{\rho}_v}{\partial z} &= \phi_w \left(\frac{z}{L} \right) \end{aligned} \tag{5.33}$$

where $\rho_{v*} = -E/u_*$, $T_* = -Q_H/\rho c_p u_*$. As noted earlier, allowing different k_v's permits to insist that $\phi_m(0) = \phi_h(0) = \phi_w(0) = 1$ for the neutral limit $z/|L| = 0$.

Their conclusion was that, within the accuracy of the experiment, $k_{vm} = k_{vh} = k_{vw} = 0.4$ (so we can call them all simply k_v) and therefore the eddy diffusivities are all equal in neutral stratification[6]. For the similarity functions in unstable stratification (in the range $-4 \leq z/L \leq -0.004$) they recommend

$$\phi_m = \left(1 - 28\,\frac{z}{L}\right)^{-\frac{1}{4}}, \tag{5.34}$$

$$\phi_h = \phi_w = \left(1 - 14\frac{z}{L}\right)^{-\frac{1}{2}}. \tag{5.35}$$

In stable stratification the result of Webb (1970) is usually used:

$$\phi_m = \phi_h = \phi_w = 1 + 5\frac{z}{L} \tag{5.36}$$

5.6 Mean Profiles

The MOST expressions for the gradients of mean properties must be height-integrated in order to obtain the mean profiles.

5.6.1 Profiles in stable stratification

$$\overline{u}(z) = \frac{u_*}{k_v}\left(\ln\,\frac{z}{z_0} + 5\,\frac{z - z_0}{L}\right), \tag{5.37}$$

$$\overline{T}(z) - \overline{T}(z_{0T}) = \frac{T_*}{k_v}\left(\ln\,\frac{z}{z_{0T}} + 5\,\frac{z - z_{0T}}{L}\right) \tag{5.38}$$

(in analysing observations from a layer whose depth exceeds more than a few metres, it is preferable express the thermal profile by way of the *potential* temperature, for which the profile law is identical). Since the diffusivities are all the same, all profiles have this log-linear form. In some contexts and some environments the distinction between the constants of integration z_0 and z_{0T} is useful.

5.6.2 Profiles in unstable stratification

The integral for the wind profile is not trivial, and the result is quoted in different forms. One version is

$$\overline{u}(z) = \frac{u_*}{k_v}\left[c\left(\frac{z}{L}\right) - c\left(\frac{z_0}{L}\right)\right] \tag{5.39}$$

where

$$c\left(\frac{z}{L}\right) = 2\,\mathrm{atan}\left({\phi_m}^{-1}\right) + \ln\left(\frac{{\phi_m}^{-1} - 1}{{\phi_m}^{-1} + 1}\right). \tag{5.40}$$

[6]Even if true within the MO layer – and a later section casts some doubt on that – this is definitely not true within the roughness sublayer.

A popular alternative (due to Paulson, 1970) shows explicitly a logarithmic term and a diabatic correction:

$$\overline{u}(z) = \frac{u_*}{k_v} \left[\ln \frac{z}{z_0} - \psi_m \left(\frac{z}{L} \right) + \psi_m \left(\frac{z_0}{L} \right) \right] , \tag{5.41}$$

where ψ_m is given in terms of ϕ_m as

$$\psi_m = 2 \ln \left(\frac{1 + {\phi_m}^{-1}}{2} \right) + \ln \left(\frac{1 + {\phi_m}^{-2}}{2} \right) - 2 \operatorname{atan} \left({\phi_m}^{-1} \right) + \frac{\pi}{2} . \tag{5.42}$$

Similarly,

$$\overline{T}(z) - \overline{T}(z_0) = \frac{T_*}{k_v} \left[\ln \frac{z}{z_0} - \psi_h \left(\frac{z}{L} \right) + \psi_h \left(\frac{z_0}{L} \right) \right] \tag{5.43}$$

where

$$\psi_h = 2 \ln \left[\frac{1}{2} \left(1 + {\phi_h}^{-1} \right) \right] . \tag{5.44}$$

5.7 Velocity Standard Deviations

We have seen that the "power in w," measured by ${\sigma_w}^2$, is controlled by a number of counter-balancing influences (notably buoyant production/extraction, redistribution to/from other components, and viscous dissipation). There is no reason to expect σ_w to have a simple distribution in the ASL. It must surely vanish "at" ground. But despite the complexity of the mechanisms which set the level of ${\sigma_w}^2$, MO similarity seems to apply above the roughness sublayer.

For given "external" conditions (u_*, L, δ, and Geostrophic windspeed $\vec{U}_G$) a velocity variance such as ${\sigma_w}^2$ can be expected to depend on the averaging period T. As $T \to 0$ the variance will vanish, while at the other extreme, if we could sustain stationary conditions (above-listed external scales constant for a very long time) we could define an asymptotic (maximal) variance for the given external conditions, say $\sigma^2_{w,\infty}$. Then it is of interest to know the (expected) variance $\sigma^2_{w,T}$ over an arbitrary, finite averaging time T.

This has been considered by Pasquill (1974), by Wollenweber and Panofsky (1989) and by Kaimal (1989). If $S_{w,\infty}(f)$ is the asymptotic (long-time) power spectrum, then on average the variance seen over interval T is:

$$\sigma^2_{w,T} = \int_0^\infty S_{w,\infty}(f) \left(1 - \frac{\sin^2(\pi f T)}{\pi f T^2} \right) df \tag{5.45}$$

For specific choices of $S_{w,\infty}(f)$ one may deduce the (expected) variance fraction $\sigma^2_{w,T}/\sigma^2_{w,\infty}$. Taking the empirical spectral curves of Hojstrup (1982), Wollenweber and Panofsky deduced that $\sigma^2_{w,T}/\sigma^2_{w,\infty}$ should have no systematic sensitivity to averaging time in the range 1 min $\leq T \leq$ 1 hr (this result pertains to stably stratified flow). Analogous calculations for σ^2_u performed by Wilson (2008) (with $\delta = 2000$ m, $L = -30$ m, $z_0 = 0.02$ m) indicate that even with a sampling duration of only 2 min, over 60% of the $u-$ variance is expected to be seen

(ie. expected velocity standard deviation will be order 80% of the long-term value; obviously the 60% of $\sigma^2_{u,\infty}$ captured in only 2 min must be rapid variability). The w signal is even more forgiving of a short averaging duration, for the w spectrum lacks the low frequency power seen in the u, v spectra.

5.7.1 Velocity standard deviations in unstable stratification

A review of MOST in relation to the velocity standard deviations is given by Wilson (2008). For the standard deviation of vertical velocity Panofsky et al. (1977) suggested

$$\sigma_w = \left[1.6 + 2.9(-z/L)^{2/3}\right]^{1/2} . \tag{5.46}$$

However in the case of the horizontal components, strict MO similarity does not apply[7]. Rather, according to Panofsky et al., the horizontal velocity standard deviations σ_u, σ_v in the unstably-stratified surface-layer obey the formula:

$$\sigma_{u,v} = u_* \left[12 + 0.5(\delta/ - L)\right]^{1/3} \tag{5.47}$$

where δ is the depth of the Planetary Boundary Layer (PBL). Notice that this formula does not entail any height-dependence: Panofsky et al. stated "under convective conditions, a change in height has negligible effect on horizontal standard deviations." An alternative and more complex formula (based on observations over a salt flat in Utah, and which do indicate a height dependence of $\sigma_{u,v}$) is provided by Wilson (2008).

5.7.2 Velocity standard deviations in stable stratification

In neutral stratification observations cluster around

$$\sigma_w = \alpha\, u_* \tag{5.48}$$

with rather more variability in the "constant" α than a reading of textbooks might suggest (Wilson, 2008). The popular choice is $\alpha = 1.25 - 1.3$.

Panofsky and Dutton (1984) note that under stable statification the ratios $\sigma_{u,v}/u_*$ retain values appropriate to neutral stratification (about 2), except for very large z/L, where they become large and unpredictable.

5.8 Velocity Spectra

Velocity spectra are covered in Sections (7.3, 7.4.2).

[7]Townsend was the first to speak of "inactive turbulence", large, quasi-horizontal eddies with which is associated very little vertical motion and very little transfer of stress. This will be evident in the later discussion of velocity spectra in the ABL

5.9 Turbulent Prandtl- and Schmidt Numbers

Ratios of the von Karman constants give us the turbulent Prandtl and Schmidt numbers:

$$\begin{aligned} \frac{k_v}{k_{vh}} &= P_r = \left(\frac{K_m}{K_h}\right)_{|L|=\infty} \\ \frac{k_v}{k_{vc}} &= S = \left(\frac{K_m}{K_c}\right)_{|L|=\infty} \end{aligned} \tag{5.49}$$

(where c denotes a gas concentration, e.g. one of the natural scalars – absolute humidity and carbon dioxide concentration – or some artifical species such as a pollutant). There is no reason to suppose the von Karman "constants" actually are constant, across the family of all possible horizontally-homogeneous ASL states. Consequently ratios of von Karman "constants" are also somewhat uncertain, and may not be universal.

According to Harman and Finnigan (2008) "there is no strong evidence that (the Schmidt or Prandtl number) differs significantly from unity" above the roughness sublayer, whereas "the scalar roughness sublayer can be defined as the layer across which (the Schmidt number) varies from its canopy-top value of 0.5 in neutral stability to its MOST value of 1.0 above the RSL." Surprisingly though, rather few micrometeorological experiments offer concrete information on this subject. Let us focus specifically on water vapour (flux-gradient experiments with eddy covariance measurements of the carbon dioxide flux are even rarer). Based on evaporation and drag as measured by a 6.1 m diameter drag-plate lysimeter matched to a grass surface, Pruitt et al. (1973) reported $k_v = 0.42$ and $k_{vw} = 0.47$ (implying the Schmidt number for water vapour $S^w = 0.89$). Analysing the ITCE 1976 experiment in Australia, which entailing the pooling of several eddy covariance systems as well as a lysimeter (and drag plates), Francey and Garratt (1981) deduced values for the von Karman constants for (e.g.) momentum or water vapour by plotting $\Delta\overline{u}_{21}/\left(u_*\ \ln(z_1/z_2)\right)$ (or $\Delta\overline{q}_{21}/\left(q_*\ \ln(z_1/z_2)\right)$) versus $\sqrt{z_1 z_2}/L'$, where

$$L' = k_v L = \frac{u_*^3\, T_{v0}}{g\ \overline{w'T'_v}}$$

is a modified Obukhov length defined without including the (sought for) factor k_v. Alternative values for the von Karman constant were extracted by presupposing one or another of the pre-existing curves for the MO similarity functions $\phi(z/L)$ or $\phi(R_i)$, for instance if adopting $\phi = (1 - 15z/L)^{0.25}$ and $\phi_w = (1 - 16z/L)^{0.5}$ (Dyer 1974) they infer $k_v = 0.38 \pm 0.06$ and $k_{vw} = 0.42 \pm 0.06$ (broadly similar outcomes follow from their alternative choices). This implies $S^w = 0.9$. FG emphasized the large scatter in their extracted values for the von Karman constants, assessing mean wind speed errors as the dominant cause. In their "alternative analysis" of the ITCE, Dyer and Bradley (1982) concluded that the von Karman constants for momentum, heat and water vapour were equal within the limits of uncertainty, with the value 0.40.

Thus there is a suggestion that in the inertial sublayer the Schmidt number for water vapour may differ from unity by up to about 10%, vapour being transported more efficiently than momentum.

Atmospheric "flux-gradient" experiments are not unanimous on the values of the von Karman constants for momentum, heat and vapour. An alternative and indirect source of information upon them stems from atmospheric tracer experiments.

Wilson (1982b) and Hassid (1983) have noted that the Schmidt number imposed in (at least some types of) Eulerian dispersion models must differ from unity, in order to attain best simulations of reliable tracer experiments such as Project Prairie Grass (PPG). More specifically, Eulerian dispersion models whose form reduces (in the limit of undisturbed, horizontally-uniform flow) to:

$$\overline{u}\,\frac{\partial \overline{c}}{\partial x} = \frac{\partial}{\partial z}\,\left(K_c(z)\,\frac{\partial \overline{c}}{\partial z}\right) \tag{5.50}$$

with $K \propto {\sigma_w}^2$ apparently require $K_c/K_m \approx 1.6$ (ie. $S_c \approx 0.63$) for optimal agreement with the observations.

5.10 Local free convection scaling

With increasing height, the shear production term $(-\overline{u'w'}\,\partial\overline{u}/\partial z)$ in the TKE budget decays (roughly as $1/z$) while buoyant production remains roughly constant. Thus it can be argued that at large $-z/L$ the scaling variable u_* might become irrelevant. If one chooses the reduced set (z, g/θ_0, $\overline{w'\theta'}$) as defining the "external" scales, the following velocity and temperature scales are implied:

$$u_f = \left(\frac{g}{\theta_0}\,\overline{w'\theta'}\,z\right)^{1/3}\,, \tag{5.51}$$

$$T_f = \frac{\overline{w'\theta'}}{u_f}\,. \tag{5.52}$$

Now suppose one sought a law for σ_w. With the set (σ_w, z, g/θ_0, $\overline{w'\theta'}$) one has $n = 4, m = 3$ and it is easy to obtain the result that

$$\frac{\sigma_w}{u_f} = \text{const}\,. \tag{5.53}$$

This in turn implies that for large $-z/L$

$$\frac{\sigma_w}{u_*} \propto \left(\frac{z}{-L}\right)^{1/3}\,, \tag{5.54}$$

a result that is well supported by experimental data. Tennekes (1970) named this scaling regime "local free convection scaling," and Panofsky (1978) refers to the layer within which it applies as the "convective matching layer."

5.11 Comment on origin and caution on effectiveness of MO Similarity Theory

Prior to the MO theory, decades of work by scientists had not succeeded to provide a theory that would reveal nature's *order*, as regardes the statistical properties of wind and temperature etc. near ground. Recall that deriving an exact theory from the governing equations (conservation pronciples) is not possible, for upon averaging those equations we obtain an infinite and unclosed set of equatons for the statistics.

Monin and Obukhov provided quite a parsimonious theory based on simplifications whose plausibility was evident from experimental work; with hindsight, the theory can seem almost inevitable. Like any exploratory similarity theory or dimensional analysis — the distinction between the two is not very clear and does not matter — MOST is justified to the extent that it is consistent with observations. Subsequently theoreticians (e.g. Mellor, 1973) have carried out numerical simulations of ideal surface layer flow using second-order closure to "predict" the MO universal functions.

As to effectiveness, published "universal" flux-gradient relationships are analytical curves fitted to scatter-plots, ie. correlations of measured data, such as $z/T_*\ \partial\overline{T}/\partial z$ versus z/L. Figures (1-4; especially the insets) from Businger et al. (1971), and Figures (1-3) from Dyer and Bradley (1982), indicate the random scatter, at given z/L , in single (short term) observations of statistics like this. This scatter amounts, certainly, to no less than about 10% of the mean value – and probably 25% is a more honest figure. Yaglom (1976) emphasizes not only this scatter inherent to a given site and given instrumentation, but also the disparity among analytic fits that have been recommended. As Dyer and Bradley concluded, "The evidence is mounting that the atmosphere does not follow the averaged laws at all places and all times even over an excellent site, and the statistical variability of the medium itself must be taken into account." The saving factor is that these stochastic errors, which might be 10% or 20% for any $15 - 30$ min period, should cancel out upon integration over much longer periods.

In a later chapter we cover special topics whose context is appropriately the horizontally-uniform ASL as described under MOST.

Chapter 6

Surface-air exchange

6.1 The surface energy balance

Consider an imaginary plane in the surface layer, standing above a horizontally-uniform surface. Because a plane has no volume, the sum of all thermodynamic energy fluxes to and from that surface must sum to zero. It is common to see the surface energy balance expressed in that form, however if we focus on the practicality of measuring its components then the balance of energy fluxes must be performed on a volume. For the following, assume horizontal homogeneity applies.

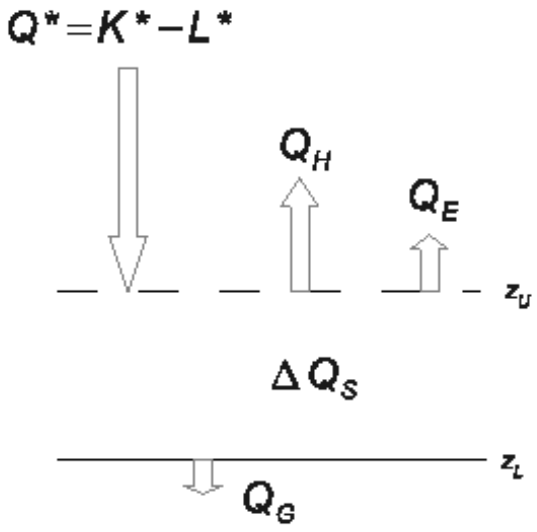


Figure 6.1: Components of the suface energy budget. The orientation of the arrows defines a convention for the signs of the individual fluxes.

We identify an imaginary upper plane at $z = z_U$ that lies above any vegetation, and corresponds to the placement of instruments to determine the vertical energy fluxes. Another imaginary plane is placed at $z = z_L$, at the soil surface or slightly below. We can sum up

all energy fluxes across these boundaries, and any residual must define energy being stored within the layer $z_L \leq z \leq z_U$. We shall label the energy storage term ΔQ_S. Energy storage may correspond to changing temperature of air, soil, plant matter and water. Note that an averaging time (or area) is implicit in any statements about the energy balance, and the magnitudes of the various terms in the balance will depend on the duration of averaging.

Across the lower plane it is assumed the vertical energy flux, Q_G for "ground", is normally due to conduction down the soil temperature gradient (latent heat transport due to diffusion of vapour, and convective transport due to percolating rain, can also play a role). If we define Q_G to be positive when energy travels into the soil, then Q_G may be quite large a millimeter or two beneath the surface, in soil exposed to the midday sun; but when averaged over a year, it is probably rather small (which is the corollary of the fact that the deep soil temperature does not change much from year to year). Indeed, the diurnal cycle in solar elevation assures that even on a daily basis (24 hr averages) Q_G may be small.

Now suppose at z_U we are able to measure the incoming shortwave and longwave radiative energy flux densities $K\downarrow, L\downarrow$ and the corresponding outgoing fluxes $K\uparrow, L\uparrow$. The net shortwave radiation is $K^* = K\downarrow - K\uparrow$, the net longwave is $L^* = L\downarrow - L\uparrow$, and the net allwave radiation is $Q^* = K^* + L^*$, in the convention outlined here, positive if directed downward to the ground[1].

The other energy fluxes we must account are the convective fluxes of heat ($Q_H(z_U)$) and latent heat ($Q_E(z_U) = L_v\ E(z_U)$) across the upper plane, fluxes which, if written (as customarily thought of) in the form of eddy covariances

$$Q_H = \rho\ c_p\ \overline{w'T'} \tag{6.1}$$

are subject to the uncertainties covered in Section (6.2). And of course with the usual sign convention that $w' > 0$ for upward motion, these convective fluxes are positive if directed away from ground.

Having set out the definitions, we may express the surface energy balance as:

$$Q^*(z_U) = Q_H(z_U) + Q_E(z_U) + \Delta {Q_S}^{(z_U, z_L)} - Q_G(z_L)\ . \tag{6.2}$$

Note that the convective fluxes, if measured, represent an average over a substantial region of the upwind surface (the flux footprint, see Sec. 6.8), a point which is irrelevant, if the site (truly) is horizontally-uniform. On the other hand the soil heat flux density is almost always a point measurement, in a notoriously non-homogeneous medium. A net radiometer may ostensibly have a field of view corresponding almost to the entire upper and lower hemispheres, but its reading is weighted to a region of the ground (and sky) that may overlap with, but certainly does not coincide with, the (convective) flux footprints. Thus measured components of the energy balance may in practice be averages over different regions of the surface and atmosphere, ie. air, canopy (if any) and soil.

[1]The one-way fluxes $K\uparrow, K\downarrow, L\uparrow, L\downarrow$ are all non-negative by definition; however the net fluxes K^*, L^* and the other fluxes Q_H, Q_E, Q_G may have either sign, depending on specific circumstances.

6.2 Eddy-Covariance

Suppose we wished to determine the near-surface vertical flux Q of an atmospheric component whose concentration is c. This covers the sensible and latent heat fluxes Q_H, Q_E, the flux of carbon dioxide Q_{CO_2} and any other case of interest.

Let us start out by supposing stationary, horizontally-homogeneous flow over an ideally horizontal, uniform surface that uniformly releases this entity, whose concentration is $c = c(x, y, z, t)$. The mean vertical convective flux density of c at a point (x, y, z) over the interval $t_m - T_{avg} \leq t \leq t_m$, where T_{avg} is typically $15 - 60$ min, is

$$Q^{EC}(x, y, z, t_m, T_{avg}) = \overline{w\, c} \tag{6.3}$$

(the time-average of the turbulent vertical convective mass flux density). By our assumption of symmetry, and neglecting any errors, this vertical flux Q^{EC} equals the flux Q off the source. Potential sources of error in the point eddy flux might include inadequate instrument spectral (temporal) response; inadequate instrument spatial resolution; poor instrument calibration (span, offset); instrument interference with the flow (flow distortion); anemometer-scalar sensor separation; cross-correlated instrument (electronic) noise; and instrument misalignment relative to the vertical.

But let us assume that of all these possible sources of error, only one arises: we have ideal instrumentation in every respect except that there is (or may be) an unknown small anemometer offset w_e. We write for the measured vertical velocity

$$w(x, y, z, t) = \overline{w}(x, y, z, t_m, T_{avg}) + w_e + w'(x, y, z, t) \tag{6.4}$$

where we acknowledge explicitly the offset error w_e, and that the (true) mean vertical velocity, $\overline{w}$, depends on averaging interval T_{avg}. Now from the definition above the (apparent) point eddy flux is,

$$Q^{EC} = (\overline{w} + w_e)\, \overline{c} + \overline{w'c'} \tag{6.5}$$

Operationally, however, one recognises the (possible) existence of error w_e (due to tower misalignment and/or terrain slope and/or instrument offset), and assumes that a better estimate of the true flux is

$$Q^{EC*} = \overline{w\, c} - (\overline{w} + w_e)\, \overline{c} = \overline{w'\, c'}\ . \tag{6.6}$$

However this neglects the possibility of a *true* mean vertical velocity that arises due to the injection of heat and/or water vapour at the surface, and therefore it is usual to apply the Webb-Pearman-Leuning (WPL) correction (Webb et al. 1980). This correction assumes that the total vertical flux of "dry air" at the surface

$$\overline{w\, \rho_a} = 0 = \overline{w}\, \overline{\rho_a} + \overline{w'\, \rho'_a} \tag{6.7}$$

and building on earlier work (for a summary see Fuehrer and Friehe 2002) WPL deduced that

$$\overline{w} = (1 + \mu\,\sigma)\ \frac{\overline{w'T'}}{\overline{T}} + \ \mu\ \frac{\overline{w'\rho_v'}}{\overline{\rho}_a} \tag{6.8}$$

where $\mu = M_a/M_v$ is the ratio of the molar masses of dry air and water vapour and $\sigma = \overline{\rho}_v/\overline{\rho}_a$ is the ratio of the mean absolute humidity to the mean density of dry air. If this correction is applied to the fluxes of carbon dioxide (concentration ρ_c) and water vapour (ρ_v), the result is

$$F_c = \overline{w'\rho_c'} + \mu\ \frac{\overline{\rho}_c}{\overline{\rho}_a}\ \overline{w'\rho_v'} + (1 + \mu\,\sigma)\ \frac{\overline{\rho}_c}{\overline{T}}\ \overline{w'T'}\ , \tag{6.9}$$

$$F_w = \left(1 + \varepsilon^{-1}\,\sigma\right)\ \left(\overline{w'\rho_v'} + \frac{\overline{\rho}_v}{\overline{T}}\ \overline{w'T'}\right)\ . \tag{6.10}$$

In effect, the WPL correction introduces an idealized mean vertical velocity (see Businger 1984; Fuehrer and Friehe 2002; Paw U et al. 2000; Massman and Lee 2002; Leuning 2004, 2007; Lee and Massman 2011). A recent review on eddy covariance is given by Gu et al. (2012).

WPL-corrected surface fluxes are usually considered to represent surface-air exchange over what are subjectively judged homogeneous surfaces, with the accompanying assumption that if the surface is homogeneous, then so is the atmosphere (which is not necessarily true). Assuming the raw measurements had been performed by a 3-dimensional anemometer the steps are: (1) rotate all statistics into a coordinate system in which $\overline{w} = 0$; (2) perform Schotanus correction (if the temperature signal derives from "sonic temperature"; (3) make the Webb-Pearman-Leuning (1980) correction, which amounts to the imposition of an *idealized* theoretical mean vertical velocity; (4) make corrections for flux loss due to sensor-sensor spacing and/or inadequate or mismatched temporal response.

As covered in Section 6.4 the sum $Q_H + Q_{LE}$ of the sensible and latent heat fluxes not uncommonly fails to match the energy supply $Q* - Q_G - \Delta Q_S$ ("non-closure" of the surface energy budget; Blanken et al. 1998; Twine et al. 2000). The emerging viewpoint is that the problem — with EC measurement over flat ground and uniform sources — lies in illegitimate neglect of the dispersive contribution to the flux, i.e. a component of flux carried by a small, mesoscale component of vertical velocity (e.g. Huang et al. 2008; Mauder et al. 2010).

6.3 Flux-gradient methods

Although eddy correlation is the most fundamental technique to measure trace gas exchange fluxes, it is inapplicable in a disturbed flow — and not without ambiguity even in the nominally-uniform case (eg. Mahrt, 1998). Furthermore for many trace gases of interest we lack sufficiently fast concentration sensors. An alternative is to deduce the vertical flux

by measuring associated vertical mean gradients. Such techniques are traditional (and acceptable) in horizontally-uniform conditions, but again, there are potentially grave errors under inhomogeneous conditions.

There are many variations on flux-gradient (FG) techniques, but it will suffice that we examine only one. At an arbitrary location on the $x-y$ plane we select a pair of heights ($z_1 < z_2$), at each of which we measure the mean windspeeds $\overline{u}_1, \overline{u}_2$; the mean temperatures $\overline{T}_1, \overline{T}_2$; and the mean concentrations of the gas $\overline{c}_1, \overline{c}_2$. According to our symmetry assumption - a conceptual idealisation of a reality that is usually more complex - the mean fluxes are absolutely constant, ie. invariant with x, y, z; and we will have chosen a site so as to attempt to uphold this assumption.

Firstly, we need to know atmospheric stability. We approximate the gradient Richardson number (eqn(5.25)) as

$$R_i{}^g = \frac{\frac{g}{T_0}\,\Delta\overline{T}\Delta z}{\Delta\overline{u}^2} \tag{6.11}$$

where $\Delta\overline{T} = \overline{T}_2 - \overline{T}_1$, etc., and the resulting $R_i{}^g$ is considered to apply at height $z_g = \sqrt{z_1 z_2}$. As an aside, one will have observed arbitrary decisions entering the picture; the choices z_1, z_2; the use of the geometric mean height. Leaving those issues aside, we exploit an empirical $R_i{}^g$ versus z/L correlation to obtain z_g/L and thus L. There are as many such correlations as there are versions of the universal MOST functions, but as an example (Hogstrom, 1996)

$$\begin{aligned} \frac{z}{L} &= 0.67 R_i{}^g,\ L < 0 \\ &= R_i{}^g\,(1 - 5R_i{}^g)^{-1},\ L \geq 0 \end{aligned} \tag{6.12}$$

Any ambiguity or inconsistency or error, eg. in having ignored that k_v/k_{vh} may not be unity, will to this stage have affected only the value of L we deduce for the flow.

Now, to get the desired flux estimate (which we shall explicitly distinguish from the true flux Q by writing Q^{FG}), we take the ratio of the flux-gradient expressions written above[2], viz.

$$\frac{Q^{FG}}{{u_*}^2} = -\frac{k_{vc}}{k_v}\,\frac{\phi_m}{\phi_c}\,\frac{\Delta\overline{c}}{\Delta\overline{u}} \tag{6.13}$$

where we continue to take pains to admit the possibility that $k_{vc}/k_v \neq 1$. Then by eliminating u_* we obtain:

$$Q^{FG} = -\frac{1}{S_c}\,{k_v}^2\,\frac{{z_g}^2}{\Delta z^2}\,\frac{1}{\phi_c\,\phi_m}\,\Delta\overline{c}\,\Delta\overline{u} \tag{6.14}$$

Since our measured information $\Delta\overline{c}, \Delta\overline{u}, \Delta\overline{T}$ determines L and thus the ϕ's (whose functional form we assume is a given), we are able to calculate Q^{FG}. Now, given that the eddy diffusivities (and von Karman constants) are determined from flux-gradient experiments in

[2]Here it will be assumed that Δz is sufficiently small to permit use of finite differences; alternatively one could use the integrated forms of the MOST flux-gradient relationships.

which (hopefully) correct fluxes are related to correct gradients, it is surely a necessary self-consistency that under situations of suitable horizontal uniformity (of the flow and the scalar sources), Q^{FG} should be a good estimate of Q. Provided we are not too unfortunate or extreme in our choices of z_1, z_2, and if the micrometeorology of the "uniform" ASL is truly universal and suitably described by MOST, and if the ${R_i}^g - z/L$ correlation we employed is "true" to MOST, there should be no problem.

Suppose we take the neutral limit; and suppose too we allow z_1 and z_2 to be close together (but we nevertheless assume ideally correct measurements of $\Delta\overline{u}, \Delta\overline{c}$ are obtainable). The expression above simplifies, and the z_g approximation is nearly exact; given that L is of infinite magnitude and so irrelevant in the neutral limit, now only the two von Karman constants kv, k_{vc} enter the picture. For given measured values of $\Delta\overline{u}, \Delta\overline{c}$, what we get for our estimate Q^{FG} depends very directly on our choice of those constants,

$$Q^{FG(N)} = -\frac{1}{S_c}\,{k_v}^2\,\frac{{z_g}^2}{\Delta z^2}\,\Delta\overline{c}\,\Delta\overline{u} \tag{6.15}$$

Dyer and Bradley (1982) concluded from the ITCE flux-gradient experiment that the von Karman constants for humidity, heat and momentum in the atmospheric surface layer were identical, with value 0.4 ± 0.02. Although some (other) flux-gradient experiments have suggested the turbulent Prandtl number (and/or turbulent Schmidt number for vapour) is/are less than unity, many micro-meteorologists treat the eddy viscosity and eddy diffusivities as being identical in the neutral limit — this despite the fact that in engineering wall shear flows it is near unanimous that they differ. In short there is conflicting evidence on these "constants," from which we conclude that, even in ideally uniform conditions, the application of FG methods to determine a source strength is not without uncertainty, or ambiguity.

From eqn. (6.15) one may infer that the effective mass diffusivity at the intermediate height z_g is implicitly posited to be

$$K_c = \frac{1}{S_c}\,{k_v}^2\,{z_g}^2\,\frac{\Delta\overline{u}}{\Delta z} \tag{6.16}$$

This makes sense in the ideal case considered (neutral, horizontally-homogeneous ASL), for which

$$k_v\,z_g\,\frac{\Delta\overline{u}}{\Delta z} = u_* \tag{6.17}$$

so that the implicit mass diffusivity is $K_c = (1/S_c)k_v z_g u_*$, which is correct, in uniform conditions.

In historical practise, how well has the FG method worked in uniform conditions? The question begs qualification: do we refer to short-term (15-60 min) figures, or to weekly, seasonal or even annual averages; and secondly, what is the standard of comparison, and the uncertainty therein (ie. how and how well is "true Q" determined)? For short term flux-gradient measurements Q^{FG}, one cannot escape stochastic errors that are inherent in

flux-gradient relationships (see discussion above). The saving factor is that these stochastic errors, which might be 10% or 20% for any 15 - 30 min period, should cancel out as we average together increasing numbers of 15 min or 30 min estimates (of trace gas fluxes inferred from flux-gradient relationships). And one would argue that if this were not the case — if a FG method did not work in the long term, at an ideal site — well then the site was not ideal, or the measurements were wrong, or (lastly on the scale of probability) MOST is not universal.

See Wilson et al. (2001) for a discussion of what can go wrong if the FG method is carried over to inhomogeneous flows.

6.4 Flux loss and energy-balance non-closure

In the early 1980's micro-meteorologists began to recognize that, commonly, measurements do not "close" the energy balance (Mahrt, 1998; Blanken et al., 1998; Twine et al., 2000; Mauder et al., 2008); the sum $Q_H + Q_E$ of the convective fluxes (of sensible and latent heat, respectively) typically underestimates the available energy $Q^* - Q_G - \Delta Q_S$. This section will focus on the supposition that the seat of the discrepancy lies with the convective fluxes, but there have been suggestions that radiometry could be an aspect of the problem (see Wilson et al., 2009a, for an analysis of the physics of the net radiometer.)

Now, why should it be that eddy covariance systematically underestimates the mean vertical flux over what are thought to be good sites? Much thought has gone into eliminating or correcting for *instrumental flux losses*, namely

- inadequate frequency response; Moore (1986) pioneered the application of frequency-response corrections based on ideal co-spectra; Horst (2000) reviews some errors that have been made in implementing frequency-response corrections
- excessive spatial smoothing
- wind/scalar sensor separation; Laubach and McNaughton (1998)

which all do necessarily produce flux losses. Currently, although transducer-wake corrections have been known to be necessary for a long time, the adequacy of calibration of sonic anemometers is under enquiry (Foken and Weisensee, 2000; Voght et al., 2000, these two being *AMS* preprints; also Heinemann et al).

On the basis of Large Eddy Simulations Huang et al. (2008) reported, as had earlier authors, that the underlying cause of the energy balance closure problem is (or can be) inadequate spatial representativity of point measurements of the vertical fluxes. Another possibility is that the horizontal homogeneity one has sought to assure by choice of the site, is illusory, and that locally, the mean vertical velocity cannot be ignored. According to Mauder

et al. (2010), "Heterogeneity-induced and buoyancy-driven quasi-stationary circulations are probably the dominant processes causing the underestimation of energy uxes."

Let us decompose any instantaneous fluid property g:

$$g(x,y,z,t) = \langle \overline{g} \rangle + \overline{g}'' + g' \tag{6.18}$$

where $\overline{g}$ is a time-average and $\langle\rangle$ denotes a spatial average (over area $A = L_x L_y$) in the xy plane (Raupach and Shaw, 1982). The middle term $\overline{g}''$ is the local time-average deviation from the space-time mean $\langle \overline{g} \rangle$, and g' is the instantaneous local fluctuation from the local time average (so $\overline{g'} = 0$). For simplicity we may sometimes write $G = \langle \overline{g} \rangle$.

Now on the basis of the incompressible continuity equation we infer that over level and uniform terrain (or ocean) the mean vertical velocity $W \equiv \langle \overline{w} \rangle$ must reduce to a small (though not necessarily negligible) residual value given by the WPL correction (Webb *et al.*, 1980), provided the averaging area is sufficiently large. But how large? We are well aware that it need not do so on the local scale (say, $L_x \sim L_y \sim 10 - 100$ m) due to inhomogeneity in soil temperatures, or vegetation cover, or whatever. We know also that large eddies in the ABL may imply inhomogeneity even for averages over lengthscales of order $L_x \sim L_y \sim 1 - 10$ km. Above this lengthscale, we have generally to accept the possibility of mesoscale inhomogeneity. Thus no matter what the spatial scale of averaging, it is hazardous to assume $\langle \overline{w} \rangle = 0$.

Now we need to specify more carefully what we mean by the mean vertical flux. Expanding the vertical velocity and scalar concentration,

$$\begin{aligned} w(x,y,z,t) &= \langle \overline{w} \rangle + \overline{w}'' + w' \\ c(x,y,z,t) &= \langle \overline{c} \rangle + \overline{c}'' + c' \end{aligned} \tag{6.19}$$

we can see the cross product wc contains nine distinct terms,

$$\begin{aligned} w\,c &= \langle \overline{w} \rangle \langle \overline{c} \rangle + \overline{w}'' \overline{c}'' + w' c' \\ &+ \langle \overline{w} \rangle \overline{c}'' + \overline{w}'' \langle \overline{c} \rangle \\ &+ \langle \overline{w} \rangle c' + w' \langle \overline{c} \rangle + \overline{w}'' c' + w' \overline{c}'' \,. \end{aligned} \tag{6.20}$$

Time-averaging, we have:

$$\begin{aligned} \overline{w\,c} &= \langle \overline{w} \rangle \langle \overline{c} \rangle + \overline{w}'' \overline{c}'' + \overline{w' c'} \\ &+ \langle \overline{w} \rangle \overline{c}'' + \overline{w}'' \langle \overline{c} \rangle \,, \end{aligned} \tag{6.21}$$

while

$$\overline{w} = \langle \overline{w} \rangle + \overline{w}'' \,. \tag{6.22}$$

Now space-averaging

$$\langle \overline{w\,c} \rangle = \langle \overline{w} \rangle \langle \overline{c} \rangle + \langle \overline{w}'' \overline{c}'' \rangle + \langle \overline{w' c'} \rangle \tag{6.23}$$

The first and last terms are familiar and obvious in their meaning, while the middle term is known as the "dispersive flux", and is due to spatially-correlated time-mean deviations from the space-time mean.

Although the convective flux seen by our instrument at a given point is affected by a wide region of the upstream surface, we may not interpret that measurement as being a spatial average of the convective flux, for it is very definitely a local time mean, that is, our instruments (this time, burying instrument offsets with the apparent local atmospheric mean $\langle\overline{w}\rangle + \overline{w}''$), give us, using eqn (6.21):

$$\begin{aligned} Q^{ECP-raw} &= \overline{w\,c} - \overline{w}\,\overline{c} \\ &= \langle\overline{w}\rangle\,\langle\overline{c}\rangle + \overline{w}''\,\overline{c}'' + \overline{w'\,c'} \\ &+ \langle\overline{w}\rangle\,\overline{c}'' + \overline{w}''\,\langle\overline{c}\rangle \\ &- (\langle\overline{w}\rangle + \overline{w}'')\,(\langle\overline{c}\rangle + \overline{c}'') \\ &= \overline{w'\,c'} \end{aligned} \tag{6.24}$$

which (even after application of the WPL correction, which invokes an *idealized* mean vertical flow) may be very different from the true spatial mean flux, eqn (6.23), even if it happened that $\langle\overline{w}\rangle = 0$.

An argument that the assumption that $\overline{w}'' = 0$ leads to flux loss can be made, on the following (flux-gradient based) argument for the four quadrants of the ($\overline{w}''$, $\overline{w'c'}$)-space:

- $\overline{w}'' > 0, \overline{w'c'} > 0$ then $\partial\overline{c}/\partial z < 0$, so, the part of the flux we neglected must carry "high c" air up locally, and low c air down elsewhere, so, the missing flux is an upward flux... same sign as the eddy flux
- $\overline{w}'' < 0, \overline{w'c'} > 0$ then $\partial\overline{c}/\partial z < 0$. The part of the flux we neglected must carry "low c" air down locally, and high c air up elsewhere, so, the missing flux is an upward flux... same sign as the eddy flux
- $\overline{w}'' > 0, \overline{w'c'} < 0$ then $\partial\overline{c}/\partial z > 0$, so, the part of the flux we neglected must carry "low c" air up locally, and high c air down elsewhere, so, the missing flux is an downward flux... same sign as the eddy flux
- $\overline{w}'' < 0, \overline{w'c'} < 0$ then $\partial\overline{c}/\partial z > 0$, so, the part of the flux we neglected must carry "high c" air down locally, and low c air up elsewhere, so, the missing flux is a downward flux... same sign as the eddy flux

Hopefully this section has made it clear that, although in principle a "tidy" and definite relationship, in practical micro-meteorology, even if all instruments have been calibrated and exposed with perfect competence, measured components of the surface energy balance

only sum to zero under conditions of exceptional good luck, and probably due to the happy cancellation of opposing errors. And if the flow is spatially variable, then eqn (6.6) for tracer flux is invalid, even if the instruments are placed close enough to ground to be within the constant (gas) flux layer... for flow disturbance almost inevitably introduces a (generally unknown) mean vertical motion $\overline{w} = \langle \overline{w} \rangle + \overline{w}''$, that may contribute to the local (or spatially-averaged) vertical flux of the subject gas (see Finnigan, 2000).

6.5 Bulk Transfer Coefficients

"Interactive feedback from the biosphere is probably as important as feedbacks from deep cumulus and from the ocean. The level of complication needed to model this mechanism is, however, a decision that atmospheric modellers must make." - Hua-Lu Pan (1990; Monthly Weather Review, Vol. 118).

Modern weather models estimate the surfaces energy and momentum fluxes, (sea/ground-air interaction) which of course modify both the soil/lake/ocean state and the airmass state. How are these fluxes to be estimated? Typical of modern weather models with respect to surface treatment is the Canadian "Gobal Environmental Model" (GEM). The GEM has its lowest grid level at z_a, the "anemometer height," which lies with the atmospheric surface layer, across which the vertical fluxes have negligible change with height. Now, let u_a, T_a, q_a be the mean windspeed, temperature, and specific humidity at the anemometer height z_a (the lowest model level). Then in the "bulk" aerodynamic treatment the surface flux densities of momentum, sensible, and latent heat are parameterized as:

$$\begin{aligned} \tau &= \rho\, {C_M}^2\, {u_a}^2 \\ Q_H &= \rho c_p\, C_M\, C_H\, u_a\, (T_0 - T_a) \\ Q_E &= L_v\, E = \rho L_v\, C_M\, C_V\, u_a\, (q_0 - q_a) \end{aligned} \tag{6.25}$$

These equations specify the fluxes "at" ground level, and so can be considered as constituting the boundary condition. Within the ABL, these fluxes are carried by the unresolved scales. Any convergence of the fluxes, of course, causes evolution of the corresponding resolved field.

u_a, T_a, q_a are "known" (from a flux-measurement perspective they are given values at some reference height, z_a; or in the context of a weather model, they are the gridpoint values at z_a). Also the surface values T_0, q_0 are "knowns" (a model will have an algorithm to calculate these). C_M, C_H, C_V are dimensionless transfer coefficients for momentum, heat, and vapour, and are defined by the above equations. Over uniform terrain, they *seem* to be

easily determinable from the MOST profiles, according to which:

$$\begin{aligned} C_M &= \frac{\tau/\rho}{u_a} \\ &= \frac{k_v}{\ln\left(\frac{z_a}{z_0}\right) - \psi_m\left(\frac{z_a}{L}\right) + \psi_m\left(\frac{z_0}{L}\right)} \end{aligned} \tag{6.26}$$

and similarly

$$\begin{aligned} C_H &= \frac{k_{vh}}{\ln\left(\frac{z_a}{z_{0T}}\right) - \psi_h\left(\frac{z_a}{L}\right) + \psi_h\left(\frac{z_{0T}}{L}\right)} \\ C_V &= \frac{k_{vw}}{\ln\left(\frac{z_a}{z_{0w}}\right) - \psi_w\left(\frac{z_a}{L}\right) + \psi_w\left(\frac{z_0}{L}\right)} \end{aligned} \tag{6.27}$$

where we have distinguished the roughness lengths for momentum, temperature and humidity.

But note that there is a buried problem here, a superficiality. When we use the MOST profiles to evaluate the bulk transfer coefficients we have improperly considered them to be valid over the entire interval $z_0 \leq z \leq z_a$.

6.6 Refinement over MOST profiles near $z = z_0$

The context of the following section is the parametrization of ocean or lake evaporation rate in weather models; we shall explore an interesting example of the crucial impact of an infinitesimally small-scale process, on the global scale!

It was noted by Miller et al. (1992) that the ECMWF (European Centre for Medium Range Weather Forecasting) model climatology for the Indonesian/Indian ocean produced (counter to the observed climatology) a double ITCZ (north and south of the equator), with an intervening dry region (a manifested "model-climate-deficiency" in a global model) and that if sea-surface temperature (SST) was arbitrarily enhanced in that region by 1^oK, a more realistic climate ensued. Why?

"The moisture supply for convection is a combination of local evaporation from the surface and advection from more remote areas. The relative importance of these two sources varies with geographical location and the scale of motion considered," (Miller et al. 1992). In the tropical "warm pool" areas, characterized by high SST and low wind speeds, local evaporation plays a particularly significant role, since advection is weak.

Up to that time, evaporation had been parametrized in the ECMWF (and most other) model(s) as:

$$E = \rho\, C_Q\, |U_a|\ (q_s - q_a) \tag{6.28}$$

where U_a is the horizontal velocity vector relative to a coordinate frame moving with the surface water; q_a the specific humidity, at the lowest model level (z_a); and q_s is the saturation

specific humidity at the ocean "surface"[3] which we may write as a function of sea-surface temperature $q_s = q_e(T_{SST})$ (saturation humidity at sea-surface temperature).

A necessary consequence of this parametrization was that, if the horizontal windspeed as resolved by the model was very small, evaporation $E \to 0$. But it is certainly the case that, even if $U_a = 0$ (and in the context of a *model*, this must be a spatial average over a grid cell, an area of say 50 km $\times$ 50 km), there is residual (unresolved) smaller-scale wind: in particular, during unstable stratification, there is buoyancy-induced turbulence, characterised by the convective turbulent velocity scale

$$w_* = \left(- \frac{g}{T_0} \frac{Q_{H0}}{\rho c_p} \delta \right)^{\frac{1}{3}} \tag{6.29}$$

where δ is the depth of the atmospheric mixed-layer (order 1 km).

Now, in the above formula for evaporation E, the transfer coefficient for moisture had (in effect) been written:

$$C_Q = {C_Q}^{(N)} \; F(L) = {C_M}^{(N)} {C_V}^{(N)} F(L) \tag{6.30}$$

where $F(L)$ was a stability correction and the neutral transfer coefficients for momentum (${C_M}^{(N)}$) and water vapour (${C_V}^{(N)}$) were specified by the formulae above (integration of the semi-logarithmic profiles MOST on the interval between z_a and the sea surface, $z = z_{0q}$. It had been assumed[4], furthermore, that $z_{0q} = z_0$.

Of course, the roughness length for momentum, too, is only a constant of integration. We have already encountered the ambiguity that results from extrapolation of the MOST profiles, valid in the turbulent surface layer at heights $z \gg z_0$, down into the sublayer where $z \to 0$. Is the implied "surface" value $q(z_{0q})$ actually equal to the true surface humidity (etc.)? Particularly when the ocean is "smooth," we should recognise a sublayer within which diffusion and (intermittent turbulent) convection are jointly responsible for vertical transport. Gordon and Hunt (1989; internal UK Met. Office note) suggested this parametrization might be inadequate at low windspeeds. The ECMWF model was therefore modified as follows:

- Convection-induced surface winds $|U_a| \to \sqrt{|U_a|^2 + \; {w_*}^2}$
- Appropriate smooth surface limits for the roughness lengths

I will focus on the second of these modifications, which is the most complex in terms of its focus on small scale processes. The improvement was possible due to the earlier work by Liu and Businger (1975).

[3] In the context of using these bulk fluxes, there is another problem in that observed ocean "surface" temperatures are sometimes "bucket" temperatures (a pail lowered from a ship), and sometimes radiometric; these temperatures can be very different from each other in times of low mixing (light winds) due to the existence of a diffusive (rather than turbulent) interfacial layer.

[4] Now, momentum and scalar roughness lengths for flow over water vary widely, in relation to the windspeed and the surface state (calm/wavy). According to Garrat (1992; see also Brutsaert, 1982, and Fairall et al., 2000) at low windspeed over an ocean the scalar roughness lengths z_{0T}, z_{0q} for heat and water vapour exceed the momentum roughness length z_0, but at high windspeed the reverse is true.

6.6.1 "Renewal" model for profiles very near the surface

Firstly, we note that there is turbulent mixing both in the lower atmosphere and in the upper ocean; and that in both cases, as we approach the interface (sea surface), $z \to 0$, we enter an interfacial layer wherein the turbulence is (at best) intermittent; molecular diffusivity must play a role. Liu and Businger (1975) provided a theory that has subsequently been applied to both sides of the interface.

Temperature of the water in the (normally-quiescent, but diffusive) sublayer undergoes continuous modification by heat conduction, which process is interrupted by sporadic ejections of sublayer elements into the turbulent layer, upon which event that region of the sublayer is "refreshed" or "flushed" with "bulk" water. Kline and others had observed this process in the laboratory.

Suppose a large parcel of air, arriving (at $t = 0^-$) from the "bulk" fluid far from the boundary, and carrying uniform temperature equal to the bulk value, T_b, has flushed clean the interfacial layer. If we neglect the lateral boundaries of this fresh, uniform layer of fluid, then the temperature of the layer is governed by:

$$\frac{\partial T}{\partial t} = \kappa \frac{\partial^2 T}{\partial z^2} \tag{6.31}$$

(but note that this entirely neglects lateral coupling: this is a 1-d transport model, ie., the structure of the temperature in the interfacial layer is assumed to be the consequence of convergences of vertical fluxes).

Now, at $t = 0^-$ we have $T(z, 0) = T_b \forall z$; but, at $t = 0$, we introduce a step change in temperature[5] at $z = 0$, $T(0, t \geq 0) = T_S$ In conjunction with the boundary-condition $T \to T_b$ as $z \to \infty$, the solution (most easily obtained by means of the Laplace transform) is:

$$T(z,t) = T_b + (T_S - T_b) \text{ erfc}\left(\frac{z}{2\sqrt{\kappa\, t}}\right) . \tag{6.32}$$

Define a distribution function $\phi(t)$ as the fractional area of the sea surface containing fluid elements that have been in contact with the surface for a time t. A reasonable choice is:

$$\phi(t) = \frac{1}{t_*}\, e^{-\frac{t}{t_*}} \tag{6.33}$$

where t_* is the average lifetime of a fluid element in the sublayer before its ejection. Then, by virtue of:

$$\begin{aligned} \overline{T}(z) &= \int_0^\infty \phi(t)\, T(z,t)\, dt \\ \overline{Q}_0 &= \int_0^\infty \phi(t)\, Q(0,t)\, dt \end{aligned} \tag{6.34}$$

[5] the essentials of the model are the same if we introduce a fixed boundary heat flux.

where $Q(z,t)$ is the heat flux, it follows that:

$$\begin{aligned} T(z) - T_b &= (T_S - T_b)\, e^{-\frac{z}{\delta_T}} \\ Q_0 &= \kappa\, \frac{T_S - T_b}{\delta_T} \end{aligned} \tag{6.35}$$

where $\delta_T = \sqrt{\kappa\, t_*}$ is a length scale characterising the depth of the interfacial layer, that depends on the sea state and thus the wind, through t_*.

Liu et al. (1979; LKB) used the above (LB) theory for the flux-profile relationship in the interfacial layer(s), matching to the MO layers higher/deeper. In effect, this amounts to a re-determination of the transfer coefficients that appear in the bulk formulation, bearing in mind that the "roughness lengths" of the extrapolated MO profiles depend on the distributions in the sublayer.

I will illustrate for the case of evaporation/atmospheric humidity in the neutral case (the case of temperature involves the interfacial layer in both fluids). The "bulk" humidity q_b in what follows is regarded as a fitting parameter; let α be the molecular diffusivity of water vapour in air; and let $q_* = -E/u_*$ be the humidity scale for the MO layer. Then, the humidity profiles in the MO layer and the underlying sublayer are:

$$\begin{aligned} q(z) - q_s &= \frac{q_*}{k_v}\, \ln\left(\frac{z}{z_{0q}}\right), \\ q(z) - q_s &= (q_s - q_b)\; e^{-\frac{z}{\delta_q}} \end{aligned} \tag{6.36}$$

where δ_q is defined (by analogy to δ_T above) by:

$$\begin{aligned} E &= \rho\, \alpha\, \frac{q_s - q_b}{\delta_q}\,, \\ \delta_q &= \sqrt{\alpha\, t_*}\,. \end{aligned} \tag{6.37}$$

LKB introduce a matching height (I'll call it z_m) at which they require continuity both in $q(z)$ and in dq/dz, which matching suffices to determine both δ_q and the roughness length z_{0Q} . They also introduce a suggestion by Brutsaert, that the renewal timescale is

$$t_* \propto \sqrt{\frac{\nu z_0}{{u_*}^3}}\,. \tag{6.38}$$

Then, defining

$$D = \frac{q_b - q_s}{q_*} = \frac{\delta_q\, u_*}{\alpha} \tag{6.39}$$

it follows that

$$D = G\, {R_r}^{1/4} {S_c}^{1/2} \tag{6.40}$$

where G is a proportionality constant; $R_r = z_0 u_*/\nu$ is the roughness Reynolds number; and $S_c = \nu/\alpha$ is the Schmidt number (ratio of kinematic viscosity to mass diffusivity) for water

vapour in air. LKB appeal to measurements of mass transfer (radioactive thorium, $S_c = 2.8$; water vapour, $S_c = 0.6$) over various surfaces with different R_r, to confirm that provided R_r exceeds about 0.5, indeed $D \propto {R_r}^{1/4} {S_c}^{1/2}$ and that the optimal value of G is $G = 9.3$. For very low R_r (smooth surface), $D = C\sqrt{S_c}$ where C is determined form the matching of the wind profile across the sublayer and the turbulent flow.

In terms of the parameter D, we can re-write the humidity profiles as

$$\begin{aligned} q(z) - q_s &= \frac{q_*}{k_v} \ln\left(\frac{z}{z_{0q}}\right) , \\ q(z) - q_s &= D\, q_* \left[1 - e^{-\frac{z\, u_*}{D\alpha}}\right] . \end{aligned} \tag{6.41}$$

Matching these profiles at height $z = z_m$ gives us:

$$\begin{aligned} ln\left(\frac{z_m}{z_{0q}}\right) &= k_v\, D\, \left[1 - e^{-\frac{z\, u_*}{D\alpha}}\right] , \\ 1 &= \frac{k_v z_m u_*}{\alpha}\, e^{-\frac{z_m u_*}{D\, \alpha}} . \end{aligned} \tag{6.42}$$

These two equations determine z_m, z_{0q} (LKB provide a table that summarises their findings for z_{0q}). Most importantly, we now have the complete mean humidity profile from $z = 0$ (where $q = q_s$) out to the base of the "model atmosphere," at $z = z_a$; so, it is straightforward to determine the bulk transfer coefficient C_Q. Far from being a constant, at low windspeeds this is found to be a strong function of stability.

6.7 Convective boundary-layer budgeting (CBLB)

The CBL is the well-mixed lower layer of the atmosphere, whose mid-afternoon mid-summer depth[6] is of order $h \sim 1$ km, and it constitutes the short-term "reservoir" from which daily biospheric CO_2 is drawn, and to which overnight CO_2 production (respiration, decay) is deposited. Indeed often at night, owing to the development of a strong surface-based temperature inversion that suppresses mixing, the CO_2 released from ground and canopy is held in a very shallow ABL (depth order 100 m) and only released to a deeper volume upon the morning re-commencement of mixing ("burning out" of the surface inversion). In response to these processes, a distinct diurnal cycle in CO_2 concentration can be observed within the ABL.

Now because of the efficient mixing in a CBL, its CO_2 concentration as seen at a point is responding, not to the local surface input $F(0)$, but to the spatial average input $\langle F(0) \rangle$ over some large region (order 100 km). In this sense the CBL's CO_2 concentration is a natural spatial integrator of the surface flux, and the CBLB technique gives us that spatial average.

[6] for which various symbols appear in these notes: here h, elsewhere δ, and commonly z_i for "height of the lowest inversion.

According to Laubach and Fritsch (2002), the first application of CBLB for CO_2 fluxes was by Wofsy et al. (1988).

To carry out a CBL budget for CO_2, it is required to determine the time changes, over intervals of the order of hours, in the volume-average CO_2 concentration (C_m for "mixed-layer" concentration), as well as the diurnal deepening and shallowing of the ABL (evolution of h). Within the scope of the simplest mathematical-conceptual model of a horizontally-uniform CBL[7], we can deduce from a simple mass balance that:

$$\frac{\Delta(C_m h)}{\Delta t} = \langle F(0) \rangle - \langle F(h) \rangle \tag{6.43}$$

where the "entrainment flux" $\langle F(h) \rangle$ is due to any leakage across the "lid" $z = h$. Thus, PBL "budgeting" permits us to measure the surface flux $\langle F(0) \rangle$ for rather large regions of uniform surface, simply by measuring the change $\Delta(C_m h) = C_{m2} h_2 - C_{m1} h_1$ over time interval $t_2 - t_1$ in the amount of CO_2 stored in the turbulent reservoir. Certain assumptions relative to the entrainment flux allow the transformation to

$$\langle F(0) \rangle = h \frac{\Delta C_m}{\Delta t} - \left(C^+ - C_m \right) \left(\frac{\Delta h}{\Delta t} - w^+ \right) \tag{6.44}$$

where C^+, w^+ are the CO_2 concentration and vertical velocity measured just above the ABL.

6.8 The flux footprint

For the interpretation of elevated point measurements of exchange fluxes between the ground and the atmosphere, it desirable to know the area of the surrounding surface which has influenced the measured flux (F). This influence is conveniently expressed in terms of the flux-footprint function Φ, in terms of which the vertical flux F at a detector at location $(x = y = 0, z = z_m)$ is given by

$$F(0, 0, z_m) = \int_{-\infty}^{\infty} \int_{-\infty}^{\infty} \Phi(x', y', z_m) \, Q_0(x', y') \, dx' \, dy' \, . \tag{6.45}$$

Here Q_0 is the (possibly spatially-varying) surface flux density, and the footprint $\Phi(x', y', z_m)$ gives the flux at $(0, 0, z_m)$ due to a continuous point source of unit strength on ground at $(-x', -y')$. For situations with symmetry in the crosswind (y) direction, one may consider the flux at $(x = 0, z = z_m)$ as being due to a composition of contributions from elementary line sources, introducing a $1 - D$ footprint ϕ defined such that

$$F(0, z_m) = \int_{-\infty}^{\infty} \phi(x', z_m) \, Q_0(x') \, dx' \, . \tag{6.46}$$

[7]If the CBL were indeed strictly uniform, there would be no need to spatially average the surface flux in the first place. However we may visualize the situation where the surface CO_2 flux is patchy, but the wind statistics sufficiently close to uniform that the formulation makes sense.

Enunciation of the concept of the flux footprint owes to Schuepp et al. (1990) and Leclerc and Thurtell (1990). Reviews on the subject are given by Vesala et al. (2008) and by Schmid (2002). Some of the other (many) papers on the topic include Wilson and Swaters (1991), Horst and Weil (1994), Flesch (1996), Schmid (1994, 1997), Hsieh et al. (2000), Kormann and Meixner (2001). Qualitatively, the along-wind limits to the footprint are easy to understand. At the nearby edge, the limitation is that there should be enough travel time to allow the tracer emitted by the elementary source on ground "time to climb" ($t_\uparrow \sim z_m/\sigma_w$) to the detector aloft. However the mere presence at the detector (eddy covariance system) of mass from a given source does not ensure a contribution by that source to the mean *flux* at the detector — for in order to contribute to the vertical flux, material arriving at the detector must have, in the mean, a non-vanishing vertical velocity. Fluid elements carrying material emitted from elements of the surface that lie very far upwind (or very far crosswind) arrive at the detector with a random vertical velocity that vanishes in the mean (Wilson & Swaters, 1991), the consequence being an upper limit ($t^\sim$, "time to forget") to the flight times contributing to the flux at the detector. Neglecting mean velocity shear, an alongwind range for the footprint can be obtained upon multiplying these time-limits by mean windspeed.

Numerous quantitative studies of the flux footprint have been made, most often for fluxes measured in the surface layer. Analytical solutions include those by Weil (1991); Hsieh et al. (2000); Kormann (2001). Numerical solutions for the footprint, based on the Lagrangian stochastic model of dispersion, have been given by . Perhaps the most detailed footprint theory to date is that of Kjlun et al. (2004), which addresses detection points at any height in the Planetary Boundary Layer, and for all stability conditions. All these studies have in common the limitation that they assume an undisturbed (ie. horizontally-uniform) flow.

6.8.1 An oversimplified analytical flux footprint

Bosanquet and Pearson (1936; see Pasquill and Smith 1983; Pasquill 1972) gave a beautifully simple solution for a continuous line source (strength q) lying at $x = z = 0$ in a flow with $\overline{u}(z) = U$ =const. and $K_c = k_v u_* z$:

$$\overline{c} = \frac{q}{k_v u_* x} \exp\left(-\frac{Uz}{k_v u_* x}\right) . \tag{6.47}$$

The flux due to a unit source ($q = 1$) is

$$\begin{aligned} F &= -\left(k_v u_* z\right) \frac{\partial \overline{c}}{\partial z} \\ &= \frac{U}{k_v u_*} \frac{z}{x^2} \exp\left(-\frac{Uz}{k_v u_* x}\right) . \end{aligned} \tag{6.48}$$

Hence the flux footprint for a measurement at $(x = 0, z = z_m)$ is:

$$\phi(x, z_m) = \frac{U}{k_v u_*} \frac{z_m}{x^2} \exp\left(-\frac{U z_m}{k_v u_* x}\right) . \tag{6.49}$$

For fixed z_m the footprint function is distributed along the (positive, ie. upwind) x-axis according to the factor $x^{-2}\ e^{-\alpha/x}$. By setting $\partial\phi/\partial x = 0$ we find the maximum of the footprint function occurs at

$$x = \frac{U\, z_m}{2\, k_v\, u_*}\ . \tag{6.50}$$

This is an incorrect footprint function, for it neglects wind shear and is restricted to neutral stratification, but it serves to illustrate the principles. We would say that the flux measured at $(x = 0, z = z_m)$ is determined by the mean value of the surface source strength $Q_0(x', y')$ over the along-wind span of the footprint.

6.9 Evapotranspiration

In the most fundamental terms, the mean vertical flux density of water vapour ("evaporative flux") across the plane $z = z_M$ is:

$$E(x, y, z_M, t, T) = \overline{w\rho_v} = \frac{1}{T}\int_{t-T}^{t} w(x, y, z_M, t')\ \rho_v(x, y, z_m, t')\ dt'\ , \tag{6.51}$$

with simplification possible if it is the case (as usually assumed) that the flow is sufficiently close to being uniform that $\overline{w} = 0$ (one would also make the WPL correction).

Given the appropriate instruments, one may measure evaporation (or evapotranspiration) at a given site. This takes some time, money and effort. Naturally it would be useful to be able to estimate evaporation from related, simpler measurements. Particularly in climatology, people have always wished to do this, and may have assumed that hotter weather entails greater evaporation, etc. The first step on the road to a satisfactory formula for evaporation was made by Penman (1948), who reasoned as follows.

Assume a surface of pure water at temperature T_s (for "surface", or "source"), where the vapour pressure is $e_s = e_*(T_s)$. This could be the surface of a lake, or a wet soil, an evaporation pan (Lim *et al.*, 2012), or a piece of blotting paper, but the point is, we invoke a "bulk" treatement; we do not think about gradients in temperature at the source. Now consider a point in the air, remote from the surface, at which temperature and vapour pressure (implicitly, mean values) are T_a, e_a. Invoke the "Ohm's Law analogy" according to which the exchange fluxes (per unit surface area of the source) are modelled as:

$$\begin{aligned} Q_H &= \rho\, c_p\, \frac{T_s - T_a}{r_h}\ , \\ Q_E &= \frac{\rho\, c_p}{\gamma}\, \frac{e_s - e_a}{r_v} \end{aligned} \tag{6.52}$$

where γ [$\mathrm{Pa\,K^{-1}}$] is the psychrometric "constant"

$$\gamma = \frac{p\, c_p}{L_v \varepsilon}$$

($\varepsilon \approx 0.63$ is the ratio of the molecular weights of water and "air"). This evidently is not in fact constant, for it involves p, the air pressure.

These equations, in which r_h, r_v are empirical transfer resistances [s m^{-1}] for the "diffusion pathway" between the "source" (evaporating body) and the sink (atmosphere), constitute an "aerodynamic transport model." The resistances may readily be related to the dimensionless Nusselt and Schmidt numbers, which in turn may be correlated to dimensionless numbers describing the body and the flow about it.

Penman's model is called the "combination model" because, in conjunction with eqns (6.52), it invokes the surface energy balance, such that the "energy supply" (in the case of a bare soil surface, $Q^* - Q_G$) constrains the sum $Q_H + Q_E$. Without going into details of the algebra, Penman's combination equation is

$$Q_E^P = \frac{s}{s+\gamma}\,(Q^* - Q_G) \;+\; \frac{\rho c_p\,(e_*(T_a) - e_a)\,/r_h(\overline{u})}{s+\gamma} \tag{6.53}$$

where $s = \partial e_*(T)/\partial T$ [Pa K^{-1}] is the slope of the saturation vapour pressure curve, $\overline{u}$ is the mean wind speed, and the Q_G in the "energy supply" term is subject to appropriate interpretation. This results hinges on an assumption that $r_h \equiv r_v$, which in many circumstances is very reasonable, though not necessarily exact. Raupach (2001) thoroughly reviews this "combination equation."

Penman's combination equation is profoundly useful, for (since $E^P = Q_E^P/L_v$) it provides a quantitative measure of "potential evapotranspiration" (also known as "atmospheric demand") — the amount of water that *would* be evaporated under the prevailing climate (as specified by weather station measurements of Q^*, T_a, e_a, $\overline{u}$) if the surface were freely supplied with water. As such, Q_E^P can be regarded as a climate variable. Correlations exist for the aerodynamic resistance r_h as function of mean wind speed.

Eq. 6.53 assures us that evaporation may take place even into a saturated atmosphere, provided there is an "external" energy supply. Conversely, even if there is no "external" energy supply evaporation may occur, the latent heat being taken from the surrounding air.

In general, the evaporating surface is not saturated, thus, there is an additional transfer resistance in the "diffusion pathway" for water vapour. For instance, consider the case of transpiration from a (single) leaf, sitting (say) at height z_l, with the reference measurements T_a, e_a made at height $z = z_R$ (reference height) in a horizontally-uniform atmosphere. Clearly the pertinent radiant energy supply is the net radiation at the leaf surface (averaged over the leaf). If the leaf surface (necessarily taken as having a constant temperature etc., in the bulk treatment) is taken as the heat source, then we may split the heat transfer resistance r_h into the sum of a leaf boundary-layer resistance r_{hb}, and an aerodynamic resistance r_{ha} from the free airstream outside that boundary layer, to the reference height. Now considering the "diffusion pathway" for water vapour (quotes, because turbulent convection is the dominant

process along at least part of the path), the stomatal resistance[8] r_s impedes water loss from the sub-stomatal cavities, whereas (as noted above) the exterior leaf surface is still considered the "source" for heat exchange. If we assume saturation within the stomatal cavity, then:

$$\begin{aligned} r_h &= r_{hb} + r_{ha} \ , \\ r_v &= r_{vb} + r_{va} + r_s \ . \end{aligned} \tag{6.54}$$

Within the compass of K-theory, the "aerodynamic" resistance between heights z_1, z_2 in the atmosphere is easily shown to be:

$$r_a = \int_{z_1}^{z_2} \frac{dz}{K(z)} \tag{6.55}$$

and we recall that many atmospheric experiments suggest that, at least in undisturbed flow not too close to sources, $K \approx K_h \approx K_v$. There are many reasons to be cautious about extrapolating that convenient "almost equals" to the case where the "diffusion pathway" includes a "leg" within a canopy, but after all, we might picture our single leaf as the sole leaf around, living in a desert, so to speak, and having negligible influence on the flow. So in that circumstance, we could argue fairly argue that $r_{ha} \approx r_{va} = r_a$, with r_a inversely proportional to windspeed, and potentially stability-dependent.

What of the leaf boundary-layer resistance? This boundary layer is neither fully "laminar" (in which case the resistances would be in the ratio of the molecular diffusivities) nor turbulent – we have already looked at how such a layer, intermittently "flushed" by eddies, may be treated in the "renewal" model. Without getting bogged down, let us hypothesize that $r_{hb} \approx r_{vb} = r_b$. It is well known that boundary layer resistances on flat plates in a laminar stream are proportional to to the speed (u) of the stream approximately as $r_b \propto u^{-1/2}$.

Accepting that vapour exchange is limited (relative to heat exchange) by a single supplementary resistance,

$$\frac{r_v}{r_h} = \frac{r_a + r_b + r_s}{r_a + r_b} = 1 + \frac{r_s}{r_h} \ . \tag{6.56}$$

Monteith generalized the Penman equation to account for this additional resistance r_s, assuming that the vapour pressure inside the stomatal cavity is $e_s = e_*(T_l)$ where T_l is the leaf temperature. The resulting Penman-Monteith equation is:

$$Q_E = \frac{s}{s + \gamma\,(1 + r_s/r_h)}\,(Q^* - Q_G) \ + \ \frac{\rho c_p\,(e_*(T_a) - e_a)\,/r_h(\overline{u})}{s + \gamma\,(1 + r_s/r_h)} \ . \tag{6.57}$$

It is common in environmental sciences to consider a full crop canopy as equivalent to a single "big leaf," and to invoke eqn(6.57) as the "big leaf model" with an effective "canopy resistance" r_c standing in place of the individual leaf stomatal resistance r_s. Experience shows

[8] Instruments exist to measure stomatal resistance, and inexact semi-empirical formulae exist for its prediction from plant- and atmospheric variables.

that r_c is a fairly well-behaved diagnostic parameter (it can be inferred from measurements), but is not easy to predict, or to relate to other properties. There are several reasons for the difficulty, including the underlying uncertainty as to stomatal resistance (even given all factors ever thought to be pertinent); the fact that in the big leaf model one overlooks the fact that there are both sunlit and shaded classes of leaves; that not all leaves experience the same humidity and temperature; and that eddy diffusion is not a valid description of transport in a plant canopy (e.g. Raupach and Finnigan 1988).

In principle, a better diagnosis of canopy evapotranspiration may be made by combining the momentum, temperature and humidity equations, as well as a canopy radiation model, to calculate a multi-layer canopy microclimate with which the leaves interact. This has been done, and even for the case of disturbed winds (Naot & Mahrer, 1991), but it may be overkill. Wang and Leuning (1998) and Leuning et al (1998) prove that a refined application of the Penman-Monteith equation that differentiates sunlit and shaded leaf classes for a single canopy layer is a sufficient level of description for diagnosing evaporation on a seasonal timescale, with half-hourly time-steps (the single-layer model was compared with a multiple-layer canopy, and differences proved unimportant).

Finally, if our reference level is just a few meters over the crop, the reference properties T_a, e_a must themselves be functions of the evaporation rate, ie. these are not "external" variables. If we are interested in evaporation over a larger region, we may wish to use values characteristic of the whole ABL. McNaughton and Spriggs (1986) and Jarvis and McNaughton (1986) initiated this approach, along the way introducing an interesting and useful distinction between short crops (eg. grass), that are relatively weakly coupled to the above-canopy flow, and at the opposite extreme, forests, which due to the vigorous large eddies, are closely coupled. This explains why evapotranspiration over short grass closely follows the radiative energy supply $Q^* - Q_G$, whereas evaporation from forests may be more closely correlated with the saturation deficit $e_*(T_a) - e_a$. The thrust of McNaughton's work was to account for the influence of surface evaporation on the state of the ABL, so that the latter is not (wrongly) considered indifferent to the injection of vapour.

6.10 Inverse dispersion method

Determination of ground-air gas emissions (e.g. methane flux to the atmosphere from a cattle feedlot) can be technically difficult, but a simple approach is to infer the emission rate (Q, $\mathrm{kg\,m^{-2}\,s^{-1}}$) from the more easily measured aerial concentration (C) that the source causes. This is the "**inverse dispersion**" approach, and is based on the use of a theoretical C/Q ratio, say $(C/Q)^*$, that is computed by an atmospheric dispersion model on the basis of the prevailing meteorological conditions: the unknown emission rate is estimated as $Q = C/\left(C/Q\right)^*$.

Flesch et al. (1995) demonstrated the advantages of using a backwards-in-time Lagrangian stochastic (bLS) trajectory model to determine the needed $(C/Q)^*$ ratio, and Flesch et al. (2004) performed a field experiment to demonstrate the very satisfatory accuracy of bLS in the ideal setting of undisturbed flow on flat terrain. Over uniform terrain wind statistics are well described by Monin-Obukhov (MO) similarity theory, and almost all the many *applications* of bLS (e.g. Flesch *et al.*, 2005b; Flesch *et al.*, 2007; Flesch *et al.*, 2009) have used "MO-bLS," this label designating that the Lagrangian model had invoked MO wind statistics.

However at most natural sites where one might contemplate to apply inverse dispersion, winds are disturbed by obstacles (terrain, animals, trees, buildings, etc.), and this compromises the validity of adopting a $C - Q$ relationship that stems from trajectories computed using MO-bLS. Flesch et al. (2005a) studied the viability of *ignoring* flow disturbance, and found that so long as the concentration (C) detector is far from any obstacles, MO-bLS sustains acceptable accuracy. Wilson et al. (2010) explore the utility of adopting in such cases a more complex, three-dimensional Lagrangian transport model, which (necessarly) must be provided (an approximation to) the disturbed wind field and show that if the concentration detector perforce must be placed close to a flow disturbance, then it *is* advantageous to adopt "3D-bLS," i.e. to approximate the spatial variation of the disturbed flow (in this case, by way of a numerical simulation as in Bourdin & Wilson, 2008) and drive a fully three-dimensional Lagrangian model to compute $(C/Q)^*$.

Consider the task of measuring gas transfer from ground to atmosphere, over a chemical spill, or a field emitting pesticide residue, etc. Standard methods are applicable only to large, uniform source areas (horizontal extent of order 100 m) and demand either fast response instruments (eddy correlation method) or sensitive differential measurements of vertical concentration gradient (gradient methods). But suppose we define a "source-receptor relationship" $UC/Q = n$, relating the strength Q of the source to the average concentration C at a nearby point (U is a reference windspeed). If n were known, Q could be inferred from the simpler measurements U, C. This is sometimes called "inverse dispersion", and requires the use of a suitable dispersion model, which must be provided measurements of the atmospheric state: at a minimum, the friction velocity u_*, Obukhov length L, roughness length z_0, and mean wind direction β. The procedure could be represented symbolically as:

$$Q^{(est)} = Q^{(est)}\left(C_P | u_*, L, z_0, \beta\right) \ . \tag{6.58}$$

This approach was introduced for circular sources by Wilson et al., (1982). A far more flexible instance of this approach was introduced by Flesch et al. (1995), based on (an

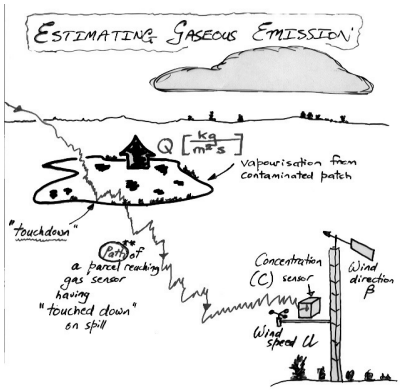


Figure 6.2: Schematic for the inference of source emission rate Q from measured concentration C and wind speed and direction, by means of knowledge of backward trajectories.

ensemble of N) *backward* trajectories (Fig. 6.2),

$$\begin{aligned} Q^{(est)} &= \frac{U\, C_P}{n} \\ n &= \frac{1}{N} \sum_i \frac{2}{w_{0i}/U} \end{aligned} \tag{6.59}$$

In this formula U is a reference windspeed (whose explicit inclusion renders the "magic number" n dimensionless). The summation runs over all "touchdowns" of trajectories on the source, and w_{0i} is the magnitude of the vertical velocity of the i^{th} touchdown. A useful feature of this approach is that the source need not be known or specified in advance; it may be of any shape, and in any position and orientation with respect to the mean wind vector and the observation point. Laser line-average concentration measurements (C) are particularly advantageous for this type of inference, since they less the uncertainty stemming from the lateral (y) spread of the plume off the source.

Part III

Above and Below the Surface Layer

Chapter 7

The "Horizontally-Uniform" ABL

If (hypothetically) we wished to compute the fate of pollutants at distances of more than a kilometer or so from their source, we should require to know the distribution of the mean wind and the turbulence statistics above the surface layer. In this course our treatment of the outer layer of the ABL will be rather schematic. We can begin by saying a few things that the ABL, taken as a whole, is *not*. The ABL (in general) is not horizontally-uniform; it is not stationary, for it grows and shrinks daily (Stull's 1988 Figure 1.7 gives a nice pictorial representation of the idealized daily cycle in the ABL state); it is not isolated from the free atmosphere (in general there are fluxes across the "entrainment layer"); and it is not necessarily possessed of a clearly-demarcated "top." Furthermore the velocity field in the ABL frequently features "coherent structures," in which (observed in a motion-following coordinate system) there is a temporally-sustained spatial velocity correlation over long distances: thermals, plumes, dust devils, and roll vortices. Relative to the mean flow, these are "unresolved motion." But they probably could usefully be distinguished from that part of the unresolved motion normally called "turbulence."

We have studied the atmospheric surface layer in some detail[1], and now consider the structure of the outer part of the ABL. What do the governing equations tell us? In their instantaneous form, they are closed, but could only be solved numerically. To solve them, we would require impossibly-high spatial and temporal resolution (eg. tiny grid spacing to resolve eddies down to the size of the Kolmogorov length). A modern numerical approach ("Large Eddy Simulation," LES) concentrates on predicting explicitly the evolution of the "large eddies." One considers volume-averaged variables $\langle w \rangle$ etc., and by volume-averaging the equations, one obtains an unclosed set. A closure scheme is adopted to model the influence of the unresolved scales on the resolved scales (ie. gradients in fluxes carried by unresolved scales). The simplest LES closure (attributed to Smagorinsky) invokes an eddy viscosity $K = q\,\ell$ to compute the subgrid fluxes; the length scale ℓ is computed as some multiple of

[1]More specifically, we have dealt with the "inertial sublayer," which is the part of the surface layer lying above the roughness sublayer, and in which Monin-Obukhov similarity theory applies. Later we will cover the structure of a canopy layer at the base of the ASL.

the size of the averaging volume (e.g. $\ell \propto \sqrt[3]{\Delta x \Delta y \Delta z}$) and the velocity scale q is based on the shear in the resolved velocity (e.g. $q \propto \ell |\partial \langle u \rangle / dz|$).

But suppose we "average over" all the eddies, ie. the turbulence is entirely unresolved, we deal only in mean properties (defined over times or distances very large compared to turbulence time and length scales). We seek guidance on the "long-time" (or "long-line") statistical properties. Clearly in general we have a very complex and unclosed set of equations governing mean properties. There is no wholly satisfactory closure scheme available. This approach, with considerable labour, can generate predictions of particular cases. But we can extract little of generality.

What if we restrict ourselves to the idealisation of horizontal-uniformity? We are certainly free to do so, and it will of course eliminate many terms from the governing equations. We have already seen an argument to the effect that the large scale pressure gradient is impressed through the entire ABL, which results in the mean wind structure having the form of a "velocity deficit" law, and we know that by introducing a constant eddy diffusivity K to close those equations, we are lead to the classical, and incorrect, Ekman wind spiral. One can (e.g. Hassid and Galerpin 1983; Wilson and Flesch 2004; Wilson 2012) use a better first-order closure scheme (than "constant K") to close the mean equations, or turn to higher-order closure (e.g. Mellor and Yamada 1974; André et al. 1978; Abdella and McFarlane 1997). It is possible to predict with a degree of skill the mean profiles in the outer ABL, but they are very sensitive to specific details of the particular flow, and it is not possible to say anything very general about those profiles except that, generally speaking (certainly in the unstable case), gradients are not as large aloft as they are near the surface: thus, in the unstable case, we often talk of the "mixed layer." The term "mixed layer" is sometimes loosely used to refer to the whole convectively-unstable ABL (the "CBL"); but more-properly it should be reserved for the outer part of the CBL, which indeed often is well-mixed, in the sense that, above the ASL and below the entrainment layer, the mean potential temperature and humidity and even the mean windspeed may show very little variation with height.

So much for what "theory," in the form of the rigorous expression of the conservation laws, can tell us. Once again, it has been found that a similarity theory lends most generality for least expenditure of effort. But only with respect to predicting properties of the turbulence: "there is no effective similarity theory for mean profiles in the mixed layer" (Wyngaard 1985), although the effort has been made (e.g. Garratt et al. 1982).

As an introduction to the idealized daily evolution of the ABL, Figure (7.1) shows the observed potential temperaure profiles of Day 33 of the Wangara experiment, along with a numerical simulation (Wilson 2012) of the heat budget

$$\frac{\partial \overline{\theta}}{\partial t} = - \frac{\partial \overline{w' \theta'}}{\partial z} \tag{7.1}$$

using a $K = \sigma_w^2 \tau$ closure. At 09:00 a "residual mixed layer" lies above the nocturnal inver-

sion, and is itself "capped" by an alevated inversion. Daytime sensible heat injection (Q_{H0}) progressively "burns out" the noctural inversion, and the mixed layer, now continuous to ground (or rather, to an unstable surface layer) continues to grow into the elevated capping inversion. (Inclusion of radiative divergence on the rhs of Eq. 7.1 is necessary, in order to properly simulate the evening cooling phase.)

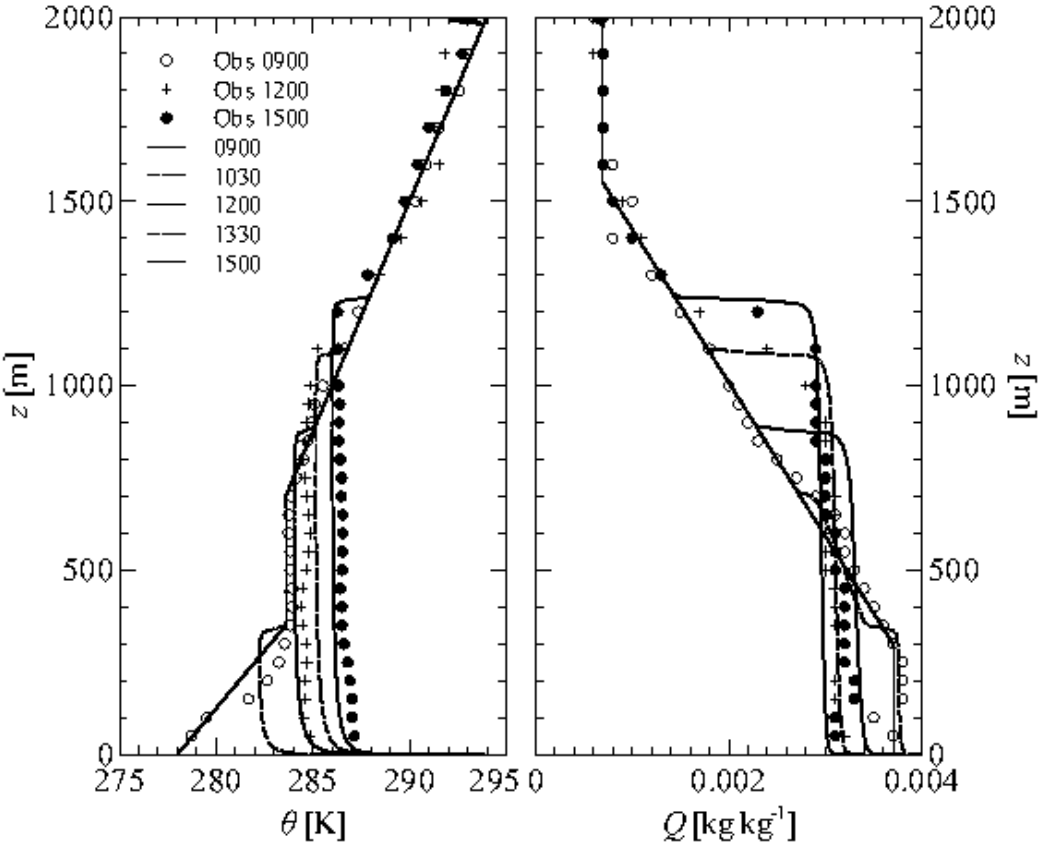


Figure 7.1: Potential temperature profiles (left) and specific humidity profiles (right) of Day 33 of the Wangara experiment (symbols), compared with a numerical solution (lines) of the heat and humidity budget equations using a K closure.

7.1 Partial list of ABL experiments

- The Wangara experiment (Clarke *et al.*, 1971; Hess *et al.*, 1981; Hicks, 1976; Hicks, 1981).
- The Minnesota experiment (Izumi & Caughey, 1976)

7.2 Multi-layer description of very convective CBL over land

For $\delta/(-L) \geq 50$, a 3-layer picture (Table 7.1) of the well-developed CBL is useful. We will focus especially on the ideal *mixed layer*, which represents the simplest state of the outer ABL. Ideally, the mean property gradients are height invariant, but they evolve with time throughout the day (for an example from the Wangara experiment, see Figure **??**). Nevertheless the CBL is interesting in the context of our course because of a phenomenon that long puzzled atmospheric dispersion theorists.

The vertical velocity in the CBL must be regarded as having a skew distribution: at a given time some roughly 40% of the horizontal plane is in a state of ascent (collectively, the thermals) and the residual area undergoes descent. This means that if a plume is released into the CBL, it will tend to *sink* until such time as reflection off ground causes it to rise. As we shall later see, that behaviour is nicely captured by the modern Lagrangian stochastic dispersion model (Luhar and Britter 1989).

Table 7.1: The three named layers of the ideal convective boundary layer. Some authors introduce a fourth layer, the "convective matching layer," covering the height range $|L| \ll z \ll \delta/10$; in this layer "local free convection scaling" applies, the controlling variables being chosen as $(z, Q_{H0}/\rho_0 c_p, g/\theta_0)$ (i.e. both u_* and δ are considered irrelevant). For most purposes, little is gained by admitting this extra layer.

Height	Layer's Name	Scaling	Scales
$0.8 - 1.2\delta$	Entrainment Interfacial	-	-
$0.1 - 0.8\delta$	Windless Convection (Mixed Lyr)	Mixed Lyr	δ, w_*, θ_*
$0 - 0.1\delta$	Surface Lyr	Monin-Obukhov	L, u_*, θ_*

Referring to Table 7.1 we note that in the mixed layer u_* is considered irrelevant: this is because there is (ideally) no wind shear, so that the whole layer is in a state of uniform translation that has no effect on its structure. However the surface heat input Q_{H0} has a profound effect, as does the depth (δ or z_i of the CBL. Thus the set of controlling variables is assumed to be $(\delta, g/\theta_0, Q_{H0}/\rho_0 c_p)$. From these we obtain a complete set of scales:

$$\delta, \quad w_* = \left(\frac{g}{\theta_0} \, \frac{Q_{H0}}{\rho_0 c_p} \, \delta \right)^{1/3} \quad , \quad \theta_* = \frac{Q_{H0}}{\rho_0 c_p w_*} \, . \tag{7.2}$$

Quasi-equilibrium of the CBL

Suppose $\delta = 2000$ m, $Q_{H0} = 200\,\mathrm{W\,m^{-2}}$. Recall that the net radiation is partitioned at ground into sensible and latent heat fluxes in such a way that the surface energy balance is

$$Q_* = Q_{H0} + Q_{E0} + Q_G \tag{7.3}$$

and that Q_* can easily be as large as $500\,\mathrm{W\,m^{-2}}$ on an early afternoon in midsummer: so this is not a particularly high estimate of Q_{H0}. From these values, $w_* = 2.5\,\mathrm{m\,s^{-1}}$, and we may define a mixing timescale for the CBL as $\Gamma = \delta/w_* \sim 15$ min. The CBL "adjusts" in about 15 min, or, we can say that if external conditions (eg. cloud cover) abruptly change, the CBL will quickly come to a new equilibrium.

Velocity statistics in the CBL

According to Hicks (1985), within the layer $0.1 \leq z/\delta \leq 0.6$:

$$\begin{aligned} \overline{w'^2} &= 1.2{u_*}^2 + 0.35{w_*}^2 \,, \\ \overline{v'^2} &= 3.6{u_*}^2 + 0.35{w_*}^2 \,, \\ \overline{T'^2} &\approx 3.2{T_*}^2 \,. \end{aligned} \tag{7.4}$$

This is not quite mixed-layer scaling, for a dependence on u_* is included.

Sometimes one needs formulae for the flow statistics that apply throughout the CBL. For example, Weil (1990) uses:

$$\frac{{\sigma_w}^2}{{w_*}^2} = \left[\frac{{u_*}^3}{{w_*}^3} \left(1.6 - \frac{z}{\delta}\right)^{3/2} + 1.2\,\frac{z}{\delta}\left(1 - 0.98\,\frac{z}{\delta}\right)^{3/2} \right]^{2/3} . \tag{7.5}$$

Empirical formulae can be found for most other statistics.

7.3 Velocity spectra

Fig. (7.2) is a schematic wavenumber spectrum. The shape of the spectrum in the energy-containing range depends on the specifics of the flow. However the smaller eddies of the universal equilibrium range are considered to be isotropic and to have statistics independent of details of energy production, depending only on the overall spectral flux[2] ϵ and (in the dissipation range) the viscosity ν (see earlier material on the Kolmogorov hypotheses). As the Reynolds number increases, the separation in scale $k_d - k_e$ between the dissipation range and the energy-production range increases.

7.3.1 Velocity spectra for the unstable ABL

Following the terminology of Kaimal et al. (1972), whose influential paper on spectra is based on the Kansas data, let n be true (**n**atural) frequency; then for observations at height z where windspeed is $\overline{u}$ define a dimensionless frequency $f = nz/\overline{u}(z)$.

[2]According to the notion of an energy "cascade", the transfer-rate down-scale is just ϵ, which is the rate of conversion of TKE to heat. That is, according to this idealized spectral equilibrium of the mix of eddies, TKE is not "accumulated" in any scale-range but rather, is produced at rate ϵ at large scales, dissipated at rate ϵ at dissipation scales, and in short, merely "passed down" the intermediate range of scales.

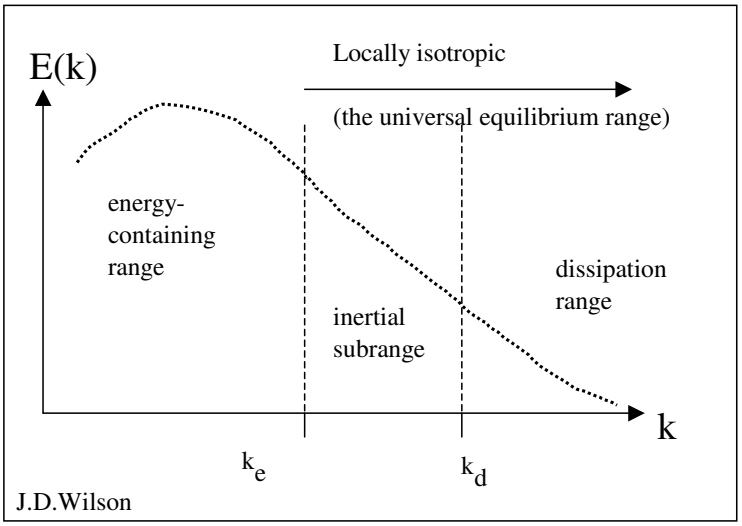


Figure 7.2: Schematic wavenumber spectrum. If l_e is a length scale characterizing the largest eddies, which are likely to be on the scale of the flow domain (eg. ABL depth δ) then a wavenumber characteristic of the production region is $k_e \sim 1/l_e$. The wavenumber marking the transition into the dissipation range (where viscosity plays a role) is $k_d \sim 1/\eta_K$ where η_K is the Kolmogorov length.

From the Kolomogorov law for the inertial subrange, it is expected that the spectra S_{uu}, S_{vv}, S_{ww} scale as:

$$\frac{nS_{\alpha\alpha}(n)}{{u_*}^2\ {\phi_\epsilon}^{\frac{2}{3}}} \propto\ f^{-\frac{2}{3}} \tag{7.6}$$

where the function $\phi_\epsilon(z/L)$ is defined by

$$\frac{k_v z}{{u_*}^3}\,\epsilon = \phi_\epsilon\left(\frac{z}{L}\right)\ . \tag{7.7}$$

Scaled this way, spectra should be universal in the inertial subrange[3]. This was confirmed by the Kansas experiments. However as regards the energy containing range, spectra of u', v' (particularly) in unstable stratification showed no particular order or consistency when plot-

[3]If local equilibrium applies

$$P = \epsilon = -\overline{u'w'}\ \frac{\partial \overline{u}}{\partial z}\ +\ \frac{g}{T_0}\ \overline{w'T'}\,, \tag{7.8}$$

and so we have

$$\phi_\epsilon\left(\frac{z}{L}\right) = \phi_m\left(\frac{z}{L}\right) + \left(\frac{z}{L}\right)\ . \tag{7.9}$$

ted this way. The later Minnesota experiment showed the wavelength λ_{mx} of the spectral peak in u', v' to be virtually independent of height z, but varying with the ABL depth δ such that $\lambda_{mx} \sim 1.5 z_i$. According to Kaimal (1978), analysis of spectra from the Kansas experiments indicated that "some length scale other than z controlled the low-frequency spectral behaviour in the horizontal components.... the evidence from the Kansas and Minnestota experiments points to a horizontal velocity field that follows different similarity laws in different regions of the spectral range in the surface layer" (see also p356 of Wilson 2008).

Hojstrup (1982) presented "a simple model that describes velocity spectra under stability ranging from neutral throughout the unstable range, from close to ground up to a height of $z_i/2$, where z_i is the height of the lowest inversion." Hojstrup's formulae are:

$$\begin{aligned}
\frac{nS_{uu}(n)}{{u_*}^2} &= \frac{0.5 f_i}{(1+2.2\ f_i)^{\frac{5}{3}}} \left(\frac{z_i}{-L}\right)^{\frac{2}{3}} + \frac{105\ f_{ru}}{(1+33 f_{ru})^{\frac{5}{3}}} \frac{(1-z/z_i)^2}{(1+15 z/z_i)^{2/3}} \\
\frac{nS_{vv}(n)}{{u_*}^2} &= \frac{0.95 f_i}{(1+2\ f_i)^{\frac{5}{3}}} \left(\frac{z_i}{-L}\right)^{\frac{2}{3}} + \frac{17\ f_{rv}}{(1+9.5 f_{rv})^{\frac{5}{3}}} \frac{(1-z/z_i)^2}{(1+2.8 z/z_i)^{2/3}} \\
\frac{nS_{ww}(n)}{{u_*}^2} &= F(f, \frac{z}{z_i}) \frac{0.95 f_i}{(1+2\ f_i)^{\frac{5}{3}}} \left(\frac{z_i}{-L}\right)^{\frac{2}{3}} + \frac{2\ f}{(1+5.3 f)^{\frac{5}{3}}} 1 - z/{z_i}^2
\end{aligned} \tag{7.10}$$

where

$$\begin{aligned}
f_i &= \frac{n z_i}{\overline{u}(z)} \\
f_{ru} &= \frac{f}{1+15 z/z_i} \\
f_{rv} &= \frac{f}{1+2.8 z/z_i} \\
F\left(f, \frac{z}{z_i}\right) &= \sqrt{\frac{f^2 + (0.3 z/z_i)^2}{f^2 + (0.15)^2}}
\end{aligned} \tag{7.11}$$

The filter function F cuts out low frequency power from w near ground.

The variances implied by these empirical formulae are:

$$\begin{aligned}
\frac{{\sigma_u}^2}{{u_*}^2} &= 0.6 \left(\frac{z_i}{-L}\right)^{2/3} + 4.8 \frac{(1-z/z_i)^2}{(1+15 z/z_i)^{2/3}} \\
\frac{{\sigma_v}^2}{{u_*}^2} &= 0.7 \left(\frac{z_i}{-L}\right)^{2/3} + 2.7 \frac{(1-z/z_i)^2}{(1+2.8 z/z_i)^{2/3}}
\end{aligned} \tag{7.12}$$

and these values agree well with those given by Panofsky et al. (1977).

Fig. (7.3) gives (similar, but earlier) idealized spectra of u, v, w in the unstable ABL, from Kaimal (1978)[4]. Firstly, notice that at large heights, the spectra for u, v, w are all similar

[4]These earlier formulae from Kaimal, according to Hojstrup, are not in good agreement with data for small $z/(-L)$. Note that the spectra have not been normalised on ϕ_ϵ, and so do not collapse at high frequency.

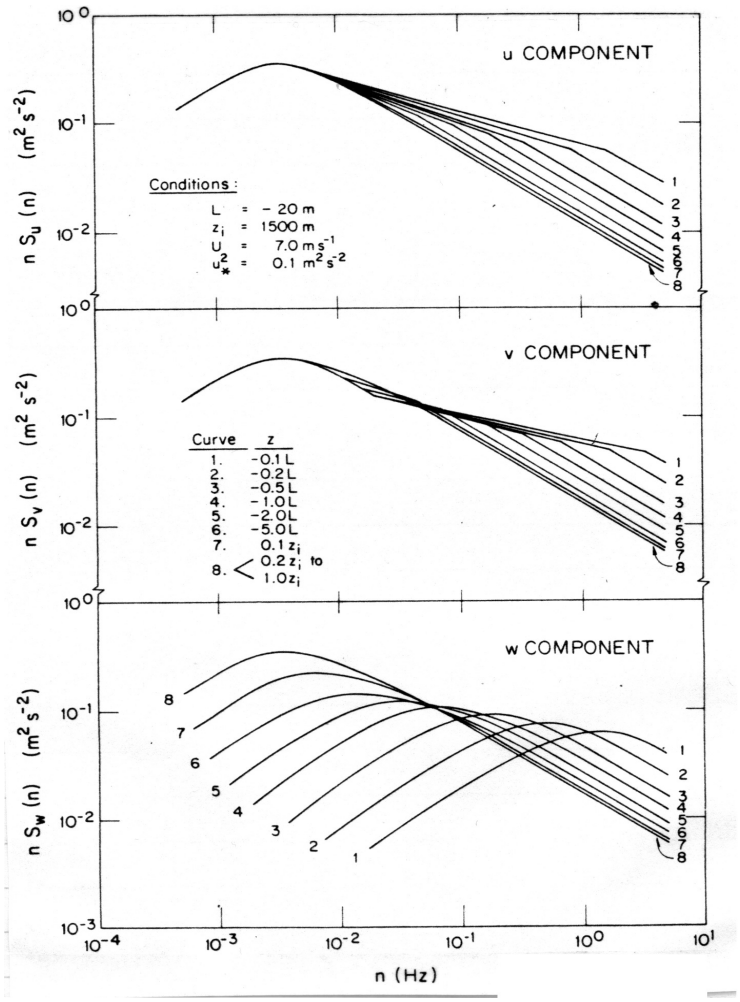


Figure 7.3: Height-dependence of power spectra in the neutral or unstable ABL (from Kaimal, 1978).

in shape, the spectral peaks all occurring at the same (true) frequency. However "the w spectrum encounters a steady depletion of energy on the low-frequency side as z approaches zero" (Kaimal), whereas as the ground is approached the low frequency ("inactive") part of the u', v' spectra is unchanged, while additional power appears at high-frequency. According to Kaimal, "in the surface layer, the velocity field is essentially two-dimensional at low frequencies ... and becomes truly three-dimensional at wavelengths shorter than the height above ground."

7.4 The stable boundary layer (SBL)

The boundary-layer *may* remain reasonably well-mixed overnight, if the winds are exceptionally strong, so that surface cooling is unable to build a strong ground-based inversion, and/or if cloud cover prevents significant stabilization (weak or non-existent surface cooling). Assuming neither of these eventualities prevails, a strong ground-based nocturnal inversion develops, beginning when Q_H turns negative, in the late afternoon. In consequence, buoyant suppression of vertical motion limits downward transport of momentum, winds die down, and the level of turbulence is low.

This makes the SBL a difficult environment in which to make measurements, for velocities are small and may be close to the noise level of the instruments. Perhaps more seriously, the extreme stability and consequent near-stagnation of the winds compromises the assumption of horizontally uniformity. Given the weakness of inertial forces at night, the slightest unevenness in the terrain will result in drainage winds (gravity-driven flow). A further factor is that gravity waves occur, and complicate the interpretation of velocity variance ${\sigma_w}^2$ as necessarily entailing mixing. And finally, radiative flux divergence may be a dominating factor in the evolution of the temperature field; from a study that coupled measurements and spectrally-resolved radiative calculations so as to evaluate the terms in

$$\begin{aligned} \frac{\partial Q_H}{\partial z} &= \frac{\partial Q*}{\partial z} - \rho\, c_p \frac{\partial \overline{\theta}}{\partial t} \\ \frac{\partial E}{\partial z} &= -\rho\, L \frac{\partial \overline{q}}{\partial t} \end{aligned} \tag{7.13}$$

(where $\overline{q}$ is the mean specific humidity), Schaller (1977; see also Ha and Mahrt, 2003) observed that "during the clear night radiative cooling exceeds the cooling caused by the sensible heat flux."

If the idealization of horizontal uniformity is upheld, and radiative divergence is neglected, then a simple "story" can be concocted for the development of the nocturnal SBL. Delage (1974) calculated the evolution of the profiles of mean wind $\overline{u}(z)$, turbulent kinetic energy $k(z)$, and mean potential temperature $\overline{\theta}(z)$ in the SBL, starting from an initially neutral state $\theta = \theta_{00}$. Delage's simulation was driven by a simplified surface boundary conditoin,

viz. an imposed (cooling) trend in surface temperature. The governing equations were

$$\begin{aligned}
\frac{\partial \overline{u}}{\partial t} &= \frac{\partial}{\partial z}\left(K \frac{\partial \overline{u}}{\partial z} \right) + f(\overline{v} - V_g) \, , \\
\frac{\partial \overline{v}}{\partial t} &= \frac{\partial}{\partial z}\left(K \frac{\partial \overline{v}}{\partial z} \right) - f(\overline{u} - U_g) \, , \\
\frac{\partial \overline{\theta}}{\partial t} &= \frac{\partial}{\partial z}\left(K \frac{\partial \overline{\theta}}{\partial z} \right) \, , \\
\frac{\partial k}{\partial t} &= \frac{\partial}{\partial z}\left(K \frac{\partial k}{\partial z} \right) \, , \\
&+ K \left[\left(\frac{\partial \overline{u}}{\partial z} \right)^2 + \left(\frac{\partial \overline{v}}{\partial z} \right)^2 \right] - \frac{g}{\theta_{00}} K \frac{\partial \overline{\theta}}{\partial z} - \epsilon \, .
\end{aligned} \tag{7.14}$$

The eddy viscosity was specified by the classic closure

$$K = \lambda(z) \sqrt{c_e \, k} \tag{7.15}$$

where $c_e = (u_*^2/k)_{eq}$ is the equilibrium value of the stress/TKE ratio, and as usual with this closure, the TKE dissipation rate was modelled as

$$\epsilon = (c_e \, k)^{3/2}/\lambda \, . \tag{7.16}$$

Delage specified the lengthscale as

$$\frac{1}{\lambda} = \frac{1}{k_v z} + \frac{1}{\lambda_\infty} + \frac{\beta}{k_v L} \tag{7.17}$$

which has the properties that in the neutral limit,

$$\begin{aligned}
\lim_{(z \to 0)} \lambda &= k_v z \, , \\
\lim_{(z \to \infty)} \lambda &= \lambda_\infty = 4 \times 10^{-4} \, \frac{|\overrightarrow{U}_G|}{f} \, .
\end{aligned} \tag{7.18}$$

Note that as L becomes small (and positive) the length-scale is limited by the *local* Obukhov length.

According to Delage's idealized simulations, the rate of deepening of the ground-based inversion is greatest early in the evening, when the inversion is still weak. As time progresses (Fig. 7.4) the inversion strengthens, suppressing TKE and thus turbulent exchange, and consequently deepens more and more slowly, due to the limpid motion under this increasingly stable layer. Eventually the depth of the inversion reaches an upper limit, set by the declining depth of the turbulent layer ($k > 0$). The entire mixing layer may have a depth that is only a few multiples of the Obukhov length. Delage's simulation also reproduces (Fig. 7.5) a feature of the nocturnal boundary layer that is often observed, the low-level jet. (See Wilson,

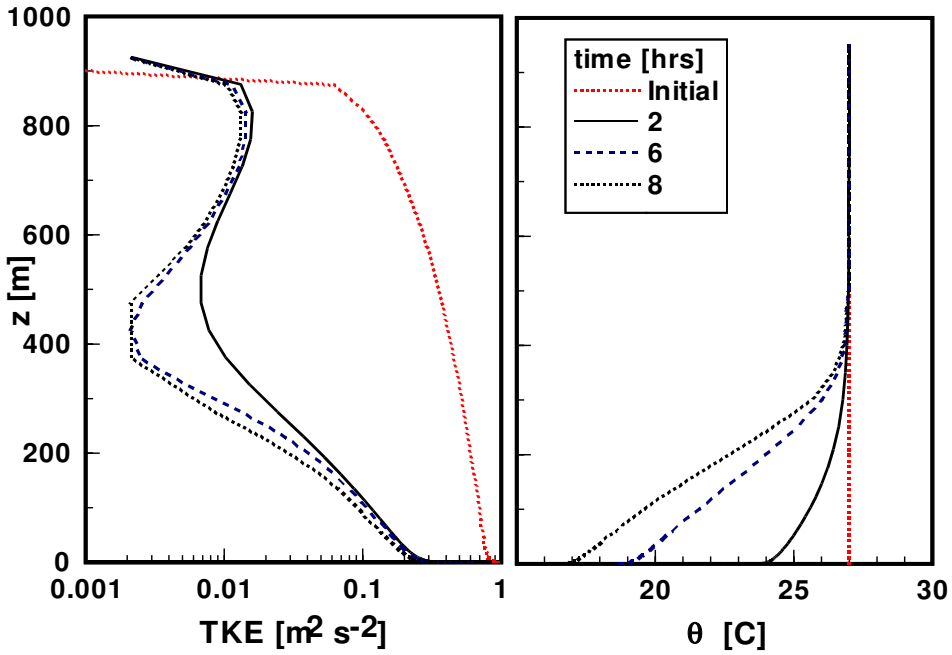


Figure 7.4: Computation of the nocturnal evolution of TKE and temperature, using the conceptual model of Delage.

2012, for similar calculations using an alternative turbulence closure. The Delage model is incomplete, in the sense that it does not include the longwave radiative divergence, which is certainly an important factor in the nocturnal evolution of the ASL during light winds.)

Delage's findings are qualitatively consistent with those that stem from the very different but equally interesting style of analysis by Nieuwstadt and Tennekes (1981), who postulated self-similar profiles for $\overline{u'w'}, \overline{w'T'}, \overline{u}$ and $\overline{\theta}$ as functions of z/δ, eg.

$$\frac{\overline{\theta}(\delta) - \overline{\theta}(z)}{\overline{\theta}(\delta) - \overline{\theta}(0)} \;=\; f_4\left(\frac{z}{\delta}\right) \tag{7.19}$$

By considering the SBL-averaged TKE productions terms, N&T deduced a first-order evolution equation for δ,

$$\frac{d\delta}{dt} = \frac{\delta_e - \delta}{\Gamma}\,. \tag{7.20}$$

According to Nieuwstadt and Tennekes, nocturnal boundary-layer depth evolves towards an equilibrium depth

$$\delta_e = c\,\frac{f\;|\mathbf{U}_G|^2\;\sin(\alpha)\;\cos(\alpha)}{\frac{g}{T_0}\,|\frac{\partial\theta(0)}{\partial t}|} \tag{7.21}$$

where α is the angle between the Geostrophic wind $\mathbf{U}_G$ and the surface wind. The rate of

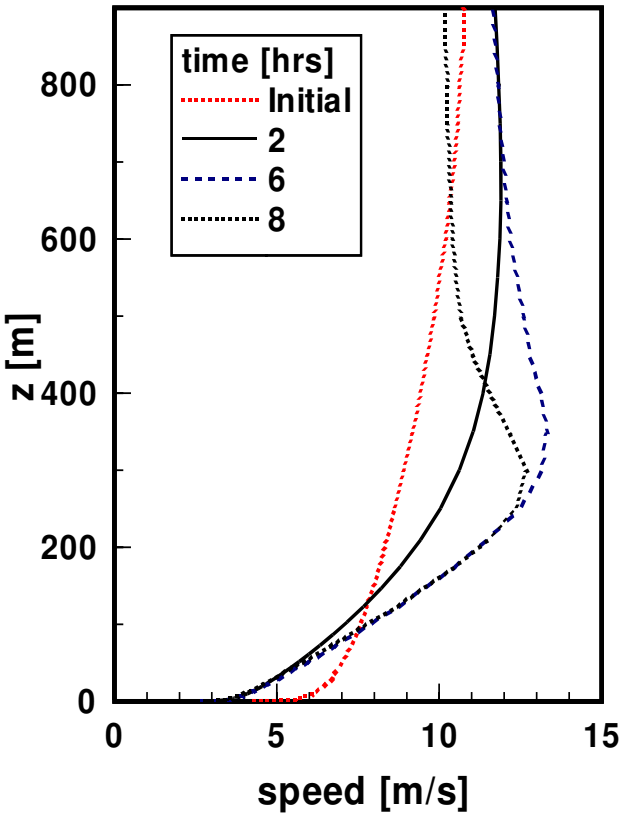


Figure 7.5: Computed evolution of the profile of windspeed, using the conceptual model of Delage. Note the low-level jet.

adjustment of δ is controlled by a timescale

$$\Gamma = \frac{3}{4} \frac{\theta(\delta) - \theta(0)}{|\partial\theta(0)/\partial t|} \tag{7.22}$$

The adjustment timescale is short early in the night, but increases as the night passes. N&T suggest that the actual SBL depth never reaches the equilibrium value, and that therefore the SBL depth cannot be considered a diagnostic parameter.

Although these theories are predicated on the questionable idealization of horizontal-uniformity, the real SBL can only be more complex than is indicated by these interesting results.

7.4.1 Intermittency in the SBL

In general terminology a "negative feedback" is a stabilizing feedback that opposes or acts in opposition to a disturbance ($\alpha < 0$ in Fig. 7.6), while a positive (destabilizing) feedback ($\alpha > 0$) accentuates or *amplifies* the original disturbance. In the stable boundary-layer, confusingly (at the level of terminology) a destabilizing feedback exists. Consider a dry

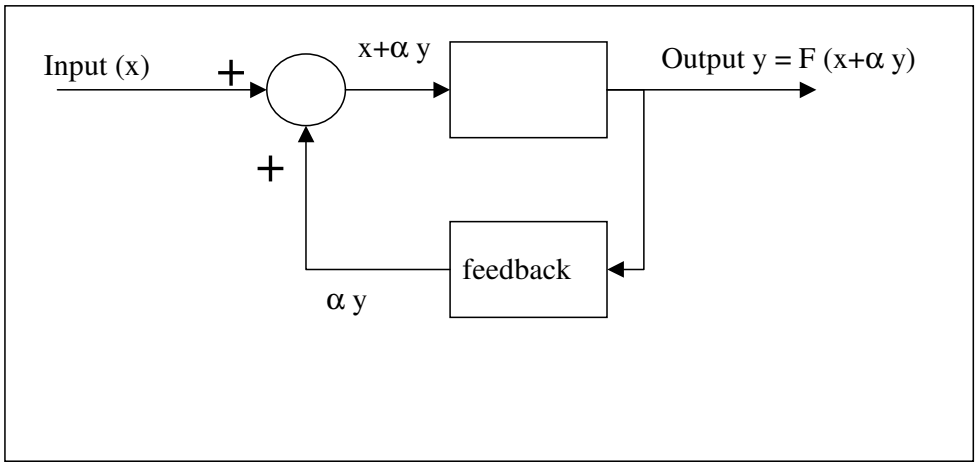


Figure 7.6: Conceptual framework of a feedback loop. Generally, the feedback is is some function $h(y)$ of the output, here simplified to a linear fraction, $h(y) = \alpha y$. The coefficient α may be positive (positive "feedback") or negative, and the "summing junction" feeds the sum $x + \alpha y$ of the input x and the feedback αy to the "system", which produces output y.

system, neglect the soil heat flux, and assume a steady radiative rate of loss of energy at the surface ($Q_* < 0$). At the base of the atmosphere a downward heat flux results, $Q_H(0) < 0$, and an inversion begins to built. As the inversion builds in strength, buoyancy acts in the direction to suppress vertical motion, ie. we may expect diminishing σ_w. However diminishing σ_w limits the ability of the atmosphere to convect heat to the ground, so accentuating the cooling of the surface, and thus strengthening the inversion, and further suppressing vertical motion. Eventually the Richardson number may become so large that vertical motion is eliminated... and the base of the surface-layer is calm. But now, of course, the still turbulent layer aloft is "decoupled" from the ground - since there is no turbulence there can be no loss of momentum into the calm layer. Thus, the winds above the calm layer increase, which increases the wind shear, until eventually shear production overwhelms buoyant suppression, and turbulence "breaks out."

It is hazardous to use statistically-valid arguments (eg. countervailing terms in the TKE budget) to defend an argument for a specific cycle of events. However this argument (intermittent periods of calm) has been given a mathematical basis by Wiel et al. (2000). Because the night-time atmosphere has this capacity to "poise itself" this way in an unstable equilibrium, the SBL state is more sensitive to idiosyncracies, such as the wake of a far-off tree, or building.

In contrast, in the CBL, a positive fluctuation $\delta Q_H(0) > 0$ in the surface heat flux accentuates the (already) unstable temperature gradient, the enhanced buoyancy of surface

parcels increasing the capacity of the atmosphere to convective heat away from the hot surface: this makes it easier to "cool" the surface, and so opposes the original change.

7.4.2 Velocity spectra for the stable ASL

Kaimal (1973) gave the following formula for spectra of u', v', w', T' in the stable surface layer:

$$\frac{nS_\alpha(n)}{{\sigma_\alpha}^2} = \frac{0.164(f/f_{0\alpha})}{1 + \ 0.164\ (f/f_{0\alpha})^{5/3}} \tag{7.23}$$

where ${\sigma_\alpha}^2$ is the variance of α ($= u', v', w',$ *or* T') in the (true) frequency range $0.005 \leq n \leq 10\ Hz$ and $f_{0\alpha}$ is a stability-dependent fitting parameter such that the (reduced) frequency at the spectral peak is about $f \approx \ 4.8 f_0$. Moraes and Epstein (1987) gave formulae for the $f_{0\alpha}$ as functions of z/L. Caughey (1977) gave spectra covering also the outer region of the stable ABL.

7.5 Theories for time-evolution of ABL depth

Because the depth of mixing is extremely important in the context (e.g.) of air pollution meteorology, and because it is reasonably difficult to measure[5], it would be of interest to have a theory of its growth and decay. Seibert et al. (2000) review progress in this regard.

We shall limit discussion here to the simplest paradigm for the simplest case, namely, the daytime growth of a well-mixed CBL by "encroachment." Let the potential temperature profile be characterized by a well-mixed layer, within which $\overline{\theta} = \overline{\theta}(t)$ is increasing with time, and a capping inversion whose lapse rate is $\Gamma > 0$ (this treatment ignores the excess heat stored in the shallow superadiabatic surface layer). The ABL depth (δ) is identified with the height where the constant θ layer meets the stable capping layer. Then the heat budget can be expressed

$$\frac{\partial \overline{\theta}}{\partial t} = -\frac{\partial\, \overline{w'\theta'}}{\partial z} \approx -\frac{\overline{w'\theta'}(\delta) - \overline{w'\theta'}(0)}{\delta}\ , \tag{7.24}$$

where $\overline{w'\theta'}(\delta)$ is the heat flux at the top of the CBL, and must be *negative* (due to downward mixing of heat from the warmer air aloft in the free troposphere). Now we write

$$\frac{\partial \delta}{\partial t} = \frac{1}{\Gamma}\ \frac{\partial \overline{\theta}}{\partial t} \tag{7.25}$$

to obtain

$$\Gamma\, \delta\ \frac{\partial \delta}{\partial t} \approx \overline{w'\theta'}(0) - \overline{w'\theta'}(\delta)\ . \tag{7.26}$$

[5]The most common method is to analyse the temperature profile returned by balloon soundings, assuming that the ABL will be "capped" by an inversion (Portelli 1977 gives a climatology of mixing depth for Canada, based on this approach). ABL depth – or rather, the depth of mixing – can be directly detected by using an acoustic sounder: thermal turbulence in the entrainment interface layer causes the back-scattering of anupwardly-propogated pulse of sound.

Since the entrainment heat flux ought to be stronger if thermals are punching the inversion, a common assumption (Carson and Smith 1974) is that

$$\overline{w'\theta'}(\delta) \;=\; -\,c\,\overline{w'\theta'}(0) \tag{7.27}$$

with $c \approx 0.2$. Wyngaard (2010) gives a variant of this solution that allows for a mean velocity ("entrainment velocity") at the top of the ABL.

Exercise: Assuming $\Gamma = 0.01\,\mathrm{K\,m^{-1}}$ and $\overline{w'\theta'}(0) = 0.2\,\mathrm{m\,s^{-1}\,K}$, what is the rate of growth of CBL depth at the moment when $\delta = 800$ m?

Chapter 8

The micrometeorology of "Uniform" Plant Canopies

The atmospheric surface layer is composed of an inertial sublayer, in which the Monin-Obukhov similarity theory is applicable, and beneath it the roughness sublayer (RSL)[1]. Over tall crops the RSL extends to an elevation of several times the canopy height h_c. In this section we shall explore the micrometeorology of the canopy layer.

When the wind blows through a plant canopy (mean height h_c), heat, mass and momentum are exchanged between the airstream and the vegetation. Turbulence in a "horizontally-uniform" canopy is markedly different from that in the surface layer above:

1. extreme vertical inhomogeneity, incl. extreme wind shear near $z = h_c$
2. high turbulence intensity
3. intermittency
4. highly non-Gaussian velocity pdf's
5. MOST is inapplicable
6. K-theory is invalid in principle (counter-gradient transport may occur)
7. transport is dominated by large eddies
8. transport terms in the stress and TKE budget equations are not negligible (flow is *not* in local equilibrium)
9. daytime TKE budget typically dominated by shear production and turbulent transport, but buoyancy can be the dominant factor during extremely calm conditions, which are usual at night

[1]At the base of the RSL there is an Unresolved Basal Layer, as defined by Wilson and Flesch (1993).

Recalling that MOST is valid at heights $z \gg z_0$ such that scales relating to the structure of the underlying surface do not appear in the theory, it makes sense to call that layer within which surface properties (e.g. length scales such as canopy height) *do* influence the flow the "roughness sublayer." The roughness sublayer, then, extends from ground to a height of about two or three times canopy height.

Finnigan (2000) reviewed the topic of wind and turbulence in "uniform" plant canopies. Fig. (8.1) from Raupach (1988) summarizes the profiles of mean windspeed, shear stress and velocity variance from a number of uniform canopies:

1. *Mean wind speed*: Strong shear near $z = h_c$. Profile concave upward above canopy, concave downward within canopy.

2. *Turbulent momentum flux (i.e. shear stress)*: Slowly height varying above canopy (to a first approximation, the surface layer above the canopy may be regarded as a constant stress layer). Rapidly absorbed within the upper canopy (the mechanism is adddressed in Sec. 8.3.1). Negligible stress transferred directly to ground (i.e. $(\overline{u'w'})_0 \approx 0$).

3. *Velocity variances and TKE*: Roughly constant above canopy. Decaying within the canopy.

Fig. (8.2) illustrates the point that velocity statistics in a plant canopy are *not Gaussian*.

8.1 Meaning of "uniformity": implicit need for horizontal averaging

A plant canopy obviously is inhomogeneous when viewed on a length scale that permits to distinguish individual leaves, and the branches and trunks: yet we readily admit that a certain forest is more "uniform" than another. On the other hand, how could we speak of a homogeneous "field" of wind velocity, when the property we speak of, wind velocity $\mathbf{u}$, is devoid of meaning, does not "exist" inside a leaf or trunk? In a plant canopy or forest, the spatial domain within which the fluid properties $\mathbf{u}$ exists is (by definition of "fluid") bounded randomly by surfaces at which the fluid is connected to non-fluid: in short, the canopy airspace is "multiply connected"[2]. This difficulty also arises in the context of soil properties, and in general the issue is that of "flow in porous media."

We may recover well-defined air-properties that vary continuously in the Cartesian space (x, y, z) by the step of defining new, spatially averaged variables, and thereby we may give sensible meaning to the idea of a "horizontally-uniform" forest; an essential precursor to rational discussion of canopy properties. The logical necessity for spatial averaging and the

[2]A multiply-connected space is a space in which not all closed curves C can be shrunk to a point without crossing boundaries of the space (excluded volume).

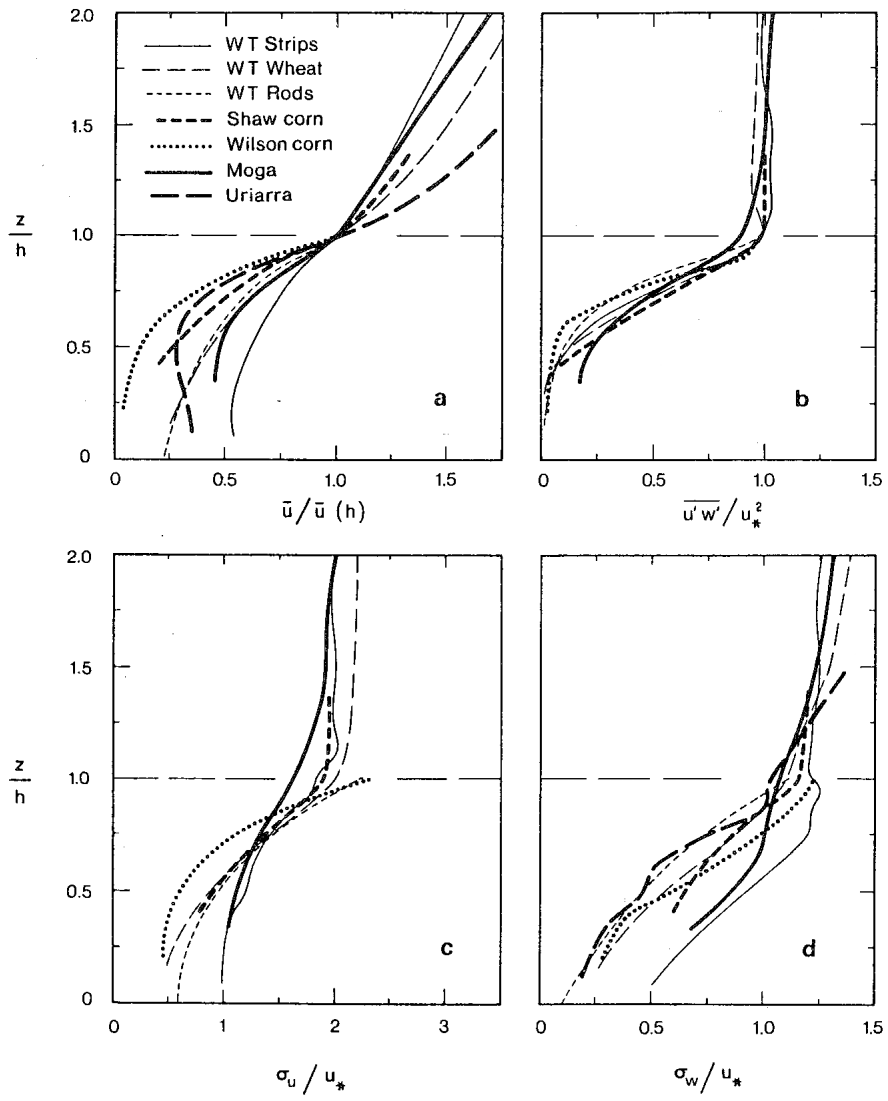


Figure 8.1: Profiles of wind statistics in canopies of height h (from Raupach, 1988; WT means "wind tunnel", Moga and Urriara were pine plantations). Friction velocity u_* is based on shear stress at $z = h$.

formalism have been developed particularly by Wilson and Shaw (1977), Raupach and Shaw (1982), Finnigan (1985) and Miguel et al. (2001), among others. See also Finnigan (2000) for a review.

8.1.1 A Spatial Average

Let $V = V_f + V_s = L_x\ L_y\ L_z$ be the volume over which we integrate to recover continuous variables, composed of a fluid sub-volume (V_f) and a solid sub-volume (V_s), and suppose we

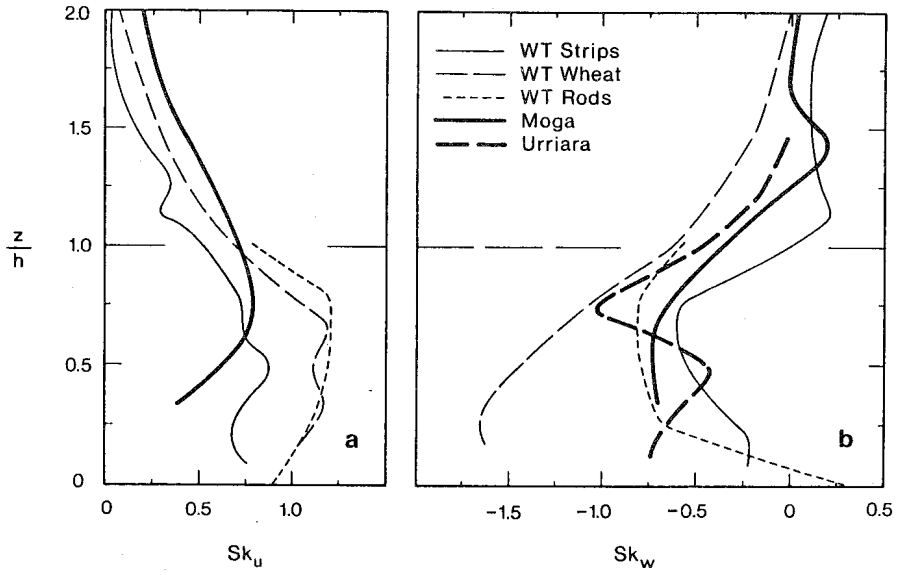


Figure 8.2: Typical profiles of velocity skewness ($Sk_u \equiv \overline{u'^3}/\sigma_u^3$, etc.) in a vegetation canopy (from Raupach, 1988).

define our averaging process as:

$$\langle g \rangle = \frac{1}{V_f} \int_{x-L_x/2}^{x+L_x/2} \int_{y-L_y/2}^{y+L_y/2} \int_{z-L_z/2}^{z+L_z/2} I(x',y',z')\; g(x',y',z')\; dx'\; dy'\; dz' \tag{8.1}$$

where the normalizing volume

$$V_f = \int_{x-L_x/2}^{x+L_x/2} \int_{y-L_y/2}^{y+L_y/2} \int_{z-L_z/2}^{z+L_z/2} I(x',y',z')\;\; dx'\; dy'\; dz' \; . \tag{8.2}$$

In eqns (8.1, 8.2), $I(x',y',z')$ is an indicator function, having unit value if the point (x',y',z') lies within the airspace, and vanishing otherwise. In order to ensure that the indicator function does not vanish *throughout* an entire averaging volume, L_x, L_y, L_z need to be large w.r.t. the scales of inhomogeneity; but to retain sufficient vertical resolution of the vertical gradients presumably $L_z \ll L_x, L_y$ (averaging volumes are 'slabs'). This choice for the averaging is termed by Miguel et al. the "intrinsic (internal) phase average", while normalization using the *total* volume yields the "superficial (external) phase average." The two averages are trivially related by the porosity V_f/V.

If we choose L_x, L_y to be much larger than a typical inter-plant (or tree) spacing we shall attain continuity of properties, but the resulting (smoothed) variables $\langle g \rangle$ will remain variable in space and time. We shall probably wish to focus on a time average, of the (already) spatially-averaged property; or in a "uniform" forest we may make L_x, L_y sufficiently large as to cover all fluctuations. Alternatively, we could first time-average fluid properties, then perform the spatial integration. Raupach and Shaw (1982) have given the governing equations for both possibilities, and the differences are not essential.

Let us then decompose any instantaneous, local (in-fluid) property g thus:

$$g(x,y,z,t) = \langle \overline{g} \rangle + \overline{g}'' + g' \tag{8.3}$$

where $\overline{g}$ is a time-average, $\overline{g}''$ is the local time-average deviation from the space-time mean $\langle \overline{g} \rangle$, and g' is the instantaneous local fluctuation from the local time average (so $\overline{g'} = 0$). For simplicity we shall write $G = \langle \overline{g} \rangle$.

With the above triple decomposiiton, a velocity cross product expands as

$$\begin{aligned} u_i u_j &= (U_i + \overline{u}_i'' + u_i')\,\left(U_j + \overline{u}_j'' + u_j'\right) \\ &= U_i U_j + \overline{u}_i''\,\overline{u}_j'' + u_i' u_j' \\ &+ \left(U_i\,\overline{u}_j'' + U_j\,\overline{u}_i''\right) + \left(U_i\,u_j' + U_j\,u_i'\right) + \left(\overline{u}_i''\,u_j' + \overline{u}_j''u_i'\right)\ . \end{aligned} \tag{8.4}$$

The resolved cross product is $\langle \overline{u_i u_j} \rangle$, and consistent application of the Reynolds averaging rules – which admittedly are not realizable – leads to the result that

$$R_{ij}^{tot} \equiv \langle \overline{u_i u_j} \rangle = U_i U_j + \langle \overline{u}_i''\,\overline{u}_j'' \rangle + \langle \overline{u_i' u_j'} \rangle\ , \tag{8.5}$$

where the first term is the momentum transport by the mean flow, the final term is the Reynolds stress, and the middle term is the dispersive momentum flux arising from the spatial covariance of local time average departures from the local space-time mean flow.

For ordinary spatial averaging in simply-connected space, the operations of spatial-differentiation and spatial integration commute, ie.

$$\overline{\frac{\partial g}{\partial x_i}} \equiv \frac{\partial \overline{g}}{\partial x_i} \tag{8.6}$$

and (for any vector g_i)

$$\overline{\frac{\partial g_i}{\partial x_i}} \equiv \frac{\partial \overline{g}_i}{\partial x_i}\ . \tag{8.7}$$

In the multiply-connected space (x,y,z), exchange of some arbitrary property (ϕ) of the atmosphere with the solid fraction implies losses or gains of ϕ from the fluid sub-volume of $L_x\ L_y\ L_z$; these exchanges are due to and representable as, surface integrals of exchange-fluxes of ϕ across the air/solid boundaries. Bearing in mind the essential form of the fluid conservation equation (1.35) the fluid-solid exchange of property ϕ (that we identify upon spatial averaging) evidently might be regarded as having to be accounted for, either by an (additional) apparent source, or by some modification of the flux-divergence term upon averaging. It is the latter interpretation that has been preferred, in the form of the 'spatial averaging theorem' (eg. Miguel et al., 2001; Finnigan, 1985) according to which eqn(8.7) must be replaced by

$$\overline{\frac{\partial g_i}{\partial x_i}} = \frac{\partial \overline{g}_i}{\partial x_i} - \frac{1}{V}\int g_i\ n_i\ ds \tag{8.8}$$

where the surface integral covers the *entire* surface area of the air-solid boundaries within $L_x\ L_y\ L_z$, and n_i is the local surface unit normal-vector vector (note: $g_i\,n_i \equiv \vec{g}\cdot\vec{n}$).

8.2 Intermittency in plant canopies

When viewing a field of wheat or corn from well above, one sees focal points of activity, where gusts are whirling slowly across the canopy, bending down the crop, which bucks and shakes and waves, before settling as the gust passes[3]. Finnigan (1979) has studied waving plant canopies, but generally we neglect the plant motion.

The relative calm that prevails inside a deep canopy is sporadically punctuated by the penetration into the canopy of a "gust" from above, which "flushes" the canopy airstream and restores properties ($T_b, \rho_{vb}, [CO_2]_b$) of the bulk ("b") airstream aloft. Standing far below the crown of a forest, one may first see the tree tops bend, the leaves commence fluttering, and hear an increased "shhhh" of wind (Lighthill 1952 is the originator of the theory of "aeroacoustics," covering sound generated by the wind; see also Kato *et al.*, 2006). Some seconds later the disturbance reaches the forest floor, and a period of gentle motion ensues, but soon dies out.

If one were to observe a trace of air temperature in the canopy, during a sunny afternoon, during the quiet periods one would see a rising trend, characterized by small scale turbulent mixing, which is abruptly terminated by the in-flushing external air which "sweeps" out the warm air and replaces it with cooler air from aloft. This trace is called a "ramp", and may be seen in other properties too — in humidity and in CO_2 concentration (in the later case the ramp is inverted, as CO_2 concentration is drawn down by leaf photosynthesis). An interesting and influential description of this process was given by Denmead and Bradley (1985; Fig. 8.3).

8.2.1 Ramps and Microfronts

Temperature "ramps" (Fig. 8.4) are a well-known phenomenon of the ASL (Webb 1988; Antonia et al. 1979). Such ramps are one of the conceptual bases upon which the "clean sweep" (or "renewal") model of canopy transport are founded. A nice example of the ramp structures in the ASL above a short grass surface is provided by Koprov et al. (1998). Ramps in temperature and humidity are also seen within the roughness sublayer, inside the plant canopy. Interestingly, within a plant canopy the associated circulations are *not buoyancy-driven*, for ramps in humidity are observed even when $|L| \sim \infty$.

Gao et al (1989) used conditional sampling to create a conditionally-averaged structural view of the coherent structures in canopy flow. The structures were defined to be the (ensemble mean) fields of T', q', u', w' viewed in a 2-d space (z, t') where time t' (loosely interpretable as equivalent to variation in space along the streamwise coordinate x) was measured relative to the sudden truncations of the characteristic "ramps" in the temperature and/or humidity fields. This analysis by Gao et al. revealed what the authors termed "micro-fronts" (Fig.

[3]These correspond with the "catspaws" on a lake.

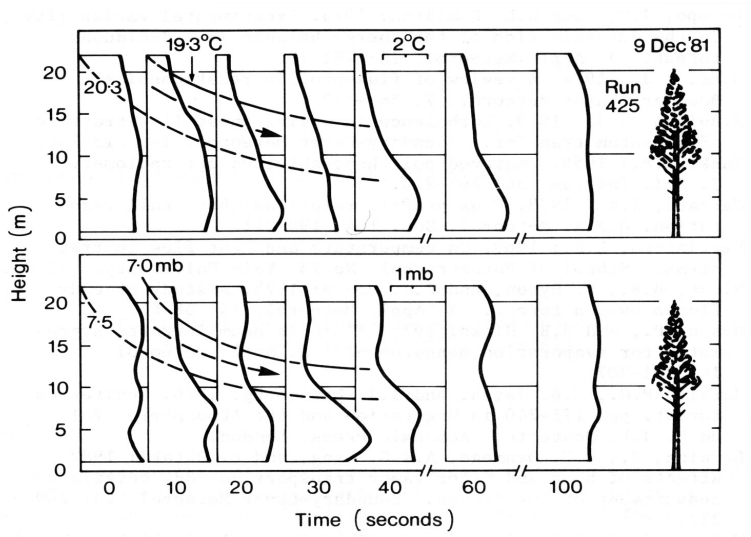


Figure 8.3: Time sequence of temperature (top) and humidity (below) during the "flushing" of the canopy by a gust of cooler, drier air from above. Long after the gust, local redistribution of the heat shed from the sunlit foliage, and of transpired vapour, have re-established the pre-gust situation of a (relatively) warm, moist, quiescent canopy airstream somewhat decoupled from the boundary-layer overhead. From Denmead and Bradley (1985).

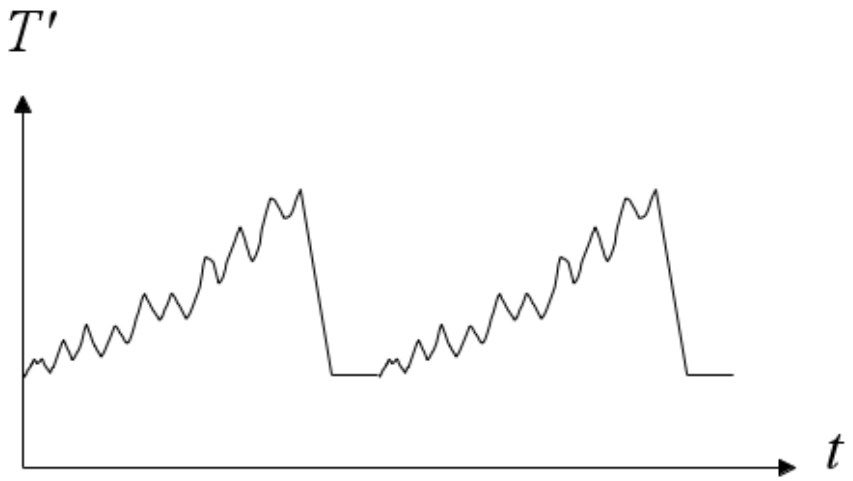


Figure 8.4: Schematic temperature "ramps". The temperature minima denote a phase where a volume of well-mixed (isothermal) air has enveloped the sensor, and so the level of fluctuation is small (Webb, 1988). Subsequently local heat production leads to an upward trend, which is truncated abruptly by a gust.

8.5). Ahead of the gust front, which is tilted downwind (to the right in the figure), is a region of gently-rising, warm, humid air, and $u' < 0$. Immediately behind the front is found fast-moving ($u' > 0$), descending ($w' < 0$), cool ($T' < 0$) and dry air. Weijers et al. (1994) show

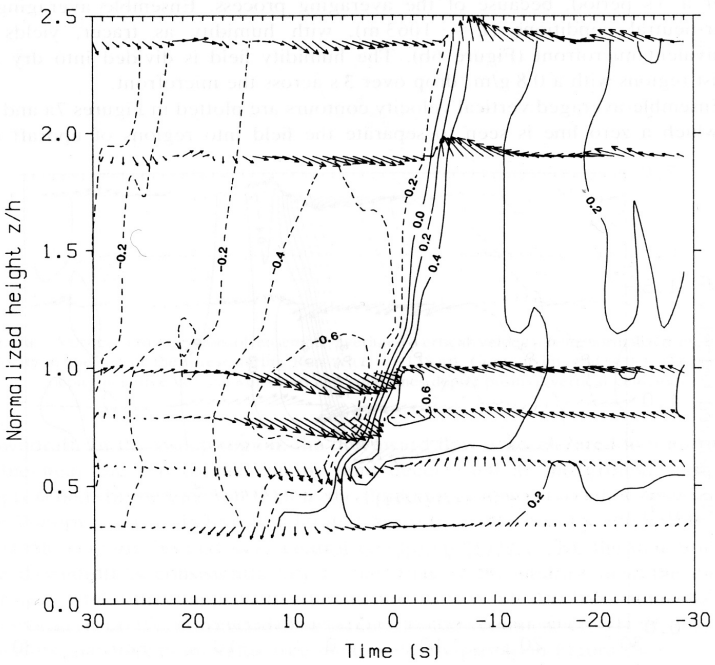


Figure 8.5: Conditionally-averaged velocity fluctuation (arrows) and temperature fluctuation (contours) in the region of the micro-front associated with penetration of a canopy by a gust. After Gao et al (1989)

an interesting diagram by Wilczak (1984; see also Wilczak & Tillman, 1980) that indicates the convergent horizontal velocity field near ground, in the proximity of a microfront.

8.2.2 Quadrant analysis

As usual, assume a coordinate system aligned with the mean flow. The $u' - w'$ plane consists of these four "quadrants"

[1] outward interaction, $u' > 0, w' > 0, u'w' > 0$

[2] ejection, $u' < 0, w' > 0, u'w' < 0$

[3] inward interaction, $u' < 0, w' < 0, u'w' > 0$

[4] gust (sweep), $u' > 0, w' < 0, u'w' < 0$.

Let I_α be an indicator function for quadrant α; for example I_1 is defined such that

$$I_1 = 1 \text{ if } u' > 0, w' > 0, |u'w'| \geq H \ |\overline{u'w'}| \tag{8.9}$$

where H is termed the "hole size". Then the stress fraction in quadrant α is:

$$\overline{u'w'}_\alpha = \frac{1}{\overline{u'w'}} \frac{1}{N} \sum_i I_\alpha(u'_i, w'_i) \ u'_i \ w'_i \tag{8.10}$$

where N is the number of samples taken over the averaging period (T). Associated with the stress fraction is a time fraction T_α, during which the stress lay in the given quadrant. It was established that a large fraction of the stress is transferred by sweeps, during a small time-fraction. Thus, these sweeps give us the periods of "action" in the canopy. They are considered the "large eddies" of particular significance in canopy transport, and their consequence is that transport terms in the budget equations cannot be neglected (e.g. $\partial\overline{w'^3}/\partial z$ in the σ_w^2 budget). Following Raupach (1981), several authors have subsequently given quadrant analyses of the shear stress in canopy flows (e.g. Shaw et al., 1983, examined the case of a corn canopy).

8.2.3 Governing equations for a uniform canopy

As might be anticipated, a proliferation of terms fall out upon averaging non-linear terms in the instantaneous, local conservation equations (eg. Navier-Stokes eqn for u). Assuming steady state, and that the time-space averaged properties are invariant in x, y (horizontal uniformity), the $\overline{u}, \overline{v}$ momentum equations (neglecting viscous transport) are:

$$\begin{aligned} 0 &= -\frac{1}{\rho_0}\frac{\partial\langle\overline{p}\rangle}{\partial x} - \frac{\partial}{\partial z}\left[\langle\overline{u'w'}\rangle + \langle\overline{u}''\overline{w}''\rangle\right] + f\langle\overline{v}\rangle + S_U \ , \\ 0 &= -\frac{1}{\rho_0}\frac{\partial\langle\overline{p}\rangle}{\partial y} - \frac{\partial}{\partial z}\left[\langle\overline{v'w'}\rangle + \langle\overline{v}''\overline{w}''\rangle\right] - f\langle\overline{u}\rangle + S_V \ . \end{aligned} \tag{8.11}$$

The right hand terms in the square brackets are dispersive momentum fluxes. It may be surprising that the Coriolis terms have been retained; the reason for this is discussed in a later section. They can be dropped in case of a wind tunnel canopy, or for shallow real world canopies.

The terminology for space-time averaged quantities is a little clumsy, so let us henceforth, in the context of canopy flows, understand that

$$\begin{aligned} U &= \langle\overline{u}\rangle \ , \\ V &= \langle\overline{v}\rangle \ , \\ \tau &= \langle\overline{u'w'}\rangle \ , \end{aligned} \tag{8.12}$$

(etc). The momentum sources S_U, S_V are a symbolic shorthand for surface integrals of momentum exchange across the intricate and unresolvable air/solid surfaces, (for their formal

expression, see Raupach and Shaw). That is, S_U is a canopy drag force. It must be sensitive to the density of vegetation, and to wind velocity, so we may parameterize it (conventionally) thus:

$$S_U = c_D\, a(z)\, U\, |\mathbf{U}| \,. \tag{8.13}$$

Here $a(z)$ [$\mathrm{m}^2\ \mathrm{m}^{-3}$] is the surface-area density (surface area per unit volume), a familiar variable in the study of plant canopies, and c_D is a dimensionless drag coefficient (not necessarily independent of windspeed, or the canopy Reynolds number $R_e = hU(h)/\nu$). The $c_D a$ product may be subdivided

$$c_D a = c_{Dl}\, a_l + c_{Db}\, a_b + c_{Dt}\, a_t \tag{8.14}$$

into leaf, branch and trunk contributions (a step we shall not pursue). As one may expect, our canopy drag term involves the square of a windspeed, or something like it: $|\mathbf{U}| = \sqrt{U^2 + V^2 + W^2}$ is the magnitude of the mean wind vector (by the assumed horizontal uniformity, $W = 0$) and the product $U\,|\mathbf{U}|$ is the projection of the vector $\mathbf{U}\,|\mathbf{U}|$ onto the x-axis.

8.3 Canopy profiles

There have been a number of comprehensive reviews of wind and turbulence in plant canopies, among them: Raupach (1988); Finnigan (2000). Fig. (8.1) given earlier provides a general picture. For profiles in the Canadian Boreal forest see Amiro (1990).

8.3.1 Canopy shear-stress profile

Now assume that at the top of the canopy we align our coordinate system such that $V = \langle \overline{v} \rangle = 0$. Recall that in the "constant stress layer" we can regard the shear stress $\overline{u'w'}$ as approximately height independent. However inside the plant canopy ($z \le h_c$) the momentum budget reduces (approximately) to a balance of two dominant terms,

$$0 = -\,\frac{\partial \langle \overline{u'w'} \rangle}{\partial z} \;+\; c_D\, a\, U^2 \tag{8.15}$$

where the so-called "dispersive flux" $\langle \overline{u}'' \overline{w}'' \rangle$ has for the moment been ignored. In the upper canopy the windspeed U and the area density a are large, and there results a rapid attenuation of the downward turbulent momentum flux (momentum flux convergence; Fig. 8.6); the convergence of that flux is equal to the momentum lost to the vegetation (and transferred via the stalks to the earth).

8.3.2 Canopy wind profile

Not surprisingly, the mean windspeed, too, is rapidly attenuated as we descend into a plant canopy — a result of the momentum absorption. Recall that aloft in the ABL, layers of the

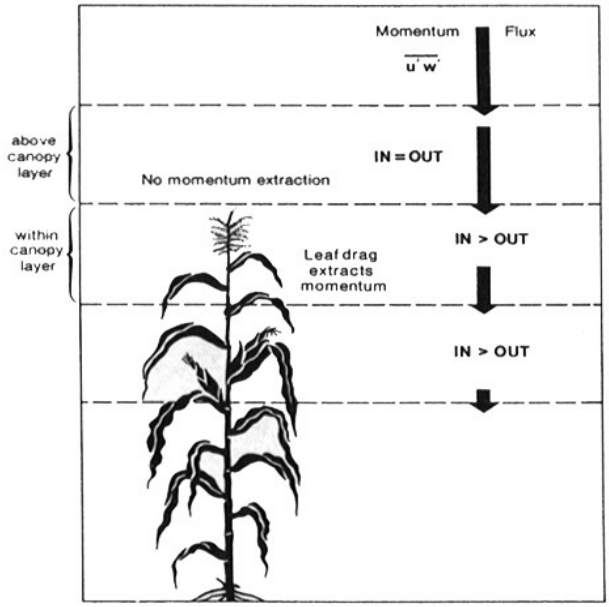


Figure 8.6: Schematic of height variation of the turbulent momentum flux $\tau(z)$ in and above a horizontally-uniform plant canopy.

atmosphere are coupled to each other by the convective exchange of momentum (fluctuating vertical motion implies parcel exchanges, and these parcels, speaking statistically, carry momentum-deficit upwards, and momentum-surplus downwards: $\overline{u'w'} < 0$). Because of the rapid attenuation of the shear stress by the canopy, the air deep in a canopy is "driven" only by a feeble shear stress, and whatever "background" synoptic pressure gradient is present.

One may obtain one of the most popular of formulae for representing the "canopy wind profile" by using an eddy viscosity $K_m = \text{const.}$ to parameterize the momentum flux,

$$\tau = -\langle\overline{u'w'}\rangle = K_m \frac{\partial U}{\partial z} . \tag{8.16}$$

Upon substitution into eqn (8.15), and upon assuming $c_D a$ independent of height, one may easily solve to find

$$U = U_h \exp\left[\beta_u \left(\frac{z}{h_c} - 1\right)\right] . \tag{8.17}$$

The parameter β_u is related to the (assumed value for the) eddy viscosity, but usually regarded as "free" (optimizable). Note that according to this formula, mean wind on ground $U(0) = U_h e^{-\beta_u}$, ie. free slip is permitted. While on first thought objectionable, this is actually a good thing. Wind speed and shear stress at the base of a deep canopy are very small, and

accordingly so is the wind shear. There is of course, as $z \to 0$, an Unresolved Basal Layer (UBL – see Wilson & Flesch, 1993), whose details remain unknown to us; but seldom have measurements ever been made that conflict with a small, near constant windspeed at small z/h_c.

Other semi-empirical wind profile formulae have been given, eg. Cowan's (1968) profile:

$$U(z) = U(h_c) \sqrt{\frac{\sinh(\beta z/h_c)}{\sinh(\beta)}} \tag{8.18}$$

is solution to the momentum budget eqn(8.15) with

$$K_m(z) = \lambda \, U(z) \; , \tag{8.19}$$

where $\lambda =$ const. and area density $a =$ const. (the lower boundary condition is that $U = 0$ at $z = 0$). The parameter β is theoretically

$$\beta = \sqrt{\frac{2h_c^2 \; c_D \; a}{\lambda}} \; , \tag{8.20}$$

but is usually treated as a fitting parameter.

Note that these canopy wind profiles – supported by observations – indicate a *positive* curvature $\partial^2 U/\partial z^2 > 0$, whereas in the surface layer above the canopy, where the log-law wind profile (see below) applies, $\partial^2 U/\partial z^2 < 0$. Thus somewhere near $z = h_c$ there must be a height where curvature vanishes — an inflexion point of the wind profile. Inflexion-point instability is a theorem from linear stability analysis (Drazin & Reid, 2004), and suggests that to a certain extent, characteristics of the canopy turbulence may be related to the form of the wind profile (more on this later).

What of observations? Measurements are usually presented in the form $U/U(h_c)$ or $U/u_*(h_c)$, versus z/h_c. Of course this normalisation does not result in a universal profile — a pine forest differs from a wheat canopy, more fundamentally that in its height (alone). And even for a particular canopy, the normalisation does not take care of the influence of stability. But while buoyancy can be a dominating influence on canopy motion during calm conditions — eg. at night — typically it has modest influence on wind and turbulence profiles; thus for example, the Elora corn measurements (Wilson, 1988) built a wind profile from days of measurements from paired split-film anemometers; the result being a universal curve (for *that* canopy).

Far above the canopy, it is habitual to suppose that the wind profile can be described by

$$U(z) = \frac{u_*}{k_v} \left[\ln \left(\frac{z-d}{z_0} \right) - \; \psi_m \left(\frac{z-d}{L} \right) + \; \psi_m \left(\frac{z_0 - d}{L} \right) \right] \tag{8.21}$$

where the displacement length $d \sim \frac{2}{3} h_c$ is simply an offset on the z-axis (as if the effect of the canopy had been to lift the atmosphere) and the roughness length $z_0 \sim h_c/10$ (these

suggested magnitudes are only very approximate, and not meant to suggest constancy across the family of all "uniform canopy flows"). The in-canopy profile formulae are easily matched to eqn. 8.21 some distance above the canopy or at the top of the canopy, by requiring continuity of $U, \partial U/\partial z$. As an example for a neutral case,

$$\begin{aligned} \frac{U}{u_*} &= \frac{U(h_c)}{u_*} \exp\left[\beta_u \left(\frac{z}{h_c} - 1\right)\right], \; z \le h \\ &= \frac{U(h_c)}{u_*} + \frac{1}{k_v} \ln\left[\frac{z/h_c - d/h_c}{1 - d/h_c}\right], \; z > h \end{aligned} \tag{8.22}$$

where the friction velocity u_* is based on the shear stress at $z = h_c$. The extinction parameter β_u may be defined in terms of the ratio of the windspeeds at $z = h_c, z = 0$,

$$\beta_u = \ln\left[\frac{U(h_c)/u_*}{U(0)/u_*}\right]. \tag{8.23}$$

For example if $(U(h_c)/u_*, U(0)/u_*) = (3.0, 0.15)$ then $\beta_u = 3.0$.

Although the K-theory notion that underpins its derivation is (as we shall see) invalid, an analytical wind profile like eqn (8.22) can be a very convenient alternative to a numerical wind profile from a numerical solution of the canopy momentum budget (eqn. 8.15) and supplementary equations. We should best regard it as a flexible curve, that may be tuned to any particular situation.

8.3.3 Turbulence profiles

In a dense plant canopy, the turbulent velocity variances $\sigma_{u,v,w}$ increase from small values deep in the canopy, to large values near $z = H$ (still larger values may occur aloft in the b.l.). However because of the attenuation of the mean wind with depth, the turbulence in a dense plant canopy is characterised by a high turbulence intensity $\sigma_u/\sqrt{\overline{u}^2 + \overline{v}^2}$ deep in the canopy.

In view of the above discussion, it will not be surprising that streamwise skewness $Sk_u > 0$, and $Sk_w < 0$.

8.3.4 Layer-resolved energy budget in the plant canopy

If we consider any finite layer Δz of a uniform plant canopy, we may express conservation of thermodynamic energy in that layer by the equation:

$$\Delta Q^* = \Delta Q_H + \Delta Q_E + \Delta Q_S \tag{8.24}$$

where ΔQ^* is the net radiant energy supply to the layer, ΔQ_S represents any storage in the layer (heating of the air and plant material), and $\Delta Q_H, \Delta Q_E$ are the increment in the

vertical fluxes of sensible and latent heat across the layer. Dividing by Δz and taking a limit, we may equivalently write that the flux-profiles are constrained by

$$\frac{\partial Q^*}{\partial z} = \frac{\partial Q_H}{\partial z} + \frac{\partial Q_E}{\partial z} + \frac{\partial Q_S}{\partial z} \tag{8.25}$$

Now, ΔQ_H is a supply of (or loss of) sensible heat to the airstream, within this layer, and it must be equivalent to heat shed to (or taken from) the airstream by leaves. Then with Q_{Hl} representing a characteristic leaf heat flux density for the layer in question, and $a(z)$ being the leaf area density, it follows that

$$\Delta Q_H = a(z)\ \Delta z\ Q_{Hl}\ . \tag{8.26}$$

Similarly, for water vapour we may write

$$\Delta Q_E = a(z)\ \Delta z\ L_v\ E_l \tag{8.27}$$

where E_l is (mean) leaf evaporation rate in this layer and L_v ($\approx 2.5 \times 10^6\,\mathrm{J\,kg^{-1}}$) is the latent heat of vapourization. To estimate E_l one might choose to partition leaves in into sunlit and shaded classes, and apply the Penman-Monteith equation to each class; this will involve the airstream temperature and humidity, the local radiation load on the leaf, and the stomatal conductance of each leaf class.

An alternative expression of eqns(8.26,8.27) is:

$$\begin{aligned} \rho c_p \frac{\partial \overline{w'T'}}{\partial z} &= a(z) Q_{Hl} = \frac{\beta}{1+\beta}\,\frac{\partial Q^*}{\partial z}\ , \\ \frac{\partial \overline{w'\rho_v'}}{\partial z} &= a(z) E_l = \frac{1/L}{1+\beta}\,\frac{\partial Q^*}{\partial z}\ , \end{aligned} \tag{8.28}$$

where

$$\beta(z) = \frac{\partial Q_H/\partial z}{\partial Q_E/\partial z} \tag{8.29}$$

is a local Bowen ratio, in terms of which we may write

$$\frac{\partial Q^*}{\partial z} = (1+\beta)\,\frac{\partial Q_E}{\partial z} = \frac{1+\beta}{\beta}\,\frac{\partial Q_H}{\partial z}\ . \tag{8.30}$$

A typical "comprehensive canopy micrometeorology model" will involve the coupled governing equations for $U, V, \overline{T}, \overline{q}$ and (assuming higher-order closure) the fluxes and variances $\overline{w'T'}, \overline{w'q'}, \overline{T'^2}$ etc., as well as canopy radiation. Necessarily the model will be numerical, and the heat and vapour sources and sinks within the layers will be modelled using the Penman-Monteith equation.

8.3.5 TKE transformations (wake production)

Drag on the vegetation converts kinetic energy of the mean flow (MKE) to turbulent kinetic energy in some range of scales of motion ('wake scales', WKE); and the (fluctuating) drag extracts energy from the eddies, re-depositing it in the wake scales (a spectral-transfer mechanism which acts in parallel with the normal vortex-stretching mechanism).

In vegetation canopies wake scales of motion are usually considered to be 'small', and thus rapidly dissipated. Although it is sometimes possible to detect a hump or peak in the power spectrum, reflecting the deposition of energy into wake scales, measurements reviewed by Seginer et al. (1976) led them to regard "eddies generated by branches and leaves as only a small perturbation on the main spectrum" and to conclude that "only a small fraction of the turbulence which can be observed inside natural canopies has its origin in the wakes of individual elements".

8.3.6 Modelling TKE transformations

Wilson (1988; W88) split the turbulence spectrum into two bands (k, k_w) where k is the 'shear kinetic energy' (SKE) and k_w the 'wake kinetic energy' (WKE). MKE lost to the drag forces was assumed to be re-deposited as (small scale, thus unimportant) WKE, while the SKE→WKE term was modelled heuristically as:

$$\epsilon = \epsilon_{cc} + \epsilon_{fd} = \frac{(c_e\ k)^{3/2}}{\lambda} + \frac{1}{2}\ C_d A\ \overline{u}\ \left(4\ \overline{u'^2} + 2\overline{v'^2} + 2\overline{w'^2}\right), \tag{8.31}$$

where A [m^{-1}] is the leaf area density and λ the turbulence length-scale. The first term represents the conventional vortex stretching mechanism (ϵ_{cc} for 'cascade conversion'). The second term (ϵ_{fd}) is due to the action of the form drag on vegetation, and was derived by assuming that momentum sinks of form $C_d A(u^2, uv, uw)$ appear in the *instantaneous* momentum equations.[4] Then the corresponding SKE sinks in the individual variance-budget equations would be (omitting the localising functions):

$$\begin{aligned}
\epsilon_{xx} &= 4c_D a(z)\ \overline{u}\ \overline{u'^2} + \frac{2}{3}\ \epsilon_{cc}, \\
\epsilon_{yy} &= 2c_D a(z)\ \overline{u}\ \overline{v'^2} + \frac{2}{3}\ \epsilon_{cc}, \\
\epsilon_{zz} &= 2c_D a(z)\ \overline{u}\ \overline{w'^2} + \frac{2}{3}\ \epsilon_{cc}.
\end{aligned} \tag{8.32}$$

[4] Ayotte et al. replaced Wilson's projections (uu, uv, uw) with the rigorous form $(u|\vec{u}|, v|\vec{u}|, w|\vec{u}|)$, where $|\vec{u}| \equiv (u_i u_i)^{1/2}$ is the magnitude of the instantaneous velocity vector $\vec{u}$. Consideration that, at the fences, space is 'multiply-connected' will show that indeed, an extra source term must be included (Wilson & Shaw, 1977, Wilson *et al.*, 1990). It can be shown that a term of this form in the instantaneous momentum equations implies loss of energy at *all* scales, which is not quite realistic, since there must be a compensating production of TKE at "wake" scales.

8.4 Velocity and TKE profiles computed from a simple closure

One of the classical first-order closures is

$$K(x,z) = \lambda \, (c_e \, k)^{1/2}, \tag{8.33}$$

where k is the turbulent kinetic energy, calculated from its simplified governing differential equation, and λ is an algebraic length scale (but see Wilson **?** for a critique of the rationality of this closure). We shall briefly describe this simple closure, which has seen use in just about every type of micrometeorological flow (eg. Delage's 1974 treatment of the nocturnal boundary layer, covered in Section 7.4).

For horizontally-uniform winds and neglecting buoyancy forces, the idealized TKE equation associated with this closure is:

$$\frac{\partial}{\partial z}\left(-\mu K \frac{\partial k}{\partial z}\right) \;=\; K\left[\left(\frac{\partial \overline{u}}{\partial z}\right)^2 + \left(\frac{\partial \overline{v}}{\partial z}\right)^2\right] \;-\; \epsilon \; . \tag{8.34}$$

The diffusion term (lhs) parameterizes turbulent and pressure transport, and μ distinguishes the eddy diffusivity for TKE (μK) from the eddy viscosity (K). The terms on the rhs are shear production, and viscous dissipation.

It makes no essential difference whether one "splits" the TKE dissipation rate as

$$\epsilon = \epsilon_{cc} + \epsilon_{fd}, \tag{8.35}$$

or (like Wilson et al. 1998) writes

$$\epsilon = \max\left[\epsilon_{cc}, \epsilon_{fd}\right] . \tag{8.36}$$

The viscous dissipation ϵ_{cc} is parameterized conventionally as

$$\epsilon_{cc} = \frac{(c_e \, k)^{3/2}}{\lambda}. \tag{8.37}$$

The "wake conversion" sink (TKE sink due to form drag) can be estimated[5] by the prescription

$$\epsilon_{fd} = \alpha \; c_D \; a(z) \; \overline{u} \; k \tag{8.38}$$

where α is a constant of order 1 (Wilson, 1985). Note that where using this closure we consider that k excludes wake-scale TKE, and so we do not include MKE $\rightarrow$ TKE conversion.

[5]Ayotte et al. have given a more precise expression.

8.4.1 Application to "uniform canopies"

"Furry Hill"

Brunet et al. (1994) reported a wind tunnel study of flow in a model aeroelastic canopy (nylon fishing line) within the CSIRO wind tunnel wall boundary layer. In the "Furry Hill" experiment (Finnigan and Brunet, 1995), this canopy was placed upwind and over a Witch of Agnesi ridge (half-width L). From a comparison with these data, Wilson et al. (1998; WFR) suggested that the K_k closure reproduces the overall character of the *mean* wind field, particularly very close to ground, in flow over hilly, forested terrain. Here we examine the simulation of the equilibrium profiles, far upwind from the ridge.

The pressure gradient in the test section of the tunnel upwind of the hill was set to zero by adjusting the height of the tunnel roof, but there was a vertical gradient in Reynolds stress above the canopy (balanced by advection). To permit simulation of the $\tau(z), k(z)$ profiles aloft, for the wind tunnel experiments we calculated an effective pressure gradient

$$\frac{1}{\rho\, u_{*0}^2}\,\frac{\partial P}{\partial x/h_c} = \frac{\partial}{\partial z/h_c}\left(\frac{\tau_0}{{u_{*0}}^2}\right) \tag{8.39}$$

which was imposed in the simulations.

Measurements of (U, τ, k) are available to height $z/h_c = 6$, at $x/L = -5$, far upstream from the ridge in the Furry hillflow experiments. Fig (8.7) compares those measured profiles, with simulations using $\alpha = c = 1, \mu = 0.2$; all other inputs are provided unambiguously by the Furry data. The numerical method is covered in Section (**??**). The agreement of model and observations is excellent (though the modelled above-canopy gradient in shear stress is only the necessary consequence of our imposed $\partial_x P$).

"Tombstone Canopy"

Raupach et al. (1986; hereafter RCL) reported wind statistics, and Legg et al. (1986) the temperature field due to a line source of trace heat, within the "Tombstone Canopy," a staggered array of vertical bars ($H = 60$ mm high, $Y_0 = 10$ mm wide, $X_0 = 1$ mm thick), arranged in a diamond pattern on the floor of a wind tunnel (cross-stream spacing $L_y = 60$ mm, along-stream spacing $\frac{1}{2}L_x = 44$ mm). Although an unnatural type of canopy, the experiment provided excellent data on scalar dispersion (trace heat) from line and area sources in the canopy, as well as a test of the importance of horizontal inhomogeneity on the scale of the "tombstone" spacing. Because this is such an unusual canopy, and because the flow is so comprehensively documented and analysed, these data are a useful challenge to the breadth of applicability of the closure we have introduced. The flow was in approximate streamwise equilibrium (ie., alongstream gradients were weak) in the test section. Velocity statistics were measured with a specially-developed 3-wire probe (Legg et al., 1984). The data used here (Table 3b) are mostly from measurements at (their) $x \approx 1.5$ m. The wind

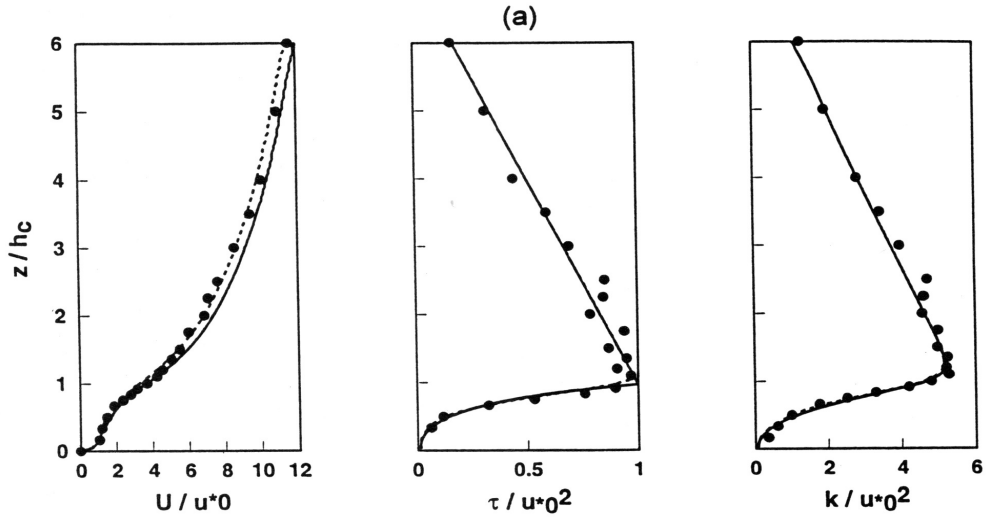


Figure 8.7: Simulation of spatial-mean profiles of mean velocity, shear stress and TKE in the Furry canopy. $K \propto \lambda\sqrt{k}$ closure.

profile is a composite, made up below $z/h_c = 1.5$ of the spatial average $\langle U \rangle$ measured by sonic anemometers at $x = 1.25$ m (their Fig 3c; Raupach et al. consider this profile their best estimate of wind in the canopy), and above, the hot wire profile from the central position (D) in the diamond cell at $x = 1.5$ m. TKE and shear stress, likewise, are from ($x = 1.5$ m; position D). From the vertical gradient in Reynolds stress above the canopy (balanced by advection) we calculated an effective $\partial_x P$. Fig. (8.8) shows the profiles computed for this canopy. This is a particularly interesting canopy in that data are provided for the spatial variation within the unit cell of the canopy[6].

8.5 Countergradient transport in plant canopies

Figure (8.9) from Denmead and Bradley shows the mean vertical profiles of temperature, specific humidity and CO_2 concentration, and the corresponding vertical eddy fluxes of heat, vapour and carbon dioxide, for a particular interval in the Urriara forest. Notice that below the crown of the canopy, the mean heat flux runs *against* the mean gradient, and that in the upper crown the CO_2 flux likewise is countergradient. As for the vapour flux, at the base of the crown it is directed upwards, yet the corresponding concentration gradient is essentially zero. Summarising their observations in the Urriara forest, Denmead and Bradley wrote: "Turbulent transport in the canopy appears as a sporadic process quite unrelated to the

[6]New studies of the Tombstone Canopy suggest that large coherent eddies of a length scale several times the unit cell width affected the dispersion. (Dr. E. Yee, pers. comm.)

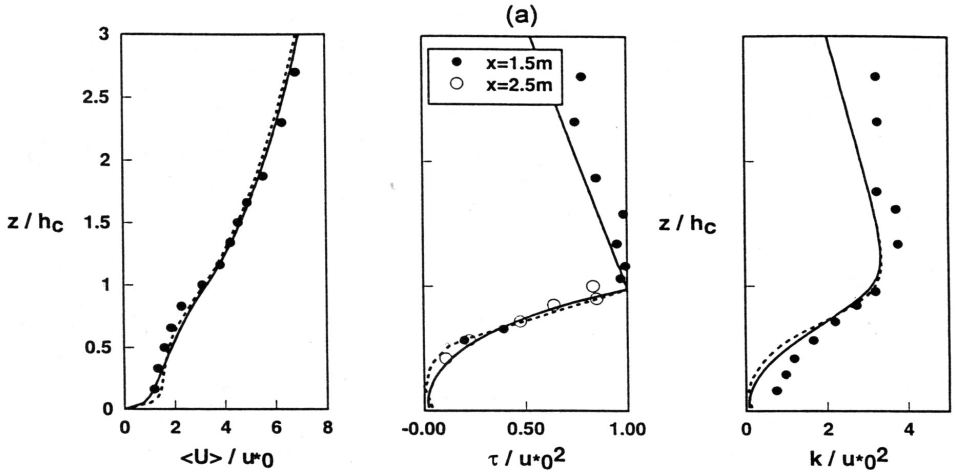


Figure 8.8: Simulation of spatial-mean profiles of mean velocity, shear stress and TKE in the Tombstone canopy. $K \propto \lambda\sqrt{k}$ closure.

shape of the mean concentration profile." These observations (counter-gradient transport)

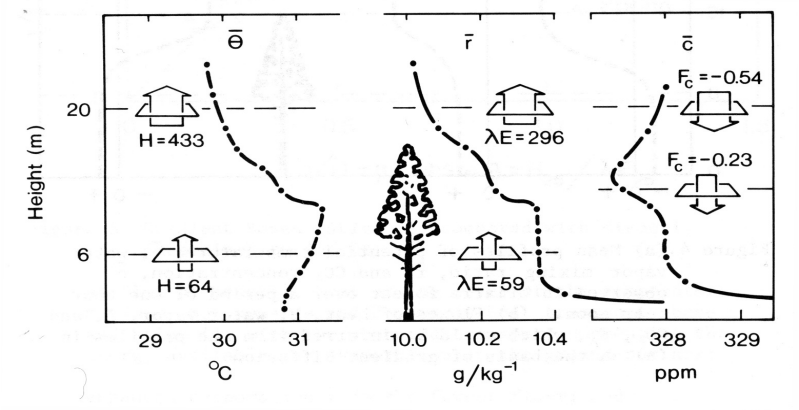


Figure 8.9: Countergradient fluxes in a uniform pine forest; from Denmead and Bradley

are incompatible with K-theory, according to which the fluxes should run down the mean gradient.

The invalidity of K-theory (in general) had been implicit since Taylor's (1921) Lagrangian treatment of dispersion, if not earlier. However K-theory continued (and still continues) to be used. Periodically problems were noted, eg. Legg and Long (1975), and from time to time

scientists addressed the issue. One of the more famous analyses is that of Corrsin (1974), who stated as a pre-condition for the validity of K-theory that: "the transport mechanism length scale must be much smaller than the distance over which the curvature of the mean transported field gradient changes appreciably."

Now, let λ be a length-scale of the turbulence, eg. $\lambda = \sigma_w \Gamma_{ww}$ where Γ_{ww} is an Eulerian integral timescale of the vertical velocity. Recall that integral scales characterize the energy-containing range of scales. If we take λ as the "transport mechanism lengthscale" then Corrsin's criterion may be interpreted mathematically as requiring:

$$\lambda \, |\frac{\partial^2 C}{\partial z^2}| \ll \, |\frac{\partial C}{\partial z}| \tag{8.40}$$

where C is the mean concentration of the transported scalar (this is just roughly the requirement that the concentration gradient be unchanging over the span of the eddy length scale). That is, we require

$$\lambda \ll \, |\frac{\partial C/\partial z}{\partial^2 C/\partial z^2}| \, . \tag{8.41}$$

Now if we refer back to Figure (8.9), we note that owing to the complex canopy source distribution, we have a very irregular concentration profile. If one is to be so bold as to cite a canopy transport lengthscale, then in view of the dominance of canopy turbulence by the gusts, that lengthscale is large, say $\lambda \sim h_c$. Thus, the condition specified by Corrsin is not met, in this flow.

An *explanation* of the failure of K-theory (as opposed to merely identifying under what conditions it may occur) relates to the fact that in the near field of sources, the transport process is definitely not "diffusion" (refer to the section on G.I. Taylor's Lagrangian theory). Raupach (1987) has given an approximate analytical theory (Localised Near Field Theory, LNF) for the source-concentration relationship in a uniform plant canopy, and this hinges on providing a better description of the contribution of nearby sources. Countergradient fluxes are unsurprising when we make observations at points that are *not* in the far field of widely separated sources.

8.6 The renewal model

We have seen evidence that mixing in a plant canopy is intermittent; that periods of relative calm are punctuated by abrupt penetration of the canopy by gusts. The exact structure of these gusts is unknown, ie. we do not have time-dependent solutions of the NS equations, etc. Many questions arise; how are they connected to the large eddies of the surface layer above? What is their relation to the inflexion-point instability? What is their relation to the hairpin eddies?

But without any further detailed knowledge of the eddies, and because it is appealing due to its physical clarity, people have proceeded to build a so-called "clean-sweep" or "renewal"

model of canopy transport, which involves periodic time-dependent vertical profiles $T = T(z,t)$ etc. At intervals ${\delta_t}^{swp}$ the canopy is considered to be "flushed", and at these instants $T(z,t) = T_b, q(z,t) = q_b$, where $T_b = \overline{T}(z_b)$ is the temperature of the "bulk" boundary layer (etc). After the "flush", follows an interval ${\delta_t}^{swp}$ of small-scale diffusion (diffusivity $K = K(z)$ during which heat and vapour from the canopy is spread. If one time averages the profile $T(z,t)$, one obtains the models's mean profile $\overline{T}(z)$.

The interval ${\delta_t}^{swp}$ between the sweeps is random, and attempts to scale its mean value with overall conditions (stability, canopy height) show a fair amount of scatter (e.g. Brunet and Irvine, 2000). In models the renewal interval is treated as an adjustable parameter; there are also other arbitrary inputs, such as the level z_b from which properties of the "flushing" air are assigned.

8.7 Canopy wind spiral

The canopy "wind spiral" has received little attention despite Shinn's (1971) early recognition of it, an exception being Holland (1989). Shinn showed that due to the Coriolis force there occurs a large swing in mean wind direction between tree-top level and the base of the canopy.

The cause of the canopy wind spiral is simple to give in qualitative terms: deep enough within a dense canopy ($z \ll h_c$) the Coriolis force and the turbulent shear-stress are "small," and it follows that the mean wind is directed parallel to the large scale pressure gradient, implying (up to) a full 90^o swing in direction between the Geostrophic-level, where the wind blows perpendicular to the pressure gradient, and ground-level. Shinn used the term "Quasi-Geotriptic" to describe that local force-balance, "a balance of the drag force and the pressure gradient force but with residual effect of the Coriolis force evident in the direction of the wind drift with respect to the geostrophic definition of the pressure gradient direction."

Directional shear is presumably then to be regarded as normal, in mid- and high-latitude canopies. It will have to be accounted for in scientific descriptions of many problems, eg. short range patterns of (pollen, seed, etc.) dispersion from localised sources.

8.8 Coherent structures in canopy flows

Finnigan et al. (2009) used Large Eddy Simulation to investigate the role of coherent structures in canopy flow. Their abstract states "The characteristic eddy consists of an upstream head-down sweep-generating hairpin vortex superimposed on a downstream head-up ejection-generating hairpin. The conjunction of the sweep and ejection produces the pressure maximum between the hairpins, and this is also the location of a coherent scalar microfront."

Chapter 9

Coherent Structures in the Lower Atmosphere

Thermals, dust devils, and roll vortices are familiar "large eddies" of the lower atmosphere. They may play an enormous role in atmospheric transport, but as yet we are generally unable to account for them is a satisfactory way. This is because they are stochastic in the sense that we do not know where or when they will occur, nor how often. Their existence does find faint reflection in theory of the atmosphere: for example we accept that the pdf for vertical velocity in the CBL (rightly or wrongly, treated as horizontally-uniform) is skewed, owing to thermals, and we can build Lagrangian dispersion models accordingly. Models that account for the skewness of w perform better than those that don't, in respect of the tendency of the plume from an elevated source to descend towards ground.

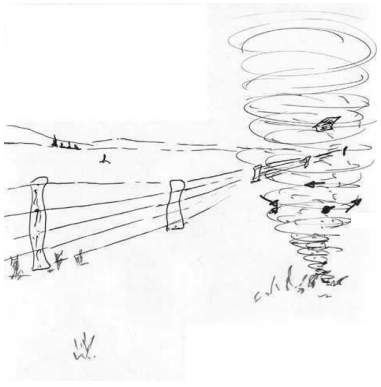


Figure 9.1: Dust Devil.

9.1 The Dust Devil (columnar vortices)

Dust devils are in general a harmless, fascinating and beautiful phenomenon (they can be dangerous for hang glider and paraglider pilots). They range in diameter from $O[1]$ m to tens of metres; and although their *visible* height is usually only a few tens of metres (or less), occasionally they are seen up to several hundred metres. Dust devils play a very important role in the micrometeorology of the Martian boundary layer, where they grow much larger and taller than do their terrestrial cousins. Dust from the dry Martian surface, raised high into the boundary layer, absorbs solar radiation, thereby stabiling the distribution of potential temperature (**?**).

As to the circulation within a dust devil, measurements indicate a downdraft at the axial core, surrounded by "a region of vigorous upflow and swirl" (Smith and Leslie, 1976), with "maximum vertical velocities (being) comparable with maximum swirling velocities." Smith and Leslie performed a numerical simulation of a "thermally driven vortex," acknowledging that their assumption of constant eddy viscosities and eddy diffusivities limits interpretation of the modelled circulation as "real." (See Kanak, 2005, for more recent simulations of the dust devil.)

Regarding the path of a dust devil, Maxworthy (1973) produced a theory that a cyclonic (anticyclonic) dust devil should drift to the right (left) of the mean wind shear vector, in accordance with his field observations (Kanak et al. 2000).

9.2 Connexion of the convective surface layer to the outer-CBL thermals

Webb (1988) made an interesting commentary on convective turbulence, indicating that a satisfactory theoretical understanding has not yet been achieved. His comments stemmed from an experiment to study "how the surface layer (the lowest 20 or so) gives rise to the extended boundary-layer convection with thermal columns up to heights of 1 or 2 km." On the basis of this experiment, over flat grassland in Australia and involving measurements near ground (an array of anemometers and thermometers) and gliders circling overhead at around 800 m, Webb infers that "Small scale turbulence and plumes transfer heat from the ground into the surface layer. In a completely decoupled mode of convection, this heated surface layer as a whole gives rise to thermal walls arranged in an irregular polygonal net; these extend up through the CBL to heights of around 300 m where they channel the warm air into the bases of columnar thermals." Webb:

- notes that the ratio $R = -Q_H(\delta)/Q_H(0)$ helps to correlate observations of CBL turbulence, or in particular, of the potential temperature variance $\overline{\theta'^2}$

- major convective elements in the CBL (as opposed to the entrainment layer) "have at least the simplification of being elongated in the vertical"
- Priestley (1955) had noted that as instability increases such that $-R_i \approx z/L$ increases through a value of about $-R_i \sim 0.03$ the heat flux-temperature gradient relationship switches from forced convection ($\partial\overline{\theta}/\partial z \propto z^{-1}$) to free convection form ($\partial\overline{\theta}/\partial z \propto z^{-4/3}$)
- the surface-based buoyant plumes only reach to about $z \sim -L$
- in moderate winds the surface flow patterns indicate convective upcurrents in the form of walls about 50 - 100 m thick, arranged in an irregular net of polygonal cells about 3 km across. The walls carry warm surface-layer air up through the CBL... to heights of around 300 m, where, probably at the junctions of walls, they channel the warm air into the bases of the columnar thermals which extend up to the top of the CBL"
- the width of the columnar thermals "is likely to be scaled to the surface-layer Obukhov length L, since they arise from the polygonal walls" while " the height of the system of walls and columns is scaled to z_i"
- "in the central areas surrounded by the cell walls, the subsiding cooler air is entirely devoid of temperature fluctuations.
- "the whole polygonal pattern travels in the general wind direction"

Webb gives many references to observations supporting the concept of these cellular patterns and the "walls". He infers that "the small scale turbulence and plumes transfer heat from the ground into the surface layer, while this heated surface layer as a whole gives rise to the boundary-layer convection walls." Telford (1972) gives a theory of plumes in the ABL.

9.3 Thermals

Lenschow and Stephens (1980; LS) define thermals as "buoyant parcels or plumes 50 to 1000 m in diameter that develop above a surface which is considerably warmer than the overlying air," while Stull (1988) terms them "large columns of rising buoyant air in the convective mixed layer." Of course, not every interval of positive vertical velocity corresponds to a thermal, and so scientific measurements of thermals always require some identification strategy. In their selection criteria, Lenschow and Stephens required that the vertical velocity remain positive over a distance exceeding 25 m, and the humidity more than $\frac{1}{2}\sigma_q$ above the mean $\overline{q}$ for the flight leg.

According to earlier aircraft measurements (at height $z = 100m$) analysed by Manton (1977), thermals occupy a fractional area of 40% of the horizontal plane, and it is stated that

observations throughout the CBL indicate about the same fraction. However the more "conservative" thermal selection process of Lenschow and Stephens indicated a smaller fraction of their aircraft record ($20 - 30\%$) occupied by thermals[1].

Thermals occur during unstable stratification (surface heat flux $Q_{H0} > 0$) in the convective boundary layer (CBL). According to Stull, 1988, thermals are "trapped within the mixed layer," and their range of penetration heights defines the entrainment zone of this CBL (zone in which bl air and air from the free atmosphere above are mixed).

[1]The experience of hang gliding in the CBL seems quite clearly to confirm that Manson's estimate is too large, although one must remember that a hang glider pilot will think of a thermal as a region with $w >\sim 2 - 3\ \mathrm{m\,s^{-1}}$, which will "select out" events that scientists may have identified as thermals. The study of Pennycuick (1998) confirms that if the definition of a thermal is based on vertical velocity alone, then the thermal fraction is very sensitive to the vertical velocity threshold chosen.

9.3.1 Thermals in a uniform CBL, according to mixed-layer scaling

According to mixed-layer scaling, one has a single length scale δ. It follows that the number-density of thermals on the landscape (number per unit area) $N_A \propto \delta^{-2}$ and thermal diameter $D \propto \delta$. Consistent with this, Lenschow and Stevens *observed* that, above the surface-layer, the number of thermals intersected per unit distance travelled is

$$N \approx 1.5\,\delta^{-1} \; . \tag{9.1}$$

Assuming a random distribution of thermals in the horizontal (and that is all the idealized theory of a uniform CBL attempts), this means that the thermal number-density (number per unit ground area) is $N_A \approx 2\,\delta^{-2}$, so that if $\delta = 1$ km, then there are about two thermals per square kilometer of ground area; and (as a statistical fact, only) on average, in flying 1 kilometer, we should encounter one.

LS also report their observation of the "average length of intersected segments of thermals", a number which is likely to be substantially smaller than the actual "diameter" of thermals (since their aircraft did not necessarily penetrate the middle of thermals). They found the segment length increases with increasing height,

$$D_{iseg} \approx 0.16\;\delta\;\left(\frac{z}{\delta}\right)^{1/3}\;\left(1 - \frac{1}{4}\,\frac{z}{\delta}\right) \; . \tag{9.2}$$

At $\delta/h = 0.5$, $D_{iseg} \approx 0.1\,\delta$, and so presumably mean thermal diameter $D \approx \delta/5$. Again taking $\delta = 1$ km, we have for the diameter of our thermal $D = 200$ m. This does not seem unreasonable, but hang glider pilots are often able to circle much more sloppily, indeed just tour around at liberty, and remain in lift... perhaps these experiences are not due to "thermals."

Note that for larger δ we have *fewer* thermals per square kilometer, ie. a thermal is harder to (randomly) find, but statistically, if found, it will be a larger thermal than under lower-δ conditions.

According to mixed-layer scaling, the turbulence velocities in the CBL scale with the convective velocity scale

$$w_* = \left(\frac{g}{T_0}\,\frac{Q_{H0}}{\rho c_p}\,\delta\right)^{1/3} \; . \tag{9.3}$$

Thus Q_{H0} is doubly important, in that it affects w_* directly, but also promotes a large δ. Furthermore the surface energy budget states that:

$$Q_{H0} = Q* - Q_{E0} - Q_G \tag{9.4}$$

so thermals will be more likely where the surface is dry (thus, hot).

In principle, updraft velocity $W \propto w_*$, and B. Stevens has found (from LES studies) that the maximum velocities are about equal in magnitude to w_*. Lenschow and Stevens *observed*

that the mean updraft velocity

$$W = w_* \Big(\frac{z}{\delta}\Big)^{1/3} \Big(1 - 1.1\,\frac{z}{\delta}\Big) \tag{9.5}$$

indicating that W "decreases approximately nearly to zero at the top of the mixed layer" from a maximum (of about $w_*/2$) at about $\delta/2$. Thus a thermalling hang glider might expect the strength of thermals to diminish with increasing elevation.

What is the structure of a thermal? Telford (1972) and Weijers et al. (1994) show an interesting diagram by Wilzak (1984; see also Wilczak & Tillman, 1980) that indicates the convergent horizontal velocity field near ground, in the proximity of a microfront.

9.4 Roll vortices

Commonly present in the PBL, and of great significance for soaring, are "roll vortices" (Fig. 9.2), i.e. paired, counter-rotating, horizontal vortices, which occupy the whole boundary-layer, and can be very persistent (lifetime $\tau \sim 1-72$ hr). The axes of rotation of the rolls are aligned with the mean wind direction, to within a smallish offset angle (ϵ, $-20^o \leq \epsilon \leq 30^o$). Pair-spacing ($\lambda/2$) varies in the range $1-2$ km, while the longitudinal extent may be huge, from 10 to 1000 km. B/l rolls are made visible when cloud streets occur, but often occur without that observable sign. Etling and Brown (1993) surveyed the observations, and noted that "rolls are ubiquitous in favourable situations" and "may be present for all moderate flows with modest unstable stratification". Analyses indicate that "dynamic (inflection-point) instabilities and thermal (convection) instabilities are still assumed to play their roles under certain situations... But it is now recognized that a single instability mode cannot explain the observed structure of large roll-like eddies in the real ABL". However "it appears that under most circumstances large roll eddies in the PBL are driven by thermal instabilities", and the "roll regime" lies in the slightly unstably stratified regime $-25 \leq \ z_i/L \ \leq -5$. Emanuel (1994; p203-204) writes: "On windy days, surface stress and/or baroclinic effects may produce reasonably strong shear on the mean horizontal wind within the ABL. If the shear is strong enough to overcome the preference of strongly nonlinear convection for three-dimensional forms, two-dimensional convection aligned with the shear vector is preferred, and the overlying cumuli occur in rows or cloud streets."

In the laboratory (where the Coriolis force has no influence), rolls may be produced not only in a sheared convective layer, but also in a neutral shear layer; indeed Etling & Brown, 1993 consider that *in theory* they may occur in the atmosphere even during slightly *stable* stratification – though most commonly they are seen in an (at least, slightly) unstable b/l: apparently they have been seen during such modest instability as $|\delta/L| \approx 2$, but more typically for $|\delta/L| \approx 5-15$, while in extreme instability $|\delta/L| \geq 25$ three-dimensional convection cells take over. Thus it appears that there may be more than one type of instability

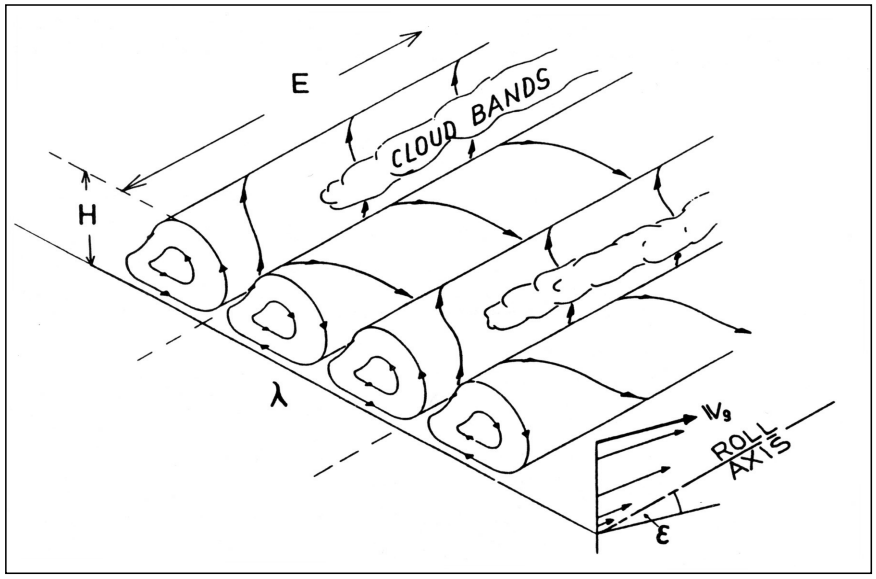


Figure 9.2: Schematic of boundary-layer roll vortices, taken from Etling and Brown (1993).

able to cause b/l rolls: an interaction of thermal convection with shear, but perhaps also (Etling & Brown, 1993 cast doubt on this, though it was earlier considered definite), an inflexion-point instability which can be present due to directional wind shear (Ekman layer turning, whether it be ideally-normal or not) through the ABL.

Drobinski et al. (1998) summarize the theoretical view of bl rolls: In neutral, barotropic conditions the rolls are theoretically aligned at $\alpha = 18^{\circ}$ relative to the direction of the Geostrophic wind, and should drift laterally at about $1\,\mathrm{m\,s^{-1}}$ (Brown, 1970). The angle α is expected to be larger (order 30°) in stable stratification and smaller (order 5°) in unstable stratification, when the lateral drift velocity is expected to vanish. Their observations (lidar; sodar; tower) of rolls on two days in a cloudless ABL agreed very well with the predictions of Brown's theory.

9.5 Wall-generated Inertial Eddies (Hairpin Vortices)

For a long time "hairpin" vortices (also called "horseshoe vortices") have been considered by some authors as the most significant "structure" in wall shear-layer turbulence (see Figure 9.3). Perry and Chong (1987) modelled wall turbulence using the hairpin as the representative eddy (see also Marusic, 2001). A recent suggestion is that these occur in spatially-correlated

trains of vortices aligned in the direction of the mean flow, an idea emerging from several directions (Theodorsen, 1952; Smith et al., 1991; Adrian et al., 2000; Christensen and Adrian, 2001; Hommema and Adrian, 2003; McNaughton, 2004a, 2004b, 2006; McNaughton and Brunet, 2002).

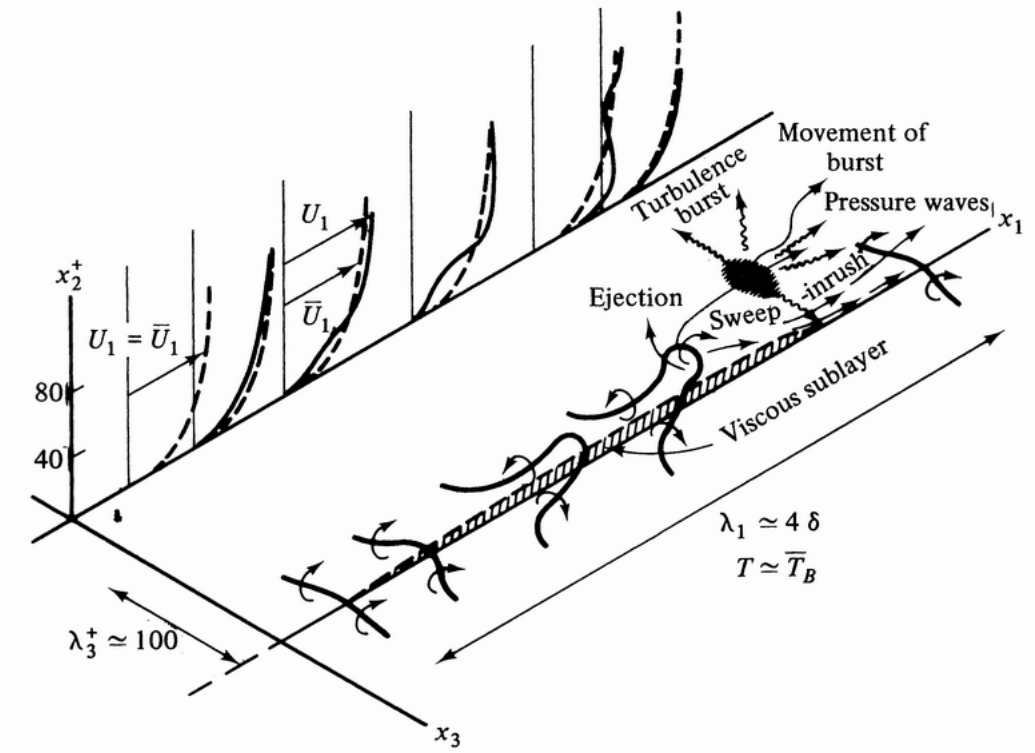


FIGURE 7-43
Conceptual model of the turbulence near the wall during a "cyclic" process, with average spacings λ_1 and λ_3.

Figure 9.3: Schematic of boundary-layer hairpin vortices, reproduced from Hinze (1975, Figure 7.43).

9.6 Bird flight in the ABL

Birds soaring in the ABL exploit the updrafts to reduce their energy expenditure. Articles on this include Woodcock (1975), Agee and Sheu (1978) and Pennycuick (1998).

Part IV

Disturbed Flows

Chapter 10

Introduction

The notion of a *horizontally-inhomogeneous* or *disturbed* ABL establishes a dichotomy, a two-fold classification of ABL's, relative to the idealization of a horizontally-uniform ABL. If the latter did not exist, neither, in a sense, would the former.

What would we mean by an "understanding" of disturbed flows? A crow understands even the wildest of winds, and would laugh at our scientific notion of understanding – the spatial pattern of 30-minute statistics, $\overline{u}(x, y, z)$, $\sigma_u(x, y, z)$ and so forth. In everyday life we do not tend to compare weather where we are, on campus walking between the library and our next class, briefly in the sun, with any reference state elsewhere. Simply we note it is sunny, or not; windy, or not; the snow is slushy, or not. Any theory for this local environment has to link the region described with the outer universe; the "weather" on campus is bounded by, and coupled to, the "weather" around and above campus, and so on. Ultimately, explaining present "weather" on campus entails knowing the weather all over planet earth. However we may construct local scientific theories for *differences* in weather variables $\Delta\overline{u}(x, y, z), \Delta\overline{T}(x, y, z)$, relative to a reference state. Typically the reference state is defined by a weather station at a local airport, in terms of reference values $\overline{u}_a, \overline{T}_a$. In this chapter we will make a few abstract points relative to disturbed flows *in general*. In later chapters we shall cover some interesting specific cases.

Horizontal gradients of mean properties in the atmospheric surface layer may be generated by

- inhomogeneity in the surface boundary conditions (inhomogeneity in surface properties and fluxes eg. ΔQ_{H0} or ΔQ_{E0}
- by purely aerodynamic disturbances (Δz_0, fences, hills, surface cover)
- a combination of these types of influences

But even in the absence of obvious disturbances originating at the boundary, the ASL and the ABL may be horizontally-inhomogeneous.

10.1 Paradigm of the Internal Boundary Layer (IBL)

Suppose we consider that upwind of a boundary at $x = 0$, the atmosphere is in equilibrium with the ground (and the surface fluxes), while, at $x = 0$ occurs a transition to a new surface.

The concept of the IBL is closely related to the idea of a deepening "plume" of tracer ejected from the downwind surface, and within that plume we identify what depth of the atmosphere has been altered by the boundary change. Clearly the growth rate of the IBL, $\partial\delta(x)/\partial x$, must have to do with the balance between the rate of vertical propagation of fluid-elements that have touched the surface (say, σ_w) and the rate at which they are whisked off downwind ($\overline{u}(z)$).

Mikaye (1965) is considered to have been one of the early proponents of this argument (see Panofsky, 1973), according to which

$$\frac{\partial\delta(x)}{\partial x} \propto \frac{u_*}{\overline{u}} \; . \tag{10.1}$$

If we assume a log wind profile, we may write

$$\frac{\partial\delta(x)}{\partial x} = \frac{A}{\ln \frac{a\,\delta}{z_0}} \tag{10.2}$$

where $a\delta$ is the effective height at which the mean wind is to be evaluated. For simplicity, set $a = 1$. Now integrate, noting that for any variable x the indefinite integral $\int \ln(x)dx = x[\ln(x) - 1]$. Then the solution for the depth of an IBL in neutral stratification is[1]

$$\frac{\delta(x)}{z_0}\left[\ln\frac{\delta(x)}{z_0} - 1\right] + \; 1 = A\,\frac{x}{z_0} \tag{10.3}$$

where (according to Panofsky, loc. cit.) $A \sim 0.6$ and z_0 should be evaluated for the rougher of the upstream and downstream surfaces. However Savelyev and Taylor (2001) reason that the upstream roughness length should be used, and draw confirmation of that proposal from observations.

More sophisticated formulae for the growth of the IBL have been given (see review article by Garratt, 1990; and textbook discussion by Garratt, 1992), but the point to be made here is that *in general*, the notion of an IBL is inappropriate. If at $x = 0$ there is a profound aerodynamic disturbance – say a cliff, or a transition from forest to field, then there will be a disturbance to the mean pressure field,

$$\frac{1}{\rho_0}\nabla^2\overline{p} = -\,\frac{\partial\overline{u}_i}{\partial x_j}\,\frac{\partial\overline{u}_j}{\partial x_i} \; - \; \overline{\frac{\partial u_i'}{\partial x_j}\,\frac{\partial u_j'}{\partial x_i}} \; - \; \frac{g}{T_0}\,\frac{\partial\overline{T}}{\partial z} \; . \tag{10.4}$$

What we learn from this equation is that the pressure field *everywhere* is sensitive to the velocity gradients everywhere (although there is a $1/r$ decay in the sense that a velocity

[1] Compare with the equation of Wilson, 1982a, for the depth of a plume in the NSL.

gradient at point $\overrightarrow{x_1}$ influences the pressure at point $\overrightarrow{x_2}$ with a proportionality factor involving $r = |\overrightarrow{x_2} - \overrightarrow{x_1}|$). But the point is that the resulting re-adjustment may occur at a pace that is not fundamentally describable in terms of a diffusing plume of velocity change $\Delta\overline{u}_i$ emanating from a source, ie. the location of the disturbance, growing in the vertical in relation to σ_w and advecting downstream in the profile $\overline{u}(x, z)$.

The chapters to follow will illustrate how micrometeorologists comprehend disturbed flows, by attacking first the idealized cases where (for instance) a spatial symmetry prevails or a hill has a precise geometric shape, etc.

Chapter 11

Local Advection

Consider the idealized situation of a long straight boundary (parallel to the y-axis, at $x = 0$) separating a uniform upstream surface with roughness length z_{00} from a *different* downstream surface with roughness length[1] z_{01}. For example the upstream (0) and downstream (1) surfaces might differ in their (constant) surface temperatures[2] T_{00}, T_{01}.

By definition, then, over the upstream surface ($x < 0$), and not too close to the step change at $x = 0$, the surface-layer wind, temperature and specific-humidity profiles $\overline{u}_0(z), \overline{T}_0(z), \overline{q}_0(z)$ are in equilibrium with the (kinematic) surface fluxes ${u_{*0}}^2, u_{*0}T_{*0}, u_{*0}\rho_{v*0}$ of momentum, heat and water vapour, where "in equilibrium" means that the relationships of MOST apply. However downstream, ie. at $x > 0$ (and probably even slightly upstream from $x = 0$), MOST does *not* apply, except possibly at large x where under suitable circumstances a new equilibrium may be established. Therefore the profiles $\overline{u}(x, z), \overline{T}(x, z), \overline{q}(x, z)$ are *not*, over the downstream region, in equilibrium with the "new" surface fluxes $\overline{u'w'}_{z=0}(x), \overline{w'T'}_{z=0}(x), \overline{w'\rho'_v}_{z=0}(x)$.

Now, the vertical fluxes of momentum, heat and vapour need not be height-independent over the downwind region, so we need to be careful with notation: these fluxes will be $Q_H(x, z), Q_E(x, z)$ (etc.) where, for $x \ll 0$, $Q_H(x, z) = const = -\rho\, c_p u_{*0} T_{*0}$ (etc).

"At" the surface, the vertical energy fluxes are constrained by the surface energy balance,

$$Q^* = Q_H(x, 0) + Q_E(x, 0) + Q_G + \Delta Q_s \tag{11.1}$$

and so whereas the upwind surface tempeature and humidity are (by assumption) constant, they may be spatially variable over the downwind surface.

This scenario is the prototype of "local advection," which occurs for example when the wind passes off arid land onto irrigated fields (or vice versa). Earliest treatments were analytical, and used unrealistic surface boundary conditions (eg. step change in surface

[1] If you consider how a roughness length is defined, as a constant of integration in the equilibrium wind profile, you see that one commits oneself to a superficial view when one speaks of a "step change" in surface roughness length; on the other hand measurable attributes of the local surface, say height h_c of the grass, may undergo a step change.

[2] In view of the complexity of the surface energy budget, this situation of constant but different surface temperatures is not likely to arise in practise, although it could be contrived in a wind tunnel.

temperature or step change in surface heat flux). The step change in roughness became something of a favourite problem, usually treated in the spirit of the longitudinal advection and vertical "diffusion" of velocity-change, sourced at the new surface. Some of the many influential local advection experiments are those of:

- Rider, Philip and Bradley (1963), who studied wind and temperature profiles on and off an airport tarmac. Analysis of these data demonstrated that much was correct in Philip's (1959) analytical treatment of local advection
- Dyer (1962) and Dyer & Pruitt (1962)
- Lang et al. (1974) and Lang et al. (1983)
- Itier & Perrier (1976)
- La Crau valley — De Bruin et al. (1991), Bink (1996), Wilson et al. (2001)

Taylor (1970, 1971) was among the first modern (numerical) treatments of local advection, although here still, there were simplifications, foremost of them an unrealistic boundary condition, and a closure based on a disturbed eddy diffusivity $K = k_v u_* z \phi^{-1}$ postulated as given by a "local" friction velocity $u_* = u_*(x, z)$ and MO length $L = L(x, z)$ in the disturbed flow. Not long afterwards Rao et al. (1974a, 1974b; hereafter RWC) simulated local advection using one of the earliest applications of second-order closure in micrometeorology. The RWC model consisted of 16 coupled partial-differential equations, governing all first- and second- order statistical properties of the flow; ie. mean velocity $(\overline{u}, \overline{w})$, mean pressure $(\overline{p})$ temperature and humidity $(\overline{T}, \overline{Q})$; variances $({\sigma_u}^2, {\sigma_v}^2, {\sigma_w}^2, {\sigma_T}^2, {\sigma_q}^2)$ of the fluctuations (u', v', w', T', q'); covariances (symbolically, $\overline{\alpha' \beta'}$), which include the turbulent convective fluxes, such as $\overline{w'T'}$; and the turbulent kinetic energy dissipation rate ϵ. This is probaby stll the most complex model applied to local advection, and has subsequently been used by many others, including N. Bink (Ph.D thesis).

Fig. (11.1) compares a simulation (Wilson *et al.*, 2001, using the RWC local advection model) of the mean temperature and humidity fields in flow from dry land onto irrigated grassland in the La Crau valley (France), and may be compared with Bink's (1996; Figure 6.4a,b) simulation of the same data. These observations are averages over a single 30 minute period (Run 42; 22 June 1987, 1130 hrs). The highly unstable near-ground temperature profile over the arid upwind plain is rapidly transformed by the growth of a moist, near-neutral internal boundary layer over the cooler, evaporating downwind surface (in other circumstances, a strong inversion develops over the cool surface).

Inputs for this simulation of Run 42 are identical to those used by Bink (1996), given in his Table (6.1). The upstream friction velocity $u_{*0} = 0.63\,\mathrm{m\,s^{-1}}$ and roughness length $z_{00} = 0.01$ m. Reference upwind temperature and specific humidity at $z_{ref} = 3.05$ m were drawn from

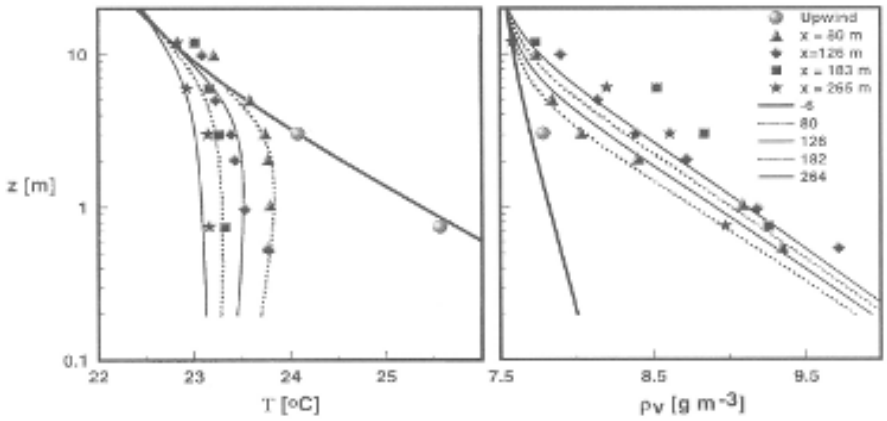


Figure 11.1: Observed (symbols) and modelled (lines) vertical profiles of mean temperature and absolute humidity in flow off dry land onto moist land (La Crau Run 42; data from Bink, 1996). Highly unstable near-ground temperature profile over the arid upwind plain is rapidly transformed by the growth of a moist, near-neutral internal boundary layer over the cooler, evaporating downwind surface.

the observed values on the upwind tower, $T_{ref0} = 24.08$°C and $Q_{ref0} = 0.0066$[kg/kg], so that Bink's specified temperature and absolute humidity at $(x = 0, z = z_{01})$ were not required. The upstream energy supply was $Q_{*0} - Q_{G0} = 434$ [W m^{-2}], with the upstream sensible heat flux accounting for $Q_{H0} = 362$[W m^{-2}]. Over the downstream surface $z_{01} = 0.07$ m, and following Bink's observation (his Table 4.4) we set the downstream available energy supply $Q_{*1} - Q_{G1} = 500$[W m^{-2}]. Over the moist surface the canopy resistance $r_{c1} = 47\,[\mathrm{s\,m^{-1}}]$.

The rather good agreement of the simulation with the observations suggests that the second-order closure model has reasonable fidelity — as indeed it should, since it captures many of the relevant processes realistically and is driven by *measured* boundary conditions.

Chapter 12

Windbreak Flows

Anyone who has stepped into the lee of a line of trees on a windy day will have noticed the pleasant relief offered. Even a ragged, leafless line of weather-beaten shrubs may offer a surprising calm. Windbreaks are of practical importance in many parts of the world, and so offer us a chance to study a well-defined "disturbed flow" that is also pertinent to human affairs. A line of trees against the storm winds may offer shelter to a wet sheep, whose newborn lamb might otherwise die from hypothermia; might prevent wind damage to the vineyards; might moderate the sway of fruit, and resulting wind-rub marks.

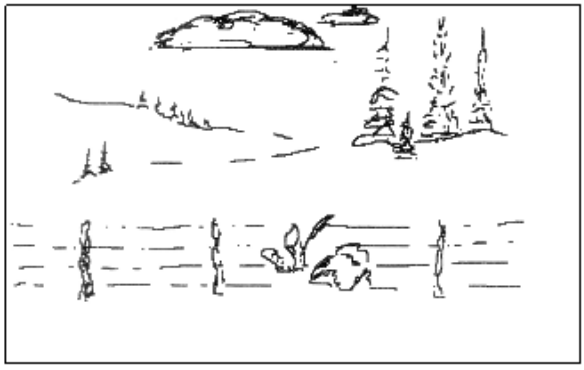


Figure 12.1:

The microclimatic effects of windbreaks are both direct (shading, wind reduction) and indirect (altered temperature, humidity, evaporation, plant size). The is no shortage of pamphlets for farmers or orchardists on the design of shelter (eg. Hanley and Kuhn, 2003). These probably suffice to answer most practical questions, but they are not very satisfying if one's interest is the aerodynamics. Here we concentrate on the purely aerodynamic aspects of a windbreak, because they are interesting.

An isolated windbreak constitutes one of the canonical disturbances of an ideal atmospheric surface layer, other examples being the step change in surface roughness z_0, and the step change in surface energy-flux densities (Q^*, Q_H, Q_E). Bradshaw (1973) stated that "the

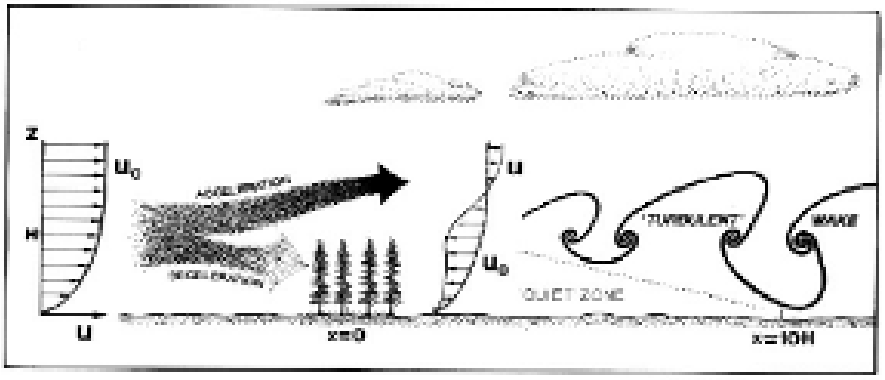


Figure 12.2: Schematic windbreak flow, showing mean velocity reduction, the "quiet zone" of reduced turbulence, and the turbulent wake due to enhanced shear at $z \sim H$.

most difficult flows to predict will be those in which a shear layer has its turbulence structure perturbed by a short region of strong pressure gradients and extra rates of strain, and then emerges into a longer region in which its Reynolds stress gradients are significant compared to smaller pressure gradients." Windbreak flow is such a flow.

12.0.1 Partial list of experiments on isolated windbreaks and windbreak arrays

1. Raine and Stevenson (1977), an influential wind tunnel study, with a focus on velocity spectra

2. Seginer (1975b,1975a), field studies on a thin windbreak in oblique, stratified winds.

3. Bradley and Mulhearn (1983; BM83), an experiment on neutral flow through a very long, isolated, porous (wooden slatted) fence standing on uniform ground. Key parameters were the windbreak height $h = 1.2$ m, surface roughness length $z_0 = 0.002$ m ($h/z_0 = 600$), and resistance coefficient $k_r = 2$ (measured in a wind tunnel by Wilson, 1985). Fig. 12.7 is a simulation of this experiment, discussed later

4. Wilson (1987): measured mean wind and turbulence behind two porous fences differing in the vertical profile of their porosity

5. Wilson (1997): measured the along-wind profile of mean ground-level pressure $\overline{p}_0(x)$ upwind and downwind from a single porous plastic fence on bare ground ($h = 1.25$ m, $z_0 = 0.008$ m, $h/z_0 = 160$, $k_r = 2.4$)

6. Wilson (2004): wind reduction versus approach angle and stratification

7. Judd et al. (1996): wind tunnel simulation of the flow through porous windbreaks standing in a model plant canopy ($h/h_c \approx 3$, where h_c is crop height), the barriers being spaced at intervals of $D_x/h = 6$ or $D_x/h = 12$.

8. Patton et al. (1998): an LES study of the Judd et al. experiment, approximating the repeated windbreaks by assuming flow through a *single* fence in a domain terminated by periodic along-wind boundary conditions. Patton et al. concluded that 'Mean fields from the numerical and physical simulations show striking resemblances', but that velocity variances were not simulated quite so well. Thus LES, though computationally far more demanding than RANS, does provisionally appear promising for the calculation of disturbed flows.

9. McAneney and Judd (1991): measured mean wind (using cup anemometers) and turbulence (using a 1-dimensional sonic anemometer) in their unique field study of the windflow about a series of 15 very long, parallel fences (their 'aeolian array'). The site was flat and unobstructed (roughness length $z_0 = 0.007$ m, displacement height $d = 0.045$ m), and data were selected for near-neutral stratification, with the mean wind direction within 10° of normal to the fences. The fences were composed of a porous, plastic windbreak cloth, had height $h = 2$ m ($h/z_0 = 290$), and were spaced along-wind at intervals $D_x/h = 6$. McAneney and Judd concluded with the observation that 'In a practical sense, the data clearly demonstrate the difficulty of simultaneously reducing both mean windspeeds and turbulence at crop levels using repeated windbreaks at conventional horticultural spacings'.

12.0.2 Overview of Windbreak Aerodynamics

We will consider the aerodynamic impact on surface layer flow of a long straight windbreak of height $H(\ll \delta)$ standing normal to the mean wind (Fig. 12.2). We mostly focus on the case of one or more *artificial* windbreaks, or *porous* barriers to the wind ("fences"), and we will assume symmetry along the y-axis. Nothing fundamental is lost in doing so, and the essentials carry over to describe natural windbreaks. An old review of many of the early measurements of windbreak flow is given by van Eimern et al. (1964). Heisler and DeWalle (1988) review the effect of windbreak structure on wind flow (in the same book, McNaughton reviews the windbreak effect on microclimate). McNaughton (1988, 1989) are useful overviews.

Characterizing the approach flow and the barrier

The simplest real windbreak flow is neutrally-stratified atmospheric surface-layer (ASL) flow perpendicular to an infinitely-long windbreak. The state of the undisturbed NSL (neutral

surface layer) can be taken as controlled by the friction velocity u_* and the surface roughness length z_0 alone.

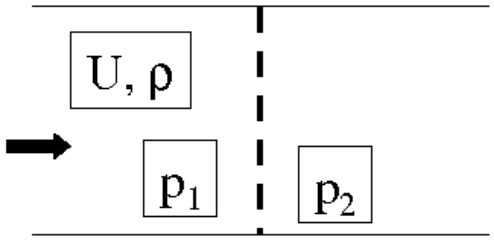


Figure 12.3: Defining the resistance coefficient k_r of a porous screen or cloth or fence. Approach flow is laminar and unsheared.

A porous barrier is conveniently characterized by its "pressure-loss" or "resistance" coefficient, $k_r(\theta)$ (Laws and Livesey, 1978). This is defined with reference to a calibration flow (Figure 12.3) wherein the barrier is mounted so as to block a uniform, shearless steady flow (velocity U) in a wind tunnel. The normal to the barrier is inclined at angle θ to the stream. The resistance coefficient is formed by normalising the pressure drop Δp across the barrier by $\rho\, U^2$,

$$k_r(\theta) = \frac{\Delta p}{\rho\, U^2}\ . \tag{12.1}$$

We will assume θ to be very small and write $k_r(0) = k_r$. Evidently, $k_r\ \rho\ u^2$ is the force per unit area exerted by the barrier on the flow and vice versa. To a first approximation one might expect that in an unbounded flow through a porous barrier, provided the streamline inclination relative to the barrier is small, the primary effect of each element $\Delta y\ \Delta z$ of barrier area would be to exert a localized retarding force $F_{Dx} = k_r\ \rho\ u\sqrt{u_i u_i}\ \Delta y\ \Delta z$ on the airstream (where u_i is the velocity at the barrier element[1]).

The resistance coefficient is easily measured, and may be correlated with the porosity and type of construction of the barrier (e.g., Baines and Peterson, 1951). Being an aerodynamic rather than a geometric property, its use as a characterizing attribute is much preferable to the use of porosity; flows through barriers of equal porosity and span may differ substantially but differences between flows through barriers of equal resistance coefficient and span but unequal porosity will be difficult to detect.

If we do wish to describe the wind resistance of a natural windbreak, we only need to introduce a spatially-varying plant area density function $a = a(x, y, z)$, $[\mathrm{m}^2\ \mathrm{m}^{-3}]$ (see section on canopy flows). If the windbreak is infinite in length and oriented along the y-axis, we may for example consider the case:

[1] F_{Dx} is the projection onto the x-axis of a vector force that is dependent on the square of the local windspeed.

$$a(x,z) = a_0(z)\ [s(x - x_{uw}) - \ s(x - x_{dw})] \tag{12.2}$$

where $s(x - x_1)$ is a unit step function at $x = x_1$,

$$\begin{aligned} s(x - x_1) &= 0,\ x < x_1 \\ &= 1,\ x \geq x_1 \end{aligned} \tag{12.3}$$

(etc.) and $a_0(z)$ describes the height-variable plant area density for a case where the foliage is uniform in x between the limits $x_{uw} \leq x \leq x_{dw}$. An even simpler case, foliage density uniform ($a_{00} = \text{const.}$) over the width $W = x_{dw} - x_{uw}$ and height H is

$$a(x,z) = a_{00}\ [s(x - x_{uw}) - \ s(x - x_{dw})]\ (1 - \ s(z - H))\ . \tag{12.4}$$

Mean velocity field

Momentum is removed from the flow at the barrier. This causes a mean velocity deficit both downstream and (as a result of pressure effects) for a shorter range upstream. Immediately cross-stream from (above, in the windbreak case) the barrier there is a sharp and shallow zone of increased velocity so that

$$\int_{z_0}^{\infty} \overline{u}(z)\ dz = \int_{z_0}^{\infty} \overline{u}_0(z)\ dz = \text{const.}, \tag{12.5}$$

where $\overline{u}_0(z)$ is the unperturbed approaching velocity profile and the integral spans the range of the cross-stream coordinate.

Between the speedup region and the velocity-deficit region is a region of very strong wind shear $\partial\overline{u}/\partial z$. The action of the shear stress $\overline{u'w'}$ (itself increased in this region) upon this shear converts mean kinetic energy to turbulent kinetic energy at an increased rate (relative to the undisturbed flow). The consequence (see Fig. 12.2) is a spreading zone of increased turbulence (again relative to the undisturbed flow). The turbulent convection of mean momentum back from the speedup region to the decelerated region causes recovery of the velocity field.

Turbulent velocity field

Formally, ie. in the conservation equations, the flow interaction with the barrier may be treated by adopting a spatial averaging procedure (see Wilson and Shaw, 1977; Raupach and Shaw, 1982; Finnigan, 1985), and as a result of the spatial averaging there appear terms which may be identified with the viscous and form drag. The (fluctuating) drag converts mean kinetic energy (MKE) to turbulent kinetic energy (TKE) at the barrier, and also exerts a drag on the turbulent flow, passing energy from larger eddies to small eddies on the scale of the barrier elements. In spite of this strong production of TKE at the barrier, observations

(Raine and Stevenson, 1977; Wilson, 1987) show a zone of reduced TKE in the near lee of a porous barrier, often called the "quiet zone". The quiet zone is bounded by the spreading wake of increased TKE generated by the increased shear production in the strong shear zone. Presumably the very small scales of motion being fed with energy at the barrier are subject to very rapid dissipation.

12.0.3 Mean Pressure

The flow approaching a porous barrier is retarded upwind of the barrier, and a portion of the flow is deflected over the top. A sharp pressure drop through the barrier drives a "bleed flow", and pressure in the lee of the barrier is well below ambient. Pressure recovers rather quickly in the lee of the barrier. Fig.(12.4) gives observations (Wilson, 1997) of the along-wind profile of mean ground-level pressure $\overline{p}_0(x)$ upwind ($x < 0$) and downwind ($x > 0$) from a single porous plastic fence on bare ground ($h = 1.25$ m, $z_0 = 0.008$ m, $h/z_0 = 160$, $k_r = 2.4$). Notice that the pressure gradient is everywhere adverse, except in an unresolved region across the barrier. The magnitude of the pressure disturbance is quite small relative to total pressure ($\Delta\overline{p} \sim 10\rho u_{*0}^2$) but nevertheless has a dramatic effect on the wind.

12.0.4 Governing Equations for mean flow and turbulence

The governing equation for $\overline{u}$ is

$$\frac{\partial}{\partial x}\left(\overline{u}^2 + \overline{u'^2} + \overline{p}\right) + \frac{\partial}{\partial z}\left(\overline{u}\,\overline{w} + \overline{u'w'}\right) = S_{\overline{u}}\ . \tag{12.6}$$

Here $\overline{p}$ is the disturbance in mean kinematic pressure (mean pressure divided by density), generated by the interaction of the wind with obstacles. The l.h.s. is the divergence of the mean flux ($\vec{F}_u$) of u-momentum, and so eqn (12.6) could be written symbolically as

$$\frac{\partial \overline{u}}{\partial t} = 0 = -\nabla \cdot \vec{F}_u + S_{\overline{u}}\ . \tag{12.7}$$

If we were to integrate eqn. (12.6) within a small cube of airspace, the transport term $\int \nabla \cdot \vec{F}_u\,\mathbf{dx}$ would measure the *net* rate of transport of $\overline{u}$-momentum across the walls, while the source term $\int S_{\overline{u}}\,\mathbf{dx}$ would quantify production or destruction of momentum inside the cube, e.g. specifically (here) windbreak drag, should it happen that the volume of integration spans the barrier.

Consideration that, at the trees or fences, space is 'multiply-connected' will show that indeed, an extra source term $S_{\overline{u}}$ must be included (Wilson & Shaw, 1977, Wilson *et al.*, 1990). In the case ofa single thin porous fence the momentum sink $S_{\overline{u}}$ may be parameterized as

$$S_{\overline{u}} = -k_r\,\overline{u}\,\sqrt{\overline{u}^2 + \overline{w}^2}\,s(z-h)\delta(x-0)\ , \tag{12.8}$$

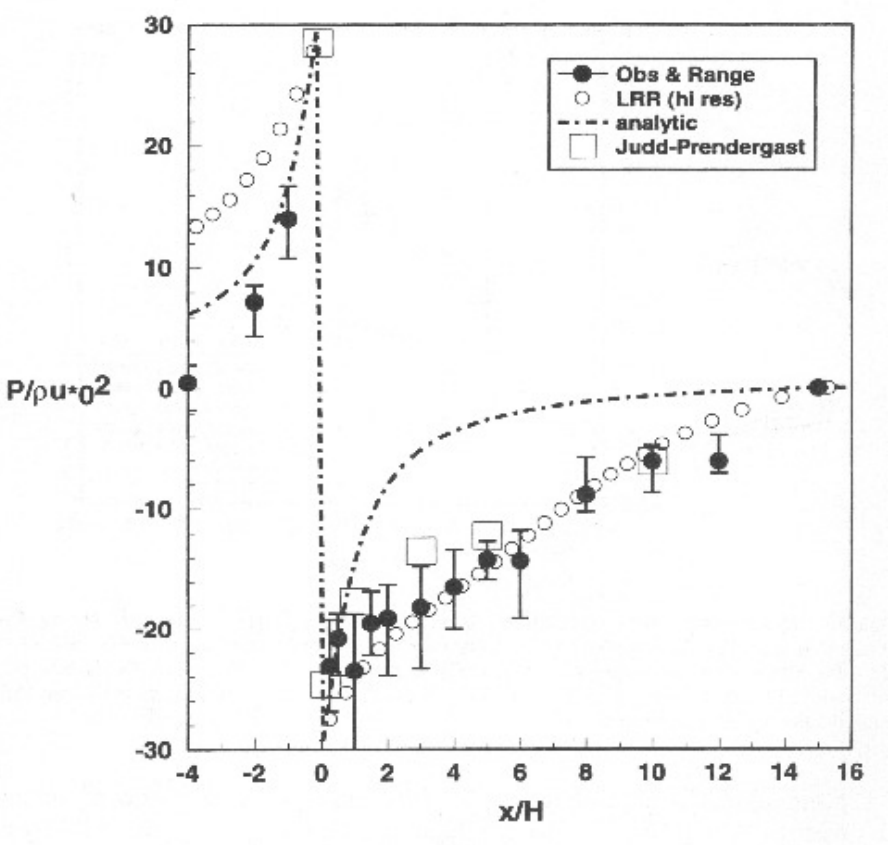


Figure 12.4: Mean ground-level pressure along a transect through a porous fence on bare ground ($h = 1.25$ m, $z_0 = 0.008$ m, $h/z_0 = 160$, $k_r = 2.4$): •, overall mean of numerous 30-minute averages; LRR labels a calculation using the second-order closure of Launder et al. (1975); □, observations under very similar conditions by Judd and Prendergast (1996; unpublished).

where k_r is the (dimensionless) resistance coefficient of the fence(s), $s(z-h)$ is a step function (unity for $z \leq h$, and zero for $z > h$) and the delta-function specifies the fence stands at $x = 0$. A corresponding sink is included in the $\overline{w}$-momentum equation, but its effect has been found to be negligible, whether in the case of a single fence or an array. If we wish instead to consider a natural windbreak, then the source is

$$S_{\overline{u}} = - \, c_D \, a(x,z) \, \overline{u} \, \sqrt{\overline{u}^2 + \overline{w}^2} \; . \tag{12.9}$$

From eqn (12.6) it is obvious that the velocity fluctuations impact the mean velocity $\overline{u}_j$ through the Reynolds stress $\overline{u_i' u_j'}$, but turbulence also impacts the mean velocity through its influence on the mean pressure. In *models*, the feedback of the computed turbulence field on the computed mean velocity depends in detail on the closure assumptions.

RANS wind simulations couple eqn (12.6) with the vertical momentum equation, the incompressible continuity equation, and a "turbulence closure" whose role is to provide the impact of the unresolved (turbulent) eddies on the mean flow.

12.0.5 TKE sources

Section(12.0.5) covered the topic "wake production" when the wind blows about vegetation. That discussion carries over to windbreak flow, but, there is an important question as to whether in the case of a windbreak the wake scales of motion really are negligibly important, and can be considered distinct from the main spectrum; ie., is it reasonable to partition the power spectrum in to two bands, k, k_{WKE}? For the time bring assuming yes, then a parameterized budget-equation for $\overline{u'^2}$ ($\equiv \sigma_u^2$) will include a variance-sink term ϵ_{fdx} given by (cf. eqn 8.32)

$$\epsilon_{fdx} = 4k_r \, \overline{u} \, \sigma_u^2 \, s(z-h) \, \sum_{k=1}^{N} \delta(x - x_{fk}) \; . \tag{12.10}$$

Thus from the current perspective we consider that the flow disturbance induced by a windbreak is "driven" by the sink terms $S_{\overline{u}}$ and ϵ_{fdx} in the $\overline{u}$- and σ_u^2-equations. Before looking at the results of these sources for computed windbreak flows, let us survey the earliest theories.

12.0.6 Evolution of theories of porous barrier flow

G.I. Taylor (1944) gave a solution for the velocity perturbation upstream of a finite or infinite porous plate perpendicular to an unbounded laminar flow. Taylor hypothesized that the effect of each area element $\Delta y \, \Delta z$ of the barrier on the flow upstream of the barrier is equivalent to the effect of a source of fluid volume of strength $k_r u \Delta y \, \Delta z$ placed at the same point. For small k_r Taylor's result for the velocity immediately upstream of a finite barrier is $u/u_0 = 1 - k_r/2$. This result agrees with later analyses (eg. Wilson et al., 1990) and with experiment (eg. Graham, 1976).

Both Tani (1958) and Kaiser (1959) correctly treated a windbreak as a source of mean velocity-deficit $\Delta\overline{u}$, but they treated $\Delta\overline{u}$ as a passive scalar, permitting free slip along the wall (no momentum flux to ground), and adopting a spatially-constant eddy viscosity to parameterise the momentum flux. This means that the spatial distribution of $\Delta\overline{u}$ was controlled by turbulent diffusion along the vertical, and advection by the approach flow $\overline{u}_0(z)$, i.e. terms that are non-linear in the velocity disturbance were ignored. These treatments also missed the essential influence of the pressure field, which is responsible for the displacement of the location of minimum mean velocity downwind from the windbreak. Despite these limitations, the Tani-Kaiser approach does predict a wind reduction of the correct order of magnitude for small k_r.

Kaiser gave solutions both for a single momentum sink of strength $Q = k_r \overline{u}_0{}^2 \, H$ placed at $z = H$, and for a collection of strip sources of width dz and strength $dQ = k_r \overline{u}_0{}^2 \, dz$

extending to $z = H$. The latter solution is

$$\frac{1}{k_r}\,\frac{\Delta\overline{u}}{\overline{u}_0} = -\frac{1}{2}\left[\mathrm{erf}\left(\frac{1+z}{2\sqrt{x/R}}\right) + \mathrm{erf}\left(\frac{1-z}{2\sqrt{x/R}}\right)\right], \tag{12.11}$$

where x, z are dimensionless (scaled on H) and $R = u_0 H/K_0$ is a turbulent Reynolds number.

Plate (1971) noted that observations of the mean wind profile in the lee of sharp-edged solid barriers reveal a region of very strong vertical shear (lying at $z \sim H$ for small x), separating the region of reduced mean velocity near ground from a region of increased mean velocity aloft. Recognizing the oversimplification involved, Plate identified an "intrinsic" streamwise coordinate lying in this strong shear region, and considered this axis to separate two slabs of air whose interaction he represented as that of an upper stream of initially (i.e., at $x = 0$) uniform velocity U_2 interacting via turbulent momentum exchange with a lower stream of (again initially) uniform velocity U_1. Assuming the eddy viscosity to vary as $K = \alpha\, x\, (U_2 - U_1)^2$, one obtains a standard mixing-layer solution involving the empirical parameter α.

Counihan et al. (1974) presented an analytical theory for the mean velocity field in the far ($x/H > 10$) wake of solid obstacles in a turbulent wall layer of depth (with obstacle height $H \ll$). The restriction to the far wake is a consequence of the fact that the flow perturbation due to a solid obstacle can never be small near the obstacle. One of the interesting findings is that the leeward fractional velocity change $\Delta u/u_0$ is approximately height-independent in the lower "wall region" of the wake; this is also the case behind porous barriers.

12.0.7 Modern (numerical) simulations of windbreak flow

With growing accessibility of computing power, and the incursion of numerical fluid mechanics into micro-meteorology, e.g. Taylor's (1970) early treatment of local advection over surface temperature changes, came more plausible simulations of windbreak flows, using RANS models. Using the k-ϵ closure, Durst et al (1980) calculated the effects of a *solid* barrier, requiring that mean velocity vanish at the barrier. Also using the k-ϵ closure, Hagen et al. (1981) treated a *porous* fence, by imposing a measured mean velocity profile in the immediate wake of the fence.

Wilson (**?**, W85) reverted to the representation of a porous barrier as a momentum sink, involving the (easily measurable) resistance coefficient (k_r) of the material, and showed that good predictions of the mean wind field near an *isolated* windbreak could be obtained[2]. This was the case irrespective of the complexity of the turbulence closure (Wilson tested a range of closures, including the classic Launder-Reece-Rodi closure of Launder et al., 1975), presumably due to the dominating influence of the pressure gradient near the fence. However

[2]Numerical method was SIMPLE, see Section **??**. Comparisons with the Bradley-Mulhearn data involves no tunable parameters, since all necessary inputs ($H/z_0, k_r$) are known.

further downwind, where the pressure gradient has relaxed and is less important than the Reynolds stress, these simulations, regardless of closure, slightly underestimated the rate of recovery of the wind[3]. Consequently W85 concluded that 'one could not with confidence simulate the more complex problem of a windbreak network'. Other RANS simulations of the BM83 fence followed, including those by Wang and Takle (1995), Wilson and Mooney (1997), Packwood (2000), and Lee et al. (2001).

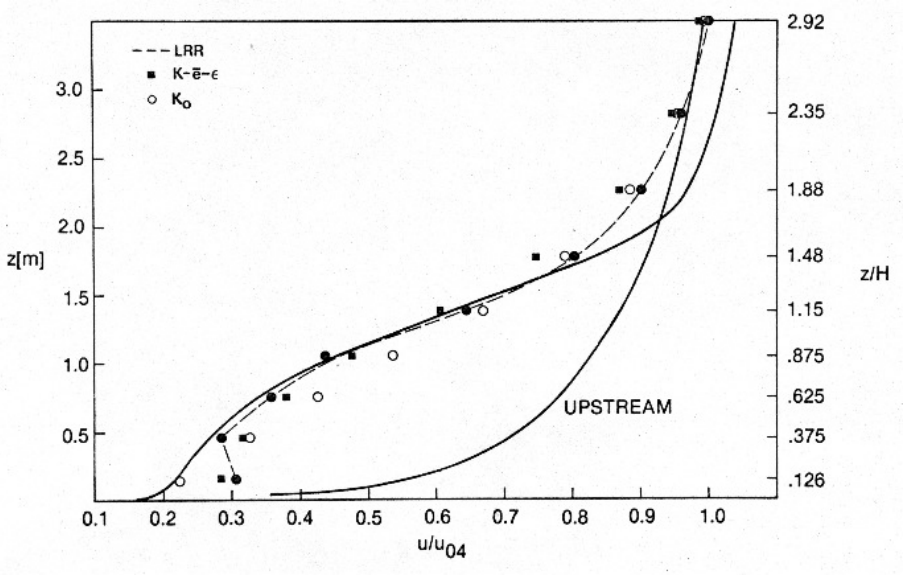


Figure 12.5: Simulations of the experiment of Bradley and Mulhearn by Wilson (1985). Mean velocity profiles at $x/H = 4.2$. U_{04} is the mean windspeed observed at $z = 4$ m, far upstream from the windbreak. Closures are those defined in Ch. 13: the K_0-closure applies the eddy viscosity of the approach flow, $K = K_0(z) = k_v u_{*0} z$); standard $k-\epsilon$ closure; and second-order closure of Launder et al. (1975).

The calculations by Wang and Takle (1995) did not manifest the problem of a slow recovery of the mean velocity field. Wilson and Mooney (1997) sought to discover why not, and thought the better performance of Wang and Takle's model *may* have been ascribable to a too-shallow computational domain. However the suggestion by W85 that perhaps all closures would manifest this failure of too-slow recovery is contradicted, if not by the Wang-Takle simulations, then certainly by later simulations using the Rao-Wyngaard-Cote second-order closure, including those shown in Fig. (12.7). Details of this particular computation (Wilson et al., 2000): Fig. (12.7) were: domain $-10 \le x \le 100$ m, $z \le 50$ m, gridlengths $\Delta x = 1$ m, $\Delta z = 0.15$ m ($\Delta x/h = 0.83$, $\Delta z/h = 0.125$. In wrangling over which (if any) of these various simulations is most correct, we must not lose sight of the fact that observations themselves are scarce, and carry their own uncertainty.

[3]This is probably related to the fact that all closures failed to produce the sharp but shallow speedup-region above the fence, see Fig.(12.5).

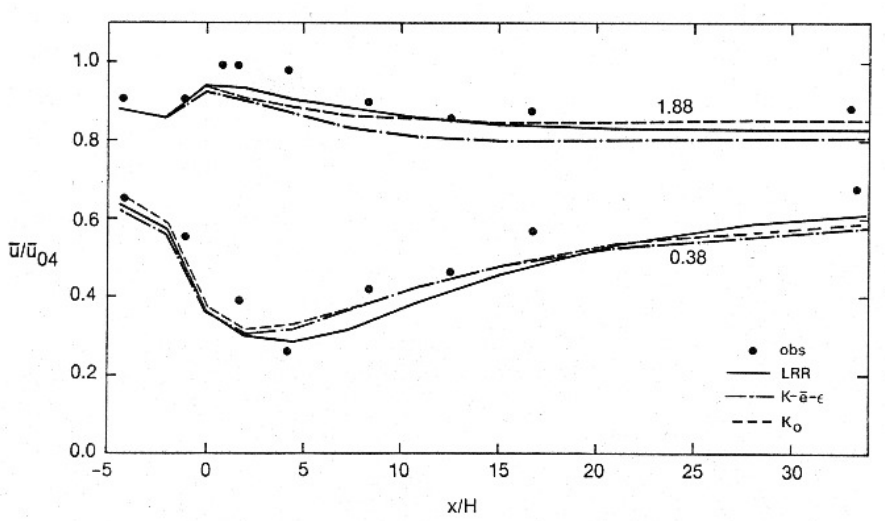


Figure 12.6: As for Fig. 12.5, simulations versus observations of Bradley and Mulhearn (1983). Profiles at $z/H = 0.38, 1.88$.

The simulations of Wilson (**?**) showed that in the case of winds about an isolated porous fence in the neutral surface layer, the K_0 closure (i.e. eddy viscosity unaffected by the flow disturbance, and given by $K = K_0 = k_v u_{*0} z$) yielded quite good simulations of the mean wind (less good for the turbulence). Later Wilson and Yee (2003) tested this most elementary of treatments of the eddy viscosity for the case of an *array* of parallel barriers, simplifying the momentum equations, viz.

$$\frac{\partial}{\partial x}\left(\overline{u}^2 - K_a \frac{\partial \overline{u}}{\partial x}\right) + \frac{\partial}{\partial z}\left(\overline{w}\,\overline{u} - K_0(z)\,\frac{\partial \overline{u}}{\partial z}\right) = -\frac{\partial \overline{p}}{\partial x} + S_{\overline{u}} \tag{12.12}$$

where K_a is a small "artificial diffusivity[4]". It was found that the K_0 closure was unsatisfactory.

Wilson's (1985) simulations established that the maximum fractional wind reduction, observed at $x/H \sim 3-5$, is approximately:

$$\frac{\Delta \overline{u}}{\overline{u}_0} \sim \frac{k_r}{(1+2k_r)^{1.8}}\ , \tag{12.13}$$

(recall that $\Delta\overline{u}/\overline{u}_0$ is more or less height independent at $z/H < 1$ in the lee of a barrier). It is interesting that this law (derived from a numerical model that had been verified relative to the Bradley-Mulhearn observations) holds for a wide range in H/z_0, and has been found to hold true in several other rather different windbreak flows.

[4]The rationale for an artificial diffusivity is to emphasize that the Boussinesq closure for the *normal* stresses is unrealistic; since K_a is small, in effect the normal stress gradients are neglected in this treatment.

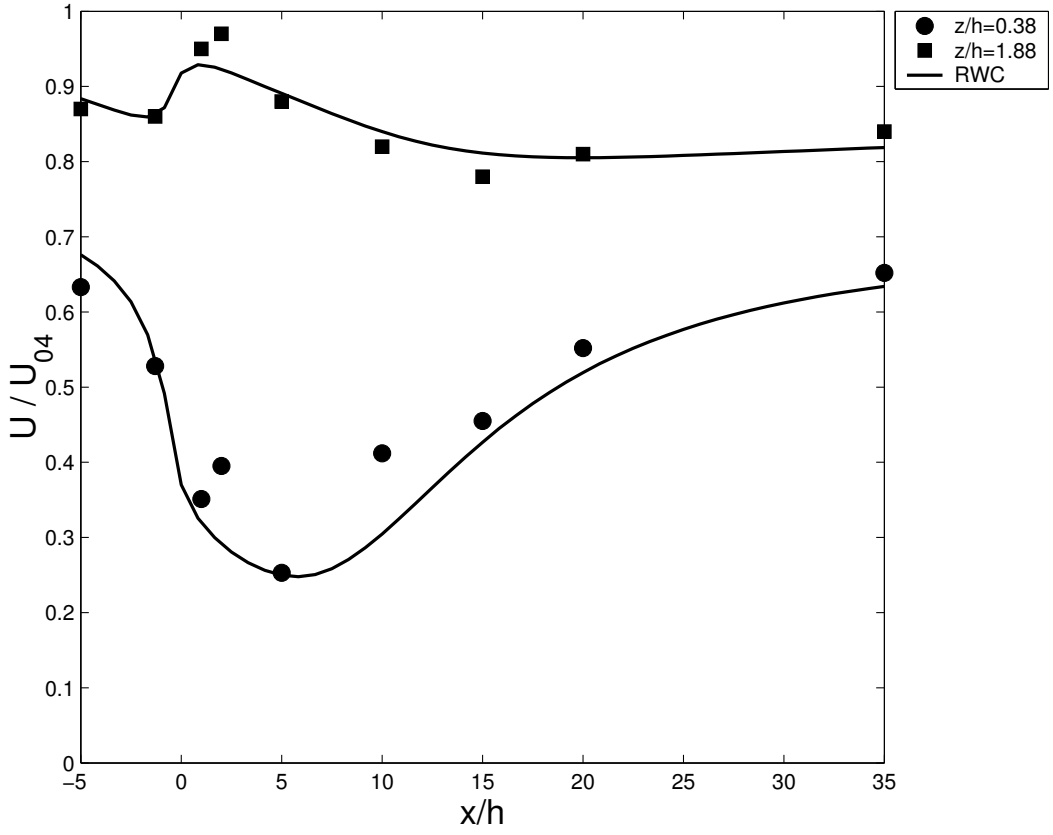


Figure 12.7: Numerical simulation of wind reduction (using the Rao-Wyngaard-Cote second-order closure model), in comparison with observations of Bradley and Mulhearn. U_{04} is the mean windspeed observed at $z = 4$ m, far upstream from the windbreak.

Chapter 13

Review of a hierarchy of turbulence closures for use in disturbed flows

In this course we briefly discuss "disturbed flows," and would wish to discuss not only measurements, but the promise of models. Therefore in this chapter we get a flavour of the range of closure schemes.

In discussing disturbed flows we will usually presume the existence of an upstream region in which the flow is at equilibrium, that is, horizontally homogeneous and with its properties described by MOST. We shall most often be considering disturbances of a sufficiently small scale that we can consider the "host flow" to be a constant stress layer, and in that case the flow may most naturally be considered "stress driven", meaning that the shear stress along the upper boundary at $z = z_{mx}$ is simply a constant, u_{*0}^2.

A feature of (small scale) wind models that is crucial to understand is that such models diagnose not the actual mean winds at some point(s), but rather, ratios of the mean velocities to some reference value U_{ref}, a reference windspeed at some point within, or at the boundary of, the model domain. U_{ref} is chosen as the reference (or "scale") on grounds of convenience, and might for example be the wind aloft at the top of the boundary layer, or possibly for models resolving only a shallower layer of the PBL, the "friction velocity" implied by the shear stress along the top of the model domain. And if on external grounds (ie. from a measurement, or as provided by some model of wider cognizance) we know or postulate a numerical value for U_{ref}, we can infer a definite value for the velocity at any other point within the model domain.

In what follows we focus only on turbulence closures, rather than specifics of the origin of flow disturbance (disturbances are "driven by" inhomogeneous boundary conditions, or internal sources). Implicitly, we regard calculation of the mean velocity field as not a problem – provided we can adequately model the disturbed Reynolds stresses.

13.1 First-order (K-theory) closures

There are many variants of the eddy-viscosity/eddy-diffusion closure, here ordered in progresion simplest to the more complex. Of course in homogeneous turbulence, by definition K =const. We are here interested in more realistic flow paradigms.

13.1.1 Eddy Viscosity of the Approach Flow ("K_0")

The eddy viscosity in a disturbed flow cannot be less complicated than the equilibrium eddy viscosity of the hh-ASL,

$$K(x,z) = K_0(z) = \frac{k_v\, u_{*0}\, z}{\phi_m(z/L)}\ , \tag{13.1}$$

where u_{*0} is the friction velocity of the approach flow, L is the Obukhov length and and k_v is von Karman's constant ("K_0-closure").

13.1.2 Prandtl closure ("K_{P_r}")

Here one specifies the distribution of a length scale λ according to intuition or experience, and obtains a velocity scale as the product of that length scale with the mean velocity shear. Assuming a unidirectional flow and that the length scale varies with height alone, then (for example)

$$K = \lambda^2(z)\ |\frac{\partial \overline{u}}{\partial z}|\ . \tag{13.2}$$

Thinking specifically of the ASL, the choice $\lambda(z) = k_v z$ guarantees that in undisturbed flow (hh-ASL) the eddy viscosity is (correctly) $K = k_v u_{*0} z/\phi(z/L)$ where ϕ is the MO function; this is easily seen by substituting the known wind shear of the hh-ASL. If in disturbed flow there is any disturbance to the mean shear (which there must be, practically by definition), then this formula will yield a disturbed eddy viscosity. Arbitrary empirical specifications $\lambda = \lambda(x,z)$ permit to "tune" this closure to types of flow, or even to specific observations – but with the danger that the tuning is of no general value.

13.1.3 One-Equation Closure ("K_k")

A classical first-order closure attributed to Prandtl and Kolmogorov expresses the eddy viscosity as the product of an imposed (heuristic) length scale λ and a velocity scale defined as the square root of the turbulent kinetic energy, viz.

$$K(x,z) = \lambda\ (c_e\ k)^{1/2}\ . \tag{13.3}$$

The TKE (k) is calculated from a simplified governing differential equation. This closure has seen use in just about every type of micrometeorological flow (eg. the nocturnal boundary layer; Delage 1974, see Section 7.4; see also Wilson **?**).

Let us write down the TKE equation in an incomplete, schematic form — retaining some horiontal derivatives and neglecting others:

$$\frac{\partial k}{\partial t} + \overline{u}\,\frac{\partial k}{\partial x} + ... = -\overline{u'w'}\,\frac{\partial \overline{u}}{\partial z} - \overline{v'w'}\,\frac{\partial \overline{v}}{\partial z} + \frac{g}{\theta_0}\,\overline{w'\theta'} - \frac{\partial}{\partial z}\,(.) - \epsilon\ . \tag{13.4}$$

Here the details of the vertical transport term have been ignored, because invariably this closure scheme (and others more complex) replaces it with a diffusion term (i.e. turbulent diffusion of TKE). Introducing the K-closure to eliminate the eddy fluxes of momentum and heat we have

$$\frac{\partial k}{\partial t} + \overline{u}\,\frac{\partial k}{\partial x} + .. = K\left[\left(\frac{\partial \overline{u}}{\partial z}\right)^2 + \left(\frac{\partial \overline{v}}{\partial z}\right)^2\right] - \frac{g}{\theta_0}\,\frac{K}{Pr}\,\frac{\partial \overline{\theta}}{\partial z} + \frac{\partial}{\partial z}\left(\frac{K}{\sigma_k}\,\frac{\partial k}{\partial z}\right) - \epsilon\ . \tag{13.5}$$

where σ_k is analogous to the Prandtl number Pr (i.e. adjusts the eddy diffusivity for TKE relative to the eddy viscosity, just as the Prandtl number adjusts the eddy diffusivity for heat). The TKE disipation rate is modelled as

$$\epsilon = c_d\,\frac{k^{3/2}}{\lambda}\ . \tag{13.6}$$

Exercise. "Tune" (i.e. evaluate) the coefficients c_e, c_d by requiring that this model reproduce the structure of an ideal, horizontally-homogeneous, neutrally-stratified surface layer, i.e. a layer of unidirectoinal flow ($\overline{v} = \overline{w} = 0$) within which horizontal derivatives vanish and which has these properties

$$\frac{\partial \overline{u}}{\partial z} = \frac{u_*}{k_v z}\ , \tag{13.7}$$

$$\lambda = k_v z\ , \tag{13.8}$$

$$K = k_v\,u_*\,z\ , \tag{13.9}$$

$$k = \text{const.} = \tfrac{1}{2}\left(c_u^2 + c_v^2 + c_w^2\right)\,u_*^2\ . \tag{13.10}$$

Assume $k_v = 0.4$, $c_u = c_v = 2$, $c_w = 1.3$.

Applying this closure in the context of flow in plant canopies, Wilson et al. (1998; WFR) wished "to avoid complicated turbulence schemes, however popular, whose basis is especially weak in the case of a canopy flow (e.g. the ϵ-equation)". With the simplest formula for λ capable of reproducing the flow structure in and above a uniform canopy, this closure performed as well or better than earlier, more complex closures for flow over a ridge, and was later applied by Wilson and Flesch (1999) to interpret measured wind variations in a periodic series of forest clearings (see also Pinard & Wilson, 2001).

13.1.4 Two-Equation Closures: k-ϵ model

By far the most popular two-equation closure is the k-ϵ model, in which model transport equations are solved for the TKE (k) and the viscous dissipation rate ϵ. From these two quantities one may form a turbulence length scale $\lambda = k^{3/2}/\epsilon$ and an eddy viscosity

$$K(x,z) = C_\mu \frac{k^2}{\epsilon} \; . \tag{13.11}$$

Here C_μ is one of five model constants in the standard $k-\epsilon$ model. Usually the k-ϵ closure is used within a linear eddy-viscosity framework, i.e. used with the Boussinesq linear constitutive relationship between stress and strain[1] as expressed in eqn (4.8).

For variety we shall adopt a more complete TKE equation, retaining horizontal and vertical advection and diffusion

$$\frac{\partial}{\partial x}\left(\overline{u}\, k - \frac{K}{\sigma_k}\frac{\partial k}{\partial x}\right) + \frac{\partial}{\partial z}\left(\overline{w}\, k - \frac{K}{\sigma_k}\frac{\partial k}{\partial z}\right) = P_k - \epsilon \; , \tag{13.12}$$

where P_k is the TKE production term (given below). The governing equation for ϵ is typically taken to be

$$\frac{\partial}{\partial x}\left(\overline{u}\,\epsilon - \frac{K}{\sigma_\epsilon}\frac{\partial \epsilon}{\partial x}\right) + \frac{\partial}{\partial z}\left(\overline{w}\,\epsilon - \frac{K}{\sigma_\epsilon}\frac{\partial \epsilon}{\partial z}\right) = \frac{\epsilon}{k}\big(C_{\epsilon 1}\, P_k - C_{\epsilon 2}\,\epsilon\big) \tag{13.13}$$

(σ_k and σ_ϵ allow the eddy diffusivities for TKE and dissipation to differ from the eddy viscosity).

In the above equations P_k is the TKE production term. Neglecting buoyant production, and if one adopts the Boussinesq eddy-viscosity approximation

$$\overline{u_i' u_j'} = -\, K \left(\frac{\partial \overline{u}_i}{\partial x_j} + \frac{\partial \overline{u}_j}{\partial x_i}\right) \tag{13.14}$$

(which, please note, has the correct tensor symmetry) the shear production rate is

$$P_k = K\left[2\left(\left(\frac{\partial \overline{u}}{\partial x}\right)^2 + \left(\frac{\partial \overline{w}}{\partial z}\right)^2\right) + \left(\frac{\partial \overline{u}}{\partial z} + \frac{\partial \overline{w}}{\partial x}\right)^2\right] . \tag{13.15}$$

It is simple to demonstrate that in a constant stress layer (e.g., log-law region of a wall-bounded turbulent flow) where production and dissipation balance, eqn (13.13) has the solution

$$\epsilon = \frac{C_\mu^{3/4} k^{3/2}}{k_v z}, \tag{13.16}$$

[1]While the linear eddy-viscosity hypothesis is reasonable in simple turbulent shear flows (e.g., boundary-layer flow) where the turbulence characteristics and mean velocity gradients change slowly following the mean flow, it is known to be unrealistic in several classes of flows (e.g., strongly swirling flows, flows with significant streamline curvature, secondary motions that occur in straight ducts with non-circular cross-section). This has led to the development of a number of non-linear eddy viscosity models (e.g., Yoshizawa, 1984, Speziale, 1987, Rubinstein & Barton, 1990, Craft *et al.*, 1996).

with the closure constants related by

$$k_v^2 = \sigma_\epsilon \, C_\mu^{1/2} \left(C_{\epsilon 2} - C_{\epsilon 1} \right). \tag{13.17}$$

Comparing this result with eqn (8.37), it is seen that $c_e = C_\mu^{1/2}$.

Different variants of the k-ϵ model arise depending on the different approaches used to determine the closure coefficients C_μ, σ_k, σ_ϵ, $C_{\epsilon 1}$, and $C_{\epsilon 2}$. The standard k-ϵ model "$(k$-$\epsilon)_0$" employs values for the closure constants that have been arrived at by comprehensive data fitting for a wide range of 'canonical' turbulent flows, with the "standard" values of the constants given by

$$C_\mu = 0.09; \quad \sigma_k = 1.0; \quad \sigma_\epsilon = 1.3; \quad C_{\epsilon 1} = 1.44; \quad C_{\epsilon 2} = 1.92. \tag{13.18}$$

These values of the constants correspond to a compromise chosen to give the "best" performance for a range of flows, and it is not likely that minor and/or *ad hoc* adjustments to their values would significantly affect the predictive accuracy.

13.2 Higher-order closures

At the level of a second-order closure, all unknown statistics such as $\overline{u_i' u_j' u_k'}$, $\overline{p' u_i'}$ (etc.) need to be expressed as functions of the 'knowns', ie. $\overline{u}_i$, $\overline{p}$, $\overline{u_i' u_j'}$, ϵ and their spatial gradients. Gosman (1999) notes that 'the only reliable guide to selection (of a turbulence closure) ... is previous experience on a similar problem,' and it is interesting that Lumley (1979), one of the pioneers of 2nd-order closure, wrote that 'The models are calibrated against certain test situations, just like the first-order models, so we can be assured that approximately the correct amounts of momentum, heat, etc. are being transported' but that 'it is usually found that the results (of simulations using 2nd-order closure) are not a substantial improvement' (over simulations using K-theory). Then in Lumley's view, one may nevertheless use a 2nd-order model because, 'if the problem is one in which first order models do not work, there is no choice.'

Lumley and Khajeh-Nouri (1974) recommend that a closure be 'based on a small number of explicitly stated, readily grasped principles... Otherwise, we will not know if an unsatisfactory result can be attributed to the omission of a vital term, the inclusion of an extraneous one, or the use of an incorrect basic principle'. They derive a turbulence closure based on an approximation of '*weak anisotropy* (which implies *weak inhomogeneity*) and quasi-steadiness,' and which they consider could be regarded as reasonable for any turbulent flow in which it is the case that 'time and length scales of inhomogeneity are large relative to time and length scales of the turbulence.' As Lumley and Khajeh-Nouri note, this restriction, of applicability to a field of fine-grained turbulence, is the same restriction that would render a gradient-diffusion (K-theory) closure workable: a widely quoted statement by Corrsin (1974) is that in order for K-theory to be a viable proposition,

"the transport mechanism length scale must be much smaller than the distance over which the curvature of the mean transported field gradient changes appreciably."

Part V

Turbulent Dispersion

Chapter 14

Passive Scalar Dispersion in Horizontally-Uniform Turbulence

We will consider the "diffusion" (really, turbulent convection) of a non-buoyant and non-reactive species whose instantaneous concentration is c. We will assume too that this additive (or contaminant) is released passively (iso-kinetically), or that we are only calculating its spread in regions far enough from any catastrophic injection point that we can consider its motion to be by regular atmospheric flow. We are therefore excluding from consideration heavy gas dispersion near overturned and burning railway cars (etc). We assume the flow itself is "known," in the sense that its statistical structure (i.e. field of velocity statistics) is provided.

What is the source of the gas? We distinguish instantaneous from continuous sources, and consider point, line and area sources, which may be on ground or aloft. All these possibilities are special cases of the general source density $Q(\mathbf{x}, t)$ [kg m^{-3} s^{-1}]. For example, for the case of an instantaneous release of q [kg] at time $t = t_0$ at the point x_0, y_0, z_0 the source density is

$$Q(x, y, z, t) = q\ \delta(t - t_0)\ \delta(x - x_0)\ \delta(y - y_0)\ \delta(z - z_0) \tag{14.1}$$

where the δ-functions localize the source, and of course carry units (the reciprocal of the units of their argument[1]). A continuous line source of strength q_l at $x = 0, z = h$ implies

$$Q(x, y, z, t) = q_l\ \delta(x - 0)\ \delta(z - h) \tag{14.3}$$

The mass conservation equation is:

$$\frac{\partial c}{\partial t} = -\nabla \cdot (\mathbf{u}\, c\ -\ D\ \nabla c)\ + Q\ , \tag{14.4}$$

[1]This can be seen from the definition of a δ function, viz.

$$g(a) = \int_{-\infty}^{\infty} g(x)\ \delta(x - a)\ dx\ . \tag{14.2}$$

and since the molecular diffusivity D is approximately constant we can write this

$$\frac{\partial c}{\partial t} = -\nabla \cdot (\mathbf{u}\, c) \; + \; D\, \nabla^2 c + Q = -\frac{\partial\, u_i\, c}{\partial x_i} + \; D\, \frac{\partial^2 c}{\partial x_i\, \partial x_i} + Q\; . \tag{14.5}$$

Now recall that our continuity equation under the Boussinesq approximation tells us $\nabla \cdot \mathbf{u} = 0$. Hence the above equation can be written

$$\frac{\partial c}{\partial t} + \mathbf{u} \; \cdot \; \nabla c = \; D\, \nabla^2 c + Q\; . \tag{14.6}$$

Anywhere the source vanishes we have

$$\frac{dc}{dt} = \; D\, \nabla^2 c \; \approx 0\; . \tag{14.7}$$

The latter equation, in the Lagrangian form, is the basis for the Lagrangian approach to turbulent dispersion. It says that away from any source, concentration is constant along trajectories, or would be if $D = 0$. That means, if a fluid element is at $t = 0$ "tagged" with concentration C_0, its concentration will remain constant at $c = C_0$ – or almost so, except for a slow "leakage" through the diffusion term on the rhs.

The "Lagrangian" approach to turbulent dispersion, then, is to set $D = 0$ in the above equation, and calculate the trajectories of a large sample of independent "tagged" (initially polluted) fluid elements. In general this is valid (i.e. transport by diffusion can be neglected relative to convection) provided the "Peclet number" $P_e = U\, L/D \gg 1$ where U, L are velocity and length scales of the turbulence.

14.1 "Relative" versus "Absolute" Dispersion

14.1.1 Plume

When we view the plume from a smoke stack, we may observe the "spread" of the plume relative to an instantaneous plume centreline that meanders in time and space. If we assign coordinates $Y(x,t), Z(x,t)$ to the meandering centreline, where x is aligned with the mean wind, then we may define relative coordinates

$$\begin{aligned} y_R &= y - Y(x,t)\; , \\ z_R &= z - Z(x,t)\; , \end{aligned} \tag{14.8}$$

and the ensemble mean spread relative to instantaneous plume centreline is termed the "relative dispersion". This is contrasted with the spread relative to fixed coordinates in space, "absolute dispersion."

14.1.2 Puff

Let $Z_i(t)$ denote the centre-of-mass of the i^{th} realization of a puff release at $z = t = 0$, and let $z_i^2(t)$ be the corresponding absolute variance in displacement in the i^{th} trial. The relative dispersion is the spread relative to the instantaneous centre-of-mass, and so is defined by a sum over all the particles of the i^{th} realization,

$$z_{iR}^2 = \sum_j \left(Z_{ij}(t) - Z_i(t)\right)^2 . \tag{14.9}$$

Relative dispersion is generally smaller than the absolute dispersion.

Consider a puff or plume of dispersing tracer gas whose instantaneous diameter is order d. Eddies of a size L very much larger than d cause meandering of the puff or plume, possibly wafting it over then away from any particular point sensor, with the result that the concentration time series will show intermittency, ie. periods of zero concentration[2]. On the other hand eddies of a size of the order of d will mix clean air into the puff/plume, and result in internal concentration gradients, that are progressively smoothed out by the finer scale eddies. Thus one can logically attribute observed concentration fluctuations to the two agencies, meandering, and internal concentration structure, whose relative importance depends both on the source size, and on the puff/plume size at the observation point. "Meandering plume" models (pioneered by Gifford, 1959; 1960) neglect the contribution of internal structure.

14.2 Project Prairie Grass

Theoretical models of turbulent dispersion range from purely empirical formulae, through analytical solutions based on severely simplistic approximations, to rather sophisticated (but numerical) solutoins based on computations of trajectories. To measure real progress one would wish for experiments, with passive tracer, over a non-absorbing surface, in horizontally-homogeneous surface layer flow. Most writers regard Project Prairie Grass (Barad 1958; Haugen 1959) as the closest approach to that ideal.

Sulphur dioxide (SO_2) was released continuously from a near ground ($h = 0.46$ m) point source over prairie land at O'Neil, Nebraska. Detectors were placed on arcs at radii $x = (50, 100, 200, 400, 800)$ m from the source, with the azimuth interval being very fine on the nearer arcs. Except at $x = 100$ m, all detectors were at height $z = 1.5$ m, but at $x = 100$ m six masts carried detectors at $z = 0.5, 1, 1.5...20$ m.

The site was well instrumented with sensors to define the surface layer flow, although no measurement of ABL depth was made. Several teams participated. The mean roughness length $z_0 \approx 0.006$ m, however detailed mean wind and temperature profiles permit to fit values (u_*, L, z_0) for each run (e.g. van Ulden 1978).

[2]If the sensor volume V_s is very large relative to plume/puff size, intermittency will be reduced.

More than 60 dispersion experiments were run, covering a wide span of values of the Obukhov length L. Many authors have compared dispersion theories with PPG, a sample being: Elliot (1961), Klug (1968), Horst (1979), Nieuwstadt (1980), Wilson (1982b, 1982a). Most investigators have assumed the surface to be non-absorbing, an exception being Gryning et al. (1983). More recently Sawford (2001) concluded deposition of the "tracer" to the surface could be neglected. A salient puzzle of PPG is that simulations best match the observations if the turbulent Schmidt number of the gas is assumed to be considerably less than unity ($S_c \approx 0.6 - 0.7$), implying that the eddy diffusivity for tracer gas exceeds the eddy viscosity. Not all authors accept this.

14.3 Eulerian Approach

For a source in turbulent flow, there is prospect of success only for a theory of concentration *statistics*. Let us begin by focusing on the mean concentration ($\overline{c}$) due to the source[3]. One may develop equations for σ_c and higher moments, but we shall delay that.

We begin by Reynolds-averaging the "box balance" equation to get:

$$\frac{\partial \overline{c}}{\partial t} = \frac{\partial}{\partial x_i}\left(\overline{u}_i\,\overline{c} + \overline{u_i'\,c'}\right) - \; D\,\frac{\partial^2 \overline{c}}{\partial x_i\,\partial x_i}\;. \tag{14.10}$$

14.3.1 Simplifications due to Symmetry

Owing to the restriction of this analysis to horizontally-uniform flows[4], we may write $\overline{w} = 0$ and $\overline{u} = \overline{u}(z)$ (by choice of axes, $\overline{v} = 0$). Then in advection form our conservation equation, for large P_e and away from any source, becomes

$$\frac{\partial \overline{c}}{\partial t} + \overline{u}\,\frac{\partial \overline{c}}{\partial x} = -\frac{\partial \overline{u'c'}}{\partial x} - \frac{\partial \overline{v'c'}}{\partial y} - \frac{\partial \overline{w'c'}}{\partial z}\;. \tag{14.11}$$

This is as far as we can go without further assumptions, for this equation is unclosed. If we try the rigorous route and derive budget equations for $\overline{w'c'}$ etc. we introduce still more unknowns.

14.3.2 First-order Closures

Suppose we presume fluxes are uniquely related to mean gradients (K-theory, or "first-order closure," so called because we make our closure approximations in the governing equation for the first moment or mean rather than in the equations for the fluxes (second order closure) or even higher-order statistics). In fact, this is not so unreasonable for undisturbed flows. We

[3]A time average concentration is appropriate for continuous sources, for which the mean concentration field is steady, $\partial\overline{c}/\partial t = 0$. In the case of an unsteady source, $\overline{c}$ will be an ensemble mean concentration.

[4]Note however that the *concentration* statistics will in general *not* be horizontally uniform.

have already seen that in the surface layer (for example) relationships between the (vertical) fluxes and (vertical) gradients of windspeed, temperature and humidity are consistent an eddy diffusivity $K = k_v u_* z/\phi(z/L)$.

So we write:

$$\begin{aligned}
\overline{u'c'} &= -K_x \frac{\partial \overline{c}}{\partial x} , \\
\overline{v'c'} &= -K_y \frac{\partial \overline{c}}{\partial y} , \\
\overline{w'c'} &= -K_z \frac{\partial \overline{c}}{\partial z} ,
\end{aligned} \tag{14.12}$$

where the K's are scalar eddy diffusivities ($\mathrm{m}^2\ \mathrm{s}^{-1}$) which we allow to be different for different directions of motion. Note that we have by assumption ruled out the possibility that a mean gradient along direction i could drive a mean flux along a different direction j. The possibility that the eddy diffusivity should be a tensor, viz.,

$$\overline{u_i'c'} = -K_{ij} \frac{\partial \overline{c}}{\partial x_j} \tag{14.13}$$

has been examined in wind tunnel simulations of flow near ground (Raupach et al. (1986)), but the off-diagonal components of K were found to be negligible.

The above parameterisations for the alongwind flux $\overline{u'c'}$ and the crosswind flux $\overline{v'c'}$ are rather poor, and it is troublesome to determine the appropriate diffusivity, because the horizontal components of the wind contain variations out to very long timescales (i.e. the power spectra $S_{uu}(f), S_{vv}(f)$ contain low frequency power that cannot be parameterized by any existing all-inclusive parameterization). Vertical motion, however, is restricted to short timescales (due to presence of the ground), so the K-model for the vertical flux is often good. Note that provided $z \gg z_0$, the typical magnitude of u' is much less than $\overline{u}$. For example in neutral stratification:

$$\frac{\sigma_u}{\overline{u}} \sim \frac{2k_v}{\ln\left(\frac{z}{z_0}\right)} . \tag{14.14}$$

Later we may assume, with no particular justification, that

$$|\overline{u}\ \frac{\partial\, \overline{c}}{\partial x}| \gg |\ \frac{\partial \overline{u'c'}}{\partial x}| \tag{14.15}$$

(neglect of divergence of streamwise mass flux carried by turbulent flow; there will be some problems for which in some regions this may be in seriously in error). Note that a consequence of that would be, that the alongwind flux is just $\overline{u}\ \overline{c}$, ie. alongwind transport occurs entirely by the mean wind, so we would be left with a model in which the total alongwind mass flux M [$\mathrm{kg\ s}^{-1}$] was

$$M = \int_{-\infty}^{y=\infty} \int_{z_0}^{z=\infty} \overline{u}\ \overline{c}\ dy\ dz . \tag{14.16}$$

However delaying (for the time being) that assumption, when we adopt the eddy diffusion closure we obtain the following advection-diffusion equation (appropriate to the restrictions already adopted):

$$\frac{\partial \overline{c}}{\partial t} + \overline{u}(z)\,\frac{\partial \overline{c}}{\partial x} = \frac{\partial}{\partial x}\left[K_x\,\frac{\partial c}{\partial x}\right] + \frac{\partial}{\partial y}\left[K_y\,\frac{\partial c}{\partial y}\right] + \frac{\partial}{\partial z}\left[K_z\,\frac{\partial c}{\partial z}\right]\,. \tag{14.17}$$

To progress we have to specify the mean wind profile, the diffusivities, and boundary/initial conditions.

"Gaussian Puff" and "Gaussian Plume" Models

Suppose one sets $\overline{u}(z) = U$ (a constant), and assumes that K_x, K_y, K_z are also constants[5]. This would be appropriate were the flow field an unsheared regime of homogeneous turbulence – though in reality there can be no such thing as homogeneous turbulence, particularly in the region of a barrier such as the ground (adjacent to which the length scale for motion normal to the wall vanishes).

With these simplifications the mass conservation equation reduces to

$$\frac{\partial \overline{c}}{\partial t} + U\,\frac{\partial \overline{c}}{\partial x} = K_x\,\frac{\partial^2 c}{\partial x^2} + K_y\,\frac{\partial^2 c}{\partial y^2} + K_z\,\frac{\partial^2 c}{\partial z^2}\,. \tag{14.18}$$

The terms on the rhs now have the form of pure "Fickian diffusion," although in fact they represent turbulent convection (we could consider diffusive transport to be included in this equation if we lump the molecular diffusivity into the K's, thus $K_x \geq D$, etc.)

Instantaneous Point Source

For the release of q[kg] at $x = y = z = t = 0$, the solution (you can prove by substitution) is:

$$\overline{c}(x,y,z,t) = \frac{q}{(2\pi)^{3/2}\,\sigma_x\,\sigma_y\,\sigma_z}\,\exp\left[-\frac{(x-Ut)^2}{2{\sigma_x}^2} - \frac{y^2}{2{\sigma_y}^2} - \frac{z^2}{2{\sigma_z}^2}\right]\,. \tag{14.19}$$

Relative to a puff centre-point $x = Ut, y = z = 0$ that is drifting with the mean wind U, we have Gaussian spread along each of the three axes independently. The spread parameters (puff standard deviations) are related to the eddy diffusivities by:

$$\begin{aligned} \sigma_x &= \sqrt{2\,K_x\,t}\,, \\ \sigma_y &= \sqrt{2\,K_y\,t}\,, \\ \sigma_z &= \sqrt{2\,K_z\,t}\,. \end{aligned} \tag{14.20}$$

The puff expands with increasing $t^{1/2}$ ("diffusive" spread).

[5]These "constants" are atmospheric statistics that are invariant in space over (i) some interval in time, the averaging interval; or (ii), if an ensemble averages are used, across the ensemble.

A direct parallel with the ensemble mean displacement of a random walker may be shown. In the so-called "drunkard's walk" in one dimension (z), a walker begins at $z = 0$ and after a sequence of independent steps Δz_i ($i = 1...N$) along the z-axis, each randomly of length L or $-L$, the walker's net displacement z_N is random with zero mean and standard deviation $\sigma_{z_N} = LN^{1/2}$ (asymptotically, i.e. for large N, the distribution of z_N is Gaussian).

Since $z_N = \sum_{i=1}^{N} \Delta z_i$ it is evident that its expected value (or ensemble mean value)

$$\langle z_N \rangle = \sum_{i=1}^{N} \langle \Delta z_i \rangle = 0 \; . \tag{14.21}$$

That the standard deviation of z_N increases with $\sqrt{N}$ is shown as follows:

$$z_N^2 = \sum_{i=1}^{N} \Delta z_i \; \sum_{j=1}^{N} \Delta z_j = \sum_{i=1}^{N} \Delta z_i^2 + \; 2 \sum_{i=1}^{N} \sum_{j \neq i} \Delta z_i \Delta z_j \tag{14.22}$$

and therefore

$$\langle z_N^2 \rangle = \sum_{i=1}^{N} \langle \Delta z_i^2 \rangle + \; 2 \sum_{i=1}^{N} \sum_{j \neq i} \langle \Delta z_i \Delta z_j \rangle \; . \tag{14.23}$$

But since the steps are independent, the covariance appearing in the second term vanishes, while $\Delta z_i^2 = L^2$ ($\forall i$). Therefore the ensemble mean square displacement after N steps is

$$\langle z_N^2 \rangle = N \, L^2 \tag{14.24}$$

and $\sigma_{z_N} = L\sqrt{N}$.

Eq.(14.19) can be modified (as below) to permit arbitrary source position, and to account for a non-absorbing or partially-absorbing ground. As the "Gaussian Puff" model, it is extremely common as an operational diffusion model. The preceeding results are easily modified to incorporate a drift in the y-direction, and the advecting velocity U is generalized to be a "large scale advecting wind" $U(\mathbf{x}, t), V(\mathbf{x}, t)$. But this is conceptually tricky: what spectral range of eddy sizes/frequencies "growes" the puff, and what spectral ranges "advects" it? This hinges on the size of the puff, which of course changes in time. Provided the puff is small compared with the distances over which U, V change, everything is clear: but it is ultimately likely one will be confounded in correctly decomposing the wind into the "advective" (U, V) and "diffusive" (contributing to the increase of σ's) parts of the wind field.

Now let us consider a steady source, so that $\partial \overline{c}/\partial t = 0$. And let us now drop the turbulent part of the alongwind flux. Then each given fluid element is moving downstream in a drifting plane normal to the x axis, and lateral motion occurs in that plane. Now we have

$$U \, \frac{\partial \overline{c}}{\partial x} = \; K_y \, \frac{\partial^2 c}{\partial y^2} + \; K_z \, \frac{\partial^2 c}{\partial z^2} \; . \tag{14.25}$$

The solution to this equation, for a source of strength q [kg s^{-1}] at $x = z = y = 0$ is:

$$\overline{c}(x,y,z) = \frac{q}{2\pi\ \sigma_y\ \sigma_z\ U}\ \exp\ \left[-\frac{y^2}{2{\sigma_y}^2} - \frac{z^2}{2{\sigma_z}^2}\ \right] \tag{14.26}$$

where again the σ's are the "plume widths"

$$\begin{aligned} \sigma_y &= \sqrt{2\ K_y\ \frac{x}{U}}\ , \\ \sigma_z &= \sqrt{2\ K_z\ \frac{x}{U}}\ . \end{aligned} \tag{14.27}$$

According to this solution, we have a Gaussian distribution along each crosswind direction, and the "spread" parameters are the standard deviations of the Gaussian distributions. The plume widths increase parabolically with x, ie. $\sigma_y \propto \sqrt{x}$. Since we have a $1-1$ relation between x and t ($x = Ut$) we can also say the plume spreads parabolically in time.

Exercise: Check that this solution satisfies the differential equation, and that at any plane perpendicular to the x-axis the total mass blowing downwind per unit time is q.

Now if the source is at $z = h$ rather than $z = 0$, we simply replace every occurrence of z with $z - h$ (except in the subscripts). What if we want to allow for the ground at $z = 0$? There are two extreme possibilities — the ground may reflect the plume upon contact, or it may absorb the plume. In the former case the lower boundary condition is the "flux boundary condition"

$$\left(-\ K_z\ \frac{\partial c}{\partial z} \right)_{z=0} = 0 \tag{14.28}$$

(no flux to ground) while in the latter case we impose the "concentration boundary condition" $\overline{c}_{z=0} = 0$. These boundary conditions are readily enforced by adding (reflection case) or subtracting (absorption case) the contribution from an imaginary "image source" of equal strength lying at equal distance h below the ground. Thus for points above $z = 0$ in the "real" world, the vertical distance to the image plume axis is $z + h$. Thus the solution for a continuous elevated point source a distance h above the ground is:

$$\begin{aligned} \overline{c}(x,y,z) &= \frac{q}{2\pi\ \sigma_y\ \sigma_z\ U}\ \exp\ \left(-\ \frac{y^2}{2{\sigma_y}^2}\ \right) \\ &\times\ \left[\exp\left(-\ \frac{(z-h)^2}{2{\sigma_z}^2}\ \right)\ \pm\ \exp\left(-\ \frac{(z+h)^2}{2{\sigma_z}^2}\ \right) \right]\ . \end{aligned} \tag{14.29}$$

For a ground-level receptor on the plume axis ($y = 0$) the concentration is

$$\overline{c}_0(x) = \frac{q}{\pi\ \sigma_y\ \sigma_z\ U}\ \exp\left(-\ \frac{h^2}{2{\sigma_z}^2}\ \right)\ . \tag{14.30}$$

Exercise: Set $\sigma_y = \sigma_z = \sqrt{2\ K\ x/U}$ and find the location of maximum concentration at ground on plume centreline.

So far we have dealt with a point source. What about a line source of strength q[kg m^{-1} s^{-1}] stretching to infinity along the y-axis at $x = 0, z = h$? Each elementary length dy of such a source may be considered a point source of strength $q\ dy$, and each therefore makes a contribution to the concentration at $(x, y, z) = (x, 0, z)$ of

$$\begin{aligned} d\overline{c}(x,y,z) &= \frac{q\ dy}{2\pi\ \sigma_y\ \sigma_z\ U}\ \exp\left(-\frac{y^2}{2{\sigma_y}^2}\right) \\ &\times \left[\exp\left(-\frac{(z-h)^2}{2{\sigma_z}^2}\right) \pm \exp\left(-\frac{(z+h)^2}{2{\sigma_z}^2}\right)\right]. \end{aligned} \tag{14.31}$$

By integration (summing over all elements dy of the line source) we obtain:

$$\overline{c}(x,z) = \frac{q}{\sqrt{2\pi}\ \sigma_z\ U}\left[\exp\left(-\frac{(z-h)^2}{2{\sigma_z}^2}\right) \pm \exp\left(-\frac{(z+h)^2}{2{\sigma_z}^2}\right)\right]. \tag{14.32}$$

An area source can similarly be dealt with by summing line sources.

Empirical Prescriptions for Plume Widths

In these Gaussian solutions the plume widths (σ_z, etc.) in principle are determined by the K's, and those in turn by the turbulence. But in reality the turbulence is not homogeneous. At what height would we evaluate K? For that matter U?

In practise U has been specified at an arbitrary height (often source height h), and the σ's specified by empirical curves $\sigma_y(x)$ and $\sigma_z(x)$ which are permitted to depend upon the atmospheric stratification. These curves, the classical ones being the "Pasquill-Gifford curves," are determined empirically by choosing values which best permit the Gaussian Plume model to agree with observations. Hanna (WMO Tech. Note #177, *A review of atmospheric diffusion models for regulatory applications*) has given formulae for the σ's in terms of the measured standard deviations σ_θ and σ_e of the wind azimuth and elevation angles. For example, for source heights $h \leq 100$ m in regions of large roughness length $z_0 \sim 0.1$ m, Hanna gives the following formulae for prediction of the mean concentration over averaging periods of order 10-min:

$$\begin{aligned} \sigma_y &= \frac{\sigma_\theta\ x}{1 + 0.031x},\ x \leq 10\ \text{km} \\ &= \frac{33}{\sqrt{x}},\ x \geq 10\ \text{km} \\ \sigma_z &= \sigma_e\ S_z \end{aligned} \tag{14.33}$$

where $S_z = 1$ for $\sigma_e x < 0.8\delta$. Corrections are given for different roughness lengths and averaging times.

More-general First-Order Models for the hh-ASL

The first route to improvement of the prediction of the GP model is to retain the correct (or at least, more realistic) wind and diffusivity profiles. Assuming still that we are dealing with a plume which lies within the horizontally-uniform surface layer, these may be written in the general stability-corrected form (see the section on Monin-Obukhov similarity)

$$\begin{aligned} \overline{u}(z) &= \frac{u_*}{k_v}\left[\ln\frac{z}{z_0} - \psi_m\left(\frac{z}{L}\right) + \psi_m\left(\frac{z_0}{L}\right)\right] \\ K_z(z) &= \frac{k_{vc}\,u_*\,z}{\phi_c\left(\frac{z}{L}\right)} = \frac{(k_v/S_c)\,u_*\,z}{\phi_c\left(\frac{z}{L}\right)}\,. \end{aligned} \tag{14.34}$$

According to flux-gradient relationships for water vapour transport, as seen in experiments to determine the universal functions like ϕ_c, we might consider that the turbulent Schmidt number $S_c = k_v/k_{vc} = 1$. But multi-dimensional diffusion experiments are usually better predicted using $S_c \sim 0.63$ or $1/S_c = k_{vc}/k_v \sim 1.6$. The reason for this is not at present understood; we shall return to this point later, after studying the superior Lagrangian dispersion treatment.

Near field correction

We will see later that in truth, there is a so-called "near field effect" that results in the diffusivity vanishing at the source, ie. the diffusivity is not just a property of the turbulence, but near the source depends too on the time/distance of travel from the source. One can approximately correct for this effect by introducing a multiplicative correction factor (Raupach and Legg 1983; Sullivan and Yip 1989)

$$K_z(z,x,x_{src}) = \frac{k_{vc}\,u_*\,z}{\phi_c\left(\frac{z}{L}\right)}\left[1 - \exp\left(-\frac{x-x_{src}}{\overline{u}(z_{src})\,T_L(z_{src})}\right)\right] \tag{14.35}$$

where $T_L(z)$ is the Lagrangian timescale (defined later).

Lateral dispersion

What about the diffusivity K_y for lateral diffusion? This is a harder problem. Vertical diffusion is accomplished by fluctuations w' whose spectral distribution is limited to "high" frequencies, due to the presence of the nearby ground. For any practical averaging time we are likely to choose (surely no less than 5 min?), the individual trajectories of the plume will have sampled many many "episodes" of the turbulence in w': consequently, the vertical distribution of mass over practical averaging times is smooth. However v' contains power at much lower frequencies — we know the wind direction and strength change on scales as slow as 10 min or so (cloud scale) through hours to days (changing large scale pressure patterns). Therefore no matter what our choice of averaging time T, there is always the likelihood of

an irregular and possibly multi-modal distribution of material along the lateral direction. In general the distribution in y cannot be predicted unless we can forecast the mesoscale fluctuations in wind direction[6].

Because of this difficulty, theorists may concentrate on the cross-wind integrated concentration

$$\chi(x,z) = \int_{-\infty}^{\infty} \overline{c}(x,y,z)\, dy \tag{14.36}$$

which (a little thought will convince you) is the same as the concentration downwind of an infinite line source along the y-axis. If χ is known, one can idealize the spread in y by assuming a Gaussian distribution in y with a σ_y as in the Gaussian Plume model. Or one can put in a specified K_y according to whatever guidance may be available, and calculate a consequent (smooth) spread in y.

Given the complexity of the MOST wind and diffusivity profiles for the hh-ASL , there is no chance of exact analytical solution, even in the neutral case. However numerous approximate solutions have been found. One may question their utility, now that we can easily solve numerically – but if nothing else, they provide a very powerful and rapid test for the accuracy of numerical solutions. For example Wilson (1982a) predicts mean concentration $\overline{c}(x,z)$ a distance x downwind from a continuous line source of strength q in the Neutral or Stable Surface Layer (equals $XWIC$ downwind of a point source). The solution given here is for the neutral case:

Define z_δ to be the upper edge of the plume. Let $\lambda = \ln(z/z_0)$ be a log-height coordinate (zero at the ground, which is defined to lie at $z = z_0$), and define $\xi = x/z_0$. Let $\delta = \ln(z_\delta/z_0)$. Then δ is found to be the solution to the implicit equation:

$$(\delta - 2)\ e^\delta + \delta = \frac{1}{2}\left(\frac{x}{z_0}\right) - 2 \tag{14.37}$$

and the solution for the dimensionless concentration (scaled to be insensitive to changes in windspeed or source strength) is:

$$\frac{z_0\ u_*\ \overline{c}}{k_v q} = \delta''\left[\left(\lambda\ e^\lambda - \delta\ e^\delta\right) - 2\ \left(e^\lambda - e^\delta\right) + (\delta - \lambda)\right] \tag{14.38}$$

where

$$\begin{aligned} \delta'' &= \frac{\partial^2 \delta}{\partial \xi^2} = -2\ \delta(\delta')^3\ e^\delta\ , \\ \delta' &= \frac{\partial \delta}{\partial \xi} = \frac{1}{2}\ \frac{1}{e^\delta\ (\delta - 1) + 1}\ . \end{aligned} \tag{14.39}$$

δ' is the rate of growth (with $\xi = x/z_0$) of the (log of the) depth of the plume, so unsurprisingly, there is a similarity here with the rate of growth of an internal boundary layer (see Section ?). Fig. (14.1) shows predicted and observed ground-level cross-wind integrated

[6]Note however that one could probably deduce the crosswind spread *diagnostically*, from a given measured time series $v'(t)$ for the period of the diffusion process.

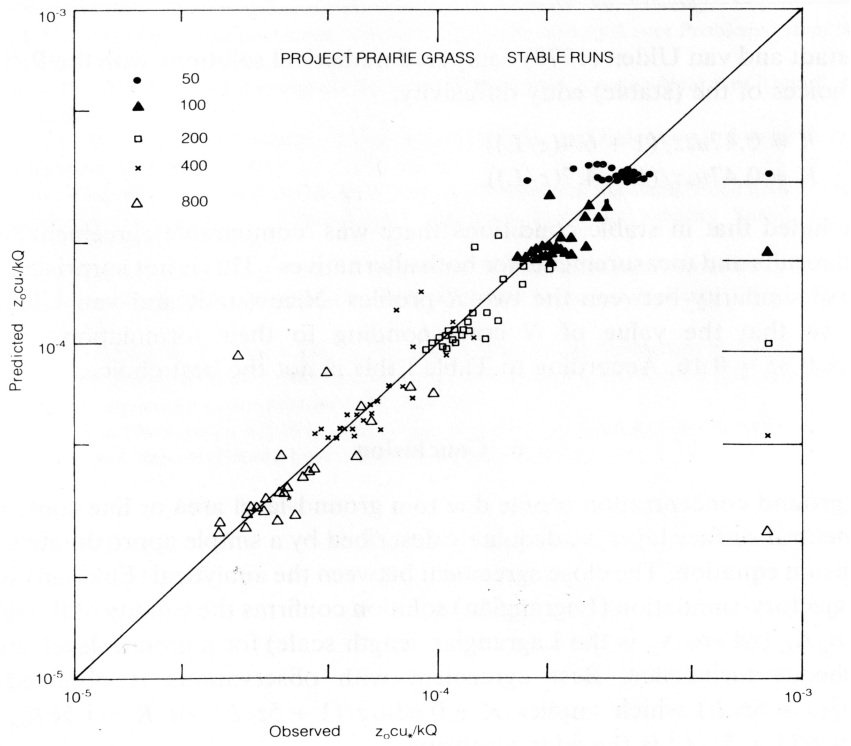


Figure 14.1: Observed versus predicted ground-level, cross-wind integrated concentration $\frac{z_0\ u_*\ \chi_0(x)}{k_v Q}$ for Project Prairie Grass, for fetches varying from 50 to 800 m. Lines on rhs indicate expected value in neutral limit, for the given fetch. Calculated according to Wilson's (1982a) analytical solution.

concentrations for the stably-stratified PPG runs.

Exact solutions for surface-layer dispersion have been given when the wind and diffusivity are approximated as power-law functions:

$$\begin{aligned} \overline{u}(z) &= \overline{u}_H \left(\frac{z}{H}\right)^m \\ K(z) &= K_H \left(\frac{z}{H}\right)^n \end{aligned} \tag{14.40}$$

For vanishing wind shear ($m = 0, \overline{u} = \overline{u}_H$) and a linear diffusivity $K(z) = k_v u_* z$ ($n = 1$), the solution for a continuous ground-level line source is (result due to Bosanquet and Pearson,

1936, but see Pasquill and Smith 1983):

$$\overline{c} = \frac{q}{k_v u_* x} \exp\left(-\frac{\overline{u}_H\, z}{k_v u_* x}\right) . \tag{14.41}$$

Sutton (cited in Pasquill and Smith, 1974) gave a more-general surface line-source solution valid provided $m - n + 2 > 0$.

A solution with power-law wind and diffusivity which has found widespread use is that of Philip (1959). Here the advection-diffusion equation was applied to the advective transport of heat and water vapour in the horizontally ***in***homogeneous surface-layer. The lower boundary-condition used is the surface energy balance. McNaughton (1981) has used Philip's solution to calculate the fraction of water distributed by a sprinkler irrigation system which evaporates before reaching the crop (irrigation efficiency). Many other analytic solutions exist, including Huang (1979); Mooney & Wilson (1993). There have also been numerous numerical solutions of the advection-diffusion equation with MO profiles of windspeed and diffusivity; early examples include Nieuwstadt & Van Ulden (1978) and Yamamoto & Shimanuki (1961).

14.4 Turbulent Schmidt Number and C_0

The von Karman constant for mass $k = k_v/S_c$, where S_c is the turbulent Schmidt number (ratio of eddy viscosity $k_v u_* z$ to the eddy diffusivity). Its numerical value is subject to considerable uncertainty (Sawford, 2001); for calculations we shall assume $S_c = 0.63$.

Chapter 15

Lagrangian approach to scalar dispersion

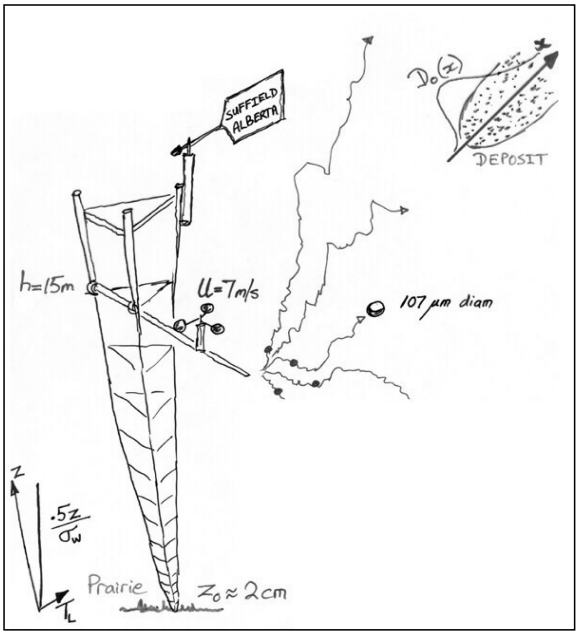


Figure 15.1: Heavy particle dispersion experiments at Suffield, Alberta.

We have covered the Eulerian approach to turbulent dispersion. In that work closure was attained by introducing assumptions concerning the joint distribution of velocity and concentration — most simply (first-order closure), by introducing the gradient-diffusion hypothesis to model the fluxes. In order to reveal a serious weakness of that approach and set the stage for a "better" method, we now take the Lagrangian approach.

The governing mass conservation equation in Lagrangian form is

$$\frac{dc}{dt} = D\,\nabla^2 c\,. \tag{15.1}$$

Assuming the Peclet number $P_e = \frac{U\,L}{D}$ is large (where U, L are velocity and length scales of the turbulence) and that there is no production/destruction ($Q = 0$), then c is constant along trajectories: ie. whatever content a given fluid element is tagged with at the source, it retains. Thus in the Lagrangian approach our attention is concentrated upon trajectories. Again, we assume the flow is "given" (in terms of statistical properties of the wind); for disturbed flows, a pre-requisite task is calculation of the flow-field itself, perhaps by Direct Numerical Simulation (e.g. John W. Brooke, 1994; Pan and Banerjee, 1996), or Large Eddy Simulation.

Consider a point source emitting N particles (or kilograms) per second, and a volume V downstream. Any given particle, say particle-i, may or may not pass through volume V. Let t_i be the time it spends in V (perhaps composed of many intervals of occupancy separated by periods of absence from V). Then if $\bar{t}$ is the average time a particle spends in V, the mean concentration therein is

$$\overline{c} = \frac{N\,\bar{t}}{V}\,. \tag{15.2}$$

Thus if we can calculate trajectories, we can calculate mean concentrations.

15.1 General Expression for Ensemble Mean Concentration

Let the source density be $Q(\mathbf{x}, t)$. If a particle is at $\mathbf{x}_0 = (x_0, y_0, z_0)$ at time $t = t_0$, then we may define a (position-) transition density such that $p(\mathbf{x}, t|\mathbf{x}_0, t_0)\; dx\; dy\; dz$ is defined to be the probability that at later time t, the particle lies within the elementary volume $\mathbf{x} \pm d\mathbf{x}/2$. In terms of this transition density, the ensemble mean concentration due to the source is:

$$\overline{c}(\mathbf{x}, t) = \int_{\mathbf{x}_0} \int_{-\infty}^{t_0=t} p(\mathbf{x}, t|\mathbf{x}_0, t_0)\, Q(\mathbf{x}_0, t_0)\; dx_0\; dy_0\; dz_0\; dt_0\,. \tag{15.3}$$

Here we see unambiguously the connection between trajectories (which in the ensemble, determine the transition density for position) and the redistribution of material from the source.

15.2 Dispersion in Homogeneous Turbulence: G.I. Taylor's Solution

Taylor's (1921) analytical theory for dispersion in homogeneous turbulence shows up the weakness in the Eulerian approach[1], and suggests the important factors in constructing a Lagrangian model. Consider the vertical motion (there is nothing special about our choice of the vertical axis) of a marked fluid element (passive "particle") released at $z = t = 0$ into an infinite domain of homogeneous and stationary turbulence in which there is no *mean* flow (Eulerian mean velocity $\overline{u}_i = 0$). At subsequent times (t) a particle's vertical coordinate is:

$$Z = \int_0^{t'=t} W(t')\, dt' \tag{15.4}$$

where $W(t')$ is the particle velocity. This vertical velocity is by definition

$$W(t') = \left(\frac{dZ}{dt}\right)_{t=t'} . \tag{15.5}$$

Now we may write

$$\frac{dZ^2}{dt} = 2\, Z(t)\, \frac{dZ}{dt} . \tag{15.6}$$

If we consider the release of many particles in such a way that they sample many realisations of the transporting velocity field, we may define an ensemble average value for any property of these fluid elements at any time t since release. For example, $\overline{Z^2}$, "mean square Z," denotes the mean value (in an ensemble average sense) of the square of the particle displacement along the z-axis at time t since release. Obviously this somehow relates to spread, and we will define the "spread" as

$$\sigma_z = \sqrt{\overline{Z^2} - \overline{Z}^2} \tag{15.7}$$

(it is apparent from Eq. 15.4 that in the case under consideration, $\overline{Z} = 0\ \forall t$). In fact σ_z is the standard deviation of the concentration distribution along z. The probability density function for the particle displacement (over time t), written $p(z, t|0, 0)$ and having the unit [m^{-1}], is defined such that $p(z_1, t|0, 0)\, dz$ is the probability that the particle released at $z = t = 0$ is at later time t between $z_1 - dz/2$ and $z_1 + dz/2$. Often this (transition) probability density will be called simply the concentration (but note again that it is a density on a line, rather than in a volume). Clearly it must satisfy

$$\int_{-\infty}^{\infty} p(z, t|0, 0)\, dz = 1 \tag{15.8}$$

[1]This is covered in Wyngaard's textbook, pp79-83.

because the particle must lie *somewhere* on the z-axis. Now by the usual rules of probability, the mean square particle displacement is

$$\overline{Z^2}(t) = \int_{-\infty}^{\infty} z^2 \; p(z,t|0,0) \; dz \tag{15.9}$$

and its square root (σ_z) is just the standard deviation of the concentration distribution.

Now we return to derivation of a prediction for σ_z. We assume, as usual, that ensemble-averaging commutes with differentiation or integration. Then

$$\begin{aligned} \frac{d}{dt}\,\overline{Z^2}(t) &= \overline{\frac{dZ^2}{dt}} \\ &= 2\,\overline{Z(t)\,\left(\frac{dZ}{dt}\right)_t} \\ &= 2\,\overline{W(t)\int_0^{t'=t} W(t')\,dt'} \\ &= 2\int_0^{t'=t} \overline{W(t)\,W(t')}\,dt' \; . \end{aligned} \tag{15.10}$$

Now define a Lagrangian velocity autocorrelation coefficient

$$R(t,t') = \frac{\overline{W(t)\,W(t')}}{{\sigma_w}^2} \tag{15.11}$$

which, defining $\tau = t - t'$, may be re-written:

$$R(t',\tau) = \frac{\overline{W(t')\,W(t'+\tau)}}{{\sigma_w}^2} \; . \tag{15.12}$$

But statistics of stationary turbulence are independent of any particular "starting time" t', so that $R(t',\tau) = R(\tau)$ (and in fact it is also true that $R(-\tau) = R(\tau)$. Therefore, noting $d\tau = -dt'$ and $\tau = 0$ when $t' = t$ and $\tau = t$ when $t' = 0$, we have

$$\frac{d\overline{Z^2}}{dt} = 2\,{\sigma_w}^2 \int_0^{\tau=t} R(\tau)\,d\tau \; . \tag{15.13}$$

This is G.I. Taylor's famous result for the rate of increase of mean square particle displacement, which is revealed to depend on the Lagrangian velocity autocorrelation function. Taylor's solution does not tell us the form of the concentration distribution, but gives us the second moment of that unknown distribution.

Note that we can define a Lagrangian integral time scale from $R(\tau)$ as

$$T_L = \int_0^{\tau=\infty} R(\tau)\,d\tau \; . \tag{15.14}$$

15.2.1 Comparison with Classical Eddy-Diffusion Solution

Remember we are considering the time-dependent evolution of the vertical position of a particle released at $z = t = 0$, and we aim to determine ensemble mean statistics (average over many trial releases). Now the governing mass conservation equation was given earlier,

$$\frac{\partial \overline{c}}{\partial t} + \overline{u}\,\frac{\partial \overline{c}}{\partial x} = \frac{\partial}{\partial x}\left(K_x\,\frac{\partial c}{\partial x}\right) + \frac{\partial}{\partial y}\left(K_y\,\frac{\partial c}{\partial y}\right) + \frac{\partial}{\partial z}\left(K_z\,\frac{\partial c}{\partial z}\right) \tag{15.15}$$

where we have assumed there is no in-situ production or destruction ($Q = 0$), and have neglected molecular transport. Now let us set the mean velocity to zero, and assume the K's are independent of position — homogeneous turbulence. Furthermore, since we don't care where on the x, y plane the particle happens to be, we can define a new concentration $c_*[\mathrm{m}^{-1}]$

$$c_*(z,t) = \int_{-\infty}^{x=\infty}\int_{-\infty}^{y=\infty} \overline{c}(x,y,z)\;dx\;dy\;. \tag{15.16}$$

Thus c_* is the earlier-mentioned probability density $p(z,t|0,0)$ for particle position, in the sense that $c_*(z_1,t)\,dz$ is the probability that a particle released at $z = t = 0$ is at time t lying in the range $z_1 - dz/2$ to $z_1 + dz/2$. By performing the double integral in x, y on the mass conservation equation we find c_* satisfies:

$$\frac{\partial c_*}{\partial t} = K_z\,\frac{\partial^2 c_*}{\partial z^2}\;. \tag{15.17}$$

It is easy to show that the solution to this equation that satisfies

$$c_*(z,0) = \delta(z-0) \tag{15.18}$$

(unit release at $t = z = 0$) is the Gaussian (ie. Normal) distribution

$$c_*(z,t) = \frac{1}{\sqrt{2\pi}\;\sigma_z}\;e^{-\frac{z^2}{2{\sigma_z}^2}} \tag{15.19}$$

with standard deviation $\sigma_z(t) = \sqrt{2\;K_z\;t}$. We could have jumped to this result straight from our earlier Gaussian Puff solution. It is pertinent that observations show that the concentration distribution *is* more or less Gaussian, for all distances from the source (but remember: this is an unbounded domain of homogeneous turbulence).

The important point is that this result states that

$$\frac{\partial {\sigma_z}^2}{\partial t} = 2\;K_z \tag{15.20}$$

while G. I. Taylor's result, which is exact, says

$$\frac{d\overline{Z^2}}{dt} = 2\;{\sigma_w}^2\int_0^{\tau=t} R(\tau)\;d\tau\;. \tag{15.21}$$

To reconcile these results we must have

$$K_z = {\sigma_w}^2 \int_0^{\tau=t} R(\tau)\, d\tau \ . \tag{15.22}$$

The eddy diffusivity, which we would have liked to consider as being a property of the turbulence statistics (alone), turns out to be (also) a function of the time since the particle was released: and only when $t \gg T_L$ (in the "far field") does the eddy diffusivity assume a value independent of t, namely the "far field limit" $K_\infty = {\sigma_w}^2\, T_L$.

Thus we conclude the classical diffusion theory, which predicts a plume width σ_z increasing as $\sqrt{t}$ for all t, is wrong at short travel times. In truth, σ_z goes linearly with t in the "near field" (when $t \ll T_L$). In the near field, travel time is so short that the particle flies with an essentially constant velocity — that it assumed (randomly) upon its release.

Taylor's result for the time-derivative of $\overline{Z^2}$ may be further integrated to obtain:

$$\sigma_z^2 = 2\ {\sigma_w}^2 \int_0^t (t-\tau)\ R(\tau)\ d\tau \ . \tag{15.23}$$

If, as is often assumed, the autocorrelation function is exponential with timescale T_L, ie.

$$R(\tau) = e^{-\frac{\tau}{T_L}} \ , \tag{15.24}$$

then Taylor's result for the spread specialises to:

$$\frac{\sigma_z^2}{2{\sigma_w}^2} = t\ T_L - \ {T_L}^2\ \left[1 - \ e^{-\frac{t}{T_L}}\ \right] \ . \tag{15.25}$$

15.2.2 Asymptotic results

The following results are valid for a general autocorrelation function.
Small time limit (near field): If $t \ll T_L$ then $R(\tau) = 1$ throughout the required integral. It follows that:

$$\overline{z^2} = {\sigma_w}^2\ t^2 \tag{15.26}$$

or $\sigma_z = \sigma_w\ t$. The plume spreads linearly in time for short times after release: that is because for short times the spread is not a diffusion process, but simply an advection at a constant random starting velocity.
Large time limit (far field):

If $t \gg T_L$ then $\sigma_z = \sqrt{2{\sigma_w}^2 T_L)}\ \sqrt{t}$.

What is important about G.I.Taylor's result?

1. If we insist on using an eddy diffusivity K to close the mass conservation equation, we have to accept that, of the totality of particles seen at a point z, a sub-ensemble of particles having been released at time t_1 may have a different diffusivity from a sub-ensemble

of particles that were released at t_2. This is logically absurd, the result of K-theory being fundamentally wrong.

2. The statistical evolution of concentration in this simple turbulence is completely governed by two statistical properties of the turbulence, σ_w, T_L.

3. The "far field" diffusivity is $K_\infty = {\sigma_w}^2\, T_L$.

15.3 Contemporary single-particle Lagrangian stochastic models

The term "Lagrangian stochastic model" (LS model) embraces a family of Lagrangian treatments of dispersion, subsuming "generalized Langevin models" (first-order LS models), as well as "random-flight" (or random-walk or Markov-chain) models, which are termed "zeroth-order LS models." The history of the LS model is covered by Thomson and Wilson in a chapter of a forthcoming AGU monograph *Lagrangian Models of the Atmosphere*.

As a starting point, let us note that the "drunkard's walk" analysed earlier is a *Markov process*, with the drunkard's position Z being the Markovian state variable: $Z(t+dt)$ depends on $Z(t)$, but not (explicitly) on any earlier positions $Z(t-dt)$ etc. The drunkard's walk is said to be a zeroth-order Lagrangian stochastic model, and we have seen that it is unsatisfactory for small travel times. Now interestingly, Taylor's superior and indeed *rigorous* result for dispersion in homogeneous turbulence can be shown to follow from the treatment of position (Z) and velocity (W) *jointly* as a compound Markovian variable $[Z, W]$. More specifically, Taylor's Eq.(15.25) follows from an analysis of (and thus, is implied by) Langevin's (1908) equation (Lemons 2002; Gardiner 2004), which was originally developed to describe spread due to Brownian motion (i.e. not turbulent dispersion). Expressed in our own notation, Langevin's equation reads

$$dW = -\frac{W}{T_L}\, dt + \sqrt{\frac{2\sigma_w^2}{T_L}}\, d\xi \tag{15.27}$$

where $d\xi$ represents an uncorrelated sequence of Gaussian random numbers having vanishing mean and variance dt, T_L is a velocity correlation time scale, and σ_w (as usual) is the standard deviation of velocity. Increments in velocity over intervals dt comprise a deterministic component (having the effect of damping the excursions in W on a timescale T_L) and a purely random component.

Obukhov (1959) was probably the first to frame a model of turbulent dispersion *explicitly* in the spirit of Langevin's equation, e.g. he states that "the evolution of the state of the selected particle in time forms a Markov process and can be described by the Fokker-Planck equation in the space (of position and velocity)." But how to comprehend the latter part of this sentence, and Obukhov's further statement that "the conditional distribution function (for velocity and position) is the principal characteristic of the motion in Lagrangian

variables"?

15.3.1 Digression: deterministic and stochastic forms of the Lagrangian stochastic model

Suppose we introduce a generalized Langevin equation (or generalized Langevin model)

$$dW = a(Z, W, t)\ dt + \ b(Z, W, t)\ d\xi \tag{15.28}$$

where $d\xi$ represents random forcing. Once the functions a, b are specified, one is able to compute an ensemble of random paths – a stochastic description of the motion. A complementary and *deterministic* approach is to frame the problem in terms of the joint density function $p(z, w, t)$ for particle location in $(z - w)$ space (this is the conditional distribution function referred to by Obukhov). For example, for release at $z = t = 0$ with a random velocity from the Eulerian pdf $g_a(w)$, the initial value of the joint density function for position and velocity is

$$p(z, w, 0) = \delta(z - 0)\ g_a(z, w)\ . \tag{15.29}$$

Now, being a statistic, $p(z, w, t)$ undergoes a *deterministic* evolution in time t (note: z, w, t are the *independent variables* upon which p depends). Over discrete intervals Δt, it evolves according to the "Chapman-Kolmogorov" equation

$$p(z, w, t + \Delta t) = \int_{z_0} \int_{w_0} p\left(z, w, t + \Delta t | z_0, w_0, t\right)\ p\left(z_0, w_0, t\right)\ dz_0\ dw_0 \tag{15.30}$$

which expresses conservation of probability (at any time after release, the particle must exist somewhere with some velocity).

It is possible to derive from the CK equation a differential equation for the evolution of the density function. Provided (only) that the random forcing ($d\xi$) in Eq. (15.28) is Gaussian (which it must be, on other grounds), the differential equation is the "Fokker-Plank equation,"

$$\frac{\partial p(z, w, t)}{\partial t} = -\ \frac{\partial}{\partial z}\ (w\ p) - \ \frac{\partial}{\partial w}\ (a\ p) + \ \frac{1}{2}\ \frac{\partial^2}{\partial w^2}\ \left(b^2\ p\right)\ . \tag{15.31}$$

The rhs is the divergence of a probability flux (in $z - w$ space): $w\ p$ is the flux along the z-axis, while $a\ p - \frac{1}{2}\ \partial(b^2\ p)/\partial w$ is the flux along the w-axis. Note that the flux of probability in w-space comprises an advection-like part ($a\, p$) and a diffusion part (the term in $\partial^2 p/\partial w^2$); since the underlying model entails random jumps in velocity it makes sense that we have a "diffusion" in w-space.

15.3.2 Reminder on relevant time scales

Recall that the Kolmogorov (inner) scales η_K (length) and t_K (time) describe the minimum intervals over which changes (in velocity) occur in the airflow. These are to be contrasted

with the Lagrangian integral (outer) scales, which measure typical spatial and temporal persistence of the turbulent velocity. In stationary, homogeneous turbulence, the Lagrangian integral timescale can be determined from the velocity variance (${\sigma_w}^2$) and the TKE dissipation rate (ϵ) as

$$T_L = \frac{2\ {\sigma_w}^2}{C_0\ \epsilon} \tag{15.32}$$

(Tennekes, 1979). Here C_0 is a dimensionless and (supposedly) universal constant, defined in Kolmogorov's similarity hypothesis

$$D_{U_i U_j} = \overline{dU_i\ dU_j} = C_0\ \epsilon\ dt\ \delta_{ij} \tag{15.33}$$

for the statistics of Lagrangian velocity increments over small dt.

15.3.3 Hierarchy of zeroth-, first-, and second-order LS models

The "zeroth-order" LS model for motion along a single axis (say z, the vertical), is a random walk in position (the drunkard's walk, or Random Displacement Model, RDM; see Wilson & Yee, 2007, and Boughton *et al.*, 1987). Over each time increment dt the increment dZ in particle position is given by

$$dZ = a\ dt + b\ d\xi \tag{15.34}$$

where a, b are deterministic coefficients, and $d\xi$ is drawn randomly from a Gaussian distribution with mean zero, and (by convention) variance dt. As we already know, this model is easily shown to be equivalent to the treatment of turbulent convection as a diffusion process, and for stationary turbulence

$$\begin{aligned} a &= \frac{\partial K}{\partial z}\ , \\ b^2 &= 2\ K\ . \end{aligned} \tag{15.35}$$

The RDM model is fundamentally wrong, and manifests as such close to a source. Although it may be adequate for description of the "far field," there remains the objection that the eddy diffusivity is not strictly a flow property, and not directly measurable. Furthermore the RDM supplies no criterion to limit the magnitude of the timestep dt, other than inhomogeneity scales like $K\ (\partial K/\partial z)^{-2}$. Choice of a timestep is therefore arbitrary, whereas the Lagrangian autocorrelation timescale T_L naturally limits the timestep of 1st - order models.

In the Random Displacement model, the position $\mathbf{X}$ is treated as Markovian, ie. correlation of particle velocity from one timestep to the next is ignored: thus the problem that the model is invalid for travel times short compared to the typical velocity correlation timescale. This deficiency is remedied in the "first-order" LS model, wherein the Markovian state variable is $(\mathbf{X}, \mathbf{U})$, and the velocity evolves in time according to a generalised Langevin equation (Thompson, 1987), whose multi-dimensional form is

$$dU_i = a_i\ dt + b_{ij}\ d\xi_j\ . \tag{15.36}$$

It is usual to require that the LS model uphold Kolmogorov's similarity theory eqn (15.33), which is accomplished provided

$$b_{ij} = \sqrt{C_0\ \epsilon}\ \delta_{ij}\ . \tag{15.37}$$

A 1^{st}- order LS model correctly predicts the rate of dispersion even in the near field of a source, where travel time t is not large w.r.t. T_L, in contradistinction to the RDM and to Eulerian models. Of course, the trajectories are not valid for travel times on the order of the acceleration timescale. To treat such exceptionally short-range trajectories, or trajectories in low Reynolds number turbulence, one may introduce a 2^{nd}-order LS model (eg. Du et al., 1995). In this case the Markovian state variable is $(\mathbf{X}, \mathbf{U}, \mathbf{A})$, where $\mathbf{A}$ is the acceleration vector, modelled as $dA_i = a_i\ dt +\ b_{ij}\ d\xi_j$.

In extremely high Reynolds number turbulence, such as occurs in the atmosphere, there is a wide separation between the smallest and largest scales of the turbulence. For many important atmospheric dispersion problems, the travel time of interest satisfies $t/t_K \gg 1$, and t/T_L finite. In this case a "first-order" LS model is appropriate (Thompson, 1987): we can choose a time step Δt in the range $t_K \ll \Delta t \ll T_L$ to resolve the evolution in velocity and position over time period t (Lagrangian acceleration correlation vanishes over timesteps $\Delta t \gg t_K$), but without need to explicitly model fluid element acceleration. Thus in these notes we emphasize the first-order LS model.

15.3.4 Thomson's well-mixed condition for first-order LS models

Accepting Eqn. (15.37), it remains to fix the coefficient a of the generalized Langevin model Eq. (15.28). Thomson (1987) proceeded as follows. One may apply an LS model to any initial distribution of tracer. Suppose, then, one applied it to the particular case where the tracer happened to be well-mixed in the flow,

$$p(z, w, 0) \propto \rho(z)\ g_a(z, w) \tag{15.38}$$

where (for the purpose of our course) the velocity statistics have been assumed stationary (the Eulerian velocity pdf g_a lacks time-dependence). For simplicity let's assume, too, that the fluid density ρ is constant. Then the joint density function at the initial time

$$p(z, w, 0) \propto g_a(z, w) \tag{15.39}$$

and since the particles are initially well-mixed, they must remain so, ie. $p(z, w, t) \propto g_a(z, w)$. Hence, g_a must be a stationary solution to the FP equation,

$$\frac{\partial}{\partial w}\ (a\ g_a) = -\ \frac{\partial (w\ g_a)}{\partial z} + \frac{1}{2}\ \frac{\partial^2\ (b^2\ g_a)}{\partial w^2}\ . \tag{15.40}$$

Since b is known (see above), this result determines the conditional mean acceleration a, for a specified Eulerian velocity pdf.

15.3.5 Unique 1-D LS Model for Gaussian Inhomogeneous Turbulence

With the exception of canopy turbulence and turbulence in the convective boundary layer, it is usual to treat boundary layer turbulence in the atmosphere as Gaussian, but vertically-inhomogeneous. And except very close to ground (or within a canopy; a case we consider later), the mean velocity is large w.r.t. the typical fluctuations (u'): thus dispersion in the streamwise direction is frequently ignored, or at least, u' is treated as independent of w. This leads to a focus on 1-component models, for the particle's vertical velocity, W.

The Eulerian velocity pdf, for now assumed Gaussian, is

$$g_a(z,w) = \frac{1}{\sqrt{2\pi}\ \sigma_w(z)}\ \exp\left(-\frac{w^2}{2{\sigma_w}^2}\right)\ . \tag{15.41}$$

It follows that the (unique) well-mixed, 1-component (here W) model for stationary Gaussian turbulence (Thompson, 1987)) is

$$\begin{aligned} a &= -\frac{C_0\ \epsilon(z)}{2{\sigma_w}^2(z)}\ W + \frac{1}{2}\frac{\partial {\sigma_w}^2}{\partial z}\ \left(\frac{w^2}{{\sigma_w}^2} + 1\right)\ , \\ b &= \sqrt{C_0\ \epsilon(z)}\ . \end{aligned} \tag{15.42}$$

The influence of atmospheric stratification enters through the turbulence parameters and the mean velocity profile $\overline{u}(z)$.

In inhomogeneous turbulence a Lagrangian timescale $T_L(z)$ can still be defined through eqn (15.32), but can no longer be interpreted as an integral time scale. In the neutral surface layer, where $\sigma_w \approx 1.3\ u_*$, inhomogeneity arises solely through the TKE dissipation rate.

It can be shown that the model compared in detail with the Project Prairie Grass field observations by Wilson et al. (1981b; hereafter WTK) is the discrete-time version of eqn (15.42). Wilson and Flesch (1993) studied the consequences of boundary treatment and time discretisation: any demixing of an initially well-mixed tracer field was attributed to the "Δt-bias error" that inevitably arises when trajectories in an inhomogeneous system are simulated with discrete time steps Δt. Using a time scale parameterisation equivalent to $C_0 = 3.1$, which value accords with latest estimates from simpler flows (Du et al., 1995), WTK showed this LS model to be in excellent agreement with the observations. They also obtained good agreement with unstable and stable PPG runs, using the parameterisations (which are consistent with $C_0 = 3.1$ in neutral conditions):

$$\begin{aligned} \frac{2\ {\sigma_w}^2}{C_0\ \epsilon} &= T_L(z) = \frac{0.5\ z}{\sigma_w}\left(1 - 6\frac{z}{L}\right)^{\frac{1}{4}},\ L < 0 \\ \frac{2\ {\sigma_w}^2}{C_0\ \epsilon} &= T_L(z) = \frac{0.5\ z}{\sigma_w}\left(1 + 5\frac{z}{L}\right)^{-1},\ L > 0 \end{aligned} \tag{15.43}$$

where L is the Monin-Obukhov length. These formulae can be used to parameterise the compound variable $C_0\epsilon$ in (modern) LS models of the equilibrium atmospheric surface layer.

Project Prairie Grass (The O'Neill Experiment)

Project Prairie Grass (Barad, 1958; Haugen, 1959) was performed 1956 in Nebraska (at an extensive flat, uniform site) by sixty personnel, directed by the Air Force Cambridge Research Center. Its objective was to determine the rate of diffusion of a tracer gas as a function of meteorological conditions. Gas concentration was measured at distances out to 800 m from the source, so this was a short range (surface-layer) dispersion experiment. It is by far the most comprehensive short range field dispersion experiment yet conducted, and still the preeminent criterion for model performance. Details:

- a point source at $z = 0.46$ m released SO_2 continuously
- detectors were placed at $z = 1.5$ m on radii at (50, 100, 200, 400, 800) m (i.e. very high azimuthal resolution of the plume, 0.5^o at $r = 50$ m)
- vertical profiles of concentration on six 20m towers at radius $r = 100$ m
- simultaneous micrometeorological measurements (wind and temperature profiles, net radiation, soil heat flux, ..)
- about 60 trials, covering the complete range of atmospheric stratification. Very good internal consistency.

Complications:

- was the surface boundary condition zero flux of SO_2, ie. no absorption? It is widely assumed so. The grass was dry; in most experiments, most of the mass emitted mass can be accounted for drifting past observation points. Sawford (2001) determined that deposition can be neglected.
- the source was a jet – what were its initial cross section and initial momentum?

LS simulations of PPG

Fig.(15.2) gives (normalized) cross-wind integrated concentration profiles at fetch $x = 100$ m for PPG runs $(16, 57, 14)$ for which the Monin-Obukhov length was, respectively, $(-3.2, -240, +4.1)$ m. Normalization on Q/u_* collapses variability due to source strength and overall windspeed, and this figure shows the remaining (and quite dramatic) dependency on stratification.

Fig. (15.3) shows simulations by WTK of PPG run 57. The simulations used $L = \infty, u_* = 0.50\,\mathrm{m\,s^{-1}}, z_0 = 0.0058$ m (effectively a neutral run). The three choices of the coefficient $a = 0.32, 0.5, 0.75$ relate to the specification of the Kolmogorov constant C_0, or equivalently to the specification of an effective timescale $T_L = \frac{2\sigma_w^2}{C_0\epsilon} = \frac{az}{\sigma_w}$. Evidently the choice $a = 0.5$ is best, and implies a turbulent Schmidt number $S_c \sim 0.63$, and $C_0 = 3.1$ (this

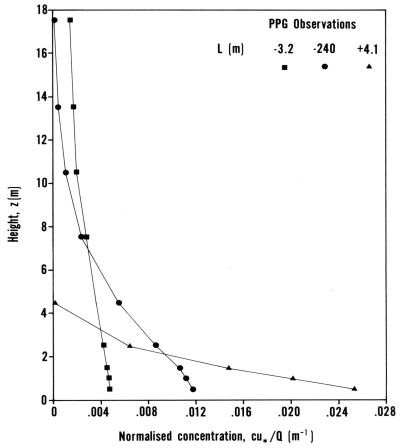


Figure 15.2: Normalized, crosswind-integrated concentration profiles at downwind distance $x = 100$ m for three PPG runs, showing the dramatic influence of stratification.

value accords with latest estimates from simpler flows; Du *et al.*, 1995). Figs. (15.4, 15.5) show the simulations by WTK of unstable ($L = -26, -8$ m) and stable ($L = +7$ m) runs. Stability corrections have been applied, viz.

$$\begin{aligned} \frac{2\ {\sigma_w}^2}{C_0\ \epsilon} &= T_L(z) = \frac{0.5\ z}{\sigma_w}\left(1 -\ 6\frac{z}{L}\right)^{\frac{1}{4}},\ L < 0 \\ \frac{2\ {\sigma_w}^2}{C_0\ \epsilon} &= T_L(z) = \frac{0.5\ z}{\sigma_w}\left(1 +\ 5\frac{z}{L}\right)^{-1},\ L > 0 \end{aligned} \tag{15.44}$$

where L is the Obukhov length. These formulae can be used to parameterise the compound variable $C_0\epsilon$ in contemporary LS models of the equilibrium atmospheric surface layer.

15.3.6 Lateral dispersion in the atmosphere

We have focused here on vertical dispersion, and ignored the important question of the impact of the fluctuating alongwind component u', which is correlated with the vertical velocity,

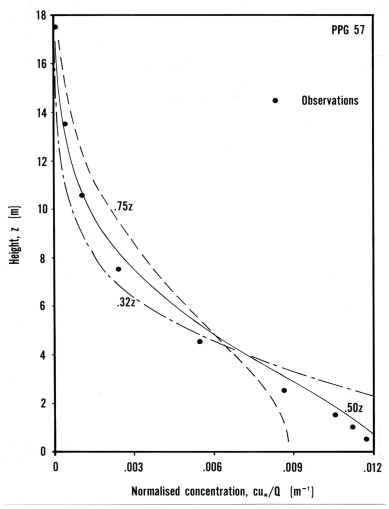


Figure 15.3: Simulations of PPG run 57 ($L = -240$ m, $u_* = 0.5\,\mathrm{m\,s^{-1}}$, $z_0 = 0.006$ m) using the unique well-mixed 1-d LS model for Gaussian inhomogeneous turbulence. The three choices of the coefficient $a = 0.32, 0.5, 0.75$ relate to the specification of the Kolmogorov constant C_0, or equivalently to the specification of an effective timescale $T_L = \frac{2\sigma_w^2}{C_0\epsilon} = \frac{az}{\sigma_w}$.

and of the lateral turbulence component. The inclusion of u' and/or v' presents a difficult problem. There is firstly the difficulty that as yet we do not have a unique well-mixed 2- or 3-dimensional LS model, even if we are prepared to accept Gaussian velocity pdfs. Particular 3-d solutions for a_i in Gaussian inhomogeneous turbulence, well-mixed (ie. satisfying), have been given by Thomson (1987) and by Borgas (see Sawford and Guest, 1988), who compared calculations for a neutral surface layer with the wind tunnel dispersion data of Legg (1983).

The second difficulty of including the horizontal velocity fluctuations, and a difficulty not peculiar to LS modelling, is that u' and v' contain energy at much lower frequencies than w'. The speed and direction of the horizontal wind change on a continuous range of scales, from the almost-microscopic (Kolmogorov) scale, up through scales of order 10 min (cloud/meso scale), to hourly and daily scales (changing large scale pressure patterns). Therefore no

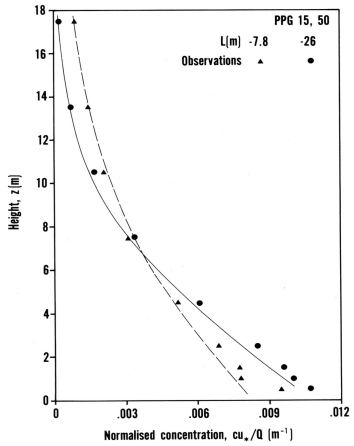


Figure 15.4: Simulations of PPG runs (15, 50) using the unique well-mixed 1-d LS model for Gaussian inhomogeneous turbulence; $a = 0.5$, and stability correction of eqn (15.44).

matter what our choice of averaging time, there is always the likelihood of an irregular and possibly multi-modal distribution of material along the horizontal direction(s). In general the (mean) mass distribution in x, y cannot be sharply predicted unless we can forecast the mesoscale fluctuations in wind direction. Practical means of accomplishing this involve prediction of the mesoscale wind variations with a prognostic mesoscale wind-field model and coupling these to a LS model for the turbulence.

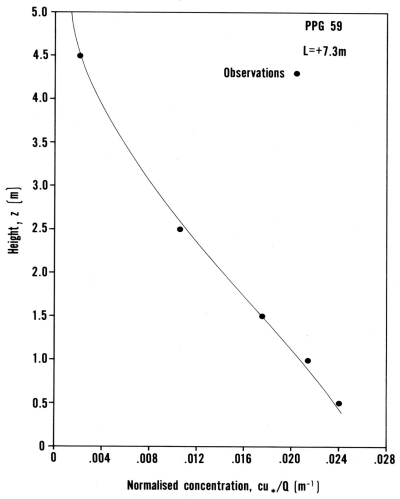


Figure 15.5: Simulations of PPG run 59; $a = 0.5$, and stability correction of eqn (15.44).

15.3.7 Multi-dimensional LS models

Gaussian inhomogeneous turbulence

Thomson's 2-dimensional model for stationary Gaussian inhomogeneous turbulence may be written

$$\begin{aligned} dU' &= -\frac{b^2}{2\sigma^2}\left[U'\,{\sigma_u}^2 - W\,\overline{u'w'}\right]\,dt + \frac{\phi_u}{g_a}\,dt + b\,d\xi_u\,, \\ dW &= -\frac{b^2}{2\sigma^2}\left[W\,{\sigma_u}^2 - U'\,\overline{u'w'}\right]\,dt + \frac{\phi_w}{g_a}\,dt + b\,d\xi_w\,, \\ dX &= \left[\,\overline{u}(Z) + U'\,\right]\,dt\,, \\ dZ &= W\,dt\,. \end{aligned} \tag{15.45}$$

Here $g_a(U', W; z)$ is the height-dependent (Eulerian) joint velocity pdf, σ is defined by

$$\sigma^2 = {\sigma_u}^2{\sigma_w}^2 - {u_*}^4\,, \tag{15.46}$$

and the ϕs are given by:

$$\begin{aligned}
\frac{\phi_u}{g_a} &= \frac{1}{2}\frac{\partial \overline{u'w'}}{\partial z} + W\frac{\partial \overline{u}}{\partial z} \\
&+ \frac{1}{2\sigma^2}\left[\frac{\partial {\sigma_u}^2}{\partial z}\left({\sigma_w}^2 U' W - \overline{u'w'} W^2\right) + \frac{\partial \overline{u'w'}}{\partial z}\left({\sigma_u}^2 W^2 - \overline{u'w'} U' W\right)\right], \\
\frac{\phi_w}{g_a} &= \frac{1}{2}\frac{\partial {\sigma_w}^2}{\partial z} \\
&+ \frac{1}{2\sigma^2}\left[\frac{\partial {\sigma_w}^2}{\partial z}\left({\sigma_u}^2 W^2 - \overline{u'w'} U' W\right) + \frac{\partial \overline{u'w'}}{\partial z}\left({\sigma_w}^2 U' W - \overline{u'w'} W^2\right)\right]
\end{aligned} \tag{15.47}$$

(one could everywhere write $\overline{u'w'} = -u_*^2$; in general u_* has to be regarded as height-dependent). As written here, the fluctuations U' and W are both simulated using the same timescale (T_L) and model coefficient $b = \sqrt{2\sigma_w^2/T_L}$. These equations simplify considerably in the case of a constant stress layer.

15.3.8 Link between C_0 and S_c

Prescription of the universal constant C_0 in an LS model is equivalent to the prescription of the turbulent Schmidt number S_c in a K-theory model, because a Lagrangian model implies an underlying diffusion model in the "diffusion limit" (Durbin, 1984). For example, Thomson's (1987) well-mixed multi-dimensional LS model for Gaussian turbulence, implies in the diffusion limit an eddy diffusivity

$$K = \frac{2\left({\sigma_w}^4 + {u_*}^4\right)}{C_0\,\epsilon} \tag{15.48}$$

for vertical diffusion in the neutral surface layer[2] (Sawford and Guest, 1988). This diffusivity may be related to an effective Lagrangian decorrelation timescale T_L, by defining $K = {\sigma_w}^2 T_L$. It has been common in LS models of the neutral ASL to write $T_L = az/\sigma_w$, thus $K = a\,\sigma_w z$. In view of Eq. (15.48), and if we assume the TKE dissipation rate $\epsilon = {u_*}^3/(k_v z)$, the relationship between C_0 and the empirical coefficient a is

$$C_0 = \frac{2\,k_v}{a}\,\frac{c_w^4 + 1}{c_w} \tag{15.49}$$

where $c_w = \sigma_w/u_*$.

The 1-d form of Thomson's model is the unique well-mixed model first-order LS model for vertical diffusion in the ASL, ie. is the correct model if fluctuations of a particle's horizontal velocity away from the local mean $\overline{u}(z), \overline{v}(z)$ are ignored (this because it proves adequate to specify the velocity pdf's of the ASL as Gaussian). The diffusion limit for the 1d model is obtained by dropping the factor ${u_*}^4$ from eqn (15.48) and (correspondingly) the factor "1" from eqn (15.49).

[2]If the $u' - w'$ correlation is neglected, the term u_*^4 is eliminated.

One may evaluate C_0 (and thus the Schmidt number S_c) by requiring that an LS model best reproduce observations of tracer dispersion (eg. Du et al, 1995). Wilson et al. (1981) "calibrated" the 1-dimensional form of Thomson's LS model against Project Prairie Grass, by tuning the formula $T_L = az/\sigma_w$. They recommended $a \approx 0.5$, which implies $S_c \approx 0.63$, and (using Eq. 15.48 with the term ${u_*}^4$ neglected) $C_0 \approx 3.1$ (if $\sigma_w/u_* = 1.25$), or $C_0 \approx 3.5$ (if $\sigma_w/u_* = 1.3$). Wilson et al.(1984) also found $a \approx 0.5$ a suitable choice, in comparing the 1d LS model with a tracer dispersion experiment on a beach in New Zealand.

Best agreement of PPG with the multi-dimensional Thomson model is still procured with $a \approx 0.5$, implying $S_c \approx 0.63$. The corresponding C_0 is larger than estimates from a 1d model, namely $C_0 \approx 4.4$ (if $\sigma_w/u_* = 1.25$), or $C_0 \approx 4.8$ (if $\sigma_w/u_* = 1.3$) . Estimates from Direct Numerical Simulations (Sawford and Yeung, 2000) suggest even larger values of $C_0 \approx 6 - 7$.

15.3.9 Reflection at Boundaries

Except in cases that permit analytic solution, an LS model will be implemented with finite timestep Δt, and it may be necessary to tack onto the model an algorithm that assures particles remain in the computational domain (not necessarily only because the timestep is finite). The best available criterion remains the w.m.c., whose satisfaction may be checked simply by calculating (numerically) the evolution of an initially well-mixed tracer distribution.

Wilson and Flesch (1993) showed how to write a discrete-time LS model that is "complete" (contains reflection; unambiguous order of operations) and how to deduce the implied transition density $p(z_2, w_2, t_2|z_1, w_1, t_1)$. The latter, defined such that $p(z_2, w_2, t_2|z_1, w_1, t_1)\ dz_2\ dw_2$ is the probability of transition during interval $(t_2 - t_1)$ from (phase space) point (z_1, w_1) into volume $(z_2 \pm dz_2/2, w_2 \pm dw_2/2)$, determines the evolution of the joint density function $p(z, w, t)$ for position and velocity, via the Chapman-Kolmogorov equation:

$$p(z_2, w_2, t_2) = \int_\Omega p\left(z_2, w_2, t_2|z_1, w_1, t_1\right)\ p\left(z_1, w_1, t_1\right)\ dz_1\ dw_1 \tag{15.50}$$

(Ω denotes the entire region of the $z - w$ domain that is accessible to a particle). Assuming constant fluid density, and stationary flow, the w.m.c. can be expressed:

$$g_a(z, w) = \int_\Omega p(z, w, \Delta t|z_0, w_0, 0)\ g_a(z_0, w_0)\ dz_0\ dw_0\ . \tag{15.51}$$

From eqn (15.51), Flesch and Wilson proved that perfect reflection is exactly valid, if applied to bound Gaussian homogeneous turbulence (multi-dimensional models that include velocity covariance will require to reverse upon reflection both normal velocity W and the correlated alongwind velocity fluctuation U'). Thomson and Montgomery (1994) give a more general trajectory reflection scheme.

15.3.10 Partially-absorbing boundaries

In Eulerian models, uptake of gases (or very small particles) at ground is usually parameterised in terms of a "deposition velocity," defined as the ratio $w_d = F/\overline{c}_0$ of the actual flux density at the surface to a mean concentration $\overline{c}_0$ measured at an arbitrary reference location. Wilson et al. (1989) derived and tested an approximate means to achieve the correct effective deposition velocity, by partial reflection at the sink. For given w_d, the corresponding reflection probability R (they found) is:

$$\frac{1-R}{1+R} = \sqrt{\frac{\pi}{2}}\,\frac{w_d}{\sigma_w}\,. \tag{15.52}$$

15.3.11 LS models for non-Gaussian turbulence

Wilson (2007) explores the LS models implied by several "toy" velocity PDFs for a neutral surface layer, showing that the Gaussian corresponds to the simplest model (namely, the Langevin equation). Several important regimes of turbulence are characterized by non-Gaussian velocity PDFs, one of the most important being the convective boundary layer.

Convective BL

The CBL can be considered as comprising a fractional area (A) of "updrafts" (wherein the mean velocity is upward, but the instantaneous velocity need not be) and a complementary fractional area ($B = 1 - A$), considered the (predominantly) subsiding environmental region. In uniform terrain and under suitable restrictions, it is possible to define a "horizontally homogeneous" CBL and to again focus on vertical dispersion. The penalty for neglecting "coherent structures" (thermals) and substituting for reality the convenient simplification of horizontal uniformity is that in consequence, the pdf $g_a(w;z)$ of the Eulerian vertical velocity in the CBL is non-Gaussian, in addition to being vertically-inhomogeneous: over much of the CBL, the skewness $Sk_w(z) = \overline{w'^3}/{\sigma_w}^3 \sim 1/2$.

A superior simulation of dispersion from sources in the CBL is considered one of the unequivocal advances offered by the (correctly designed) Lagrangian stochastic model. Shortly after Thomson (1987) demonstrated how a correctly model should be formulated, papers by Weil (1988) and Luhar and Britter (1989) demonstrated the application to sources in the CBL.

In an earlier paper Baerentsen and Berkowicz (1984; hereafter BB) had constructed a skewed pdf $g_a(w;z)$ for the CBL as a linear combination of Gaussians for the updraft and downdraft regions,

$$g_a(z,w) = A\,G(\overline{w}_A, \sigma_{wA}) + (1-A)G(\overline{w}_B, \sigma_{wB}) \tag{15.53}$$

where $G(\overline{w}, \sigma)$ represents a Gaussian pdf with mean $\overline{w}$, and standard deviation σ. This form of pdf has been used in most subsequent LS studies of the CBL, although procedures for specifying the parameters of the pdf have varied.

To reproduce the velocity moments one requires that:

$$A(z) \int_{-\infty}^{\infty} w^n \, P_A(w;z) \, dw + \; B(z) \int_{-\infty}^{\infty} w^n \, P_B(w;z) \, dw = \; \overline{w'^n} \; . \tag{15.54}$$

BB assumed

$$\sigma_{wA} = \overline{w}_A, \; \sigma_{wB} = \overline{w}_B$$

and applied eqns(15.54) for $n = 0...3$ (no constraint on kurtosis). Luhar and Britter (1989) followed BB, but Weil (1988) instead wrote

$$R = \sigma_{wA}/\overline{w}_A = - \, \sigma_{wB}/\overline{w}_B$$

with $R = 1.5$.

Profiles of vertical velocity statistics for the CBL

The LB and Weil models differ only in their tuning of the parameters of the velocity pdf, and in their parameterisations for the turbulence statistics, which in particular differed markedly near the boundaries. LB did not resolve a surface layer, but imposed at $z = 0, \delta$ vanishing σ_w and τ_L and a very large gradient $\partial\sigma_w/\partial z$.

$$\begin{aligned} \frac{\sigma_w^2}{w_*^2} &= 1.1 \left(\frac{z}{\delta}\right)^{2/3} \left(1 - \frac{z}{\delta}\right)^{2/3} \left(1 - \frac{4 \, \left(\frac{z}{\delta} - 0.3\right)}{\left(2 + |\frac{z}{\delta} - 0.3|\right)^2}\right) \\ \frac{\overline{w'^3}}{\sigma_w^3} &= \left(\frac{\sigma_w^2}{w_*^2}\right)^{3/2} . \end{aligned} \tag{15.55}$$

The TKE dissipation rate (needed for $b = \sqrt{C_0 \, \epsilon}$) was parameterized as:

$$\frac{\epsilon \, \delta}{w_*^3} = 1.5 - \; 1.2 \left(\frac{z}{\delta}\right)^{1/3} . \tag{15.56}$$

In contrast to the LB parametrization, Weil's gave the semblance of a normal surface layer near ground ($\sigma_w = 1.3 u_*$, and a small and linearly-increasing length scale). In both cases $\overline{w'^3}$ vanished at $z = (0, \delta)$, but LB set $Sk_w = 0.8$ (for all z) while Weil's parametrization resulted in $Sk_w = 0$ at the boundaries.

Validity of reflection algorithm

Both models imposed perfect reflection at $z = 0, \delta$. Wilson and Flesch (1993) examined the legitimacy of the reflection algorithm, bearing in mind the velocity skewness, which they argued implies there is no reflection algorithm that *exactly* upholds the well-mixed

constraint (but see Thompson and Mongomery, 1994). Their implementation of the LB and Weil models indicated "In the case of the LB model (which was implemented so as to make $\Delta t/T_L$ everywhere small), confinement resulted from making the boundaries unattainable (reflection, which would be invalid, did not occur). On the other hand Weil's near-wall flow statistics are such that, though reflection did occur, it was applied to particles coming from such close proximity to the boundary that neither inhomogeneity nor skewness in that shallow region compromised excessively the use of perfect reflection."

Model coefficient

The form of the 1-d LS model is

$$dW = a(W)\,dt + \sqrt{C_0\,\epsilon}\,d\xi\ . \tag{15.57}$$

In this case the well-mixed condition implies a unique solution for the conditional mean acceleration a corresponding to the BB velocity pdf,

$$a = -\frac{\sigma_w^2}{T_L}\frac{Q}{g_a} + \frac{\phi}{g_a} \tag{15.58}$$

where

$$Q(W) = \frac{A}{\sigma_{wA}^2}\,(W-\overline{w}_A)\,P_A(W;z) + \frac{1-A}{\sigma_{wB}^2}\,(W+\overline{w}_B)\,P_B(W;z) \tag{15.59}$$

and

$$\begin{aligned}\phi(W) = &-\frac{1}{2}\left(A\,\frac{\partial\overline{w}_A}{\partial z} + \overline{w}_A\,\frac{\partial A}{\partial z}\right)\,\mathrm{erf}\left(\frac{W-\overline{w}_A}{\sqrt{2}\,\sigma_{wA}}\right)\\ &+\frac{1}{2}\left(B\,\frac{\partial\overline{w}_B}{\partial z} + \overline{w}_B\,\frac{\partial B}{\partial z}\right)\,\mathrm{erf}\left(\frac{W+\overline{w}_B}{\sqrt{2}\,\sigma_{wB}}\right)\\ &+\left[\frac{A}{2}\,\frac{\partial\sigma_{wA}^2}{\partial z}\,\left(\frac{W^2}{\sigma_{wA}^2}+1\right) + \sigma_{wA}^2\,\frac{\partial A}{\partial z}\right]\,P_A(W;z)\\ &+\left[\frac{B}{2}\,\frac{\partial\sigma_{wB}^2}{\partial z}\,\left(\frac{W^2}{\sigma_{wB}^2}+1\right) + \sigma_{wB}^2\,\frac{\partial B}{\partial z}\right]\,P_B(W;z)\ .\end{aligned} \tag{15.60}$$

Example: CBL simulation of Du et al.

Du et al. (1994) slightly modified the Luhar-Britter model, assuming a constant area-fraction for thermals, $A = 0.4$. This area-fraction for thermals is supported by the aircraft observations of (Manton, 1977) and others. However observations by Lenschow and Stephens (1980), using a more conservative selection procedure for thermals, gave a smaller value of $A \sim 0.2 - 0.3$ which seems more compatible with the experience of hang glider pilots (who, however, will tend to consider thermals as events with $w \geq 2 - 3\,\mathrm{m\,s^{-1}}$).

The fitting procedure of Luhar-Britter did not specify kurtosis. Du et al. required that Kurtosis $K_w = 3$, ie. that $\overline{w'^4} = 3\,\sigma_w^4$, and so eqns(15.54) were applied for $n = 0...4$. This

results in

$$\begin{aligned}
\overline{w}_A &= \overline{w'^3}^{1/3} , \\
\overline{w}_B &= \frac{2}{3}\,\overline{w'^3}^{1/3} , \\
\sigma_{wA} &= \sqrt{\sigma_w^2 - 0.280\,\overline{w'^3}^{\,2/3}} , \\
\sigma_{wA} &= \sqrt{\sigma_w^2 - 0.927\,\overline{w'^3}^{\,2/3}} .
\end{aligned} \tag{15.61}$$

Because A=const., the ϕ term in the deterministic part of the acceleration simplifies slightly for the Du et al. model,

$$\begin{aligned}
\frac{\phi}{g_a} &= -\frac{A}{2\,g_a}\,\frac{\partial \overline{w}_A}{\partial z}\,\mathrm{erf}\left(\frac{W-\overline{w}_A}{\sqrt{2}\,\sigma_{wA}}\right) + \frac{1-A}{2\,g_a}\,\frac{\partial \overline{w}_B}{\partial z}\,\mathrm{erf}\left(\frac{W+\overline{w}_B}{\sqrt{2}\,\sigma_{wB}}\right) \\
&+ \sigma_{wA}\,\frac{\partial \sigma_{wA}}{\partial z} + \frac{W\;(W-\overline{w}_A)}{\sigma_{wA}}\,\frac{\partial \sigma_{wA}}{\partial z} + W\,\frac{\partial \overline{w}_A}{\partial z} \\
&+ \sigma_{wB}\,\frac{\partial \sigma_{wB}}{\partial z} + \frac{W\;(W+\overline{w}_B)}{\sigma_{wB}}\,\frac{\partial \sigma_{wB}}{\partial z} - W\,\frac{\partial \overline{w}_B}{\partial z} .
\end{aligned} \tag{15.62}$$

Fig.(15.6), from Du et al., gives calculated contours of normalized crosswind-integrated ensemble-mean concentration χ from a continuous point source in the CBL, as a function of normalised height $Z = z/\delta$ and downwind distance $X = (x/U)/(\delta/w_*)$ (where U is the unsheared CBL windspeed). Trajectories were reflected at $z = 0, \delta$. At large x, $\chi \to 1$ (tracer well mixed along the vertical). The most interesting aspect of this is that plume centreline initially slopes downwards from the source, until reflections off ground begin to occur. This is due to (and would not be predicted without allowing for) the skewed vertical velocity pdf; with probability 0.6, the emerging plume is caught in a weak downdraft. Similar results had been given by Luhar and Britter, and by Weil. And these results are in rather good agreement with the laboratory experiments of Willis and Deardorff (1976, 1978, 1981).

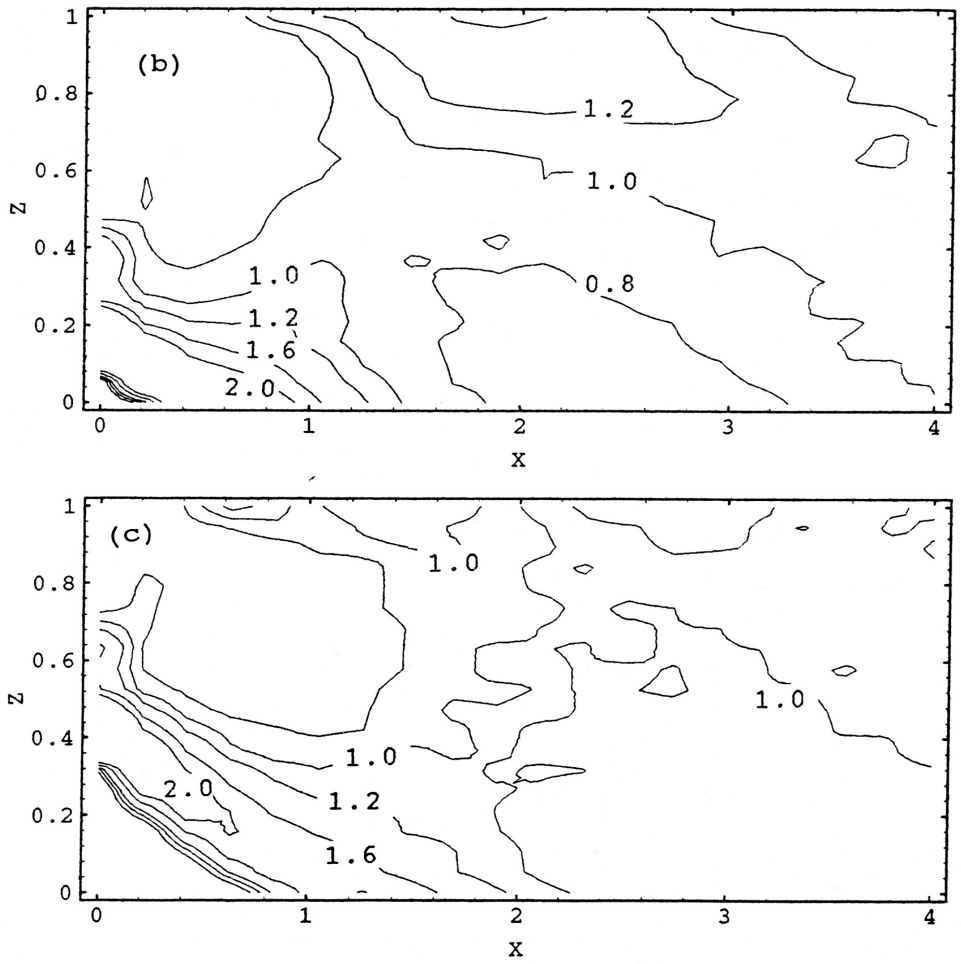


Figure 15.6: Contours of normalized crosswind-integrated mean concentration χ from a continuous point source in the CBL, at height (b) $z_{src} = 0.24\,\delta$ and (c) $z_{src} = 0.49\,\delta$. Normalized coordinates are $Z = z/\delta$, $X = \frac{x/\overline{u}}{\delta/w_*}$.

LS models for a plant/forest canopy

Turbulent velocity statistics within a crop or forest canopy are non-Gaussian, and extremely vertically-inhomogeneous, with a characteristic inhomogeneity scale

$$I_s = {\sigma_w}^{-1} T_L \partial {\sigma_w}^2 \partial z \tag{15.63}$$

being of the order of unity. Much of the vertical exchange is accomplished by intermittent large eddies, whose origin possibly owes to an instability with respect to the inflexion-point in the wind profile. The pdf of the vertical velocity $g_a(w)$ is highly skewed, $Sk_w \approx -1$, and in much of the canopy space, turbulence intensity is large ($\sigma_u, \sigma_v > \overline{u}$).

We expect K-theory to be useful when the turbulence is "fine-grained" relative to the length scale over which there is curvature in the concentration distribution (Corrsin, 1974; for an extended explanation of the failure of K-theory in a canopy, see Wilson 1989). Such is not (usually) the case in a canopy. A dramatic demonstration (that K-closure is unworkable) owes to Denmead and Bradley (1985), who by simultaneous measurement of mean profiles and eddy fluxes, demonstrated the routine occurrence of counter-gradient heat and vapour fluxes in a pine forest. Using a Lagrangian model, Raupach (1987) showed that in a canopy a substantial proportion of the scalar concentration (of heat or vapour) is contributed by the non-diffusive "near field" wakes of the nearby leaves, shedding heat and vapour to the airstream. It is natural, then, to turn to a Lagrangian description, irrespective of any wish to account for the highly non-Gaussian turbulence.

The first LS models were heuristic, not linked to the form of $g_a(w)$, and accounting only for the variance ${\sigma_w}^2(z)$. When applied to the extremely vertically-inhomogeneous canopy flow, these failed miserably the (as yet not clearly stated) well-mixed constraint: particles were found to spuriously acccumulate in regions of small turbulent velocity scale (Wilson et al. 1981a). These difficulties spurred ad hoc "drift corrections," until the clarification provided by Thomson (1984, 1987).

Since w-skewness is the signature of the intermittent large gusts, and since those gusts have been proven by quadrant analysis (eg. Shaw et al. 1983) to dominate the transport process; and furthermore since accounting for skewness had improved LS predictions of the CBL, one naturally expected an LS model properly derived from the skew Eulerian pdf ought to best handle canopy dispersion. Flesch and Wilson (1992) constructed such a model. Of course, if this was to well-simulate dispersion in a canopy, it must include both the vertical and the alongwind fluctuations. Two problems then arise: (a) even given the joint pdf $g_a(u, w)$, Thomson's criteria do not provide a unique multi-dimensional LS model; and (b) given only the low-order moments of u and w, what is the p.d.f.? Concerning (a), non-uniqueness was resolved by postulating that $\vec{\phi}$ (as defined in) should act to conserve the direction of the Lagrangian velocity fluctuation vector. Concerning (b), following the idea of Baerentsen and

Berkowizc, Flesch and Wilson superposed two joint Gaussians. Means and covariances of the individual joint-Gaussians were tailored to reproduce the lowest five moments of w, the lowest four moments of u, and the covariance $\overline{u'w'}$. This was quite arbitrary, and entailed the hazard that correctly fitting the low moments might constrain other moments to unrealistic values. Fig.(15.7) ilustrates two pdf's that *both* fit what one might consider the most important low-order moments, and this emphasizes the difficulty of formation of the pdf, even given a rather large set of moments.

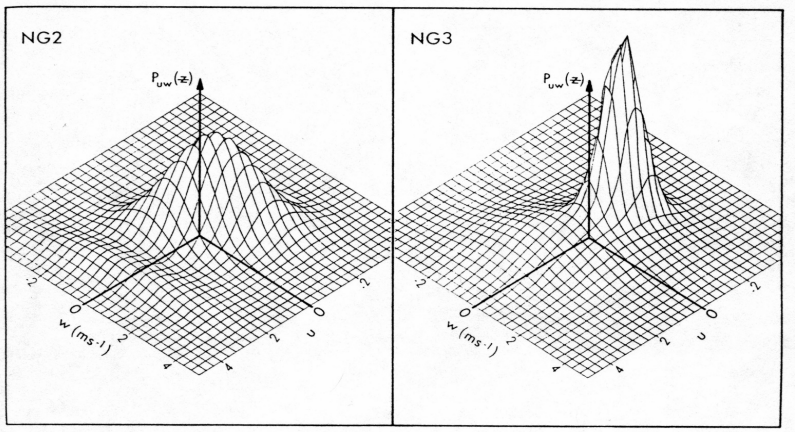


Figure 15.7: Joint probability density function for velocity at height $z/h_c = 0.85$ in the Tombstone Canopy. Constructed by linear combinations of two joint-Gaussians, constrained to reproduce (fitted curves to measured) low-order moments: $\overline{u}, \overline{w}, \sigma_u^2, \sigma_w^2, \overline{u'w'}, \overline{u'^3}, \overline{w'^3}, \overline{u'^4}, \overline{w'^4}$. PDF's differ in relation to other moments.

Flesch and Wilson simulated experiments (Raupach et al. 1986; Legg et al. 1986; Coppin et al. 1986) in which heat was released as a tracer, from line and area sources, within a model crop in a turbulent wind tunnel boundary layer. The surprising outcome of the work was that the more-complex LS model which accounted for the known skewness and kurtosis of the canopy velocity statistics performed worse than Thomson's (1987) multi-dimensional model based on Gaussian Eulerian statistics (see Figs.15.8, 15.9). The authors suspected the cause was their adoption of an ad hoc pdf: the "best" (or least biased) choice would have been the mmi pdf. However it may also be that the extreme vertical inhomogeneity of canopy flow ($I_s \sim 1$) in contrast to CBL flow ($I_s \ll 1$) implies a less critical dependence (of canopy dispersion) on the velocity skewness. It is pertinent here to quote Dr. J. Hunt: "I believe that inhomogeneity will dominate over the niceties of third and fourth moments."

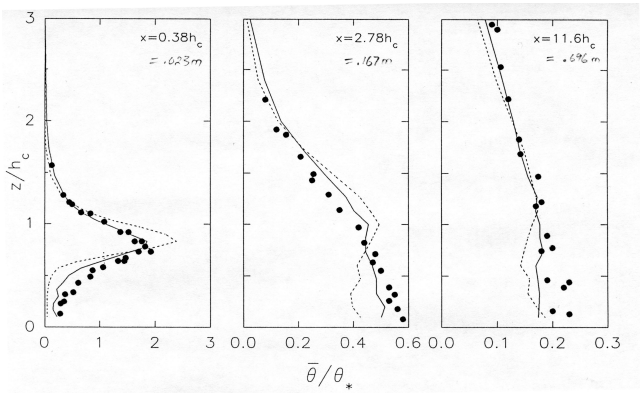


Figure 15.8: Measured versus modelled mean scalar concentration (temperature rise) due to a line source at $z_{src}/h_c = 0.85$ in the Tombstone Canopy. Solid line, Thomson's well-mixed multi-dimensional LS model for Gaussian inhomogeneous turbulence (ie. joint-pdf approximated as Gaussian); dashed line, Flesch-Wilson LS model based on non-Gaussian joint-pdf.

15.4 Fundamental Superiority of Lagrangian models

For turbulent flows usually we are interested in statistics of the velocity and concentration fields. The problem with the Eulerian theories for them is that they contain nonlinear advection terms and so the evolution equations for the mean velocity $\overline{u}$ and mean concentration $\overline{c}$ are not closed; i.e. they involve unknown higher order statistics such as the Reynolds stresses $\overline{u_i' u_j'}$ and scalar flux densities, $\overline{u_i' c'}$. Closure approximations introduced to overcome this insuperable problem depend on the concentration field itself, and so are not uniformly valid, ie., the closure approximations pertain to joint statistics of velocity and concentration whereas in general, these must depend on the source distribution.

The key advantage of the Lagrangian framework is that one is able to avoid seeking uni-

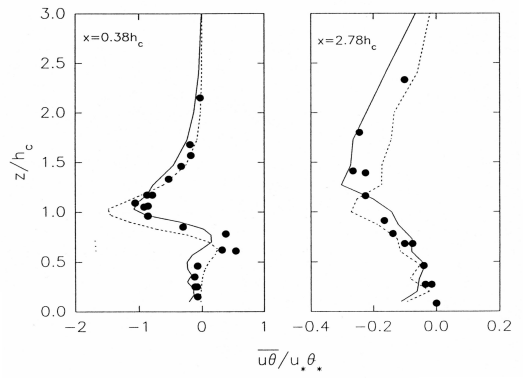


Figure 15.9: Measured versus modelled streamwise turbulent heat flux density due to a line source at $z_{src}/h_c = 0.85$ in the Tombstone Canopy. Solid line, Thomson's well-mixed multi-dimensional LS model for Gaussian inhomogeneous turbulence (ie. joint-pdf approximated as Gaussian); dashed line, Flesch-Wilson LS model based on non-Gaussian joint-pdf.

versal relationships for joint statistics of velocity and concentration. A further fundamental advantage of LS models is that they are able to exploit all given (statistical) information on the wind. A less fundamental but no less significant advantage is that, being grid-free, LS solutions are trivial to compute.

15.5 Heavy particle dispersion

Many authors have attempted to determine an effective (particle) eddy diffusivity K_p (eg. Yudine n.d.; Csanady 1963; Reeks 1977; Raupach, 2002; and many others), but a general formulation, for arbitrary types of particles in inhomogeneous turbulence, is probably impossible. Lightstone and Raithby (1998) proposed an empirical gradient-diffusion closure for the conservation equation governing the probability density function (pdf) for particle velocity, but its generality remains to be established. Recall that the advantage of a Lagrangian approach (trajectory-simulation) is that there is no call for assumptions relative to joint moments of tracer concentration (c) and Eulerian velocity (u_i).

Perhaps the most common heavy particle random flight model is the "eddy interaction model" (eg. Graham 1996). This explicitly resolves particle acceleration $d^2\mathbf{X}/dt^2$ (models of this character will here be called "Inertial Particle Models"), but treats the "driving" fluid velocity $\mathbf{u}(\mathbf{X}(t))$ at the location of the particle as constant across "patches" of the fluid, and as changing discontinuously from eddy to eddy. Others attempt to more-realistically account for the time-evolution of the driving fluid velocity (eg. Sawford and Guest 1991). At a less faithful level of description, one may model the stochastic particle velocity $\mathbf{U}_p$ itself directly, usually by means of a Langevin-type equation, which will require to be provided the heavy particle velocity variance, and the auto-correlation timescale (Γ_p) along the trajectory (eg. Walklate, 1987).

15.5.1 Inertial particle models

Assume rigid, non-rotating spherical particles, whose density ρ_p greatly exceeds the fluid density ρ. Then a simplified particle equation of motion can be adopted, and for the purposes of this paper it will suffice that we define the "Inertial Particle" class of particle trajectory models to have the form:

$$\begin{aligned} \frac{dU_{pi}}{dt} &= \frac{u_i(\mathbf{X}) - U_{pi}}{F(t)} - g\,\delta_{3i}\ , \\ dX_i &= U_{pi}\,dt\ . \end{aligned} \tag{15.64}$$

If the slip Reynolds number

$$R_e = \frac{d\,|\mathbf{u}(\mathbf{X}) - \mathbf{U}_p|}{\nu} \tag{15.65}$$

is small (d is particle diameter, and ν is fluid kinematic viscosity), then F is the the particle acceleration timescale

$$F = \tau_p = \frac{w_g}{g} \tag{15.66}$$

(particle inertial time constant, or Stokesian time scale) and is related to the gravtitational settling velocity (terminal velocity) w_g.

In eqn (15.64) $u_i(\mathbf{X})$ is the air velocity at the (moving) position of the particle, and the crux of the proplem is to determine a realistic sequence for it: it is neither a fluid Lagrangian nor an Eulerian (fixed point) series.

15.5.2 Heuristic driving fluid velocity for IP model

In one of the earliest heavy particle trajectory models to be developed after the provision (by Thomson 1987, and Pope 1987) of selection criteria for LS models of passive tracer dispersion, Sawford and Guest (1991) "attempted to combine the understanding of heavy particle effects gained from studies in idealised stationary homogeneous turbulence with a good model of passive scalar dispersion for more realistic flows." Treating particle motion in decaying homogeneous isotropic turbulence (an analogue for grid turbulence), Sawford and Guest commenced from the well-mixed LS model for tracer dispersion in that system,

$$dU_i = -\,U_i\,\left(\frac{1}{\Gamma} + \,\sigma^2 2\,\frac{d\sigma^{-2}}{dt}\right)\,dt + \,\sqrt{C_0\,\epsilon}\,d\xi_i \tag{15.67}$$

where $\Gamma = 2\sigma^2/(C_0\epsilon)$ and σ^2 is the Eulerian velocity variance. Sawford and Guest reasoned that correlation in fluid velocity along a heavy particle trajectory should be reduced relative to correlation along a fluid element trajectory, so, the above (generalised) Langevin equation, but with a reduced timescale, was considered to generate an appropriate driving fluid velocity for imposition in the particle equation of motion.

Taking two key particle parameters τ_p and w_g, which suffice to characterize the simplest types of particles, and two fluid turbulence parameters (σ, T_L), we have two non-dimensional ratios $(\tau_p/T_L, w_g/\sigma)$, and if we consider τ_p/T_L to be small enough, these two notional limiting cases:

(a) if $\tau_p/T_L \ll 1$ and $w_g/\sigma \ll 1$, the driving velocity correlation reduces to the fluid Lagrangian correlation, and the timescale τ_p is simply $\tau_p = T_L$.

(b) if $\tau_p/T_L \ll 1$ but $w_g/\sigma \gg 1$, the particle is essentially always falling through the fluid at its terminal velocity, ie. takes a ballistic trajectory through the eddy. If the timestep is $\Delta t(\ll T_L)$ then the particle traverses distance $w_g\Delta t$ through the eddy in each timestep, during which time the eddy velocity is essentially unchanged. Then we can estimate a temporal correlation timescale along the particle trajectory as L_E/w_g where L_E is the Eulerian lengthscale.

Following Csanady (1963), Sawford and Guest assumed the correlation timescale Γ_p along a heavy particle trajectory to be an interpolation in w_g/σ between these limiting cases:

$$\Gamma_p = \,\frac{T_L}{\sqrt{1 + \,\left(\frac{\beta\,w_g}{\sigma}\right)^2}} \tag{15.68}$$

Here $\beta = \sigma T_L / L_E$ is an empirical dimensionless constant which in principle differs, by a factor of two, for velocity components parallel and perpendicular to the external force. Sawford and Guest found that for dispersion lateral to the external force, their trajectory model was in reasonably good agreement with the laboratory experiments of Snyder and Lumley (1971) if they set $\beta = 3$. The external force ($\vec{g}$) in the atmosphere is parallel to the most important fluctuation velocity (W_p), so when Γ_p is reduced according to eqn (15.68), the constant β has in principle a value of one half that found by Sawford and Guest to be optimal for dispersion lateral to the external force, ie. for the atmosphere $\beta = 3/2$ is consistent with Sawford and Guest. However it is a very long stretch between the ideal turbulence envisaged by those authors and the atmospheric case, and there is no reason to treat β as other than a flexible parameter of order unity.

Other Inertial Particle models, that perform comparably well relative to the limited observations available, have been reported (eg. Zhuang et al. 1989, whose IP model was more complex, in that the trajectories of both the heavy particle and a driving fluid element were tracked).

15.5.3 Langevin class of particle trajectory models

Several authors (perhaps first Yudine, 1959 and earlier; Csanady, 1963; and others since) have suggested that for typical atmospheric problems, particle inertia is not very important, even (eg.) for liquid droplets of diameter as large as $d = 400\mu$m. Wilson et al. (1981b) simulated their field experiments (glass beads, $\tau_p = 0.012$ s) by tacking a gravitational settling velocity ($w_g = 0.12\,\mathrm{m\,s^{-1}}$) to a 1st-order Lagrangian stochastic model for tracer trajectories. Recent treatments of aerial spray dispersion have taken the same line, and the main distinction between them rests on whether the underlying (tracer) trajectory model respects (or otherwise) Thomson's well-mixed constraint (wmc); results of MacInnes and Bracco (1992), who examined several models not satisfying the wmc, usefully illustrate the seriousness of errors that can result. To give a few examples of these recent Langevin treatments of spray dispersion, Wang et al. (1995) adopted Thomson's two-dimensional well-mixed tracer dispersion model for a Gaussian velocity pdf, and used eqn (15.68) to specify the correlation timescale Γ_p in terms of $T_L = 2{\sigma_w}^2/(C_0\epsilon)$. Hashem and Parkin (1991) earlier had used a tracer model pre-dating the well-mixed constraint, and reduced Γ_p relative to T_L according to an equation differing from Eq. (eq:reducetimescale). Wallace et al. (1995) also used an old LS tracer model (though it may have been well-mixed), but did not reduce Γ_p.

In none of these Langevin treatments of aerial spray was the particle vertical velocity variance (σ_{wp}^2) treated as distinct from (ie. potentially smaller than) the fluid Eulerian velocity variance ${\sigma_w}^2$. On that point, while the ratio σ_{wp}/σ_w is known for some idealised cases, such as "oscillating Stokes flow" (eg. Wilson et al. 1988), in general its value is inaccessible,

and any theory fixing it implicitly has already solved the heavy particle trajectory problem. In their Langevin model for transport of evaporating ocean sprays, a model based on the Legg-Raupach (1982) LS treatment for passive tracer, Edson and Fairall (1994) reduced both σ_{wp} and Γ_p relative to their counterparts for a fluid element trajectory, invoking to that end formulae drawn from analytical studies. Essentially the same treatment was adopted by Lakehal et al. (1995) in calculations of raindrop trajectories in complex, urban windflows.

Turbophoresis

The existence of "turbophoresis" was first suggested (and the effect named) by Camparaloni et al. (1975), who reasoned that a (mean) particle mass flux can occur in conjunction with a uniform particle distribution, in response to spatial inhomogeneity of the turbulent velocity fluctuations. By "assuming that the motion of a particle under non isotropic turbulent 'shocks' is analogous to the motion of a particle under asymmetrical molecular shocks (thermophoresis) as described by Einstein," they derived a formula for the turbophoretic drift velocity. Reeks (1983) gave a more formal analysis (an approximation for the evolution of the joint probability density function for particle position and velocity), deriving a turbophoretic velocity component that is related to the spatial gradient in the particle mean-square velocity tensor (μ_{ij}),

$$U_i^{turb} = \tau_p \frac{\partial \mu_{ij}}{\partial x_j} \ . \tag{15.69}$$

Reeks cautioned, however, that "the precise form of the turbophoretic term... depends upon... the closure approximation we adopt." It is interesting to note that turbophoretic drift occurs even in the case of particles in a flow that is inhomogeneous only by virtue of a gradient in turbulence timescale, such as the (idealised) neutrally-stratified atmospheric surface layer, where, if we follow convention and overlook the "Unresolved Basal Layer" we have a system with constant velocity variance, but with timescale T_L decreasing to zero at the ground.

Reeks (1983) considers the turbophoretic term "a manifestation of the skewness in the velocity distribution of the particle." In any case, as regards selection criteria for heavy-particle trajectory models, the well-mixed condition clearly does not apply in its original sense (even in the absence of body forces). A properly formulated heavy particle trajectory model should reproduce turbophoresis – but this will presumably arise quite naturally, for a large ratio τ_p/T_L (eg. near the ground) will result in a reduced mean square particle velocity... and turbophoresis.

However if a Langevin-type model is adopted, and it is a well-mixed model (according to Thomson's criterion), then it cannot reproduce turbophoresis; for even if provided the (proper) near-ground gradient in particle velocity variance, by virtue of being a well-mixed model it will present a well-mixed state as the equilibrium condition. This objection to the Langevin class of model does not appear to be very serious, for in problems of practical

interest, only very close to ground is τ_p/T_L sufficiently small to induce turbophoresis.

15.5.4 Suffield heavy particle dispersion trials

Hage (1961) and Walker (1965) reported observations of the deposition of glass beads (mass mean diameter $d = 49, 56$ or 107μm), released continuously over durations of $30 - 60$ min, from a point source at height $h = 7.4$ or 15 m over prairie land at the Suffield Research station in southern Alberta. Fifteen such trials covered a wide range in atmospheric stratification, and for each trial micro-meteorological data are available, including the mean wind speed $\overline{u}(z)$ at heights $z = (0.5, 1, 2, 4, 8, 16)$ m, and the mean temperature difference between $z = 0.5$ m and $z = 4$ m. Surface layer scales u_*, L, z_0 can be determined for each trial.

The number-density of beads deposited (n, m^{-2}) was observed as a function of azimuth (θ) and downwind distance (x), on arcs at increasing radii up to (in some trials) a maximum of $x = 1100$ m. By attributing to each particle an identical mass M [kg], Hage and Walker constructed from $n(x, \theta)$ a normalised, crosswind-integrated mass density

$$D_0(x) = \frac{M}{Q} \int n(x, \theta)\ x\ d\theta \tag{15.70}$$

where Q [kg s^{-1}] is the source strength. Hage reported that graphical integrations (to downstream distance X from the source) for the "recovery"

$$R = \int_0^{x=X} D_0(x)\ dx \tag{15.71}$$

indicated that the fraction of released mass deposited in the measurement array ranged from $0.85 - 1.05$ (Trials 1-9), while Walker cited recoveries ranging from $0.65 - 1.00$ (Trials A-L). Observed deposition $D_0(x)$ is subject to some small degree of error due to the assignment of equal masses to all observed particles, and unless the streamwise integration for R extends adequately far downwind, i.e. unless X is sufficiently large, there is no requirement that $R = 1$. But the form of the $D_0(x)$ profiles given strongly suggests the observational array provided sufficient downwind span, and so one suspects serious experimental error (perhaps a sub-period of lateral drift carrying particles outside the array of deposition cards) in any trial for which $|R - 1|$ exceeds about 0.1, and certainly 0.2.

For the Suffield bead diffusion trials we may define a normalised travel time[3]

$$\frac{x}{\overline{u}(h)\ T_L(h)} \approx \frac{k_v\ \frac{\sigma_w}{u_*}\ x}{a\ h\ \ln\left(\frac{h}{z_0}\right)} \approx \frac{x}{h\ \ln\left(\frac{h}{z_0}\right)} \tag{15.72}$$

from the source to any downstream range (x). Taking $x = 100$ m, which is near the location of peak deposition for near-neutral trials, one finds $x/\overline{u}(h)T_L(h) \approx 1.0$. By this criterion, we

[3]Assume $T_L(z) = az/\sigma_w$ with $a \approx 0.5$.

should regard the Suffield trials as examining the "near field" of the source, within which a strong memory of the initial (release) velocity is sustained.

Wilson (2000) compared predictions of both Langevin-class and IP trajectory models against the Suffield data. Fig. (15.10a) compares observations and simulations of the along-wind profile of crosswind-integrated surface deposition rate, for the Suffield heavy particle dispersion trial C (near-neutral, $L = 341$ m). Particles ($w_g = 0.6\,\mathrm{m\,s^{-1}}, \tau_p = 0.06$ s) were released at $h = 15$ m. The Lagrangian stochastic simulations, except where indicated, were 1-dimesnional (streamwise velocity fluctuation u' neglected). In ascending order of complexity, the models of Fig. (15.10a) were

- RR, "Random Release." Particle is released with vertical velocity $W_0 - w_g$, where W_0 is a random vertical velocity from the Eulerian pdf. That (random) release velocity is sustained.
- RDM, "Random Displacement Model."
- SFE "Sticky Fluid Element." Particle behave as fluid elements, but adhere to the ground
- SSFE "Settling Sticky Fluid Element" (Langevin-class model, with added w_g)

Fig. (15.10b) gives further simulations in which

- SSFE "Settling Sticky Fluid Element" (Langevin-class, with added w_g). Same as on (a)
- SSFE + u' (alongwind fluctuation included)
- SSFET, $\beta = 2, 5$ (Langevin model with w_g, and reduced timescale along trajectory, $\Gamma_p < T_L$)
- IP, Inertial Particle model with $\beta = 2$

This work confirmed the usefulness of the simple Langevin scheme, for the calculation of an ensemble of heavy particle trajectories, released from "high" sources (large h/z_0) in the unperturbed atmospheric surface layer. The Random Displacement Model (zeroth-order LS) was shown to be clearly inferior, while the Inertial Particle model was found to be superfluous, in the sense that while more rigorous, it gave predictions equivalent to the simpler Langevin model. This work suggested that statistics of the particle concentration- and deposit- clouds will most often be calculated by a Langevin model to within an accuracy of about 20%, except near the outer fringes of the pattern.

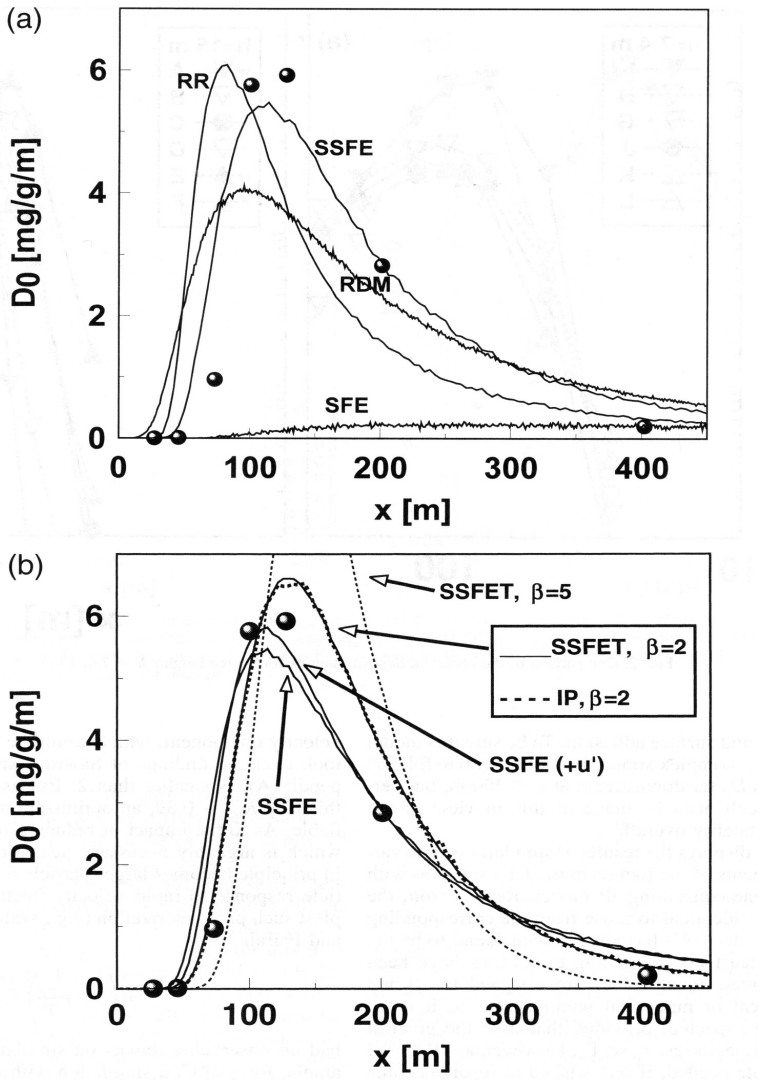


Figure 15.10: Deposition pattern of glass beads in Suffield dispersion trial "C" ($L = 341$ m). Observations (symbols) versus simulations by the various LS models described in the text.

Regarding the finding that an IP model is redundant, some qualification is needed. Very near ground, where τ_p/T_L is not small, and particle inertia reduces the particle velocity variance, trajectories ought to be calculated using an Inertial Particle model, eg. because a "turbophoretic" flux (Caporaloni et al., 1975; Reeks, 1983; Brooke et al., 1994) of particles down the near-ground gradient in particle velocity variance cannot occur in the Langevin-class model. But there is an inevitable superficiality in the treatment of wind and dispersion very near ground, within the "Unresolved Basal Layer" (UBL). Over the range of $(u_*, L, z_0, h, \tau_p, w_g)$ space covered in the Suffield experiments, the observations did not permit

to distinguish any disadvantage of the Langevin model relative to the Inertial Particle model, for calculations of practical relevance.

In the case where heavy particles trajectories intersect a tall crop canopy, uncertainties in the treatment of deposition overwhelmed nuances of the trajectory algorithm.

15.6 LS models applicable in disturbed flows

To this point we have mostly assumed the flow and turbulence to be horizontally-uniform, so that the joint pdf for the Eulerian velocity fluctuations $g_a(u', v', w'; z)$ is a function only of the height z. In a disturbed flow, $g_a = g_a(\mathbf{u}', \mathbf{x})$.

Provided an analytical description of g_a is given, it remains possible to derive a well-mixed LS model for the disturbed flow — and this is a significant advance over the Eulerian description, where any such attempt would be exceeedingly complex to implement.

Suppose that g_a remained Gaussian. Then the turbulence would be described by the velocity standard deviations ($\sigma_u = \sigma_u(x, y, z)$, etc.) and covariances like ($\overline{u'w'} = \overline{u'w'}(x, y, z)$). The LS model would involve not only vertical derivatives of flow statistics, but also the horizontal derivatives, such as $\partial\sigma_u/\partial x$, $\partial\overline{u'w'}/\partial y$ and so on.

Of course, such an LS model demands that all these flow statistics be provided — it must be "driven" by this information. It is laborious to supply such data. Measurements are presumably out of the question. The only possibility, if it must be done, is a judicious combination of a sufficient number of measurements in the disturbed flow that one can prove (establish the correctness of) a disturbed flow model, which can then be used interpolatively and extrapolatively to "procure" all the needed derivatives, which are provided to the LS model on a grid ("gridded LS model). In the case where g_a is presumed Gaussian, the flow model must provide all components of $\overline{u}$, of $\partial\overline{u}_i/\partial x_j$ and of $\partial/\partial x_k \overline{u'_i\, u'_j}$ (and in addition, the TKE dissipation rate ϵ). Examples of this approach include Wilson et al. (2009b, 2010).

Chapter 16

Lagrangian similarity theory

At the origin of Lagrangian similarity theory for dispersion in the ideal atmospheric surface layer (hh_ASL) is Batchelor's (1957, 1964) hypothesis that for a marked fluid element (with position Z and vertical velocity $W = dZ/dt$), the variable $W(t)/\sigma_w(Z(t))$ is a stationary random function of a scaled time $t/T_L(Z(t))$. Cermak (1963) built on this to suggest that for a puff released at $(t = 0, z = h)$, and provided the travel time $t \gg h/u_*$, the ensemble mean concentration $\overline{c}_{ips}$ ("ips" for instantaneous point source) obeys a self-similarity law

$$\overline{c}_{ips}(x, y, z, t) \propto \psi \left(\frac{x - \overline{x}}{\overline{z}},\ \frac{y}{\overline{z}},\ \frac{z}{\overline{z}} \right) \tag{16.1}$$

where $\psi()$ is a dimensionless function (to be determined), and $\overline{x}(t), \overline{z}(t)$ define the ensemble mean puff position (puff centroid) as function of time. Cermak suggested

$$\frac{d\overline{z}}{dt} = b\, u_* \,, \tag{16.2}$$

$$\frac{d\overline{x}}{dt} = \overline{u}(\overline{z}) \tag{16.3}$$

where b was named "Batchelor's constant". Later Eq. (16.3) was generalised to

$$\frac{d\overline{x}}{dt} = \overline{u}(\beta\ \overline{z}) \tag{16.4}$$

where β is a constant, determined below.

Starting from eqn (16.1) Cermak developed more specific formulations for instantaneous and continuous point sources, viz.

$$\overline{c}_{ips}(x, y, z, t) = \frac{Q_{ips}}{\overline{z}^3}\ \psi \left(\frac{x - \overline{x}}{\overline{z}},\ \frac{y}{\overline{z}},\ \frac{z}{\overline{z}} \right) \tag{16.5}$$

(where Q_{ips} is the mass released) and

$$\overline{c}_{cps}(x, y, z) = Q \int_0^\infty \frac{1}{\overline{z}^3}\ \psi \left(\frac{x - \overline{x}}{\overline{z}},\ \frac{y}{\overline{z}},\ \frac{z}{\overline{z}} \right)\ dt \tag{16.6}$$

where Q is the mass released per second. Using a (now) obsolete formulation for stability, Cermak compared his equations with observations.

Chatwin (1968) compared LST with a diffusion analysis for the neutral surface layer, and showed that

- $b = K_c/(u_* z)$ where K_c is the eddy diffusivity of the species concerned. Thus $b = k_{vc} = k_v/S_c$). It had earlier been suggested by Ellison (1959) that $b = k_v$ (Gifford, 1962, exploited LST following Ellison in order to model the Project Prairie Grass trials)
- $\beta = 0.562$

Pasquill (1966; see also Pasquill 1974 or Pasquill and Smith 1983) concluded that the Project Prairie Grass data indicate the effects of stratification are more severe than is implied by the Cermak formulation. Chaudhry and Meroney (1973) repeated Chatwin's analysis, but with MOST corrections to the profiles $\overline{u}(z), K_c(z)$, and concluded it was acceptable to write

$$\begin{aligned} \frac{d\overline{z}}{dt} &= \frac{k_v\, u_*}{\phi_h\left(\frac{\overline{z}}{L}\right)}\,, \\ \frac{d\overline{x}}{dt} &= \overline{u}(\overline{z})\,, \end{aligned} \tag{16.7}$$

(i.e. $\beta = 1$ "is reasonable when considering diffusion at large distances").

Horst (1979) developed LST further, starting from

$$\begin{aligned} \frac{d\overline{z}}{dt} &= \frac{k_v\, u_*}{\phi_h\left(\frac{\overline{z}}{L}\right)}\,, \\ \frac{d\overline{x}}{dt} &= \overline{u}(\beta\,\overline{z})\,, \end{aligned} \tag{16.8}$$

with β regarded potentially as a function of $\overline{x}$. Integrating the second of eqns. (16.8) one has:

$$\overline{x} = \frac{1}{k_v}\int_{z_0}^{\overline{z}} \frac{\overline{u}(\beta\, z)}{u_*}\,\phi_h\left(\frac{z}{L}\right)\,dz \tag{16.9}$$

which relates $\overline{x}$ to $\overline{z}$.

Horst assumes a functional form for crosswind integrated concentration:

$$\chi(x,z) = \chi_0(x)\exp\left[-\left(\frac{z}{c_2\,\overline{z}}\right)^s\right] \tag{16.10}$$

where $s = 1.5$ is satisfactory. Accepting that value, then from the definition

$$\overline{z} = \frac{\int_0^\infty z\,\chi(x,z)\,dz}{\int_0^\infty \chi(x,z)\,dz} \tag{16.11}$$

it follows that $c_2 = 1.51$. Next, the centroid advection velocity is determined as:

$$\overline{u}(\beta\,\overline{z}) = \frac{\int_0^\infty \overline{u}(z)\,\chi(x,z)\,dz}{\int_0^\infty \chi(x,z)\,dz} \tag{16.12}$$

from which one can deduce (needs correction: c_3 is not defined – find my notes — may be with my hard copy of Horst 1979?) that

$$\frac{k_v\ \overline{u}(\beta\ \overline{z})}{u_*} = \frac{k_v\ Q}{u_*\ \chi_0(x)}\ \frac{1}{\overline{z}(x)\ \frac{c_3}{c_2\Gamma(1/c_3)}}\ . \tag{16.13}$$

Finally, the constraint

$$\int_0^\infty\ \overline{u}(z)\ \chi(x,z)\ dz\ =\ Q \tag{16.14}$$

leads to the equation

$$\frac{\chi_0(x)\ u_*}{k_v\ Q} = \int_{z_0}^{\infty} e^{-\left(\frac{z}{c_2\ \overline{z}}\right)^{c_3}}\ \frac{k_v\ \overline{u}(z)}{u_*}\ dz\ . \tag{16.15}$$

To evaluate the solution $\chi(x,z)$ for given (u_*, z_0, L, Q) one begins by specifying a value for $x = \overline{x}$: then an iteration is necessary. Here are the essentials of the algorithm:

1. Guess β
2. solve eqn(16.8) for $\overline{z}$
3. evaluate $\frac{\chi_0\ u_*}{k_v Q}$ using eqn(16.15)
4. Calculate $N = \frac{k_v\ \overline{u}(\beta\ \overline{z})}{u_*}$ using eqn(16.13)
5. compare this value against $N^* = \left[\ln\left(\frac{\beta\ \overline{z}}{z_0}\right) -\ \psi_m\left(\frac{\beta\ (\overline{z}-z_0)}{L}\right)\right]$
6. loop through guesses in β to minimise $|N - N^*|$

Horst's solution is closely related to that of Van Ulden (1978). Van Ulden noted that if the wind and diffusivity profiles are approximated as power-law functions[1]:

$$\begin{aligned} u(z) &= u_H\left(\frac{z}{H}\right)^m \\ K(z) &= K_H\left(\frac{z}{H}\right)^n \end{aligned}$$

then for a line source (strength Q) near ground the advection-diffusion equation for crosswind-integrated concentration

$$u(z)\ \frac{\partial\chi}{\partial x} = \frac{\partial}{\partial z}\ \left(K\ \frac{\partial\chi}{\partial z}\right) \tag{16.16}$$

has the solution

$$\frac{\chi(x,z)}{Q} = \frac{A}{\overline{z}(x)\ \overline{u}(x)}\ \exp\left[-\left(\frac{B\ z}{\overline{z}}\right)^s\right]\ , \tag{16.17}$$

[1]Here the overbar has been dropped so as to avoid confusion with the overbars introduced below, for the plume-averaged variables.

where constants A, B depend only on s, and $\overline{z}(x), \overline{u}(x)$ are defined by

$$\begin{aligned} \overline{z} &= \frac{\int_0^\infty z\, \chi(x,z)\, dz}{\int_0^\infty \chi(x,z)\, dz} \\ \overline{u} &= \frac{\int_0^\infty u(z)\, \chi(x,z)\, dz}{\int_0^\infty \chi(x,z)\, dz} \end{aligned} \tag{16.18}$$

which are essentially equations (16.11, 16.12). Horst's parameter β is defined by the equation $\overline{u}(x) = u(\beta z)$ for the effective height at which the velocity advecting the (local) plume applies.

The surface-layer dispersion solution developed in this section is tied strictly to the undisturbed case where MOST applies, but it is both interesting (for the creativity it exhibits) and lastingly useful — even though by virtue of our computers we now have the facility to easily solve the underlying Eulerian mass conservation equation(s), or can even more easily address dispersion problems using the Lagrangian stochastic method. Kormann and Meixner (2001) have developed the LST solution into an analytical formulation for the flux footprint. Note that Lagrangian similarity theory has built-in flexibility, in the sense that it can be (and has been) tuned to observations, by optimizing β, S_c and the choice of the puff shape function ψ.

Bibliography

Abdella, K., & McFarlane, N. 1997. A New Second-Order Turbulence Closure Scheme for the Planetary Boundary Layer. *J Atmos Sci*, **54**, 1850–1867.

Adrian, R.J., Meinhart, C.D., & Tompkins, C.D. 2000. Vortex Organization in the Outer Region of the Turbulent Boundary Layer. *J Fluid Mech*, **422**, 1–54.

Agee, E.M., & Sheu, P.J. 1978. MCC and Gull Flight Behaviour. *Boundary-Layer Meteorol*, **14**, 247–251.

Amiro, B.D. 1990. Comparison of Turbulence Statistics Within Three Boreal Forest Canopies. *Boundary-Layer Meteorol*, **51**, 99–121.

André, J.C., Moor, G. De, Lacarrere, P., Therry, G., & Vachat, R. Du. 1978. Modeling the 24-Hour Evolution of the Mean and Turbulent Structures of the Planetary Boundary Layer. *J Atmos Sci*, **35**, 1861–1883.

Anthes, R.A. 1977. A Cumulus Parameterization Scheme Utilizing a One-Dimensional Model. *Mon Weather Rev*, **105**, 270–286.

Antonia, R.A., Chambers, A.J., Friehe, C.A., & Van Atta, C.W. 1979. Temperature Ramps in the Atmospheric Surface Layer. *J Atmos Sci*, **36**, 99–108.

Aris, R. 1989. *Vectors, tensors, and the basic equations of fluid mechanics*. Dover.

Arya, S. Pal. 1988. *Introduction to Micrometeorology*. Academic Press.

Baerentsen, J.H., & Berkowicz, R. 1984. Monte Carlo Simulation of Plume Dispersion in the Convective Boundary Layer. *Atmos. Env.*, **18**, 701–712.

Baines, W. D., & Peterson, E. G. 1951. An Investigation of Flow Through Screens. *Trans ASME*, **Vol. 73**, 467–480.

Barad, M.L. 1958. *Project Prairie Grass, a Field Program in Diffusion (Vol. 2)*. Tech. rept. Geophysical Research Papers No. 59, TR-58-235(II). Air Force Cambridge Research Center.

Batchelor, G.K. 1957. Diffusion in Free Turbulent Shear Flows. *J Fluid Mech*, **3**, 67–80.

Batchelor, G.K. 1964. Diffusion from Sources in a Turbulent Boundary Layer. *Archiwum Mechaniki Stosowanej*, **3**, 661–670.

Batchelor, G.K. 1985. *An Introduction to Fluid Dynamics*. Cambridge University Press.

Bergstrom, Hans. 1986. A Simplified Boundary Layer Wind Model for Practical Application. *American Meteorological Society*, **Vol. 25**, 813–824.

Bink, N.J. 1996. *The structure of the atmospheric surface layer subject to local advection Ph.D. thesis*. Wageningen Agricultural University, 206 pp. ISBN 90-5485-513-4.

Bird, R.B., Stewart, W.E., & Lightfoot, E.N. 1960. *Transport Phenomena*. John Wiley and Sons.

Blanken, P.D., Black, T.A., Neumann, H.H., Hartog, G. Den, Yang, P. C., Nesic, Z., Staebler, R., Chen, W., & Novak, M. D. 1998. Turbulent Flux Measurements Above and Below the Overstory of a Boreal Aspen Forest. *Boundary-Layer Meteorol*, **89**, 109–140.

Boughton, B.A., Delaurentis, J.M., & Dunn, W.E. 1987. A Stochastic Model of Particle Dispersion in the Atmosphere. *Boundary-Layer Meteorol*, **40**, 147–163.

Bourdin, P., & Wilson, J.D. 2008. Windbreak Aerodynamics: Is CFD Reliable? *Boundary-Layer Meteorol*, **126**, 181–208.

Bradley, E.F., & Mulhearn, P.J. 1983. Development of velocity and shear stress distribution in the wake of a porous shelter fence. *J. Wind Eng. Indust. Aero.*, **15**, 145–156.

Bradshaw, P. 1973. *Effects of Streamline Curvature on Turbulent Flow*. Tech. rept. 169. North Atlantic Treaty Organization Advisory Group for Aerospace Research and Development.

Bradshaw, P. 1978. *Introduction*. Topics in Applied Physics. Springer-Verlag. 339pp. Chap. 1, pages 1–44.

Bridgman, P.W. 1922. *Dimensional analysis*.

Brunet, Y., & Irvine, M.R. 2000. The Control of Coherent Eddies in Vegetation Canopies: Streamwise Structure Spacing, Canopy Shear Scale and Atmospheric Stability. *Boundary-Layer Meteorol*, **94**, 139–163.

Brunet, Y., Finnigan, J.J., & Raupach, M.R. 1994. A Wind Tunnel Study of Air Flow in Waving Wheat: Single-Point Velocity Statistics. *Boundary-Layer Meteorol*, **70**, 95–132.

Buckingham, E. 1914. On Physically Similar Systems: Illustrations of the Use of Dimensional Equations. *Phys. Rev.*, **4**, 345–376.

Businger, J. A., Wyngaard, J. C., Izumi, Y., & Bradley, E. F. 1971. Flux-Profile Relationships in the Atmospheric Surface Layer. *J Atmos Sci*, **28**, 181–189.

Businger, J.A. 1984. *Equations and Concepts*. D. Reidel Publ. Co.

Calder, K. L. 1968. In Clarification of the Equations of Shallow-Layer Thermal Convection for a Compressible Fluid Based on the Boussinesq Approximation. *QJRMS*, **Vol. 94**, 88–92.

Caporaloni, M., Tampieri, F., Trombetti, F., & Vittori, O. 1975. Transfer of particles in nonisotropic air turbulence. *J. Atmos. Sci.*, **32**, 565–568.

Carson, D.J., & Smith, F.B. 1974. Thermodynamic Model for the Development of a Convectively Unstable Boundary Layer. *Adv. Geophys.*, **18A**, 111–124.

Caughey, S. J. 1977. Boundary-Layer Turbulence Spectra in Stable Conditions. *Boundary-Layer Meteorol*, **11**, 3–14.

Cermak, J.E. 1963. Lagrangian similarity hypothesis applied to diffusion in turbulent shear flow. *J. Fluid Mech.*, **15**, 49–64.

Charuchittipan, D., & Wilson, J.D. 2009. Turbulent Kinetic Energy Dissipation in the Surface Layer. *Boundary-Layer Meteorol*, **132**, 193–204.

Chatwin, P.C. 1968. The dispersion of a puff of passive contaminant in the constant stress region. *.J.R. Met. Soc.*, **94**, 350–360.

Chaudhry, F.H., & Meroney, R.N. 1973. Similarity Theory of Diffusion and the Observed Vertical Spread in the Diabatic Surface Layer. *Boundary-Layer Meteorol*, **3**, 405–415.

Chou, P.Y. 1945. On Velocity Correlations and the Solutions of the Equations of Turbulent Fluctuation. *Quarterly of Applied Math.*, **3**, 38–54.

Christensen, K. T., & Adrian, R. J. 2001. Statistical Evidence of Hairpin Vortex Packets in Wall Turbulence. *J Fluid Mech*, **431**, 433–443.

Clarke, R.H., Dyer, A.J., Brook, R.R., Reid, D.G., & Troup, A.J. 1971. *The Wangara Experiment: Boundary Layer Data*. Tech. rept. 19. Commonwealth Scientific and Industrial Research Organization. 362pp.

Coppin, P.A., Raupach, M.R., & Legg, B.J. 1986. Experiments on Scalar Dispersion Within a Model Plant Canopy, Part II: An Elevated Plane Source. *Boundary-Layer Meteorol*, **35**, 167–191.

Corrsin, S. 1974. Limitations of Gradient Transport Models. *Adv. Geophys.*, **18A**, 25–60.

Counihan, J., Hunt, J. C. R., & Jackson, P. S. 1974. Wakes Behind Two-Dimensional Surface Obstacles in Turbulent Boundary Layers. *J Fluid Mech*, **64**, 529–563.

Cowan, I.R. 1968. Mass, Heat and Momentum Exchange Between Stands of Plants and Their Atmospheric Environment. *Q.J.R. Meteorol. Soc.*, **94**, 523–544.

Craft, T.J., Launder, B.E., & Suga, K. 1996. Development and application of a cubic eddy-viscosity model of turbulence. *Int J Heat Fluid Flow*, **17**, 108–115.

Csanady, G. T. 1963. Turbulent Diffusion of Heavy Particles in the Atmosphere. *Journal of the Atmos. Sciences*, **Vol. 20**, 201–208.

D. Lakehal, P.G. Mestayer J. B. Edson S. Anquetin, & Sini, J. F. 1995. Eulero-Langrangian Simulation of Raindrop, Trajectories and Impacts Within the Urban Canopy. *Atmos. Environ.*, **Vol. 29 ,NO. 23**, 3501–3517.

De Bruin, H.A.R., Bink, N.J., & Kroon, L.J.M. 1991. *Fluxes in the Surface Layer under Advective Conditions*. Springer-Verlag. Chap. 9, pages 157–169.

Delage, Y. 1974. A Numerical Study of the Nocturnal Atmospheric Boundary Layer. *Q J R Meteorol Soc*, **100**, 351–364.

Denmead, O.T., & Bradley, E.F. 1985. Flux-gradient relationships in a forest canopy. *Pages 421–442 of:* Hutchison, B.A., & Hicks, B.B. (eds), *The forest-atmosphere interaction*. D. Reidel Pub. Co. 708pp.

Drazin, P.G., & Reid, W.H. 2004. *Hydrodynamic Stability*. 2 edn. Cambridge Mathematical Library.

Drobinski, P., Brown, R.A., Flamant, P.H., & Pelon, J. 1998. Evidence of Organized Large Eddies by Ground-Based Doppler Lidar, Sonic Anemometer and Sodar. *Boundary-Layer Meteorol*, **88**, 343–361.

Du, S., Wilson, J.D., & Yee, E. 1994. Probability Density Functions for Velocity in the Convective Boundary Layer, and Implied Trajectory Models. *Atmos. Environ.*, **28**, 1211–1217.

Du, S., Sawford, B.L., Wilson, J.D., & Wilson, D.J. 1995. Estimation of the Kolmogorov Constant (C_0) for the Lagrangian Structure Function, Using a Second-Order Lagrangian Model of Grid Turbulence. *Phys. Fluids*, **7**, 3083–3090.

Durst, F., & Rasogi, A.K. 1980. *Turbulent flows over two-dimensional fences*. Turbulent Shear Flows, vol. 2 Selected papers from the 2nd. Int'l Symp. on Turbulent shear flows, London, 1979. Springer-Verlag, Berlin.

Dyer, A. J. 1962. The Adjustment of Profiles and Eddy Fluxes. *Quart. J. Roy. Meteorol. Soc.*, **89**, 276–280.

Dyer, A. J., & Hicks, B. B. 1967. The Fluxatron-A Revised Approach to the Measurement of Eddy Fluxes in the Lower Atmosphere. *Journal of Applied Meteorology*, **6**(2), 408–413.

Dyer, A.J., & Bradley, E.F. 1982. An Alternative Analysis of Flux-Gradient Relationships at the 1976 ITCE. *Boundary-Layer Meteorol*, **22**, 3–19.

Dyer, A.J., & Pruitt, W.O. 1962. Eddy-Flux Measurements over a Small, Irrigated Area. *J Appl Meteorol*, **1**, 471–473.

Dyer, A.J., Hicks, B.B., & King, K.M. 1967. The fluxatron – a revised approach to the measurement of eddy fluxes in the lower atmosphere. *J. Appl. Meteorol.*, **6**, 408–413.

Edson, J.B., & Fairall, C.W. 1994. Spray droplet modelling. Part 1: Lagrangian model simulation of the turbulent transport of evaporating droplets. *J. Geophys. Res.*, **99**, 25295–25311.

Elliott, W.P. 1961. The Vertical Diffusion of Gas from a Continuous Source. *Int J Air and Water poll.*, **4**, 33–46.

Ellison, T. H. 1959. Meteorology. *Science Progress*, **47**, 495–506.

Emanuel, K.A. 1994. *Atmospheric Convection*. Oxford University Press.

et Al., Wofsy. 1988. Carbon Dioxide in the Atmosphere over the Amazon Basin. *J Geophys Res*, **93**, 1377–1387.

Etling, D., & Brown, R.A. 1993. Roll Vortices in the Planetary Boundary Layer: A Review. *Boundary-Layer Meteorol*, **65**, 215–248.

Finnigan, J.J. 1979. Turbulence in Waving Wheat. I Mean Statistics and Honami. *Boundary-Layer Meteorol*, **16**, 181–211.

Finnigan, J.J. 1985. Turbulent transport in flexible plant canopies. *Pages 443 – 480 of:* Hutchison, B.A., & Hicks, B.B. (eds), *The forest-atmosphere interaction*. D. Reidel Pub. Co.

Finnigan, J.J. 2000. Turbulence in plant canopies. *Ann. Rev. Fluid Mech.*, **32**, 519–571.

Finnigan, J.J., & Brunet, Y. 1995. *Wind and Trees*. Cambridge University Press, UK. Chap. Turbulent Airflow in Forests on Flat and Hilly Terrain, pages 3–40.

Finnigan, J.J., Shaw, R.H., & Patton, E.G. 2009. Turbulence structure above a vegetation canopy. *J. Fluid Mech.*, **637**, 387–424.

Flesch, T. K., Wilson, J. D., & Harper, L. A. 2005a. Deducing Ground-to-Air Emissions from Observed Trace Gas Concentrations: A Field Trial with Wind Disturbance. *J Appl Meteorol*, **44**, 475–484.

Flesch, T.K. 1996. The Footprint for Flux Measurements, from Backward Lagrangian Stochastic Models. *Boundary-Layer Meteorol.*, **78**, 399–404.

Flesch, T.K., & Wilson, J.D. 1992. A Two-Dimensional Trajectory-Simulation Model for Non-Gaussian, Inhomogeneous Turbulence Within Plant Canopies. *Boundary-Layer Meteorol*, **61**, 349–374.

Flesch, T.K., Wilson, J.D., & Yee, E. 1995. Backward-Time Lagrangian Stochastic Dispersion Models, and their Application to Estimate Gaseous Emissions. *J Appl Meteorol*, **34**, 1320–1332.

Flesch, T.K., Wilson, J.D., Harper, L.A., Crenna, B.P., & Sharpe, R.R. 2004. Deducing Ground-Air Emissions from Observed Trace Gas Concentrations: A Field Trial. *J Appl Meteorol*, **43**, 487–502.

Flesch, T.K., Wilson, J.D., Harper, L.A., & Crenna, B.P. 2005b. Estimating Gas Emission from a Farm Using an Inverse-Dispersion Technique. *Atmos. Environ.*, **39**, 4863–4874.

Flesch, T.K., Wilson, J.D., Harper, L.A., Todd, R.W., & Cole, N.A. 2007. Determining Ammonia Emissions from a Cattle Feedlot with an Inverse Dispersion Technique. *Agric. Forest Meteorol.*, **144**, 139–155.

Flesch, T.K., Harper, L.A., Powell, J. M., & Wilson, J.D. 2009. Inverse-Dispersion Calculation of Ammonia Emissions from Wisconsin Dairy Farms. *Trans. ASABE*, **52**, 253 – 265. Submitted Sept. 2008.

Foken, T. 2006. 50 Years of the Monin-Obukhov Similarity Theory. *Boundary-Layer Meteorol*, **119**, 431–447.

Francey, R.J., & Garratt, J.R. 1981. Interpretation of flux-profile observations at ITCE (1976). *J. Appl. Meteorol.*, **20**, 603–618.

Frisch, U. 1995. *Turbulence : The Legacy of A. N. Kolmogorov*. Cambridge University Press.

Fritschen, L.J., & van Bavel, C.H.M. 1963. Micrometeorological data handling system. *J. Appl. Meteorol.*, **2**, 151–155.

Fuehrer, P.L., & Friehe, C.A. 2002. Flux Corrections Revisited. *Boundary-Layer Meteorol*, **102**, 415–457.

Gao, W., & Shaw, R.H. 1989. Observation of Organized Structure in Turbulent Flow Within and Above a Forest Canopy. *Boundary-Layer Meteorol*, **47**, 349–377.

Gardiner, C.W. 2004. *Handbook of Stochastic Methods for Physics, Chemistry and the Natural Sciences*. Third edn. Springer Series in Synergetics. Springer.

Garratt, J.R. 1990. The Internal Boundary Layer - a Review. *Boundary-Layer Meteorol*, **50**, 171–203.

Garratt, J.R. 1992. *The Atmospheric Boundary Layer*. Cambridge University Press. 316pp.

Garratt, J.R., Wyngaard, J.C., & Francey, R.J. 1982. Winds in the Atmospheric Boundary Layer - Prediction and Observation. *J Atmos Sci*, **39**, 1307–1316.

Gifford, F. A. 1962. Diffusion in the Diabatic Surface Layer. *J. Geophys. research*, **67**, 3207–3212.

Gill, G.C. 1982. Comments on "A Revaluation of the Kansas Mast Influence on Measurements of Stress and Cup Anemometer Overspeeding". *J Appl Meteorol*, **21**, 437–440.

Gosman, A.D. 1999. Developments in CFD for industrial and environmental applications in wind engineering. *J. Wind Eng. Indust. Aero.*, **81**, 21–39.

Graham, D. I. 1996. An Improved Eddy Interaction Model for Numerical Simulation of Turbulent Particle Dispersion. *Journal of Fluids Engineering*, **Vol. 118**, 819–823.

Graham, J. M. R. 1976. Turbulent Flow Past a Porous Plate. *J Fluid Mech*, **73**, 565–591.

Gryning, S.-E., Van Ulden, AAD P, & Larsen, S.E. 1983. Dispersion from a continuous ground-level source investigated by a K model. *Quart. J. R. Meteorol. Soc.*, **109**, 355–364.

Gu, L., *et al.* 2012. The fundamental equation of eddy covariance and its application in flux measurements. *Agric. For. Meteorol.*, **152**, 135–148.

Ha, K.-J., & Mahrt, L. 2003. Radiative and Turbulent Fluxes in the Nocturnal Boundary Layer. *Tellus A*, **55**, 317–327.

Hage, K.D. 1961. On the Dispersion of Large Particles from a 15 m Source in the Atmosphere. *J. Meteorol.*, **18**, 534–539.

Hagen, L. J., Skidmore, E. L., Miller, P. L., & Kipp, J. E. 1981. Simulation of Effect of Wind Barriers on Airflow. *Transactions of the ASAE*, 1002–1008.

Halstead, M.H., Richman, R.L., Covey, W., & Merryman, J.D. 1957. A Preliminary Report on the Design of a Computer for Micrometeorology. *J. Meteorology*, **14**, 308–325.

Hanjalic, K., & Launder, B.E. 1972. A Reynolds stress model of turbulence and its application to thin shear flows. *J Fluid Mech*, **52**, 609–638.

Hanley, D.P., & Kuhn, G. 2003. *Trees Against the Wind*. Tech. rept. PNW0005. Pacific Northwest Extension, Washington State University.

Harman, I.N., & Finnigan, J.J. 2008. Scalar Concentration Profiles in the Canopy and Roughness Sublayer. *Boundary-Layer Meteorol.*, **129**, 323–351.

Hashem, A., & Parkin, C. S. 1991. A Simplified Heavy Particle Random-Walk Model for the Prediction of Drift from Agricultural Sprays. *Atmos. Env.*, **Vol. 25A**, 1609–1614.

Hassid, S., & Galperin, B. 1983. A Turbulent Energy Model for Geophysical Flows. *Boundary-Layer Meteorol*, **26**, 397–412.

Haugen, D.A. 1959. *Project Prairie Grass, a Field Program in Diffusion (Vol. 3)*. Tech. rept. Geophysical Research Papers No. 59, TR-58-235(III). Air Force Cambridge Research Center.

Heisler, G.M., & Dewalle, D.R. 1988. Effects of Windbreak Structure on Wind Flow. *Agriculture, Ecosystems and Environment*, **22/23**, 41–69.

Hess, G.D., Hicks, B.B., & Yamada, T. 1981. The impact of the Wangara Experiment. *Boundary-Layer Meteorol*, **20**, 135–174.

Hicks, B. B. 1985. Behavior of Turbulence Statistics in the Convective Boundary Layer. *J. Clim. Appl. Meteorol.*, **24**, 607–614.

Hicks, B.B. 1976. Wind Profile Relationships from the 'Wangara' Experiment. *Q J R Meteorol Soc*, **102**, 535–551.

Hicks, B.B. 1981. *An Analysis of Wangara Micrometeorology: Surface Stress, Sensible Heat, Evaporation and Dewfall*. Tech. rept. NOAA Technical Memorandum ERL ARL-104. NOAA Air Resources Laboratories.

Hinze, J.O. 1975. *Turbulence*. 2nd edn. McGraw-Hill.

Hogstrom, U. 1985. Von Karman's Constant in Atmospheric Boundary Layer Flow: Reevaluated. *J Atmos Sci*, **42**, 263–270.

Hojstrup, J. 1982. Velocity Spectra in the Unstable Planetary Boundary Layer. *J Atmos Sci*, **39**, 2239–2248.

Holland, J.Z. 1989. On Pressure-Driven Wind in Deep Forests. *J Appl Meteorol*, **28**, 1349–1355.

Hommema, S.E., & Adrian, R.J. 2003. Packet Structure of Surface Eddies in the Atmospheric Boundary Layer. *Boundary-Layer Meteorol*, **106**, 147–170. see also a conference note Keith sent me, files as 1121; I have the pdf file saved as "smokeviz_asl.pdf" and as hommema_adrian01.pdf.

Horst, T. W., & Weil, J. C. 1994. How Far is Far Enough? The Fetch Requirements for Micrometeorological Measurement of Surface Fluxes. *J. Atmos. Ocean. Technol.*, **11**, 1018–1025.

Horst, Thomas W. 1979. Lagrangian Similarity Modeling of Vertical Diffusion from a Ground-Level Source. *J Appl Meteorol*, **18**, 733–740.

Horst, T.W. 2000. On Frequency Response Corrections for Eddy Covariance Flux Measurements. *Boundary-Layer Meteorol*, **94**, 517–520.

Hsieh, C.-I., Katul, G., & Chi, T. 2000. An Approximate Analytical Model for Footprint Estimation of Scalar Fluxes in Thermally Stratified Atmospheric Flows. *Adv. Water Resources*, **23**, 765–772.

Huang, C.H. 1979. A Theory of Dispersion in Turbulent Shear Flow. *Atmos. Environ.*, **13**, 453–463.

Huang, J., Lee, X., & Patton, E.G. 2008. A Modelling Study of Flux Imbalance and the Influence of Entrainment in the Convective Boundary Layer. *Boundary-Layer Meteorol*, **127**, 273–292.

Itier, B., & Perrier, A. 1976. Presentation D'Une Etude Analytique de L'Advection. *Ann. Agron.*, **27**(2), 111–140.

Izumi, Y., & Caughey, J.S. 1976. Minnesota 1973 Atmospheric Boundary Layer Experiment Data Report. *Environmental Research Papers*, **547**.

Jarvis, P.G., & McNaughton, K.G. 1986. Stomatal Control of Transpiration: Scaling Up from Leaf to Region. *Adv. Ecol. Res.*, **15**, 1–49.

John W. Brooke, T. J. Hanratty J.B. McLaughlin. 1994. Free-Flight Mixing and Deposition of Aerosols. *Phys. Fluids.*, **Vol. 6, No. 10**, 3404–3415.

Judd, M.J., Raupach, M.R., & Finnigan, J.J. 1996. A wind tunnel study of turbulent flow around a single and multiple windbreaks; Part 1: Velocity fields. *Boundary-Layer Meteorol*, **80**, 127–165.

Kaimal, J. C. 1973. Turbulence Spectra, Length Scales and Structure Parameters in the Stable Surface Layer. *Boundary-Layer Meteorol*, **4**, 289–309.

Kaimal, J.C. 1978. Horizontal Velocity Spectra in an Unstable Surface Layer. *J Atmos Sci*, **35**, 18–24.

Kaimal, J.C., Wyngaard, J.C., Izumi, Y., & Coté, O.R. 1972. Spectral Characteristics of Surface-Layer Turbulence. *Quart. J. Roy. Meteorol. Soc.*, **98**, 563–589.

Kaimal, J.C., Clifford, S.F., & Lataitis, R.J. 1989. Effect of Finite Sampling on Atmospheric Spectra. *Boundary-Layer Meteorol*, **47**, 337–347.

Kaiser, H. 1959. Die Stromung an Windshutzstreifen The airflow through shelterbelts. *Berichte Deutscher Wetterdienstes*.

Kanak, K. 2005. Numerical Simulation of Dust Devil-Scale Vortices. *Q. J. R. Meteorol. Soc.*, **131**, 1271–1292.

Kanak, Katharine M., Lilly, Douglas K., & Snow, John T. 2000. The Formation of Vertical Vorticies in the Convective Boundary Layer. *Quart. J. Roy. Meteorol. Soc.*, **126**, 2789–2810.

Kato, C., Yamade, Y., Wang, H., Guo, Y., Miyazawa, M., Takaishi, T., Yoshimura, S., & Takano, Y. 2006. Numerical Prediction of Sound Generated from Flows with a Low Mach Number. *Computers and Fluids*, **36**, 53–68. Numerical computations of sound generated from flows with a low Mach number are presented based on Lighthill's acoustic analogy with an assumption that sound does not alter the flow field from which it is generated... The method is applied to the prediction of ... far-field sound generated from flow around a bluff body... computed frequency spectra of the sound show a fairly good agreement with the measured spectra.

Kljun, N., Calanca, P., Rotach, M., & Schmid, H. 2004. A Simple Parameterisation for Flux Footprint Predictions. *Boundary-Layer Meteorology*, **112**, 503–523.

Klug, W. 1968. Diffusion in the Atmospheric Surface Layer: Comparison of Similarity Theory with Observations. *Quart. J. Roy. Meteorol. Soc.*, **94**, 555–562.

Koprov, B. M., Zubkovsky, S. L., Koprov, V. M., Fortus, M. I., & Makarova, T. I. 1998. Statistics of Air Temperature Spatial Variability in the Atmospheric Surface Layer. *Boundary-Layer Meteorol*, **88**, 399–423.

Kormann, R., & Meixner, F.X. 2001. An Analytical Footprint Model for Non-Neutral Stratification. *Boundary-Layer Meteorol.*, **99**, 207–224.

Lang, A. R. G., Evans, G. N., & Ho, P. Y. 1974. The Influence of Local Advection of Evapotranspiration from Irrigated Rice in a Semi-Arid Region. *Agricultural Meteorology*, **13**, 5–13.

Lang, A. R. G., McNaughton, K. G., Fazu, Chen, Bradley, E. F., & Ohtaki, E. 1983. An Experimental Appraisal of the Terms in the Heat and Moisture Flux Equations for Local Advection. *Boundary-Layer Meteorol*, **25**, 89–102.

Langhaar, H.L. 1951. *Dimensional analysis and theory of models.*

Laubach, J., & Fritsch, H. 2002. Convective Boundary Layer Budgets Derived from Aircraft Data. *Agric. For. Meteorol.*, **111**, 237–263.

Laubach, J., & McNaughton, K.G. 1998. A Spectrum-Independent Method for Correcting Eddy Flux Measurements with Separated Sensors. *Boundary-Layer Meteorol*, **89**, 445–467.

Launder, B. E., Reece, G. J., & Rodi, W. 1975. Progress in the Development of a Reynolds-Stress Turbulence Closure. *J. Fluid Mech*, **68**, 537–566.

Laws, E.M., & Livesey, J.L. 1978. Flow Through Screens. *Ann. Rev. Fluid Mech.*, **10**, 247–266.

Leclerc, M. Y., & Thurtell, G. W. 1990. Footprint prediction of scalar fluxes using a Markovian analysis. *Boundary-Layer Meteorol.*, **52**, 247–258.

Lee, S.-J., Lim, H.-C., & Kim, H.-G. 2001. A numerical study on flow around a triangular prism located behind a porous fence. *Fluid Dynamic Research*, **28**.

Lee, X., & Massman, W.J. 2011. A Perspective on Thirty Years of the Webb, Pearman and Leuning Density Corrections. *Boundary-Layer Meteorol*, **139**, 37–59.

Legg, B.J., & Long, I.F. 1975. Turbulent Diffusion Within a Wheat Canopy:II. Results and Interpretation. *Quart. J. Roy. Meteorol. Soc.*, **101**, 611–628.

Legg, B.J., & Raupach, M.R. 1982. Markov-Chain Simulation of Particle Dispersion in Inhomogeneous Flows: The Mean Drift Velocity Induced by a Gradient in Eulerian Velocity Variance. *Boundary-Layer Meteorol*, **24**, 3–13.

Legg, B.J., Raupach, M.R., & Coppin, P.A. 1986. Experiments on Scalar Dispersion Within a Model Plant Canopy, Part III: An Elevated Line Source. *Boundary-Layer Meteorol*, **35**, 277–302.

Lemons, D.S. 2002. *An Introduction to Stochastic Processes in Physics.* John Hopkins University Press.

Lenschow, D.H., & Stephens, P.L. 1980. The Role of Thermals in the Convective Boundary Layer. *Boundary-Layer Meteorol*, **19**, 509–532.

Lettau, H. 1954. Notes on the transformation of mechanical energy from and to eddying motion. *J. Meteorol.*, **11**, 196–201.

Leuning, R., Dunin, F.X., & Wang, Y.P. 1998. A Two-Leaf Model for Canopy Conductance, Photosynthesis and Partitioning of Available Energy. II. Comparison with measurements. *Agric. Forest Meteorol.*, **91**, 113–125.

Lighthill, M.J. 1952. On Sound Generated Aerodynamically. I. General Theory. *Proc. R. Soc. Lond.*, **A211**, 564–587.

Lightstone, M. F., & Raithby, G. D. 1998. A Stochastic Model of Particle Dispersion in a Turbulent Gaseous Environment. *Combustion and Flame*, **Vol. 113**, 424–441.

Lim, W.H., *et al.* 2012. The aerodynamics of pan evaporation. *Agric. For. Meteorol.*, **152**, 31–43.

Liu, W.T., & Businger, J.A. 1975. Temperature Profile in the Molecular Sublayer Near the Interface of a Fluid in Turbulent Motion. *Geophys. Res. Letters*, **2**, 403–404.

Liu, W.T., Katsaros, K.B., & Businger, J.A. 1979. Bulk Parameterization of Air-Sea Exchanges of Heat and Water Vapor Including the Molecular Constraints at the Interface. *J Atmos Sci*, **36**, 1722–1735.

Luhar, A.K., & Britter, R.E. 1989. A Random Walk Model for Dispersion in Inhomogeneous Turbulence in a Convective Boundary Layer. *Atmos. Env.*, **23**, 1911–1924.

Lumley, J.L. 1979. Prediction methods for turbulent flows. von Karman Institute for Fluid Dynamics.

Lumley, J.L., & Khajeh-Nouri, B. 1974. Computational modeling of turbulent transport. *Adv. Geophys.*, **18A**, 169–192.

MacInnes, J. M., & Bracco, F. V. 1992. Stochastic Particle Dispersion Modeling and the Tracer-Particle Limit. *Phys. Fluids A*, **Vol. 4, No. 12**, 2809–2824.

Mahrt, L. 1998. Flux Sampling Errors for Aircraft and Towers. *J. Atmos. Ocean. Tech.*, **15**, 416–429.

Manton, M.J. 1977. On the Structure of Convection. *Boundary-Layer Meteorol*, **12**, 491–503.

Marusic, I. 2001. On the Role of Large-Scale Structures in Wall Turbulence. *Phys. Fluids*, **13**, 735–743.

Mauder, M., Desjardins, R.L., Pattey, E., Gao, Z., & van Haarlem, R. 2008. Measurement of the Sensible Eddy Heat Flux Based on Spatial Averaging of Continuous Ground-Based Observations. *Boundary-Layer Meteorol.*, **128**, 151–172.

Mauder, M.R., Desjardins, R.L., Pattey, E., & Worth, D.E. 2010. An Attempt to Close the Daytime Surface Energy Balance Using Spatially-Averaged Flux Measurements. *Boundary-Layer Meteorol*, **136**, 175–191.

Maxworthy, T. 1973. A Vorticity Source for Large Scale Dust Devils and Other Comments on Naturally Occurring Columnar Vortices. *J Atmos Sci*, **30**, 1717–1722.

McAneney, K.J., & Judd, M.J. 1991. Multiple windbreaks: an aeolean ensemble. *Boundary-Layer Meteorol*, **54**, 129–146.

McBean, G.A., & Elliot, J.A. 1975. The Vertical Transports of Kinetic Energy by Turbulence and Pressure in the Boundary Layer. *J Atmos Sci*, **32**, 753–766.

McNaughton, K.G. 1981. Net Interception Losses During Sprinkler Irrigation. *Agric. Meteorol.*, **24**, 11–27.

McNaughton, K.G. 1988. Effects of Windbreaks on Turbulent Transport and Microclimate. *Agriculture, Ecosystems and Environment*, **22/23**, 17–39.

McNaughton, K.G. 1989. Micrometeorology of Shelterbelts and Forest Edges. *Phil. Trans. R. Soc. Lond. Series B*, **B324**, 351–368.

McNaughton, K.G. 2004a. Attached Eddies and Production Spectra in the Atmospheric Logarithmic Layer. *Boundary-Layer Meteorol*, **111**, 1–18. Davidson (2004, "Turbulence", Oxford U. Press) p135 states: "Townsends model is based on the idea that a typical eddy of diameter d is centred a distance $d/2$ from the wall, and so eddies of all size are in contact with the wall — the so-called *attached eddy hypothesis*.".

McNaughton, K.G. 2004b. Turbulence Structure of the Unstable Atmospheric Surface Layer and Transition to the Outer Layer. *Boundary-Layer Meteorol*, **112**, 199–221.

McNaughton, K.G. 2006. On the Kinetic Energy Budget of the Unstable Atmospheric Surface Layer. *Boundary-Layer Meteorol*, **118**, 83–107.

McNaughton, K.G., & Brunet, Y. 2002. Townsend's Hypothesis, Coherent Structures and Monin-Obukhov Similarity. *Boundary-Layer Meteorol*, **102**, 161–175.

McNaughton, K.G., & Spriggs, T.W. 1986. A Mixed-Layer Model for Regional Evaporation. *Boundary-Layer Meteorol*, **34**, 243–262.

Mellor, G. L. 1973. Analytic Prediction of the Properties of Stratified Planetary Surface Layers. *J Atmos Sci*, **30**, 1061–1069.

Mellor, George L., & Yamada, Tetsuji. 1974. A Hierarchy of Turbulence Closure Models for Planetary Boundary Layers. *J Atmos Sci*, **31**, 1791–1806.

Miguel, A.F., van de Braak, N.J., Silva, A.M., & Bot, G.P.A. 2001. Wind-induced airflow through permeable materials Part 1: the motion equation. *J. Wind Eng. Indust. Aero.*, **89**, 45–57.

Milleretal. 1992. . *J. Climate*, **5**, –.

Miyake, M. 1965. Transformation of the Atmospheric Boundary Layer over Inhomogeneous Surfaces.

Monin, A.S., & Obukhov, A.M. 1954. Basic Laws of Turbulent Mixing in the Ground Layer of the Atmosphere. *Trudy Geofiz. Inst. Akad. Nauk SSSR*, **151**(A 1959 translation (under auspices of American Meteorological Society) is available from Defense Technical Information Center (URL http://handle.dtic.mil/100.2/AD672723)), 163–187.

Monin, A.S., & Yaglom, A.M. 1977. *Statistical Fluid Mechanics*. MIT Press. 769 pp.

Mooney, C.J., & Wilson, J.D. 1993. Disagreements between gradient-diffusion and Lagrangian stochastic dispersion models, even for sources near ground. *Boundary-Layer Meteorol*, **64**, 291–296.

Moore, C.J. 1986. Frequency Response Corrections for Eddy Correlation Systems. *Boundary-Layer Meteorol.*, **37**, 17–36.

Moraes, O.L.L., & Epstein, M. 1987. The Velocity Spectra in the Stable Surface Layer. *Boundary-Layer Meteorol*, **40**, 407–414.

Naot, O., & Mahrer, Y. 1991. Two-Dimensional Microclimate Distribution Within and Above a Crop Canopy in an Arid Environment: Modeling and Observational Studies. *Boundary-Layer Meteorol*, **56**, 223–244.

Nieuwstadt, F. T. M. 1980. Application of Mixed-Layer Similarity to the Observed Dispersion from a Ground-Level Source. *J Appl Meteorol*, **19**, 157–162.

Nieuwstadt, F. T. M., & Ulden, A. P. Van. 1978. A Numerical Study on the Vertical Dispersion of Passive Contaminants from a Continuous Source in the Atmospheric Surface Layer. *atmos. envt*, **12**, 2119–2124.

Nieuwstadt, F.T.M., & Dop, H. Van. 1984. *Atmospheric Turbulence and Air Pollution Modelling*.

Nieuwstadt, F.T.M., & Tennekes, H. 1981. A Rate Equation for the Nocturnal Boundary-Layer Height. *J Atmos Sci*, **38**, 1418–1428.

Obukhov, A.M. 1959. Description of Turbulence in Terms of Lagrangian Variables. *Adv. Geophys.*, **6**, 113–116.

Packwood, A. R. 2000. Flow Through Porous Fences in Thick Boundary Layers: Comparisons Between Laboratory and Numerical Experiments. *J. Wind Eng. Ind. Aero.*, **88**, 75–90.

Panofsky, H. A. 1978. Matching in the Convective Planetary Boundry Layer. *J Atmos Sci*, **35**, 272–276.

Panofsky, H.A. 1973. *Tower micrometeorology*. In 'Workshop on Micrometeorology', American Meteorol. Soc. Chap. 4, pages 151–176.

Panofsky, H.A., Tennekes, H., Lenschow, D.H., & Wyngaard, J.C. 1977. The Characteristics of Turbulent Velocity Components in the Surface Layer under Convective Conditions. *Boundary-Layer Meteorol*, **11**, 355–361.

Panton, R.L. 1984. *Incompressible flow*. Wiley.

Pasquill, F. 1966. Lagrangian similarity and vertical diffusion from a source at ground level. *Q J R Meteorol Soc*, **92**, 185–.

Pasquill, F. 1972. Some Aspects of Boundary Layer Description. *Quarterly Journal of the Royal Meteorological Society*, **98**(417), 469–494.

Pasquill, F. 1974. *Atmospheric Diffusion*. Second edn. J. Wiley and Sons. 429 pp.

Pasquill, F., & Smith, F. B. 1983. *Atmospheric Diffusion*. E. Horwood.

Patton, E.G., Shaw, R.H., Judd, M.J., & Raupach, M.R. 1998. Large-eddy simulation of windbreak flow. *Boundary-Layer Meteorol*, **87**, 275–306.

Paulson, C.A. 1970. The Mathematical Representation of Wind Speed and Temperature Profiles in the Unstable Atmospheric Surface Layer. *J Appl Meteorol*, **9**, 857–861.

Penman, H.L. 1948. Natural Evaporation from Open Water, Bare Soil and Grass. *Proc. R. Soc. London Series A.*, **193**, 120–146.

Pennycuick, C.J. 1998. Field Observations of Thermals and Thermal Streets, and the Theory of Cross-Country Soaring Flight. *J. Avian Biology*, **29**, 33–43.

Perry, A.E., & Chong, M.S. 1987. A Description of Eddying Motions and Flow Patterns Using Critical-Point Concepts. *Ann. Rev. Fluid Mech.*, **19**, 125–155. Critical points are points in the flow field where the streamline slope is indeterminate and the velocity is zero relative to an appropriate observer.

Philip, J. R. 1959. The Theory of Local Advection. *J. Meteorol.*, **16**, 535–547. (I have clarifying correspondence with JRP in a folder.).

Pinard, J.-P., & Wilson, J.D. 2001. First- and second-order closure models for wind in a plant canopy. *J Appl Meteorol*, **40**, 1762–1768.

Plate, Erich J. 1971. The Aerodynamics of Shelter Belts. *Agricultural Meteorology*, **Vol. 8**, 203–222.

Portelli, R. V. 1977. Mixing Heights, Wind Speeds and Ventilation Coefficients for Canada. *Climatological Studies*, **No. 31**.

Priestley, C.H.B. 1955. Free and Forced Convection in the Atmosphere Near the Ground. *Quart. J. Roy. Meteorol. Soc.*, **81**, 139–143.

Pruitt, W.O., Morgan, D.L., & Lourence, F.J. 1973. Momentum and mass transfers in the surface boundary layer. *Quart. J. R. Met. Soc.*, **99**, 370–386.

Raine, J.K., & Stevenson, D.C. 1977. Wind Protection by Model Fences in a Simulated Atmospheric Boundary Layer. *J. Indust. Aero.*, **2**, 159–180.

Rao, K. S., Wyngaard, J. C., & Coté, O. R. 1974a. Local Advection of Momentum, Heat, and Moisture in Micrometeorology. *Boundary-Layer Meteorol*, **7**, 331–348.

Rao, K. S., Wyngaard, J. C., & Coté, O. R. 1974b. The Structure of the Two-Dimensional Internal Boundary Layer over a Sudden Change of Surface Roughness. *J Atmos Sci*, **31**(3), 738–746.

Raupach, M. R., & Legg, B. J. 1983. Turbulent Dispersion from an Elevated Line Source: Measurements of Wind-Concentration Moments and Budgets. *J Fluid Mech*, **136**, 111–137.

Raupach, M. R., Coppin, P. A., & Legg, B. J. 1986. Experiments on Scalar Dispersion Within a Model Plant Canopy Part 1: The Turbulence Structure (See also erratum, BLM 39, 423-424.). *Boundary-Layer Meteorol*, **35**, 21–52.

Raupach, M.R. 1981. Conditional statistics of Reynolds stress in rough-wall and smooth-wall turbulent boundary layers. *J Fluid Mech*, **108**, 363–382.

Raupach, M.R. 1987. A Lagrangian Analysis of Scalar Transfer in Vegetation Canopies. *Quart. J.R. Meteorol. Soc.*, **113**, 107–120.

Raupach, M.R. 1988. Canopy transport processes. *Pages 95–127 of:* Steffen, W.L., & Denmead, O.T. (eds), *Flow and transport in the natural environment: advances and applications*. Springer-Verlag.

Raupach, M.R. 2001. Combination Theory and Equilibrium Evaporation. *Quart. J. Roy. Meteorol. Soc.*, **127**, 1149–1181.

Raupach, M.R. 2002. Diffusion of heavy particles in a turbulent flow. *Pages 301–316 of:* Raats, P. A.C., Smiles, D., & Warrick, A.W. (eds), *Environmental Mechanics: Water, Mass and Energy Transfer in the Biosphere*. Geophys. Monogr. Series, vol. 129. AGU. doi:10.1029/129GM25.

Raupach, M.R., & Finnigan, J.J. 1988. Single-Layer Models of Evaporation from Plant Canopies are Incorrect But Useful, Whereas Multilayer Models are Correct But Useless': Discuss. *Australian Journal of Plant Physiology*, **15**, 705–716.

Raupach, M.R., & Shaw, R.H. 1982. Averaging procedures for flow within vegetation canopies. *Boundary-Layer Meteorol*, **22**, 79–90.

Raupach, M.R., Coppin, P.A., & Legg, B.J. (1986). Experiments on scalar dispersion within a model plant canopy. Part I: The turbulence structure. (See also erratum, BLM 39, 423-424.). *Boundary-Layer Meteorol*, **35**, 21–52.

Reeks, M. W. 1977. On the Dispersion of Small Particles Suspended in an Isotropic Turbulent Fluid. *J Fluid Mech*, **Vol. 83, part 3**, 529–546.

Reeks, M. W. 1983. The Transport of Discrete Particles in Inhomogeneous Turbulence. *J. Aerosol Sci.*, **Vol. 14, No. 6**, 729–739.

Reynolds, O. 1895. On the Dynamical Theory of Incompressible Viscous Fluids and the Determination of the Criterion. *Philosophical Transactions of the Royal Society of London. A.*, **186**, 123–164.

Rider, N. E., Philip, J. R., & Bradley, E. F. 1963. The Horizontal Transport of Heat and Moisture - a Micrometeorological Study. *Quart. J. Roy. Meteorol. Soc.*, **382**, 507–531.

Rubinstein, R., & Barton, J.M. 1990. Nonlinear Reynolds stress models and the renormalization group. *Phys. Fluids A*, **2**, 1472–1476.

Savelyev, S.S., & Taylor, P.A. 2001. Notes on an Internal Boundary-Layer Height Formula. *Boundary-Layer Meteorol*, **101**, 293–301.

Sawford, B. L. 2001. Project Prairie Grass – A Classic Atmospheric Dispersion Experiment Revisited14th Australian Fluid Mechanics Conference, for 14th Australian Fluid Mechanics Conference.

Sawford, B. L., & Guest, F. M. 1991. Lagrangian Statistical Simulation of the Turbulent Motion of Heavy Particles. *Boundary-Layer Meteorol*, **54**, 147–166. Applies only to homogeneous turbulence. Heuristic adaptation of well-mixed LS model for the driving fluid element.The copy that I reviewed is indexed 1615.

Sawford, B.L., & Guest, F.M. 1988. Uniqueness and Universality of Lagrangian Stochastic Models of Turbulent Dispersion. *Pages 96–99 of: Preprints of 8th AMS Symposium on Turbulence and Diffusion, San Diego, CA*. American Meteorological Society.

Schaller, E. 1977. Time and Height Variability of the Sensible Heat Flux in the Surface Layer. *Boundary-Layer Meteorol*, **11**, 329–354.

Schlichting, H. 1968. *Boundary Layer Theory*. 6 edn. McGraw-Hill.

Schmid, H.P. 1994. Source areas for scalar and scalar fluxes. *Boundary-Layer Meteorol.*, **67**, 293–318.

Schmid, H.P. 1997. Experimental design for flux measurements:matching scales of observations and fluxes. *Agric. Forest Meteorol.*, **87**, 179–200.

Schmid, H.P. 2002. Footprint modeling for vegetation atmosphere exchange studies: a review and perspective. *Agric. Forest Meteorol.*, **113**, 159–183.

Schmidt, R.K., & Housen, K. 1995. Problem solving with dimensional analysis. *The Industrial Physicist*, **1**(1), 21–24.

Schuepp, P.H., Leclerc, M.Y., MacPherson, J.I., & Desjardins, R.L. 1990. Footprint prediction of scalar fluxes from analytical solutions of the diffusion equation. *Boundary-Layer Meteorol.*, **50**, 355–373.

Seginer, I. 1975a. Atmospheric-Stability Effect on Windbreak Shelter and Drag. *Boundary-Layer Meteorol*, **8**, 383–400.

Seginer, I. 1975b. Flow Around a Windbreak in Oblique Wind. *Boundary-Layer Meteorol*, **9**, 133–141.

Seginer, I., Mulhearn, P. J., Bradley, E. F., & Finnigan, J. J. 1976. Turbulent Flow in a Model Plant Canopy. *Boundary-Layer Meteorol*, **10**, 423–453.

Seibert, P., Beyrich, F., Gryning, S.-E., Joffre, S., Rasmussen, A., & Tercier, P. 2000. Review and Intercomparison of Operational Methods for the Determination of the Mixing Height. *Atmos. Environ.*, **34**, 1001–1027.

Shaw, R.H., Tavangar, J., & Ward, D.P. 1983. Structure of the Reynolds Stress in a Canopy Layer. *J. Clim. Appl. Meteorol.*, **22**, 1922–1931.

Shinn, J.H. 1971. *Steady-State Two-Dimensional Air Flow in Forests and the Disturbance of Surface Layer Flow by a Forest Wall*. Ph.D. thesis, University of Wisconsin, Madison.

Smith, C. R., Walker, J. D. A., Haidari, A. H., & Sobrun, U. 1991. On the Dynamics of Near-Wall Turbulence. *Philosophical Transactions of the Royal Society of London, A: Physical Sciences and Engineering*, **336**, 131–175.

Smith, R.K., & Leslie, L.M. 1976. Thermally Driven Vortices: A Numerical Study with Application to Dust-Devil Dynamics. *Q J R Meteorol Soc*, **102**, 791–804.

Speziale, C.G. 1987. On nonlinear k-l and k-ϵ models of turbulence. *J Fluid Mech*, **178**, 459–475.

Stubbley, G.D., & Rooney, D.R. 1986. The Sensitivity of $k-\epsilon$ Model Computations of the Neutral Planetary Boundary Layer to Baroclinicity. *Boundary-Layer Meteorol*, **37**, 53–70.

Stull, R.B. 1988. *An Introduction to the Boundary Layer Meteorology*. Kluwer Academic Publishers. 666pp.

Sullivan, P. J., & Yip, H. 1989. Near-source dispersion of contaminant from an elevated line-source. *Journal of Applied Mathematics and Physics (ZAMP)*, **40**, 297–299.

Tani, N. 1958. On the wind tunnel test of the model shelter-hedge. *Bull. Nat'l Inst. Agric. Sci. Japan*, **Ser A, No. 6**, 75–80 Summary in English.

Taylor, G.I. 1921. Diffusion by Continuous Movements. *Proc London Math Soc, Ser. 2*, **A20**, 196–211.

Taylor, G.I. 1944. *Air Resistance of a Flat Plate of Very Porous Material*. Tech. rept. 2236. Aeronautical Research Council (Reports and Memoranda). Reprinted (1963) as No. 43, pp383-386 in "The scientific papers of G.I. Taylor,III", G.K. Batchelor (editor).

Taylor, P. A. 1970. A Model of Airflow Above Changtes in Surface Heat Flux, Temperature and Roughness for Neutral and Unstable Conditions. *Boundary-Layer Meteorol*, **1**, 18–39.

Taylor, P. A. 1971. Airflow Above Changes in Surface Heat Flux, Temperature and Roughness: An Extension to Include the Stable Case. *Boundary-Layer Meteorol*, **1**, 474–497.

Telford, J.W. 1972. A Plume Theory for the Convective Field in Clear Air. *J Atmos Sci*, **29**, 128–134.

Tennekes, H. 1970. Free Convection in the Turbulent Ekman Layer of the Atmosphere. *J Atmos Sci*, **27**, 1027–1034.

Tennekes, H. 1979. The Exponential Lagrangian Correlation Function and Turbulent Diffusion in the Inertial Subrange. *Atmos. Env.*, **13**, 1565–1567.

Tennekes, H., & Lumley, J.L. 1972. *A First Course in Turbulence.* M.I.T. Press. (300 pages).

Theodorsen, T. 1952. Mechanism of Turbulence. *Pages 1–18 of: Bulletin No. 149.* Ohio State University Engineering Experiment Station. Ohio State University Engineering Experiment Station.

Thomson, D. J. 1984. Random Walk Modelling of Diffusion in Inhomogeneous Turbulence. *Quart. J. Roy. Meteorol. Soc.*, **110**, 1107–1120.

Thomson, D. J., & Montgomery, M. R. 1994. Reflection Boundary Conditions for Random Walk Models of Dispersion in Non-Gaussian Turbulence. *Atmos. Environ.*, **Vol. 28, No. 12**, 1981–1987.

Thomson, D.J. 1987. Criteria for the selection of stochastic models of particle trajectories in turbulent flows. *J Fluid Mech*, **180**, 529–556.

Twine, T.E., Kustas, W.P., Norman, J.M.., Cook, D.R., Houser, P.R., Meyers, T.P., Prueger, J.H., Starks, P.J., & Wesley, M.L. 2000. Correcting Eddy-Covariance Flux Underestimates over a Grassland. *Agric. Forest Meteor.*, **103**, 279–300.

Van de Wiel, B.J.H., Ronda, R.J., Moene, A.F., De Bruin, H.A.R., & Holtslag, A.A.M. 2000. Intermittent Turbulence and Oscillations in the Stable Boundary Layer: A System Dynamics Approach. *Pages 593–595 of: Preprints, 14th Symposium on Boundary Layer and Turbulence, Aspen, CO*American Meteorol. Soc., for AMS.

van Eimern, J., Karschon, R., Razumova, L.A., & Robertson, G.W. 1964. *Windbreaks and Shelterbelts.* Tech. Note., no. 59. World Meteorol. Org.

van Ulden, A. P. 1978. Simple Estimates for Vertical Diffusion From Sources Near the Ground. *Atmos. Environ.*, **Vol. 12**, 2125–2129.

Vesala, T., Kljun, N., Rannik, U., Rinne, J., Sogachev, A., Markkanen, T., Sabelfeld, K., Foken, Th., & Leclerc, M.Y. 2008. Flux and concentration footprint modelling: State of the art. *Env. Poll.*, **152**, 653–666.

Walker, E.R. 1965. A Particulate Diffusion Experiment. *J. Appl. Meteor.*, **4**, 614–621.

Wallace, D.J., Picot, J.C., & Chapman, T.J. 1995. A numerical model for forestry aerial spraying. *Agric. For. Meteor.*, **76**, 19–40.

Wang, H., & Takle, E.S. 1995. A numerical simulation of boundary-layer flows near shelterbelts. *Boundary-Layer Meteorol*, **75**, 141–173.

Wang, Y., Miller, D.R., Anderson, D.E., & McManus, M.L. 1995. A Lagrangian stochastic model for aerial spray transport above an oak forest. *Agric. For. Meteor.*, **76**, 277–291.

Wang, Y.P., & Leuning, R. 1998. A Two-Leaf Model for Canopy Conductance, Photosynthesis and Partitioning of Available Energy. I. Model Description. *Agric. Forest Meteorol.*, **91**, 89–111.

Webb, E. K., Pearman, G. I., & Leuning, R. 1980. Correction of Flux Measurements for Density Effects Due to Heat and Water Vapour Transfer. *Quart. J. Roy. Meteorol. Soc.*, **106**, 85–100.

Webb, E.K. 1970. Profile Relationships: The Log-Linear Range and Extension to Strong Stability. *Quart. J. Royal Meteorol. Soc.*, **96**, 67–90.

Webb, E.K. 1988. Convective processes in the lower atmosphere: Commentary. *Pages 261–269 of:* Steffen, W.L., & Denmead, O.T. (eds), *Flow and transport in the natural environment: advances and applications*. Springer-Verlag.

Weber, R.O. 1999. Remarks on the definition and estimation of friction velocity. *Boundary-Layer Meteorol*, **93**, 197–209.

Weijers, E.P., van Ulden, A., & Vugts, H.F. 1994. Kinematic Estimate Within Surface-Layer Thermal Structures. *Boundary-Layer Meteorol*, **67**, 145–160.

Weil, J. C. 1988. *Langevin Model Simulations of Bottom-Up and Top-Down Dispersion in a Nonhomogeneous Turbulent Boundary Layer.*

Weil, J. C., & Horst, T.W. 1991. Footprint Estimates for Atmospheric Flux Measurements in the Convective Boundary Layer. 1–12.

Weil, J.C. 1990. A Diagnosis of the Asymmetry in Top-Down and Bottom-Up Diffusion Using a Lagrangian Stochastic Model. *J Atmos Sci*, **47**, 501–515.

Wieringa, J. 1980. A Revaluation of the Kansas Mast Influence on Measurements of Stress and Cup Anemometer Overspeeding. *Boundary-Layer Meteorol*, **18**, 411–430.

Wilczak, J.M. 1984. Large Scale Eddies in the Unstably Stratified ASL: Part I: Velocity and Temperature Structure. *J Atmos Sci*, **41**, 3537–3550.

Wilczak, J.M., & Tillman, J. E. 1980. The Three-Dimensional Structure of Convection in the Atmospheric Surface Layer. *J Atmos Sci*, **37**, 2424–2443.

Willis, G.E., & Deardorff, J.W. 1976. A Laboratory model of diffusion into the Convective Planetary Boundary Layer. *Quart. J. Roy. Meteorol. Soc.*, **102**, 427–445.

Willis, G.E., & Deardorff, J.W. 1978. A Laboratory Study of Dispersion from an elevated source within a modeled Convective Planetary Boundary Layer. *Atmos. Environ.*, **12**, 1305–1311.

Willis, G.E., & Deardorff, J.W. 1981. A Laboratory Study of Dispersion from a Source in the Middle of the Convective Boundary Layer. *Atmos. Environ.*, **15**, 109–117.

Wilson, J D, & Yee, E. 2003. Calculation of Winds Disturbed by an Array of Fences. *Agric. For. Meteorol.*, **115**, 31–50.

Wilson, J.D. 1982a. An Approximate Analytical Solution to the Diffusion Equation for Short-Range Dispersion from a Continuous Ground-Level Source. *Boundary-Layer Meteorol*, **23**, 85–103.

Wilson, J.D. 1982b. Turbulent dispersion in the atmospheric surface-layer. *Boundary-Layer Meteorol*, **22**, 399–420.

Wilson, J.D. 1985. Numerical studies of flow through a windbreak. *J. Wind Eng. Indust. Aero.*, **21**, 119–154.

Wilson, J.D. 1987. On the Choice of a Windbreak Porosity Profile. *Boundary-Layer Meteorol*, **38**, 37–49.

Wilson, J.D. 1988. A second-order closure model for flow through vegetation. *Boundary-Layer Meteorol*, **42**, 371–392.

Wilson, J.D. 1989. *Turbulent Transport Within the Plant Canopy.* Tech. rept. 177. Int. Assoc. Hydrol. Sci.

Wilson, J.D. 1997. A field study of the mean pressure about a windbreak. *Boundary-Layer Meteorol*, **85**, 327–358.

Wilson, J.D. 2000. Trajectory Models for Heavy Particles in Atmospheric Turbulence: Comparison with Observations. *J Appl Meteorol*, **39**, 1894–1912.

Wilson, J.D. 2004. Oblique, Stratified Winds About a Shelter Fence, I: Measurements. *J Appl Meteorol*, **43**, 1149–1167.

Wilson, J.D. 2007. Turbulent Velocity Distributions and Implied Trajectory Models. *Boundary-Layer Meteorol*, **125**, 39–47.

Wilson, J.D. 2008. Monin-Obukhov Functions for Standard Deviations of Velocity. *Boundary-Layer Meteorol*, **129**, 353–369.

Wilson, J.D. 2012. An Alternative Eddy-Viscosity Model for the Horizontally Uniform Atmospheric Boundary Layer. *Boundary-Layer Meteorol.*, **145**, 165–184. DOI 10.1007/s10546-011-9650-0.

Wilson, J.D., & Flesch, T.K. 1993. Flow Boundaries in Random Flight Dispersion Models: Enforcing the Well-Mixed Condition. *J Appl Meteorol*, **32**, 1695–1707.

Wilson, J.D., & Flesch, T.K. 1999. Wind and Tree Sway in Forest Cutblocks, III: A Windflow Model to Diagnose Spatial Variation. *Agric. Forest Meteo.*, **93**, 259–282.

Wilson, J.D., & Flesch, T.K. 2004. An Idealized Mean Wind Profile for the Atmospheric Boundary-Layer. *Boundary-Layer Meteorol*, **110**, 281–299.

Wilson, J.D., & Mooney, C. J. 1997. Comments on 'A numerical simulation of boundary-layer flows near shelterbelts' by H. Wang and E. Takle. *Boundary-Layer Meteorol*, **85**, 137–149.

Wilson, J.D., & Swaters, G.E. 1991. The source area influencing a measurement in the planetary boundary-layer: the footprint and the distribution of contact distance. *Boundary-Layer Meteorol*, **55**, 25–46.

Wilson, J.D., & Yee, E. 2007. A Critical Examination of the Random Displacement Model of Turbulent Dispersion. *Boundary-Layer Meteorol*, **125**, 399–416.

Wilson, J.D., Thurtell, G.W., & Kidd, G.E. 1981a. Numerical Simulation of Particle Trajectories in Inhomogeneous Turbulence. II. Systems with Variable Turbulent Velocity Scale. *Boundary-Layer Meteorol*, **21**, 423–44.

Wilson, J.D., Thurtell, G.W., & Kidd, G.E. 1981b. Numerical Simulation of Particle Trajectories in Inhomogeneous Turbulence. III. Comparison of Predictions with Experimental Data for the Atmospheric Surface-Layer. *Boundary-Layer Meteorol*, **21**, 443–463.

Wilson, J.D., Lozowski, E.P., & Zhuang, Y. 1988. Comments on a relationship between fluid and immersed-particle velocity fluctuations proposed by Walklate(1987). *Boundary-Layer Meteorol.*, **43**, 93–98.

Wilson, J.D., Ferrandino, F.J., & Thurtell, G.W. 1989. A Relationship Between Deposition Velocity and Trajectory Reflection Probability for Use in Stochastic Lagrangian Dispersion Models. *Agric. Forest Meteorol.*, **47**, 139–154.

Wilson, J.D., Swaters, G.E., & Ustina, F. 1990. A perturbation analysis of turbulent flow through a porous barrier. *Quart. J. Royal Meteorol. Soc.*, **116**, 989–1004.

Wilson, J.D., Finnigan, J.J., & Raupach, M.R. 1998. A first-order closure for disturbed plant canopy flows, and its application to windflow through a canopy on a ridge. *Quart. J. Roy. Meteorol. Soc.*, **124**, 705–732.

Wilson, J.D., Flesch, T.K., & Harper, L.A. 2001. Micro-meteorological Methods for Estimating Surface Exchange with a Disturbed Windflow. *Agric. For. Meteorol.*, **107**, 207–225.

Wilson, J.D., Massman, W.J., & Swaters, G.E. 2009a. Dynamic Response of the Thermometric Net Radiometer. *Agric. Forest Meteorol.*, **149**, 1358–1364.

Wilson, J.D., Yee, E., Ek, N., & d'Amours, R. 2009b. Lagrangian Simulation of Wind Transport in the Urban Environment. *Quart. J.R. Met. Soc.*, **135**, 1586–1602.

Wilson, J.D., Flesch, T.K., & Bourdin, P. 2010. Ground-to-Air Gas Emission Rate Inferred from Measured Concentration Rise within a Disturbed Atmospheric Surface Layer. *J Appl Meteorol Climatol.*, **49**, 1818–1830.

Wilson, N.R., & Shaw, R.H. 1977. A higher-order closure model for canopy flow. *J Appl Meteorol*, **16**, 1197–1205.

Wollenweber, G.C., & Panofsky, H.A. 1989. Dependence of Velocity Variance on Sampling Time. *Boundary-Layer Meteorol*, **47**, 205–215.

Woodcock, A.H. 1975. Thermals over the Sea and Gull Flight Behaviour. *Boundary-Layer Meteorol*, **9**, 63–68.

Wyngaard, J. C. 1981. The Effects of Probe-Induced Flow Distortion on Atmospheric Turbulence Measurements. *J Appl Meteorol*, **20**, 784–794.

Wyngaard, J. C., Businger, J. A., Kaimal, J. C., & Larsen, S. E. 1981. Comments on 'a Revaluation of the Kansas Mast Influence on Measurements of Stress and Cup Anemometer Overspeeding'. 245–269.

Wyngaard, J.C. 1985. Structure of the Planetary Boundary Layer and Implications for its Modelling. *J. Clim. Appl. Meteo.*, **24**, 1131–1142.

Wyngaard, J.C. 2010. *Turbulence in the Atmosphere*. Cambridge University Press. 393pp.

Wyngaard, J.C., & Brost, R.A. 1984. Top-Down and Bottom-Up Diffusion of a Scalar in the Convective Boundary Layer. *J Atmos Sci*, **41**, 102–112.

Yaglom, A. M. 1977. Comments on Wind and Temperature Flux-Profile Relationships. *Boundary-Layer Meteorol*, **11**, 89–102.

Yaglom, A.M. 1990. ALEXANDER MIKHAILOVICH OBUKHOV, 1918-1989. *Boundary-Layer Meteorol.*, **53**, v–xi.

Yamamoto, G., & Shimanuki, A. 1961. Numerical Solution of the Equation of Atmospheric Turbulent Diffusion (1). *Sci. Repts. Tohoku Univ., Series V, Geophysics*, **12**, 24–35.

Yoshizawa, A. 1984. Statistical analysis of the deviation of the Reynolds stress from its eddy viscosity representation. *Phys. Fluids*, **27**, 1377–1387.

Yudine, M. I. Physical Considerations on Heavy Particle Diffusion. *Heavy-particle diffusion*, 185–191.

Zhuang, Y., Wilson, J.D., & Lozowski, E.P. 1989. A Trajectory-Simulation Model for Heavy Particle Motion in Turbulent Flow. *J. Fluids Eng. (Trans. Am. Soc. Mech. Eng.)*, **111**, 492–494.

Index

body forces, 22

Canopy layer
  velocity statistics, 210
Coherent structures, 140
  Bird flight, 147
  dust devils, 141
  hairpin vortices, 146
  roll vortices, 145
  thermals, 142
Conservation eqn
  advection or transport form, 24
  Boussinesq approximation, 29
  Cauchy's equation of motion, 22
  continuity equation, 21
  Euler's equation of motion, 22
  generalized, 19
  mean momentum equations, 43
  mean pressure disturbance, 44
  mean temperature, 46
  Navier-Stokes equation, 24
  passive scalar concentration, 47
  passive scalar concentration variance, 47
  passive scalar flux, 47
  relative variables, 11
  Reynolds stress tensor, 44
  Reynolds-averaged water vapour conservation equation, 41
  sensible heat flux, 46
  temperature variance, 47
  turbulent kinetic energy, 45
  water vapour, 21
Continuum hypothesis, 12
  fluid element, 13, 18
Corrsin, 172

Delage, 113, 168
Diffusivity
  molecular thermal diffusivity, 13
  units, 14
Dimensional analysis, 4
  Buckingham Pi theorem, 4
  drag on a cylinder, 6
  method of indices, 6
  plane Poiseuille flow, 7
Dispersion
  advection-diffusion equation, 179
  drunkard's walk, 180
  Fickian, 179
  Gaussian plume model, 181
  Gaussian puff model, 179
  surface layer
    Bosanquet and Pearson, 96, 186
    Calder's solution, 96, 186
    Wilson's equation, 184
Disturbed flows
  hills
    Furry Hill experiment, 135
  local advection, 152
    experiments, 153
    simulation using second-order closure, 153
  paradigm of the internal boundary layer, 150
  their generation, 149
  windbreaks
    aerodynamic characterization of the windbreak, 158, 160, 161
    aerodynamics, 157
    early analytical studies, 162
    formula for fractional wind reduction, 165
    mean velocity field, 159

Eddy covariance
  Webb-Pearman-Leuning correction, 82
eddy diffusivity
  tensor, 178
Eddy flux divergence, 41
Evapotranspiration, 97
  big leaf model, 99
  Penman equation, 98
  Penman-Monteith equation, 99

Fick law, 14

Fluid element, 13
  acceleration, 17
Flux footprint, 95
  surface layer
    analytical, 96
Flux-gradient method, 84
Fluxes
  convective, 17
    generic, 17
    kinetic energy flux density, 17
    momentum flux density, 17
    water vapour, 17
  diffusive
    Fick's law, 14
    Fourier's law, 13
    heat flux density, 13
    mass flux density, 14
    momentum flux density, 15
    Newton's law, 14
  momentum
    shear stress tensor, 15
Fourier law, 13

Geostrophic wind, 51
Governing equations
  canopy layer
    form drag, 128
    mean momentum, 127
    simplified mean momentum budget, 128

Helmholtz decomosition, 26
Homogenization, 14
Horizontally homogeneous ASL
  Monin-Obukhov similarity theory
    fundamental premises, 64
Horizontally-homogeneous ABL
  baroclinicity, 50
  convective boundary layer, 107
  Ekman spiral, 52
  entrainment interface layer, 107
  geostrophic force balance aloft, 51
  geostrophic velocity deficit, 51
  imposiiotn of the synoptic scale pressure gradient, 50
  inner and outer layers, 49
  mixed layer, 107
  mixed layer scaling, 107
    convective potential temperature scale, 107
    convective time scale, 108
    convective velocity scale, 107
  momentum equations, 51
  shear stress divergence, 51
  temperature variance, 108
  vanishing mean vertical velocity, 50
  velocity variance, 108
Horizontally-homogeneous ASL
  constant flux layer, 53
  heat flux budget, 61
  Lagrangian similarity theory, 223
    the algorithm, 225
  local equilibrium, 60
  semi-logarithmic mean wind profile, 55
  shear stress budget, 61
  streamwise velocity variance budget, 57
  turbulent kinetic energy budget, 59
  vertical velocity variance budget, 57

Idealized flows
  inviscid flow, 26
  irrotational flow, 26
  non-divergent flow, 26
  potential flow, 26
  two-dimensional flow, 26
Incompressible flow, 21, 25
Inertial sublayer, 64

Kolmogorov
  hypotheses, 28
    inertial subrange, 28
  inner scales, 28
  Kolmogorov energy spectrum, 28
  Kolmogorov length, 12, 28
  Kolmogorov time scale, 28
  Kolmogorov velocity scale, 28
  Lagrangian velocity structure function, 195

Lagrangian, 18
Lagrangian (material) derivative, 18
Lagrangian stochastic model
  concentration–source strength relationship, 188
  transition density for position, 188
Langevin equation, 193

Markov process, 193
Molecular transport law
  Fick, 14
  Fourier, 13
  Newton, 14
Momentum flyux divergence, 35
Monin Obukhov similarity theory
  implied eddy diffusivities, 70

Monin-Obukhov similarity
imperfect scaling of horiz. velocity variances, 110
Monin-Obukhov similarity theory, 64
dimensionless mean profiles, 67
dimensionless wind shear, 65
fundamental premises, 64
its partial justification by non-dimensionalizing the conservation equations, 66
mean velocity and temperature profiles, 74
Obukhov length, 65
relationships are stochastic, 79
scaling variables, 65
temperature scale, 65
turbulent velocity variance, 75
dependence on averaging duration, 75
horizontal velocity, 76
vertical velocity, 76
universal functions, 65
Dyer and Bradley (ITCE76), 74
Dyer and Hicks, 71
Kansas, 72

Newton's law of viscosity, 14
Newtonian fluid, 23
Non-divergent flow, 21, 25
Notation
summation convention, 12
tensor notation, 11

Peclet number, 14
Penman, 97
Penman-Monteith equation, 132
Potential evapotranspiration, 98

Resolved/Unresolved scales of motion, 37
effect of the unresolved scales on the resolved flow, 41
Reynolds averaging, 39
Reynolds (mean momentum) equations, 43
Reynolds averaging, 39
Richardson, 28
Richardson number
flux Richardson number, 71
gradient Richardson number, 71
relationship between flux and gradient Richardson numbers in MO layer, 71
Roughness sublayer, 64, 119
dispersive flux, 123
dispersive fluxes, 127
flexible neutral mean wind profile, 131
plant canopy layer, 119
canopy wind spiral, 139
counter-gradient vertical transport, 136
intermittency and "ramps", 124
layer-wise energy budget, 131
leaf-level heat flux, 132
mean wind profile, 129
microfronts, 124
necessity for spatial averaging, 120
quadrant analysis, 126
renewal (clean sweep) model, 138
simulation using K a closure, 134
sweeps (gusts) and ejections, 126
wake production of turbulent kinetic energy, 133
Schmidt number, 77
Tombstone canopy experiment, 135

Similarity theory, 9
Complete similarity, 9
Lagrangian similarity theory for turbulent dispersion in hhASL, 223
the algorithm, 225
Monin-Obukhov similarity theory for hhASL, 64
Stable ABL, 112
Strain rate tensor, 15
Stress-strain relationship, 23
Newton's law, 15
Newtonian fluid
Stokes' hypothesis, 24
Surface energy balance, 80
surface forces, 22
Surface layer experiments, 71
ITCE76, 73
Kansas, 72
local advection, 153
Project Prairie Grass, 185, 197, 198
Suffield particle dispersion trials, 218
windbreak flows, 156
Surface-atmosphere exchange
bulk transfer coefficients, 89
convective boundary layer budgeting, 94
Flux footprint, 226
flux footprint, 95
vertical fluxes by eddy covariance, 82
sources of error, 82
vertical fluxes by flux-gradient method, 83
vertical fluxes by inverse dispersion, 100

Terminology

homogeneity, 35
horizontal homogeneity, 49
incompressibility, 25
inviscid, 26
irrotational, 26
stationarity, 35
Turbulence
definition, 3, 26
energy cascade, 3, 27
range of scales of motion, 3
Turbulence closure problem, 41, 167
eddy diffusion closure
limited validity, 172, 210
eddy viscosity
units, 55
eddy viscosity closure, 52
higher-order closure, 171
Large Eddy Simulation, 105
Prandtl closure, 168
Turbulence closures
eddy viscosity closure
its conditional validity demonstrated, 61
Turbulence statistics
autocorrelation coefficient, 35
dissipation rate, 12
energy dissipation rate, 27
friction velocity, 54
ideal surface layer
Obukhov length, 65
turbulent temperature scale, 65
in the convective boundary layer, 205
integral time scale, 35
mean potential temperature
its height-independence in a neutrally stratified layer, 67
notation, 31
Obukhov length
relationship to flux Richardson number, 70
probability density function
Gaussian, 33
spectra
kinetic energy, 28, 108
velocity variance spectrum, 33
wavenumer-to-frequency transformation, 28
turbulent Prandtl number, 77
turbulent Schmidt number, 77, 78, 203
velocity covariance, 33
velocity variance, 32
vertical vapour flux
eddy diffusion model, 56
Turbulence statistics:flux Richerdson number, 60
Turbulent dispersion
crosswind-integrated concentration, 184
eddy diffusion paradigm, 178
advection-diffusion equation, 179
Gaussian puff and plume, 179
MOST profiles, 183
neglecting streamwise diffusion, 178
power-law profiles, 185
generalized Langevin equation, 195
consistency with Kologorov structure function, 196
Lagrangian similarity theory, 223
the algorithm, 225
Lagrangian stochastic model
2-D Gaussian turbulence, 202
application to plant canopy layer, 211
calibration for ideal ASL, 197
Chapman-Kolmogorov equation, 194
diffusion limit, 203
Fokker-Planck equation, 194
inhomogeneity index, 210
joint density for position and velocity, 194
partially absorbing surfaces, 205
simulations of Project Prairie Grass, 198
skewed 1-D turbulence (application to CBL), 207
trajectory reflection at boundaries, 204
tuning the Kolmogorov constant, 203
unique well-mixed LS model for 1-D Gaussian turbulence, 197
well-mixed constraint, 196
lateral (crosswind) dispersion, 199
lateral (crosswind) spread, 183
passive scalar mass conservation equation, 174
Peclet number, 175, 188
Random Displacement Model, 195
relative and absolute dispersion, 175
Reynolds-averaged mass conservation equation, 177
Taylor's Lagrangian theory, 189
eddy diffusivity, 192
far field eddy diffusivity, 192
far field limit, 192
irreconcilable with eddy diffusion paradigm, 191
Lagrangian integral time scale, 190
Lagrangian velocity correlation, 190
mean square displacement, 189

near field limit, 192
puff growth rate, 190
volumetric source density, 174
Turbulent dispersion of particles
inertial particle model, 214
Lagrangian simulations of Suffield bead diffusion trials, 219
Langevin model, 216
Settling Sticky Fluid Element (SSFE), 219
turbophoresis, 217
Turbulent friction, 35
Turbulent kinetic energy budget, 45
buoyant production, 46
pressure-strain, 45
redistribution term, 45
shear production, 46
viscous dissipation, 46

Unresolved Basal Layer, 130, 220
Unresolved basal layer, 52

Velocity gradient tensor, 15
Virtual potential temperature, 68
Virtual temperature, 68
Volumetric dilatation, 21
von Karman constant, 55, 77
challenge of measuring, 72
for properties other than momentum, 67
values from ITCE, 74